



**HAL**  
open science

## Contribution to intelligent vehicle platoon control

Jin Zhao

► **To cite this version:**

Jin Zhao. Contribution to intelligent vehicle platoon control. Other. Ecole Centrale de Lille, 2010. English. NNT : 2010ECLI0010 . tel-00586081

**HAL Id: tel-00586081**

**<https://theses.hal.science/tel-00586081>**

Submitted on 14 Apr 2011

**HAL** is a multi-disciplinary open access archive for the deposit and dissemination of scientific research documents, whether they are published or not. The documents may come from teaching and research institutions in France or abroad, or from public or private research centers.

L'archive ouverte pluridisciplinaire **HAL**, est destinée au dépôt et à la diffusion de documents scientifiques de niveau recherche, publiés ou non, émanant des établissements d'enseignement et de recherche français ou étrangers, des laboratoires publics ou privés.

N° d'ordre : 

1	2	9
---	---	---

**ÉCOLE CENTRALE DE LILLE**

**THÈSE**

présentée en vue  
d'obtenir le grade de

**DOCTEUR**

Spécialité : Automatique et Informatique Industrielle

par

**ZHAO Jin**

Doctorat délivré par l'École Centrale de Lille

# Contribution à la Commande d'un Train de Véhicules Intelligents

Soutenue le 2 septembre 2010 devant le jury :

Rapporteurs:	Prof. Abdellah EL MOUDNI	UTBM - Montbéliard
	Prof. Claude H. MOOG	Directeur de Recherche, EC Nantes
	Prof. Shaoping WANG	Beihang University - Pékin, Chine
Examineurs:	Prof. Philippe BONNIFAIT	UTC - Compiègne
	Prof. Pierre BORNE	EC Lille
	Prof. Abdelkader EL KAMEL	EC Lille / Directeur de thèse
	Dr. El Miloudi EL KOURSI	Directeur de Recherche à l'INRETS - Lille

Thèse préparée au Laboratoire d'Automatique, Génie Informatique et Signal  
L.A.G.I.S.- École Centrale de Lille  
École Doctorale Sciences pour l'ingénieur Université Lille Nord-de-France - 072



Serial N° : | 1 | 2 | 9 |

**ECOLE CENTRALE DE LILLE**

**THESIS**

Presented to obtain  
the degree of

**DOCTOR**

Topic : Automatic Control and Computer Engineering

by

**ZHAO Jin**

Ph.D. awarded by Ecole Centrale de Lille

# Contribution to Intelligent Vehicle Platoon Control

Defended on September 2, 2010 in presence of the committee :

Rapporteurs:	Prof. Abdellah EL MOUDNI	UTBM - Montbéliard
	Prof. Claude H. MOOG	Research Director, EC Nantes
	Prof. Shaoping WANG	Beihang University - Beijing, China
Examiners:	Prof. Philippe BONNIFAIT	UTC - Compiègne
	Prof. Pierre BORNE	EC Lille
	Prof. Abdelkader EL KAMEL	EC Lille / Thesis supervisor
	Dr. El Miloudi EL KOURSI	Research Director, INRETS - Lille

L.A.G.I.S.- Ecole Centrale de Lille  
Ecole Doctorale Sciences pour l'ingénieur Université Lille Nord-de-France - 072



## Acknowledgments

The PhD work presented in this thesis has been done at "Laboratoire d'Automatique, Génie Informatique et Signal" (LAGIS) in Ecole Centrale de Lille, from September 2007 to September 2010. This work is partly supported by the China Scholarship Council (CSC).

This thesis would not have been possible without the help and support of so many people in so many ways. I would like to take the opportunity to express my gratitude to all those who contributed to this work.

First of all, my sincere thanks go to my supervisor, Prof. Abdelkader EL KAMEL, for his valuable guidance, continuous encouragement and the share of his research experience.

I would like to thank Prof. Pierre BORNE for his generous cooperation and helpful discussions and the share of his outstanding research experience. A special acknowledgement should be shown to Prof. Shaoping WANG, during her visiting period in LAGIS, I benefited a lot from her helpful suggestions and discussions.

I would like to express my sincere gratitude to Prof. Abdellah EL MOUDNI and Prof. Claude H. MOOG, who have kindly accepted the invitation to be the reviewers of my PhD thesis. My heartfelt thanks go to Prof. Philippe BONNIFAIT and Dr. El Miloudi EL KOURSI, for their kind acceptance to be the members of my PhD Committee.

I am also very grateful to the staff in EC Lille. Virginie LECLERCQ, Marie-Françoise TRICOT, Christine YVOZ, and Brigitte FONCEZ have helped me in the administrative works. Many thanks go also to Bernard SZUKALA, Hilaire ROSSI, Gilles MARGUERITE, Jacques LASUE, Patrick GALLAIS and Régine DUPLOUICH, for their kind help and hospitality.

I wish to express my special appreciation to Prof. Hélène CATSIAPIS, my French teacher. In her courses, I learned not only the language but also the culture, history, especially the many trips, which enrich my life in France.

I would like also to thank my colleagues and friends, Ismahène, Yahong, Minzhi, Andreea, Lian, Yifan, Pengfei, Yang, Dapeng, Jinlin, Jian, Huarong, Hui, Guoguang, Bo, Wenhua... for their friendship and supports.

Finally, my parents and my brother have provided me with their supports throughout, as always, for which my mere expression of gratitude does not suffice. Thanks to my wife, Ting, for her love, understanding and great patience during the past 3 years, even if that meant sacrificing the time we spent together. Thanks to my son, Pengpeng, for all the joy and happiness he brings to me.



# Contents

<b>List of Figures</b>	<b>xiii</b>
<b>List of Tables</b>	<b>xvii</b>
<b>Acronyms</b>	<b>xix</b>
<b>General Introduction</b>	<b>1</b>
<b>Chapter 1 Automated Highway System &amp; Intelligent Vehicle Control</b>	<b>7</b>
1.1 Background . . . . .	7
1.2 ITS & Automated Highway System . . . . .	9
1.2.1 What's ITS? . . . . .	9
1.2.2 What does Automated Highway System stand for? . . . . .	10
1.2.3 Intelligent vehicle . . . . .	12
1.3 Previous research . . . . .	14
1.3.1 Research projects . . . . .	14
1.3.1.1 Projects in U.S. . . . .	14
1.3.1.2 Projects in Asia . . . . .	15
1.3.1.3 Projects in Europe . . . . .	16
1.3.2 Control architecture for a vehicle platoon in AHS . . . . .	18
1.3.3 Longitudinal control . . . . .	19
1.3.4 Lateral control . . . . .	22
1.3.5 Integrated longitudinal and lateral control . . . . .	24
1.4 Conclusion . . . . .	25
<b>Chapter 2 Modeling of Four Wheeled Vehicles for AHS</b>	<b>27</b>
2.1 Introduction . . . . .	28

2.2	Principle movements of vehicle & decoupling of longitudinal and lateral models . . . . .	29
2.2.1	Principle movements of vehicle . . . . .	29
2.2.2	Decoupling of longitudinal and lateral models . . . . .	30
2.3	Modeling of Longitudinal Vehicle Dynamics . . . . .	31
2.3.1	Longitudinal dynamics . . . . .	31
2.3.1.1	Simple vehicle model . . . . .	31
2.3.1.2	Longitudinal tyre force . . . . .	32
2.3.1.3	Aerodynamic forces . . . . .	33
2.3.1.4	Rolling resistance . . . . .	34
2.3.1.5	Normal tyre force . . . . .	35
2.3.1.6	Effective tyre radius . . . . .	36
2.3.2	Powertrain dynamics . . . . .	38
2.3.2.1	Engine model . . . . .	38
2.3.2.2	Torque converter . . . . .	39
2.3.2.3	Gearbox . . . . .	40
2.3.2.4	Drive shaft, Final drive & Differential . . . . .	44
2.3.2.5	Braking system modeling . . . . .	45
2.3.3	Longitudinal model for simulation . . . . .	46
2.3.3.1	Assumptions . . . . .	46
2.3.3.2	Longitudinal model . . . . .	47
2.3.4	Simulations . . . . .	49
2.4	Modeling of Lateral vehicle dynamics . . . . .	51
2.4.1	Lateral kinematic model . . . . .	51
2.4.2	Lateral dynamic model . . . . .	54
2.4.3	Simulations . . . . .	60
2.4.3.1	Kinematic model simulations . . . . .	60
2.4.3.2	Dynamic model simulations . . . . .	60
2.5	Conclusion . . . . .	61

**Chapter 3 Longitudinal Control for Vehicle Platoons 63**

3.1	Introduction . . . . .	64
3.2	Architecture of longitudinal control system . . . . .	65
3.3	Upper level control . . . . .	66
3.3.1	Introduction . . . . .	66

---

3.3.2	String stability . . . . .	68
3.3.2.1	Definition of string stability . . . . .	68
3.3.2.2	String stability in vehicle following system . . . . .	69
3.3.3	Traffic flow stability . . . . .	71
3.3.3.1	Definition of traffic flow stability . . . . .	72
3.3.3.2	Effect of spacing policy on traffic flow stability . . . . .	73
3.3.4	Evaluation of the Constant Time Gap spacing policy . . . . .	74
3.3.4.1	The Traditional Constant Time-gap (CTG) Spacing Policy . . . . .	75
3.3.4.2	String stability of CTG . . . . .	75
3.3.4.3	Traffic flow stability of CTG . . . . .	78
3.3.5	Proposed Safety Spacing Policy . . . . .	78
3.3.5.1	String stability of SSP . . . . .	80
3.3.5.2	Traffic flow stability of SSP . . . . .	83
3.3.5.3	Traffic flow capacity comparison between SSP & CTG . . . . .	84
3.3.6	Simulation tests . . . . .	86
3.4	Lower level control . . . . .	89
3.4.1	Introduction . . . . .	89
3.4.2	Coordinated Throttle and Brake Fuzzy Controller . . . . .	90
3.4.2.1	Coordinated Throttle and Brake Fuzzy Control System Architecture . . . . .	90
3.4.2.2	Throttle and Brake Fuzzy Controllers . . . . .	91
3.4.2.3	Switch Logic Between Throttle and Brake . . . . .	94
3.4.3	Simulation tests . . . . .	96
3.4.3.1	Longitudinal vehicle model for simulation . . . . .	97
3.4.3.2	Horizontal road condition . . . . .	97
3.4.3.3	Inclined road condition . . . . .	100
3.5	Conclusion . . . . .	101
<b>Chapter 4 Vehicle Lateral Control</b>		<b>105</b>
4.1	Introduction . . . . .	106
4.2	Methodology-Multiple model approaches . . . . .	109
4.2.1	Introduction . . . . .	109
4.2.2	The operating regime approach& multiple model/controller approach	110
4.2.2.1	Framework of operating regime approach . . . . .	110

4.2.2.2	Dilemma between local and global . . . . .	111
4.2.2.3	Combination of local models and controllers . . . . .	111
4.2.2.4	Conclusion of multiple model approach . . . . .	115
4.3	Architecture of lateral control system . . . . .	115
4.4	Analysis of vehicle lateral dynamics . . . . .	117
4.4.1	Bicycle Model . . . . .	117
4.4.2	Open-Loop Response to the Parameter Variations . . . . .	117
4.5	Lateral controller design . . . . .	119
4.5.1	PID with anti-windup . . . . .	120
4.5.1.1	Traditional PID controller . . . . .	120
4.5.1.2	PID with Anti-Windup . . . . .	122
4.5.2	Fuzzy control for vehicle steering . . . . .	124
4.5.2.1	Vehicle lateral model . . . . .	126
4.5.2.2	Input and output variables . . . . .	126
4.5.2.3	Fuzzy control rules . . . . .	126
4.5.2.4	Simulation tests . . . . .	126
4.5.3	Multi-model fuzzy control . . . . .	128
4.5.3.1	Decomposition of the operating regime . . . . .	129
4.5.3.2	Multi-model fuzzy controller design . . . . .	130
4.5.4	Virtual desired trajectory for lane change maneuver . . . . .	133
4.6	Simulation tests . . . . .	134
4.6.1	Test 1: Lane keeping control at different speeds (1) . . . . .	135
4.6.2	Test 2: Lane keeping control at different speeds (2) . . . . .	135
4.6.3	Test 3: Lane keeping control under different loads and Cornering Stiffness . . . . .	137
4.6.4	Test 4: Lane changing scenarios at different speeds . . . . .	137
4.6.5	Test 5: Lane changing scenarios under different loads and Cornering Stiffness . . . . .	140
4.7	Conclusion . . . . .	141

**Chapter 5 Global Control System Design-Integration of Longitudinal and Lateral Controllers** **143**

5.1	Introduction . . . . .	143
5.2	System integration . . . . .	144
5.2.1	Uncoupled longitudinal and lateral control system . . . . .	144

---

5.2.2	Integrated longitudinal and lateral control system . . . . .	144
5.3	Simulation experiments . . . . .	146
5.4	Conclusion . . . . .	147
<b>Chapter 6 Observation of Vehicle States and Multi-Sensor Intelligent Vehicle Prototype</b>		<b>151</b>
6.1	Introduction . . . . .	152
6.2	Observation of vehicle states . . . . .	152
6.2.1	Introduction . . . . .	152
6.2.2	Kalman-Bucy Filter for LTV system . . . . .	154
6.2.3	Yaw rate and lateral velocity estimation using Kalman-Bucy filter .	155
6.2.4	Estimation results . . . . .	158
6.3	Presentation of reduced scale multi-sensor intelligent vehicle prototype . .	159
6.3.1	Technologies . . . . .	159
6.3.1.1	Multi-sensor system . . . . .	159
6.3.1.2	The microcontroller . . . . .	163
6.3.1.3	Wireless communication . . . . .	163
6.3.2	Integration . . . . .	164
6.3.3	Control strategies and first tests . . . . .	164
6.4	Conclusion . . . . .	164
<b>Conclusions and Perspective</b>		<b>167</b>
<b>Résumé étendu en français</b>		<b>171</b>
<b>Bibliography</b>		<b>177</b>



# List of Figures

1.1	World motor vehicle production . . . . .	8
1.2	Intelligent Transportation System (ITS) illustration . . . . .	10
1.3	Vehicle platoon in the NAHSC demonstration . . . . .	15
1.4	ITS development chronology in the world . . . . .	18
1.5	Hierarchical architecture for automated driving . . . . .	19
1.6	Two-level structure for longitudinal control . . . . .	20
2.1	Six degrees of freedom vehicle model . . . . .	29
2.2	Friction ellipse represents the interdependence of longitudinal and lateral forces for several constant value of the slip angle . . . . .	31
2.3	Vehicle on a inclined road . . . . .	32
2.4	Longitudinal tyre force as a function of slip ratio . . . . .	34
2.5	Pressure distribution at a non-rotation and rotation tyre . . . . .	35
2.6	Calculation of tyre effective radius . . . . .	37
2.7	Vehicle powertrain system . . . . .	39
2.8	Example of engine map . . . . .	40
2.9	Block diagram of torque converter subsystem . . . . .	41
2.10	Gear shift schedule . . . . .	41
2.11	Model of automatic gear shift control . . . . .	42
2.12	Stateflow diagram of the gear shift logic . . . . .	43
2.13	Typical braking system . . . . .	45
2.14	The different forces acting on the body and wheels . . . . .	48
2.15	Vehicle longitudinal system diagram . . . . .	50
2.16	Throttle and brake input for simulation . . . . .	51
2.17	Simulation of longitudinal model . . . . .	52
2.18	Kinematic bicycle model . . . . .	53
2.19	Bicycle model for vehicle lateral dynamics . . . . .	55
2.20	The vehicle lateral system . . . . .	58
2.21	Kinematic model results with different steering angles $\delta$ . . . . .	60
2.22	Dynamic model results with different speeds . . . . .	61
3.1	Two-level structure for longitudinal control . . . . .	66
3.2	Vehicle platoon . . . . .	66
3.3	Fundamental diagram . . . . .	71
3.4	Main lane and inlet ramp . . . . .	73

3.5	Vehicle platoon . . . . .	75
3.6	Impulse response of the CTG system . . . . .	77
3.7	Inter-vehicle spacing with different safety coefficients $\gamma$ . . . . .	80
3.8	Impulse responses at different velocities of the SSP system . . . . .	83
3.9	$Q - \rho$ curves of the CTG and SSP . . . . .	84
3.10	Single lane highway . . . . .	85
3.11	$Q - v$ curves of CTG and SSP . . . . .	86
3.12	Results of longitudinal control . . . . .	88
3.13	Coordinated throttle and brake control system diagram . . . . .	90
3.14	Variables of fuzzy throttle controller . . . . .	93
3.15	Block diagram of logic switch . . . . .	94
3.16	Switching regions and conditions . . . . .	95
3.17	Flowchart of switch logic . . . . .	96
3.18	Longitudinal car model . . . . .	97
3.19	Leading vehicle's speed and acceleration . . . . .	98
3.20	Following vehicle's speed and speed error . . . . .	99
3.21	Inter-vehicle spacing and spacing error . . . . .	99
3.22	Control results of throttle and brake (horizontal road) . . . . .	100
3.23	Road grade, speed error and spacing error (inclined road) . . . . .	102
3.24	Control results of throttle and brake (inclined road) . . . . .	103
4.1	Road fatalities in U.S.A. . . . .	106
4.2	Multiple model/controller approach . . . . .	110
4.3	Decomposition of a complex system . . . . .	111
4.4	Hierarchical decomposition of a complex system . . . . .	112
4.5	Approximation methods for local models . . . . .	112
4.6	Hard partitions example . . . . .	113
4.7	Fuzzy membership functions of <i>LOW</i> and <i>HIGH</i> . . . . .	114
4.8	Hierarchical architecture for vehicle lateral control . . . . .	116
4.9	Open-loop responses to parameter variations . . . . .	119
4.10	Block diagram of PID controller . . . . .	120
4.11	P control system . . . . .	121
4.12	Step response of PID controller after the first tuning . . . . .	122
4.13	Step response of PID controller after the fine-tuning . . . . .	122
4.14	PID controller with saturation constraint . . . . .	123
4.15	PID controller with Anti-Windup . . . . .	124
4.16	PID with anti-windup control system: step responses at different speed . . . . .	124
4.17	Simple bike model . . . . .	125
4.18	Membership functions . . . . .	127
4.19	Traditional fuzzy controller: step responses at different speeds . . . . .	128
4.20	Decomposition of operating regimes . . . . .	131
4.21	Lateral controller: Multi-model fuzzy controller block diagram . . . . .	131
4.22	Variables in multi-model fuzzy controller . . . . .	132
4.23	Trapezoidal acceleration profile . . . . .	133
4.24	Multi-model fuzzy controller: step responses at different speeds . . . . .	135

---

4.25	Desired trajectory (1)	136
4.26	Lane keeping control results at different speeds (1)	136
4.27	Desired trajectory (2)	138
4.28	Lane keeping control results at different speeds (2)	138
4.29	Lane keeping control results under different loads	139
4.30	Virtual Desired Trajectory	140
4.31	Lane changing control results at different speeds	140
4.32	Lane changing control results under different loads	141
5.1	Uncoupled longitudinal and lateral control system	144
5.2	Integrated control system	145
5.3	Speed and road profiles	147
5.4	Longitudinal control results	149
5.5	Lateral control results	150
6.1	Bicycle model for vehicle lateral dynamics	156
6.2	Steering angle input and vehicle longitudinal velocity	160
6.3	Measured and estimated lateral acceleration	160
6.4	Estimation results	160
6.5	Two-car platoon	161
6.6	Multi-sensor system	162
6.7	Magnetic field	162
6.8	Platoon communication system	163
6.9	Vehicle structure	164

*List of Figures*

---

# List of Tables

1.1	Potential benefits of AHS . . . . .	11
1.1	Potential benefits of AHS . . . . .	12
3.1	Parameters for longitudinal controller . . . . .	80
3.2	Platoon vehicles' braking capacities ( $m/s^2$ ) . . . . .	87
3.3	Fuzzy Rule Base . . . . .	92
4.1	Nomenclature of Bicycle Model . . . . .	118
4.2	Ziegler-Nichols tuning rule based on critical gain $K_{cr}$ and critical period $P_{cr}$ (Second Method) . . . . .	121
4.3	Fuzzy Rule Base . . . . .	128
4.4	Membership Function Variables . . . . .	133
4.5	Fuzzy Rule Base . . . . .	133
4.6	Parameter Variations . . . . .	139
5.1	Parameters for longitudinal controller . . . . .	146
6.1	Nomenclature of Bicycle Model . . . . .	157



# Acronyms

**ACC** - Adaptive Cruise Control

**AHS** - Automated Highway System

**CTG** - Constant Time-Gap spacing policy

**LTI** - Linear Time Invariant

**LTV** - Linear Time Variant

**SSP** - Safety Spacing Policy

**VDT** - Virtual Desired Trajectory



# General Introduction

The research presented in this thesis addresses the longitudinal and lateral control strategies for intelligent vehicles in highway, with the main aims of alleviating traffic congestion and improving traffic safety. The background of this research is the significant development of automobile industry in the past decades, which makes the automobiles play an important role in the evolution of industry and even of our society. However, the traffic problems such as traffic congestion, safety, pollution and fuel consumption are becoming more and more serious all over the world. To cope with these problems and to achieve the goal of “Sustainable Mobility”, the conception of AHS (Automated Highway System) has been proposed, in which, vehicles can travel together in tightly spaced platoons. In the past two decades, researches on AHS have seen significant progresses. As one of the most active research topics in AHS, the longitudinal and lateral control for automated vehicles is currently being studied by researchers and automotive manufactures.

- **Longitudinal control**

Vehicle longitudinal control system provides assistance to the driver in the task of longitudinal control by using automatic throttle and brake controllers. The first generation of longitudinal control systems like ACC system (Adaptive Cruise Control system) are primarily being developed for improving driving comfort with some potential in increasing vehicle safety. However, the impacts of these systems on highway traffic have been inadequately studied [Swaroop 1999]. In this work, the longitudinal controller design is considered for the operations of vehicle platoon. Thus, we need to consider not only the requirements of driving comfort and vehicle safety but also the challenges of string stability, traffic flow capacity and stability, etc. To meet these challenges, the structure of the longitudinal control system is generally designed to be hierarchical, with an upper level controller and a lower level controller. The upper level controller determines the desired acceleration or speed for the controlled vehicle, while the lower level controller decides the required throttle and brake commands to track the desired acceleration or speed.

The principle design tasks in the upper level control include the design of spacing policy and its associated control algorithm. The spacing policy plays an important role in vehicle longitudinal control because it has great influences on vehicle safety and traffic capacity. In this work, a safety spacing policy (SSP) is proposed, which is a nonlinear function of vehicle velocity. It uses both the information of vehicle's state and braking capacity to adjust the position and velocity of the controlled vehicle. Furthermore, the special efforts are devoted to the analysis of the string stability, traffic flow capacity and stability of the proposed SSP. A comparison between the SSP and the traditional CTG (constant time gap) policy is also presented.

The nonlinearities and uncertainties in vehicle longitudinal dynamics are the main challenges to be met in the design of throttle and brake controllers (lower level control). For instance, the exact engine model and brake system dynamics are always complex nonlinear models with numerous parameters. And in most cases, these models are hard to get. Another difficulty is that the throttle and brake pedals should work coordinately. To cope with these problems, a coordinated throttle and brake fuzzy control system is proposed. At first, an additive fuzzy controller is proposed to realize the throttle and brake control. The main advantage of this approach is that it can realize the accurate and smooth vehicle speed control without the knowledge of the exact engine and brake system dynamic models. Second, a logic switch is designed to coordinate the two speed actuators.

- **Lateral control**

As far as lateral control is concerned, the lateral control system generates steering commands to keep the vehicle running along the desired path or steer the vehicle into an adjacent lane. The design requirement of vehicle lateral control is to ensure small lateral errors and small relative yaw angles while maintaining ride comfort under different conditions. Lane keeping and lane changing are the two basic functions of lateral control system.

At first, lane keeping control is studied. The vehicle lateral dynamics is presented by the well-known "bicycle model". Since in highway operation, the vehicle parameters such as speed, load, movement inertia, wheel cornering stiffness, may vary in a wide range. The lateral model is thus a LTV (Linear Time Variant) model with parameter uncertainties. A multi-model fuzzy controller is proposed for the lane keeping operation. The proposed solution combines the strong points of multi-model and fuzzy approaches. It can provide stable performances during the whole

---

range of operation speed, and it can also repel the system uncertainties in vehicle load, movement inertia, wheel cornering stiffness, etc.

Second, the main difficulty in the lane changing maneuver is that the vehicle must travel a certain distance without sensor feedback if the onboard sensors can not measure vehicle's location between the adjacent two lanes, for instance, if the magnet-magnetometer sensing system is employed. The virtual desired trajectory (VDT) is then introduced for the lane changing maneuver. By using VDT, the lane changing operation is then investigated as a lane keeping problem. In order to effectuate flexible switch between different lateral operations, such as lane keeping, lane changing, overtaking, and etc, a hierarchical architecture is then proposed for vehicle lateral control system.

Based on the given results in both longitudinal and lateral control, we propose a global control system, which integrates the designed longitudinal and lateral control systems, to realize the final goal of automated vehicle control.

In addition, the vehicle state estimation is also studied as a step towards the application of the proposed vehicle controllers. Since in the controller design process, the required vehicle states are always assumed to be available. However, in practice, this assumption is not always correct. Then the vehicle state observer is required. Considering the sensor system configuration and the required states for the vehicle controllers, we choose the vehicle yaw rate as the parameter to be estimated. Since the control plant is a LTV system, the traditional Luenberger observer is not available in this case. A Kalman-Bucy filter is then designed for the LTV system estimation.

Finally, a reduced scale (1:10) multi-sensor intelligent vehicle prototype is introduced. The different aspects of the prototype from the multi-sensor system, vehicle structure, communication system, and HMI are presented. This prototype provides a platform for advanced technology integration, reliability analysis, real time control and monitoring. In the first-step tests with the prototype, the basic functions such as vehicle following and lane tracking were realized. In the future work, the more complex scenarios will be tested.

## Outline of the thesis

**Chapter 1** reviews the developments in automated vehicle control. At first, the background of the current traffic situation and problems are introduced. Second, ITS, AHS, and intelligent vehicle, which are considered as the most promising solutions (at different

levels) to the traffic problems, are introduced. Finally, the evaluations of the outstanding projects and the developments in vehicle longitudinal and lateral control have been surveyed in detail.

In **Chapter 2**, the vehicle longitudinal and lateral models are presented, which will be employed in the controller design in the following chapters. For the longitudinal model, at first, we establish the non-linear **longitudinal dynamic model** based on the Newton's second law, with the hypothesis of no-slip at the tyre-road interface. Second, the **powertrain dynamic model** of a passenger car with an automatic gearbox is built, which includes the sub-models of different parts in the powertrain system, the engine, torque converter, automatic gearbox, drive shafts, final drive and differential, as well as the braking system. By using this powertrain model, we can simulate the vehicle behavior thus to test the controllers' performances in the following chapters.

For the lateral model, the **kinematic** and **dynamic** models are studied respectively. The kinematic model provides a mathematic description of the vehicle motion without considering the forces that affect the motion, and it considers only the geometric parameters. A "bicycle" model is adopted to express the vehicle lateral dynamics. Under the assumptions of small steering angle and small slip angle, the bicycle model can be described by a 4<sup>th</sup> order linear model.

**Chapter 3** concentrates on the vehicle longitudinal control system design. The longitudinal control system architecture is designed to be hierarchical, with an upper level controller and a lower level controller. In the **upper level controller** design, a safety spacing policy (SSP) is proposed, which uses both the information of vehicle state and vehicle braking capacity to determine the desired spacing from the preceding vehicle. A comparison between the SSP and the traditional CTG (constant time gap) policy is also presented. In the **lower level controller** design, a coordinated throttle and brake fuzzy controller is proposed. And a logic switch is designed to avoid frequent switching between the two actuators and simultaneous operations of them. Finally, the above proposed longitudinal control system is validated to be effective through a series of simulations.

**Chapter 4** is devoted to the vehicle lateral control. A multi-model fuzzy controller is designed to perform lane keeping and lane changing operations. For the lane changing maneuver, the concept of VDT "Virtual Desired Trajectory" is introduced to provide a smooth and efficient lane changing trajectory. In order to effectuate flexible switch be-

---

tween different lateral operations, a hierarchical architecture is then proposed for vehicle lateral control system.

**Chapter 5** proposes a global control system, which integrates the longitudinal and lateral control systems that we have given in chapter 3 and 4. By using this system, the vehicle longitudinal controller and lateral controller can work coordinately.

**Chapter 6** discusses two aspects relating to the practice, the observation of vehicle states and the design of a reduced scale multi-sensor intelligent vehicle prototype. A Kalman-Bucy filter is introduced to estimate the yaw rate for vehicle later control. And the different aspects of the design of a multi-sensor intelligent vehicle prototype are presented.



# Chapter 1

## Automated Highway System & Intelligent Vehicle Control

### Contents

---

<b>1.1</b>	<b>Background . . . . .</b>	<b>7</b>
<b>1.2</b>	<b>ITS &amp; Automated Highway System . . . . .</b>	<b>9</b>
1.2.1	What's ITS? . . . . .	9
1.2.2	What does Automated Highway System stand for? . . . . .	10
1.2.3	Intelligent vehicle . . . . .	12
<b>1.3</b>	<b>Previous research . . . . .</b>	<b>14</b>
1.3.1	Research projects . . . . .	14
1.3.2	Control architecture for a vehicle platoon in AHS . . . . .	18
1.3.3	Longitudinal control . . . . .	19
1.3.4	Lateral control . . . . .	22
1.3.5	Integrated longitudinal and lateral control . . . . .	24
<b>1.4</b>	<b>Conclusion . . . . .</b>	<b>25</b>

---

## 1.1 Background

With the development of the automobile industry, the world vehicle production rose significantly during the past decades. Ten million vehicles were produced worldwide in 1950,

and this number rose to 30 million in 1970. By 2008, more than 70 million vehicles were produced, see Fig. 1.1 [Freyssenet 2009, OCIA ].

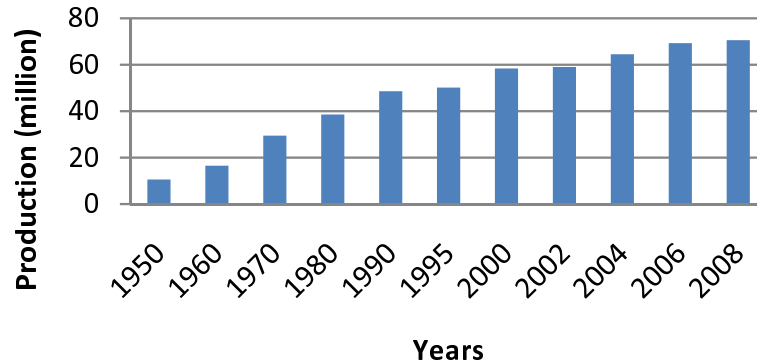


Figure 1.1: World motor vehicle production

Accompanying with this augmentation, on one hand, we benefit the vehicles in different aspects. Take Europe for instance, road transport is the largest share of intra-EU transport, which accounts for 44% of freight and around 85% of passenger transport. In addition, the annually growth rate in the above two fields are 2.8% and 1.9% respectively [COMMUNITIES 2006a]. on the other hand, we have to face the spreading traffic problems as traffic congestion, safety, pollution and fuel resources, etc.

Traffic congestion has been regarded as one of the most serious social and economical and environmental problems in the world. Take the Europe Union (EU) as an example, congestion costs amount to € 50 billion per year or 0.5% of Community GDP, and by 2010 this figure could go up to 1% of EU GDP [COMMUNITIES 2006b].

Concerning energy consumption and emissions, in 2002 the transport sector consumed 338 million tonnes oil equivalent (MToe) representing 31% of the total energy consumption in the EU. Road transport consumed 281 MToe, 83% of the energy consumed by the whole transport sector. Road transport CO<sub>2</sub> emissions account for 835 million tonnes per year representing 85% of the total transport emissions [COMMUNITIES 2006b].

Traffic safety is one of the most serious problems that impacts our daily life. According to a WHO <sup>1</sup> forecast, by 2020 traffic accidents will rank as the third biggest cause of deaths and disability ahead of such other problems as malaria, HIV/AIDS, and war <sup>2</sup>. In 2004, the “Road Safety” has been selected as the theme of the year of WHO.

In the White paper of 2001, the European Commission has set the ambitious aim of halving the number of road traffic fatalities by 2010 (from 50 000 to 25 000). Much

---

<sup>1</sup>WHO: World Health Organization.

<sup>2</sup>The first and second causes are Ischemic heart disease and Unipolar major depression. Source:“ The Gloval Burden of Disease,” by the WHO, 1996.

progress has been achieved, road fatalities in the EU-25 in 2005 were 41 247, which have been reduced by 18,1% compared with 2001. If the trend continues at the same rate, 32 500 people will die from road accidents in 2010, the EC's goal of 25 000 deaths in 2010 will thus not be achieved. The cost of traffic accidents is around € 200 billion every year, account 2% of EU GDP [Hoeglinger 2008].

One suggestion to the traffic problems is to build adequate highways and streets. However, the fact that it is becoming increasingly difficult to build additional highway, for both financial and environmental reasons. Data shows that the traffic volume capacity added every year by construction lags the annual increase in traffic volume demanded, thus making traffic congestion increasingly worse. Therefore, the solution to the problem must lie in other approaches, one of which is to optimize the use of highway and fuel resources, provide safe and comfortable transportation, while have minimal impact on the environment. It is a great challenge to develop vehicles that can satisfy these diverse and often conflicting requirements. To meet this challenge, the new approach of "Intelligent Transportation System" (ITS) has shown its potential of increasing the safety, reducing the congestion, and improving the driving conditions. Early studies show that it is possible to cut accidents by 18%, gas emissions by 15%, and fuel consumption by 12% by employing ITS approach [Unsal 1998].

## 1.2 ITS & Automated Highway System

### 1.2.1 What's ITS?

The origin of Intelligent Transportation System (ITS) was shown in "Futurama", which is a concept transportation system exhibited at the World's Fair 1940 in New York. After a long story via many researches and projects between 1980 to 1990 in Europe, North America and Japan, today's mainstream of ITS was formed. ITS is a transport system which is comprised of an advanced information and telecommunications network for users, roads and vehicles. By sharing vital information, ITS allows people to get more from transport networks, in greater safety, efficiency, and with less impact to the environment. The principle of ITS is illustrated in Fig. 1.2. (Source: [Japanese Ministry of Land a])

ITS is actually a big system which concerns a broad range of technologies and diverse activities. According to the Action plan for the deployment of Intelligent Transport System in Europe [COMMUNITIES 2008], the six priority areas for action and related measures in the short-to-medium term are:

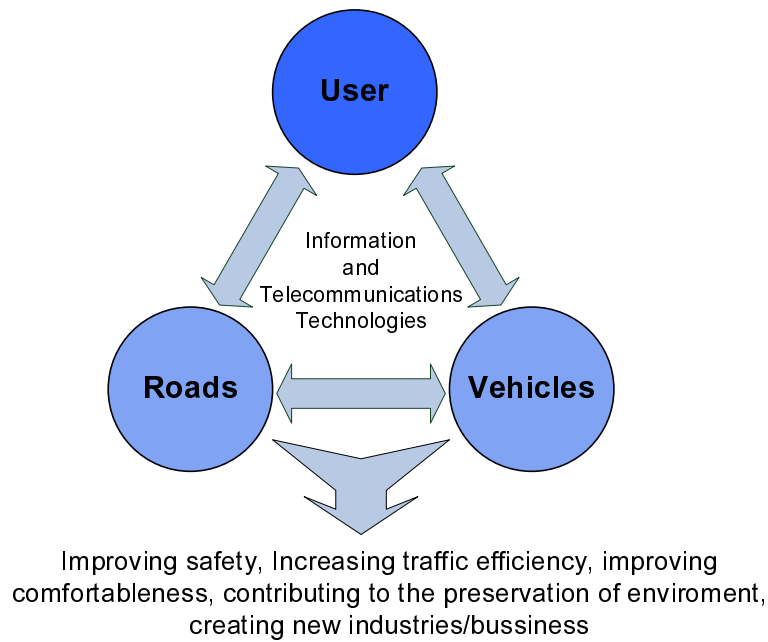


Figure 1.2: Intelligent Transportation System (ITS) illustration

- Optimal use of road, traffic and travel data
- Continuity of traffic and freight management ITS services on European transport corridors and in conurbations
- Road safety and security
- Integration of the vehicle into the transport infrastructure
- Data security and protection, and liability issues
- European ITS cooperation and coordination

### 1.2.2 What does Automated Highway System stand for?

The Automated Highway System (AHS) is one of the most important items among the diverse topics in the research of ITS. The AHS concept defines a new relationship between vehicles and the highway infrastructure. The fully automated highway systems assume the existence of dedicated highway lanes, where all the vehicles are fully automated, with the steering, brakes and throttle being controlled by a computer [Tomizuka 1993]. AHS uses communication, sensor and obstacle-detection technologies to recognize and react to external infrastructure conditions. The vehicles and highway cooperate to coordinate

vehicle movement, avoid obstacles and improve traffic flow, improving safety and reducing congestion. In brief, the AHS concept combines on-board vehicle intelligence with a range of intelligent technologies installed onto existing highway infrastructure and communication technologies that connect vehicles to highway infrastructure [Cheon 2002].

The potential benefits that might acquire from the implementation of AHS could be summarized in Table 1.1. Note that some of the benefits are fairly speculative, the system they would depend upon are not yet in practical application.

Table 1.1: Potential benefits of AHS

<b>Elements</b>	<b>Benefits</b>
Road capacity	In AHS, vehicles travel in closely packed platoons can provide a highway capacity that is three times the capacity of a typical highway [Varaiya 1993].
Safety	Human error is involved in almost 93% of accidents, and in almost three-quarters of the cases, the human mistake is solely to blame [COMMUNITIES 2006b]. Only a very small percentage of accidents are caused by vehicle equipment failure or even due to environmental conditions (for example, slippery roads). Since automated systems reduce driver burden and provide driver assistance, it is expected that the employment of well-designed automated systems will certainly lead to improve traffic safety.
Weather	Weather and environmental conditions will impact little on high performance driving. Fog, haze, blowing dirt, low sun angle, rain, snow, darkness, and other conditions affecting driver visibility and thus, safety and traffic flow will no longer impede progress.
Mobility	All drivers using AHS can be safe, efficient drivers. AHS offers enhanced mobility for the elderly, and less experienced drivers, etc.
Energy consumption and air quality	Fuel consumption and emissions can be reduced. In the short term, these reductions will be accomplished because vehicles travel in a more efficient manner, lesser traffic congestion occurs. In the long term, the AHS can support future vehicle propulsion/fuel designs.
Land use	AHS help us to use the road efficiently, thus using the land in a efficient way.

to be continued...

Table 1.1: Potential benefits of AHS

Elements	Benefits
Travel time saving	AHS can save travel time by reducing congestions in urban highway travel, and permitting higher cruise speed than today's driving.
Commercial and transit efficiency	More efficient commercial operations and transit operations. Commercial trucking can realize better trip reliability and transit operations can be automated, extending the flexibility and convenience of the transit option to increase ridership and service.

### 1.2.3 Intelligent vehicle

Implementation of AHS requires automatically controlled vehicles. Nowadays, automobiles are becoming more and more “intelligent”, with increasingly equipping with electromechanical sub-systems that employ sensors, actuators, communication systems and feedback control. Thanks to the advances in solid state electronics, sensors, computer technology and control systems during the last two decades, the required technologies to create an intelligent transportation system is already available, although still expensive for full implementation. According to Ralph K [Ralph 2008], today's cars normally have 25 to 70 ECUs ( Electronic Control Unit), which perform the monitoring and controlling tasks. Few people realize, in fact, that today's car has four times the computing power of the first Apollo moon rocket [Andrew H 1993].

Intelligent vehicle control is the vital part of the AHS applications. A variable of vehicle control systems are being developed. In our work, we will concentrate in the design of the two most basic control systems: longitudinal control and lateral control. Before introducing the state of art technologies in these two systems, we will briefly introduce some of the major electromechanical feedback control systems related to the longitudinal and lateral control, which are under developed in the automotive industry and the research laboratories.

- **Adaptive Cruise Control (ACC)** systems perform longitudinal control by controlling the throttle and brakes so as to maintain a desired spacing from the preceding vehicle. A significant benefit of using ACC is to avoid rear-end collisions. The SeiSS study reported that it could save up to 4 000 accidents in Europe in 2010 if only 3% of the vehicles were equipped [Abele 2005].

- Lateral support includes **Lane Departure Warning (LDW)** and **Lane Change Assistant (LCA)** systems. The LDW system will warn the driver if his or her vehicle leaves its lane unintentionally, while a LCA will check for obstacles in a vehicle's course when the driver intends to change lanes. The same study estimated that 1 500 accidents could be avoided in 2010 given a penetration rate of only 0.6%, while a penetration rate of 7% in 2020 would lead to 14 000 fewer accidents.
- **Collision Avoidance (CA)** operates like a cruise control system to maintain a constant desired speed in the absence of preceding vehicles. If a preceding vehicle appears, the CA system will judge the operation speed is safe or not, if not, the CA will reduce the throttle and/or apply brake so as to slow the vehicle down, at the same time a warning is provided to the driver.
- **Drive-by-wire** technology replaces the traditional mechanical and hydraulic control systems with electronic control systems using electromechanical actuators and human-machine interfaces such as pedal and steering feel emulators. The benefits of applying electronic technology are improved performance, safety and reliability with reduced manufacturing and operating costs. Some sub-systems using "by-wire" technology have already appeared in the new car models.
- **Vehicle navigation system** typically uses a GPS navigation device to acquire position data to locate the user on a road in the unit's map database. Using the road database, the unit can give directions to other locations along roads also in its database.
- **Automated Vehicle Identification (AVI)** and **Automated Vehicle Location (AVL)** systems: the AVI system was first applied for the Electronic Toll Collection (ETC) system to determine the identity of a vehicle subject to tolls. Most current AVI systems rely on radio-frequency identification, where an antenna at the toll gate communicates with a transponder on the vehicle via Dedicated Short Range Communications (DSRC). While, the AVL automatically determines the geographic location of a vehicle and transmits the information to a requester. Normally, the GPS and a radio communication system are required. As a result of AVI and AVL, processing real-time information on vehicle locations will be possible. A special application of these technologies can be found in vehicle platoon control, will be mentioned in Chapter 3.

## 1.3 Previous research

### 1.3.1 Research projects

#### 1.3.1.1 Projects in U.S.

After the first appearance of the concept of automated driving in the 1940 World's Fair, in the late of 1950s, RCA (Radio Corporation of America) in collaboration with the GM (General Motors) proposed the concept of Automated Highway System. The full AHS concept was initially examined by GM with sponsorship from U.S. department of Transportation (DOT) during the late 1970s.

With the rapid evolution of automobile and the appearance of the problems of congestion around the big cities, the program PATH (Partners for Advanced Transit and Highways), one of the most fruitful organization in transportation researches, was created by the Caltrans (California Department of Transportation) and ITSUC (Institute of Transportation Studies of the University of California) in Berkeley in 1986 [PATH]. The current research projects are mainly in the following three fields:

- Transportation Safety Research
- Traffic Operations Research
- Modal Applications Research

In later 1994, the U.S. Department of Transportation launched the National Automated Highway System Consortium (NAHSC). The consortium attempted to expand the programme's expertise and resources, and contribute to the goal of fully automated highway systems.

In 1997, a demonstration was conducted in San Diego by PATH programme. Eight fully automated cars traveled together in a tightly spaced platoon guided by the magnetic plots fixed on the center of the road, see Fig. 1.3. This demonstration is regarded as the first milestone of the AHS programme, and showed the feasibility of the AHS.

Although the demonstration showed that the progress had been made, the U.S. DOT withdrew financial support from NAHSC and shifted its priorities to short-term, safety oriented technology development. Also in 1997, the project Intelligent Vehicle Initiative (IVI) Programme was carried out, which is a government-industry partnership to accelerate the development and commercialization of safety, and driver assistance systems.



Figure 1.3: Vehicle platoon in the NAHSC demonstration

### 1.3.1.2 Projects in Asia

In the Asia region, road transport problems are becoming increasingly serious in the big cities because of the growth of motorization in many countries. To cope with these problems, several countries and regions begun to install electronic toll collection systems (e.g. Singapore, Malaysia, and Hong Kong). While, works on ITS have been started in other countries as well.

- **Activities in Japan** [Japanese Ministry of Land b]

In 1973, works on CACS (Comprehensive Automobile Traffic Control System) were initiated by the Ministry of International Trade and Industry, with the development of a route guidance system and test operations.

Since the 1980s, a number of projects had been carried out, among them some representative ones are: RACS (Road/Automobile Communication System) was carried out by the Ministry of Construction. ARTS (Advanced Road Transportation Systems), in which the overall concept on advancement of road traffic through integration of roads and vehicles was structured, was pursued. Accompanying this project were various others, including SSVS (Super Smart Vehicle System) intended for the intelligent vehicle traffic system, ASV (Advance Safety Vehicle) intended for promotion of research and development of vehicle safety technologies, and UTMS (Universal Traffic Management System) aimed at development of information system as a part of social infrastructure such as traffic signal and navigation system, and etc.

- **Activities in China** [ITSC ]

Established in 1999, the ITSC (National Intelligent Transport Systems Center of Engineering and Technology) aims at improving traffic safety and efficiency by using the communication and information technologies, and it is supported by the Ministry of Science and Technology. Its current research projects cover a wide field from society science to technology: Electronic toll collection and short range communication, traffic data analysis, safety monitoring and early-warning technology for commercial vehicles, automated snow sweeping vehicle, policy consultation and planning, and etc.

### 1.3.1.3 Projects in Europe

In Europe, a number of projects have been carried out since 1970s. The development of ALI (Autofahrer Leit und Information System) was promoted in the middle of 1970s in Germany. The programme PROMETHEUS ( PROgramM for a European Traffic with Highest Efficiency and Unprecedented Safety) was implemented during 1986 and 1994, leaded by EUREKA (Europe Research Coordination Agency). Its objective was to improve traffic safety and the management of road transport. Contemporaneously, the programme DRIVE (Dedicated Road Infrastructure for Vehicle Safety in Europe) and DRIVE II (1989-1994) studied traffic infrastructure such as road pricing and park and ride for reducing the volume of traffic in city area. These programmes have been succeeded by the current PROMOTE (Programme for Mobility in Transportation in Europe) Programme and the Telematics Applications Programme. In 1991, ERTICO - ITS Europe was founded, which is a multi-sector, public/private partnership pursuing the development and deployment of Intelligent Transport System and Services [ERTICO ]. More recently, the programme ADASE (Advanced Driver Assistance Systems) was promoted to improve road safety, efficiency and comfort. It provided the communication and dissemination platform between experts in the field, authorities and the public.

- **Activities in France**

In France, PREDIT is a programme of research, experimentation and innovation in land transport, started and implemented by the ministries in charge of research, transport, environment and industry, the ADEME (Agence gouvernementale De l'Environnement et de la Maîtrise de l'Énergie) and the ANVAR (Agence National de Valorisation de la Recherche) [PREDIT ]. Since 1990, the PREDIT has past three phases, the first phase PREDIT 1(1990-1994) was mainly devoted to technological innovations in vehicles; PREDIT 2 (1996-2000) covered a wider field includ-

ing the aspects of human and society sciences and transport services organization, etc. PREDIT 3 (2002-2006) aimed at the goods transportation and energy and environment issues, as well as a diversified research on safety. More recently, the project ARCOS (Action de Recherche pour une COnduite Sécurisée) was founded in 2001, which associates different partners (universities, industries) aiming at the improvement of road safety. Now the PREDIT 4 (2008-) is currently implemented, its objective is to improve 20% of energy efficiency in 2020, priority the other transportation methods (no-road), develop the ecological tax, and etc.

Beside the above national research projects, many universities, institutes, and research centers launched also divers projects aiming at solving current traffic problems. Among them, some results can be cited: the urban congestion problems have been studied by the researchers from SeT (laboratoire Systèmes et Transports) in UTBM (université de Technologie de Belfort-Montbéliard), autonomous vehicle control and traffic signal control using vehicle-infrastructure communication were proposed to improve the traffic efficiency in the intersection, by F. Yan, J. Wu, and A. El Moudni, see [Yan 2009, Wu 2009]. The problems of vehicle localization and autonomous navigation in the urban areas were studied by the researchers from UTC (Université de Technologie de Compiègne), the GIS-Based (Geographical Information system) localization and navigation systems, which are adapted to the real-time applications, were proposed in [Bonnifait 2007, Bonnifait 2008]. For the automated vehicles in low speed automation, divers results were given by researchers from INRETS (Institut national de recherche sur les transports et leur sécurité), see [Nouveliere 2003, Mammari 2004]. An interesting solution called “virtual drawbar” was proposed by the AUTORIS (AUTOMatique pour la Route Intelligent et Sûret). A virtual link is supposed to build a two-car platoon [Toulotte 2006]. The issues of bus guidance in station and safe tunnel control were studied in LAGIS, see [El Kamel 2002, El Kamel 2005, El Kamel 2006]. Special efforts to improve common transport (i.e. railway, bus) safety have been made by researchers from ESTAS (Evaluation des Systèmes de Transport Automatisés et de leur Sécurité), see [EL-KOURSI 2006, EL-KOURSI 2007].

A brief chronology of the ITS development in the world is given in Fig. 1.4.

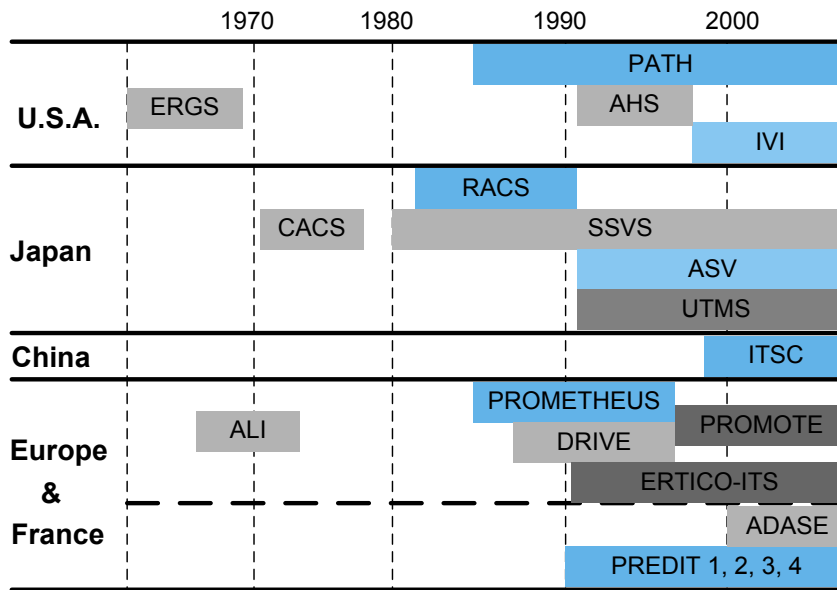


Figure 1.4: ITS development chronology in the world

### 1.3.2 Control architecture for a vehicle platoon in AHS

The intelligent vehicles in an automated cooperative driving network have to execute several maneuvers. All the maneuvers of cooperative driving can be divided into the elementary maneuvers: split, merge, follow and change lane. The control architecture design for the automated vehicles in AHS should aim at more flexible platooning of automated vehicles including smooth merging and lane changing for the compatibility for both the safety and efficiency.

In 1994, the group of PATH has proposed a four-layer control architecture. The proposed four layers are: Link, Coordination, Regulation, and Vehicle dynamics. Among them, the Link layer is on the roadside system and the other three layers are in the vehicle system [Hedrick 1994]. This four-layer constructor can be viewed as the base for the more recently proposed architectures. In 2000, R. Horowitz and P. Varaiya [Horowitz 2000], also researchers from PATH, presented a five-layer architecture, which added a Network layer to the former four-layer constructor. And it can be viewed as a continued work of the former one.

Also in 2000, a group of Japanese researchers proposed an architecture for the AVCSS (Advanced Vehicle Control and safety System), which consists of three layers: vehicle control layer, vehicle management layer, and traffic management layer [Tsugawa 2000]. This architecture has a vehicle centered structure, which will enable well-organized design of the vehicle systems.

More recently, another three-layer control architecture was proposed by Simon Halle, this hierarchical architecture was inspired by Tsugawa's architecture [Tsugawa 2000] and other concepts coming mainly from the PATH project [Lygeros 1998]. The resulting architecture has three major layers: guidance layer, management layer and traffic control layer, as indicated in Fig. 1.5. This architecture gives the more detailed descriptions to the coordination activities of the vehicles platoon, such as inter-platoon coordination and intra-platoon coordination.

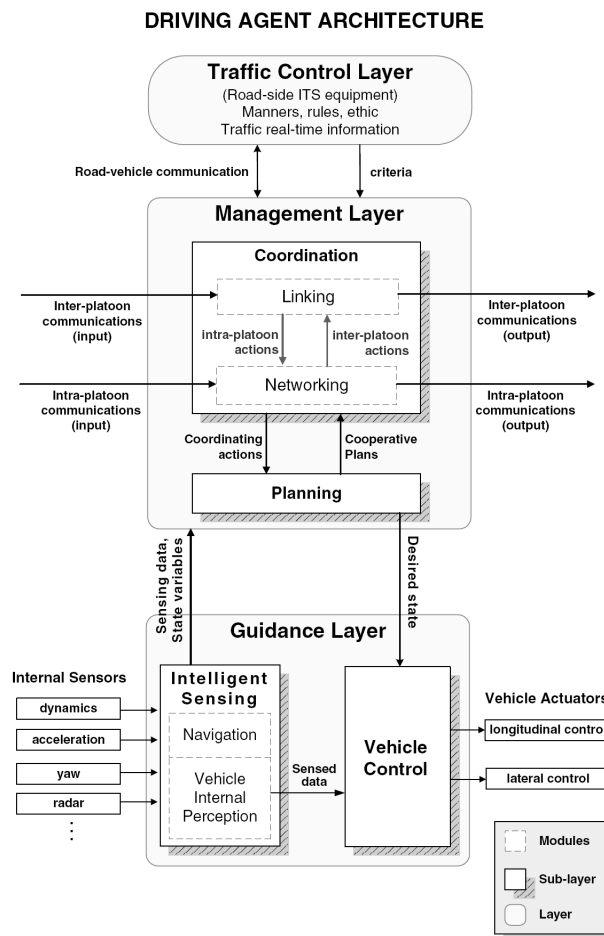


Figure 1.5: Hierarchical architecture for automated driving

### 1.3.3 Longitudinal control

Longitudinal control and lateral control are the two basic functions of the vehicle automation. Vehicle longitudinal control systems are currently being developed by researchers and automotive manufactures for highway vehicle automation [Marsden 2001, Wang 2004a, Zhou 2005]. It provides assistance to the driver in the task of longitudinal control by us-

ing automatic throttle and brake controllers. It can be classified into two categories: “autonomous” and “non-autonomous”. An autonomous system means all the required information for the controlled vehicle could be gathered by on board sensors, whereas inter-vehicle communication or vehicle-road communication are required for a non-autonomous system.

Regarding the longitudinal control system design, it needs to handle several challenges, such as nonlinear vehicle dynamics, spacing policy and its associated control law design, string stability and traffic flow stability, as well as operation at all speed: from high-speed to a complete stop, etc. [Rajamani 2000, Santhanakrishnan 2003]. To meet these challenges, the structure of the longitudinal control subsystem is generally designed to be hierarchical, with upper and lower level controllers, see Fig. 1.6. The upper level controller determines the desired acceleration or speed for the controlled vehicle, while the lower level controller decides the throttle and brake commands required to track the desired acceleration or speed [Rajamani 2006, Zhou 2005]. Therefore, we will introduce the state of the arts technologies in the longitudinal control along the two paths.

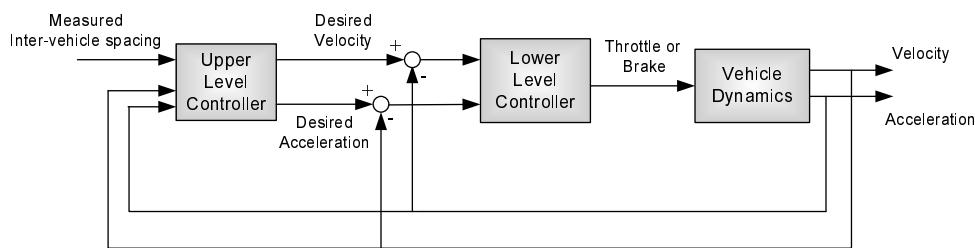


Figure 1.6: Two-level structure for longitudinal control

### *Lower level control*

The nonlinearities and uncertainties in vehicle longitudinal dynamics are the main challenges to be met in the design of throttle and brake controllers. Researches have been pursued for several decades and at many different levels by researchers and automotive manufactures. From 1970s to 1980s, there appeared some researches in the control system design for vehicle engines and brake systems, as shown in [Fisher 1970, Guntur 1972, Guntur 1980, Moskwa 1987, Powell 1987]. Since then, some first generation of engine control systems appeared in [Cho 1989, Grizzle 1994], and some results in the brake system control have obtained great success, such as the ABS (Anti-lock Brake System), which have been widely accepted in the automobile industry.

Based on the above results, and since 1990s, the researches in the longitudinal control combined with throttle and brake control has become steadily more attractive. Ioannou P.A. and Chien C.C. proposed a fixed gain and gain scheduling PID controllers as well as the adaptive control method for vehicle longitudinal control, see [Ioannou 1993]. The controllers were simulated using a validated full order nonlinear longitudinal model and tested also on a real vehicle, and the results are satisfied. However, in order to use these PID based controllers, an exact throttle angle to vehicle speed and position model is required as a premise. To get this model, it needs a lot of experiments to determine the required parameters and in some cases it is confidential. In [Gerdes 1997], Gerdes J.C. and Hedrick J.K. presented a combined engine and brake control system based on multiple-surface. The proposed system consists of three basic elements: an upper sliding controller that incorporates vehicle acceleration as a synthetic input, a logic switch that chooses between throttle or brake control, and lower sliding controllers for the engine and brake operations.

The fuzzy logic is also proposed for this subject. In [Naranjo 2006], Naranjo. J.E. et al. designed a throttle and brake fuzzy control system to perform the ACC+Stop&Go maneuvers. Two separate fuzzy controllers were designed to control the throttle and brake pedals. In order to avoid simultaneous actions of both the pedals, the values of the membership functions of the two controllers were well defined. The constant time gap spacing policy was used to give the desired spacing for the controlled vehicle. This system has been equipped in a two-vehicle platoon. The results showed that the automated vehicle behaved very similarly to human-driven car and was adaptive to the speed variations.

### *Upper level control*

The upper level controller determines the desired acceleration or speed of the controlled vehicle. The principle design tasks in the upper level control include the design of spacing policy and its associated control algorithm. The spacing policy denotes the desired spacing that an automated vehicle attempts to maintain with respect to the preceding vehicle [Santhanakrishnan 2003, Wang 2004a]. In general, the desired spacing policy is a function of the vehicle velocity but could be also a constant distance or a function of other variables such as relative velocity between the controlled vehicle and the proceeding one. It plays an important role in vehicle longitudinal control system as it has great influences on vehicle safety and traffic capacity. Spacing policy and its associated control algorithm can be evaluated from the point of view of string stability, traffic flow stability and traffic flow capacity [Swaroop 1999, Santhanakrishnan 2003].

A variety of spacing policies have been proposed in early works e.g. [Shladover 1991a, Ioannou 1994, Rajamani 2000, Wang 2004a, Zhou 2005]. From the traffic capacity point of view, a constant spacing headway of about 1  $m$  was suggested by Shladover [Shladover 1991a]. With such a tight following model, the traffic capacity increases considerably. However, it was shown that the vehicle controller needed information about the leading vehicle of the platoon to ensure string stability [Rajamani 2000, Rajamani 2006]. Therefore, an inter-vehicle communication protocol is needed to supply the information of the platoon leader to the followers. At present, the most common spacing policy used by researchers and vehicle manufactures is the constant time-gap (CTG) spacing policy [Wang 2004a]. Unlike the constant spacing policy, the tracking requirement in CTG policy can be easily obtained without any inter-vehicular communication. Much works have been done by using CTG spacing policy, and some manufactures have more recently launched their cruise systems based on CTG algorithms [Ioannou 1994, McDonald 1999, Marsden 2001, Nouveliere 2003]. However, there still exists some problems in the use of CTG algorithm:

- Using the CTG policy, the current cruise control system is not suitable for use in high-density traffic conditions, and the operating speed should be higher than 40 km/h [Marsden 2001].
- Using the standard CTG policy, traffic flow stability cannot be ensured [Swaroop 1999].

### 1.3.4 Lateral control

Lane departure is the number one cause of fatal accidents, and account for over 25,000 deaths annually, almost 60% of the total deaths in the highway crashes in the United States. It is also reported that the average crash rate in the curves is about 3 times that for straight segments [A.A.S.H.T.O 2008]. Vehicle lateral control systems provide a possible solution to cope with the steering problems of vehicles. It senses the road centerline using a road based reference system and other on-board sensors. Then, it generates steering commands to keep the vehicle running along the desired path or steer the vehicle into an adjacent lane. The design requirement of vehicle lateral control is to ensure small lateral errors and small relative yaw angles while maintaining ride comfort under different conditions. Lane-keeping and lane-changing are the two basic functions of vehicle lateral control system [Huang 2005].

A lane keeping system automatically controls the steering to keep the vehicle in its lane and also follow the lane as it curves around. In [Fenton 1988], Fenton R.E. and Selim

I designed a velocity-adaptive lateral controller using an optimization approach. The resulting controller, which is nonlinear with velocity, requires full-state feedback and thus an observer is included. In [Choi 2001], the vehicle is steered to follow the reference yaw rates which are generated by the deviations of lateral distance and the yaw angle between the vehicle and the reference lane. A PI controller was designed to minimize the error between the reference yaw rate and the measured one. In [Taylor 1999], three vision-based lateral control strategies: lead-lag control, full state feedback and input-output linearization were introduced and compared through a series of experiments. Although these unique model based approaches can lead to acceptable control results, their performance may be too sensitive to model mismatch and unmodeled dynamics. Besides, some controllers such as sliding mode solutions in [Zhang 2000], H-infinity controller in [Chaib 2004], and the self-turning regulator in [Netto 2004], appear rather complex for realtime embedded control of autonomous vehicles.

The lane changing system automatically steers the vehicle from the current lane to an adjacent lane. In fact, lane changing and lane keeping maneuvers become virtually identical when the lateral sensor can measure its location in both lanes. One major solution is Look-ahead lateral reference/sensing system (e.g. machine vision system). It can provide a long and wide range measurement of vehicle lateral displacement. By using this measurement, the lateral controller mimics human driver's behavior to perform the lane changing maneuver, see [Taylor 1999, Lee 2002]. However, the reliability of machine vision system is susceptible to variations in light or inclement weather conditions. The fact that Look-down lateral reference/sensing system (e.g. magnetic markers installed in the center of highway) improves the reliability of the sensing system can be another solution. But it suffers from the small sensor range. In this case, the lane changing control problem becomes complicated as the lateral sensing system cannot sense both lanes and the vehicle must travel a certain distance without seeing the road reference system.

The virtual desired trajectory (VDT) for a lane change operation is then designed considering passenger's ride comfort and transition time. Four candidate trajectories as (1) circular trajectory (2) cosine trajectory (3) 5th order polynomial trajectory, and (4) trapezoidal acceleration trajectory were evaluated using the transition time as a performance index, the lateral acceleration and jerk as constraints, and vehicle speed as a design parameter. The trapezoidal acceleration trajectory is selected to be the optimal trajectory [Chee 1994, Hedrick 1994]. By using VDT, the lane change maneuver is then investigated as a lane tracking problem. In this way, we consider using a uniform control algorithm to perform the lane tracking tasks for both the lane keeping and the lane

changing, so as to make the lateral control system simpler and more compact.

### 1.3.5 Integrated longitudinal and lateral control

For a totally automated vehicle on automated highway, the combined longitudinal and lateral control should be envisaged. There are two types of combination method: uncoupled and coupled. The uncoupled method neglects the coupling effects between the longitudinal and lateral dynamics, and then the designed longitudinal and lateral controllers are totally independent. Consequently, the global controller can be obtained by simply combining the two separate controllers together. However, in the coupled method, the coupling effects between the two movements are no longer neglected. Therefore, a coupling controller will be considered. Obviously, with the consideration of the coupling effects of the two movements, the controller design task becomes more complex than in the uncoupled case.

Wijesoma and Kodagoda have shown an uncoupled fuzzy control system for a golf car-like AGV (Autonomously Guided Vehicle) [Kodagoda 2002, Wijesoma 1999]. In their work, the coupling effects of vehicle speed on steering angle (and hence angular velocity), and vice versa, was not explicitly accounted for. The speed and steering controllers were independent of each other. The proposed fuzzy control system was tested extensively on an AGV prototype and has been demonstrated to operate satisfactory even in the simultaneous operations of the speed and steering control. But, the variation of speed is only from 3 to 7  $m/s$ , which is enough for a Golf car but not sufficient for the highway vehicles. In [Bom 2005], Bom J. et al. proposed a global control strategy for the urban vehicles. The longitudinal control and lateral control are fully decoupled using nonlinear control theory. However, in their experiments and simulations, the maximum speed is only 5  $m/s$ , which appears reasonable for the urban vehicles but very limited for the highway vehicles.

On the contrary, some coupled solutions were also proposed. Lim and Hedrick considered the coupling effects which exist in the vehicle longitudinal and lateral dynamics, and proposed a sliding mode controller to realize automated vehicle following, see [Lim 1999]. The proposed method was validated through simulation and field test, and it was also compared with a PID controller. In [Mammar 2004] and [Chaibet 2005], sliding mode control and backstepping control methods have been proposed for the automated vehicles in the low speed operations ( $v < 60 km/h$ ). More recently, in [Toulotte 2006], a T-S model based fuzzy control law, which takes into account the coupling between both the

longitudinal and lateral modes, was proposed. The “virtual drawbar” strategy was used in the longitudinal and lateral controller design. Simulation results showed that the longitudinal spacing error was less than 5% of safety distance. However, the orientation error (orientation difference between the follower and leader) was more than 40%. In order to limit this orientation error, a communication system was proposed as a possible solution.

## 1.4 Conclusion

This chapter reviewed the developments in automated vehicle control. At first, the background of the current traffic situation and problems were introduced. Second, we briefly introduced ITS, AHS and intelligent vehicle, which were considered as the most promising solutions to the traffic problems. Finally, the evaluation of the outstanding projects and the developments in vehicle longitudinal and lateral control were surveyed in detail.

The automated vehicle control task can be divided into two parts: longitudinal control and lateral control. The vehicle longitudinal control system is designed to be hierarchical with an upper level controller and a lower level controller. The longitudinal controller design needs to meet diverse challenges and requirements as nonlinearities in vehicle longitudinal dynamics, vehicle safety, string stability, traffic flow stability, traffic capacity, driving comfort, etc. In the lateral control design, the complexity in vehicle lateral dynamics, the selection of vehicle reference (measure) system, different operation scenarios, ride comfort are the main problems need to be envisaged. Finally, the coupling effects between the longitudinal and lateral dynamics should be also a question to be considered.

In the following chapters, we will firstly build up a complete vehicle dynamic model, and then the different control strategies for the automated vehicle will be developed.



## Chapter 2

# Modeling of Four Wheeled Vehicles for AHS

### Contents

---

<b>2.1</b>	<b>Introduction</b>	<b>28</b>
<b>2.2</b>	<b>Principle movements of vehicle &amp; decoupling of longitudinal and lateral models</b>	<b>29</b>
2.2.1	Principle movements of vehicle	29
2.2.2	Decoupling of longitudinal and lateral models	30
<b>2.3</b>	<b>Modeling of Longitudinal Vehicle Dynamics</b>	<b>31</b>
2.3.1	Longitudinal dynamics	31
2.3.2	Powertrain dynamics	38
2.3.3	Longitudinal model for simulation	46
2.3.4	Simulations	49
<b>2.4</b>	<b>Modeling of Lateral vehicle dynamics</b>	<b>51</b>
2.4.1	Lateral kinematic model	51
2.4.2	Lateral dynamic model	54
2.4.3	Simulations	60
<b>2.5</b>	<b>Conclusion</b>	<b>61</b>

---

## 2.1 Introduction

Modeling of the vehicle dynamics is the first step for control system design. It is known that the vehicle system dynamic is normally a complex system where always exists non-linear parts (tyre, clutch...) and parameter variations (mass, tyre-road friction coefficient, ...). Basically, the modeling of vehicle dynamics is essentially dependent on the forces created at the tyre/road interface and the different mechanical parts of the vehicle.

Firstly, considering the tyre force, different approaches have been studied. For example, Pacejka has developed a series of tyre design models, incorporated these models into vehicle models, and presented an applied understanding of how the tyre influences vehicle behavior [Pacejka 2006]. While, Gim and Nikravesh have proposed a series detailed analyses on tyre modeling by using Finite Element Method [Gim 1990, Gim 1991a, Gim 1991b].

Secondly, in order to get the expression of vehicle dynamic, it is necessary to choose a list of mechanical parts need to be considered: tyre, suspension geometry, steering angle, anti-roll bar, etc. The complexity and the accuracy of the expression of vehicle model are depended on the list. Usually, we need to find a compromise between the accuracy and complexity.

The modeling of vehicle dynamic have been pursued at many different levels by researchers and automotive manufactures. Generally, the complexity and accuracy of the vehicle model is always dependent on the final purpose of implementation [Day 1995, Pham 1997, Hingwe 1997, Nouvelière 2002]. One of the most complex model with 28 degrees of freedom was proposed by [Lowndes 1998], which included the detailed models for each element of vehicle: sprung mass, independent suspensions, wheels. In [Addi 2005], a complex model with 18 degrees of freedom was employed, which considered rigid body dynamics, dynamics of tyre suspensions system, as well as tyre dynamics. At present, the 6 degrees of freedom model is widely accepted, which can describe the principal movements of vehicle. The six principal movements of a vehicle are as follows: three translation along  $x$ ,  $y$  and  $z$ -axes and three rotational motions about three axes (roll-pitch-yaw).

According to the early literatures, the vehicles models could be classified into three types [Nouvelière 2002]:

- Longitudinal model of vehicle
- Lateral model of vehicle
- Coupled longitudinal/lateral model of vehicle

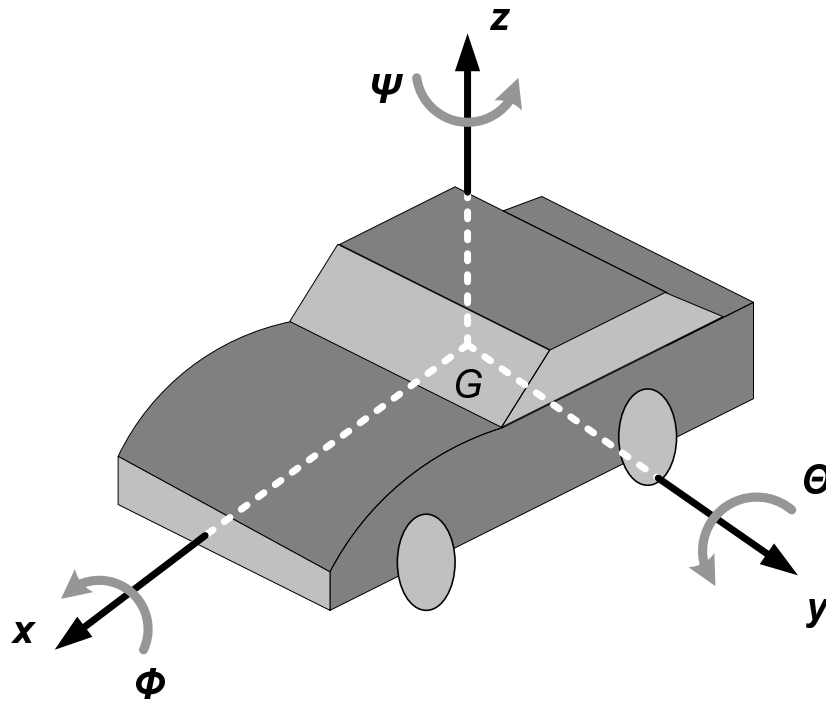


Figure 2.1: Six degrees of freedom vehicle model

In this chapter, we will firstly analyse the principle movement of a road vehicle, and then the vehicle longitudinal model and lateral model will be established. The models that we established will be employed in control systems design in the following chapters.

## 2.2 Principle movements of vehicle & decoupling of longitudinal and lateral models

### 2.2.1 Principle movements of vehicle

The principal vehicle movement can be described as a 6 degrees of freedom system within the vehicle-fixed frame, which includes translations and rotations about the three orthogonal axes:  $X$ - $Y$ - $Z$ , as shown in Fig. 2.1.

- **Translations:**

- Longitudinal movement: translation along the  $\vec{x}$  axis
- Lateral movement: translation along the  $\vec{y}$  axis
- Vertical movement: translation along the  $\vec{z}$  axis

- **Rotation motions:**

- Roll angle  $\phi$ : Rotation about the  $\vec{x}$  axis
- Pitch angle  $\theta$ : Rotation about the  $\vec{y}$  axis
- Yaw angle  $\psi$ : Rotation about the  $\vec{z}$  axis

### 2.2.2 Decoupling of longitudinal and lateral models

The tyre dynamics is one of the essential elements of the vehicle dynamics. Forces and moments from the road act on each tyre of the vehicle and highly influence the dynamics of the vehicle. The modeling of tyre road interface is difficult because there exists numerous important parameters (tyre pressure, dimension, road condition, weather condition,...) and the variations of their values with time.

One of the most famous tyre model is the “Magic Formula” model, which was proposed by Pacejka and Bakker [Pacejka 2006]. This model provides a method to calculate lateral and longitudinal tyre forces and aligning moment for a wide range of operating conditions including large slip angle and slip ratios as well as combined lateral and longitudinal force generation.

In addition, the conception of “friction ellipse” was proposed by Gillespie [Gillespie 1992]. It was shown that the amount of traction available from the tyre patch is necessarily limited, and hence, there must exist some relationship between the lateral and longitudinal forces. This relationship is generally expressed in the idea of a friction ellipse as shown in Fig. 2.2.

Consequently, there exists the coupling phenomenon between the longitudinal and the lateral motions of the tyre. Thus, the longitudinal and lateral movements of the vehicle are coupled.

However, we can decouple the dynamics of the two movements, under the assumption of small varying velocity and steering angle. Thus, the control problem can be simplified into two separate tasks: longitudinal control and lateral control. In fact, the method of decoupling the two systems are accepted in a many researches [Jia 2000, Nouvelière 2002, Shing-Jen Wu 2005, Chiang 2006, Yang 2007], and it has been tested on automated vehicle prototypes as well as in vehicle platoon operations [Lim 1999, Kodagoda 2002].

By using the separate models in stead of the complex coupling model, we can better understand the role of each model in vehicle dynamics and it is easier for us to analyze the different phenomenon in vehicle dynamics. In the following section, we will present

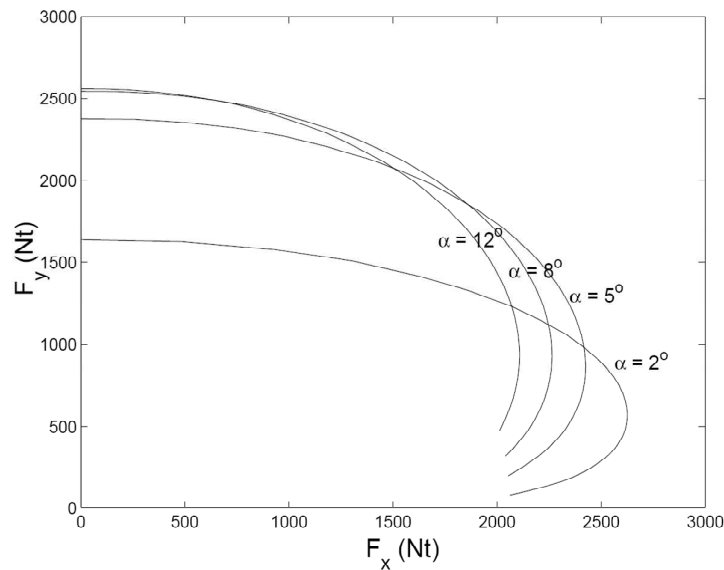


Figure 2.2: Friction ellipse represents the interdependence of longitudinal and lateral forces for several constant value of the slip angle

separately the longitudinal and lateral vehicle models. Each model that we present will be validated through a series of simulation experiments.

## 2.3 Modeling of Longitudinal Vehicle Dynamics

The vehicle longitudinal dynamics includes two major parts: *longitudinal dynamics* and *powertrain dynamics*. The longitudinal dynamics are influenced by longitudinal tyre forces, aerodynamic forces, rolling resistance forces and etc. Modeling of these forces are discussed in section 2.3.1. The powertrain dynamics consists of the dynamics of the subsystems, such as internal combustion engine, torque converter, transmission and wheels. These elements are discussed in section 2.3.2. Finally, the vehicle longitudinal model is set up in section 2.3.3, which sums up the analyses in the two former subsections.

### 2.3.1 Longitudinal dynamics

#### 2.3.1.1 Simple vehicle model

The vehicle is considered as one rigid body moving along an inclined road as shown in Fig. 2.3. At each axle the forces in the wheel contact points are combined in one normal and one longitudinal force. The other external forces acting on the vehicle include aerodynamic drag forces, rolling resistance forces, gravitational forces. These forces will

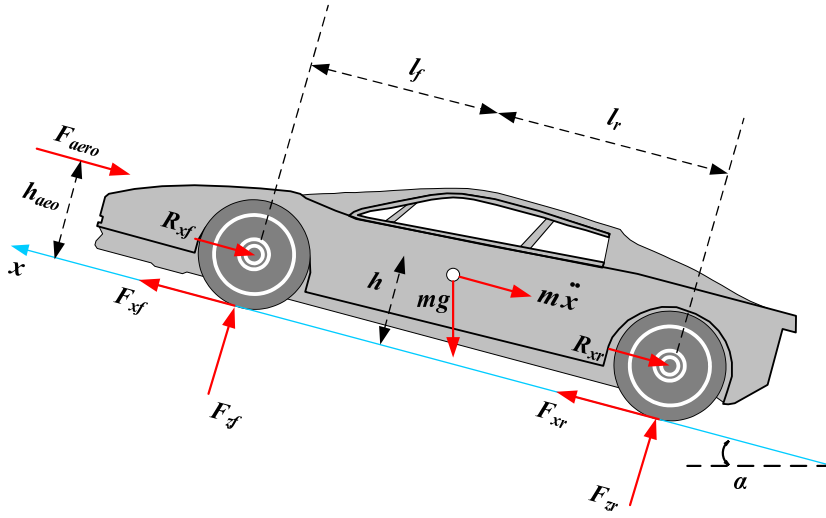


Figure 2.3: Vehicle on a inclined road

be described in the sub-sections that follow.

A force balance along the vehicle longitudinal axis yields:

$$m\ddot{x} = F_{xf} + F_{xr} - F_{aero} - R_{xf} - R_{xr} - mg \sin(\alpha) \quad (2.1)$$

where

- $F_{xf}$  is the longitudinal tyre force at the front tyres
- $F_{xr}$  is the longitudinal tyre force at the rear tyres
- $F_{aero}$  is the equivalent longitudinal aerodynamic drag force
- $R_{xf}$  is the force due to rolling resistance at the front tyres
- $R_{xr}$  is the force due to rolling resistance at the rear tyres
- $m$  is the mass of the vehicle
- $g$  is the gravitational acceleration
- $\alpha$  is the angle of inclination of the road

### 2.3.1.2 Longitudinal tyre force

#### 1. Slip ratio

For calculating the longitudinal tyre force, the conception “slip ratio” is widely used. **Slip ratio** means the difference between the actual longitudinal velocity at the axle of the wheel  $V_x$  and the equivalent rotational velocity  $r_{eff}\omega_w$  of the tyre. The value of slip ratio varies according to the vehicle movement:

For traction ( $r_{eff}\omega_w - V_x \geq 0$ ):

$$s_x = \frac{r_{eff}\omega_w - V_x}{V_x} \quad (2.2)$$

For braking ( $r_{eff}\omega_w - V_x < 0$ ):

$$s_x = \frac{r_{eff}\omega_w - V_x}{r_{eff}\omega_w} \quad (2.3)$$

where,  $s_x$  denotes the slip ratio,  $V_x$  is the actual longitudinal velocity,  $r_{eff}$  represents the effective radius of rotating tyre,  $\omega_w$  means the angular velocity of wheel.

## 2. Expression of longitudinal tyre force

The longitudinal tyre forces  $F_{xf}$  and  $F_{xr}$  are friction forces from the ground that act on the tyres. Assume that the tyre-road interface is dry and the normal force is a constant, the typical variation of longitudinal tyre force as a function of slip ration is shown in Fig. 2.4. From this figure, we can find that in the case where the slip ratio is small (typically in the region of  $(-0.1 \sim 0.1)$ ), as in normally driving, the longitudinal tyre force is proportional to the slip ratio. The tyre longitudinal force in the small slip region can be modeled as:

$$F_{xf} = C_{sf}s_{xf} \quad (2.4)$$

$$F_{xr} = C_{sr}s_{xr} \quad (2.5)$$

where  $C_{sf}$  and  $C_{sr}$  are the longitudinal tyre stiffness of the front and rear tyres respectively.  $s_{xf}$  and  $s_{xr}$  are the slip ratio at the front and rear tyre respectively.

### 2.3.1.3 Aerodynamic forces

Consider a moving vehicle, the shape of vehicle produces aerodynamic forces, the effect of these forces can be represented by a equivalent force applied at the center of gravity, as shown in (2.6)

$$F_{aero} = \frac{1}{2}\rho C_d A_F (V_x + V_{wind})^2 \quad (2.6)$$

where

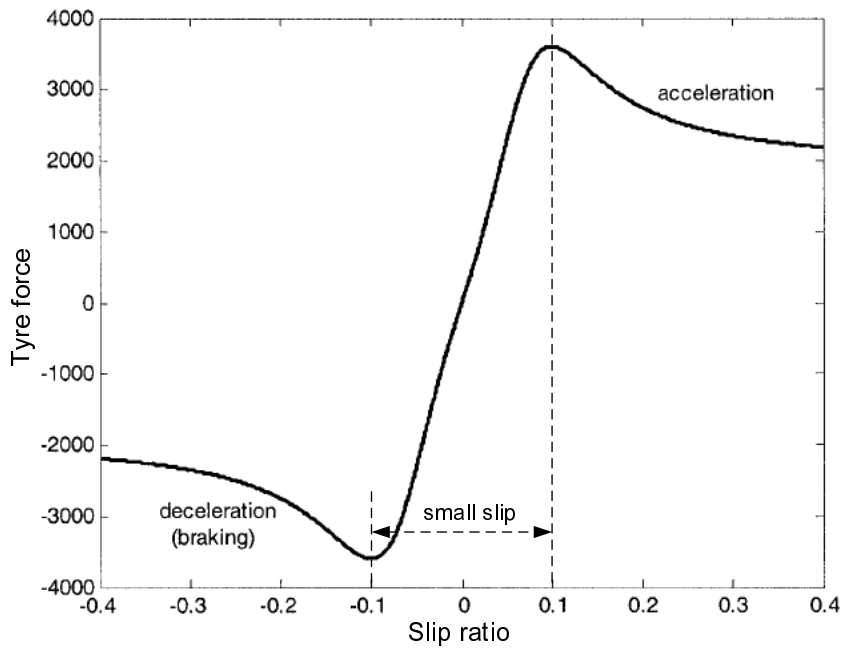


Figure 2.4: Longitudinal tyre force as a function of slip ratio

- $\rho$  is the mass density of air
- $C_d$  is the aerodynamic drag coefficient
- $A_F$  is the frontal area of the vehicle
- $V_x$  is the longitudinal vehicle velocity
- $V_{wind}$  is the wind velocity (positive for a headwind and negative for a tailwind)

#### 2.3.1.4 Rolling resistance

If a non-rotating tyre has contact to a flat ground, the pressure distribution in the contact patch will be symmetric from the front to the rear. The resulting normal force  $F_z$  acts in the center  $c$  of the contact patch and hence, will not generate a torque around the rotating axis of the tyre.

However, in the case of rotating tyre, the distribution of the normal tyre force is non-symmetric, as shown in Fig. 2.5. The normal force generates the rolling resistance torque

$$T_y = F_z \Delta x \quad (2.7)$$

Usually the variable  $\Delta x$  is difficult to be measured, and the rolling resistance is mod-

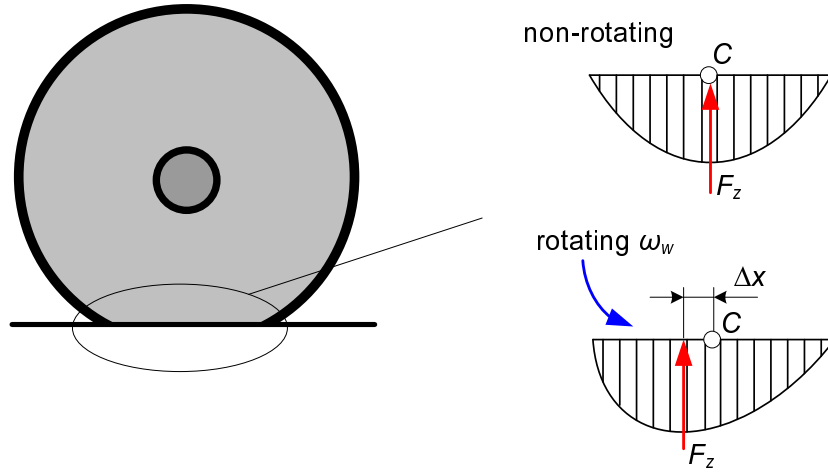


Figure 2.5: Pressure distribution at a non-rotation and rotation tyre

eled as being roughly proportional to the normal force of each tyre i.e.

$$R_x = R_{xf} + R_{xr} = f(F_{zf} + F_{zr}) \quad (2.8)$$

where

- $R_x$  rolling resistance force of vehicle
- $R_{xf}, R_{xr}$  rolling resistance forces acting on front and rear tyres respectively
- $F_{zf}, F_{zr}$  normal forces acting on front and rear tyres respectively
- $f$  rolling resistance coefficient

According to the above analysis, we find, to a rolling tyre, it is the rolling resistance torque but not the rolling resistant force that prevents the rolling movement. In fact the rolling resistance force does not exists in reality. However, in order to facilitating the analysis of longitudinal forces, we use the concept of “rolling resistance force”, which can be obtained directly from the rolling resistance coefficient, in stead of resistance torque.

### 2.3.1.5 Normal tyre force

In order to calculate the normal tyre force on the tyres, we come back to Fig. 2.3, where  $F_{zf}$  and  $F_{zr}$  denote the normal forces acting on the front and rear tyre respectively. Assuming that the net pitch torque acting on the vehicle is zero, which means the pitch angle of the vehicle is in a steady state value. Then, we can get the moments equation about the contact point of the front tyre:

$$F_{zr}(l_f + l_r) - F_{aero}h_{aero} - m\ddot{x}h - mgh \sin(\alpha) - mgl_f \cos(\alpha) = 0 \quad (2.9)$$

Solving for  $F_{zr}$ ,

$$F_{zr} = \frac{F_{aero}h_{aero} + m\ddot{x}h + mgh \sin(\alpha) + mgl_f \cos(\alpha)}{l_f + l_r} \quad (2.10)$$

Similarly, the moments equation about the contact point of the rear tyre is written by:

$$F_{zf}(l_f + l_r) + F_{aero}h_{aero} + m\ddot{x}h + mgh \sin(\alpha) - mgl_r \cos(\alpha) = 0 \quad (2.11)$$

Solving for  $F_{zf}$ ,

$$F_{zf} = \frac{mgl_r \cos(\alpha) - F_{aero}h_{aero} - m\ddot{x}h - mgh \sin(\alpha)}{l_f + l_r} \quad (2.12)$$

Regarding equations (2.10), (2.12), the normal force distribution on the tyres is affected by the acceleration of the vehicle. When the vehicle accelerates, the normal load on the front tyres decreases whereas the normal load on the rear tyres increases.

### 2.3.1.6 Effective tyre radius

As the tyre is a flexible body in contact with the road surface, the effective radius is normally slightly less than the nominal tire radius because the tyre deforms under its vertical load when it is rolling. If the rotational speed of the wheel is  $\omega_w$ , the linear speed of the wheel axle is [Kiencke 2005]

$$V_w = r_{eff}\omega_w \quad (2.13)$$

where,  $r_{eff}$  means the effective radius of rotating tyre.

As shown in Fig.2.6, let  $\Delta\varphi$  be the angle made by the center line of the wheel to the beginning of the contact patch,  $2a$  be the longitudinal length of the contact patch. We get

$$a = r_0 \sin(\Delta\varphi) \quad (2.14)$$

$$\cos(\Delta\varphi) = \frac{r_s}{r_0} \quad (2.15)$$

where,  $r_0$  is the unloaded tyre radius, and  $r_s$  is the loaded or static tyre radius.

Let  $t$  be the time taken by the tyre to move through half of the contact patch. We

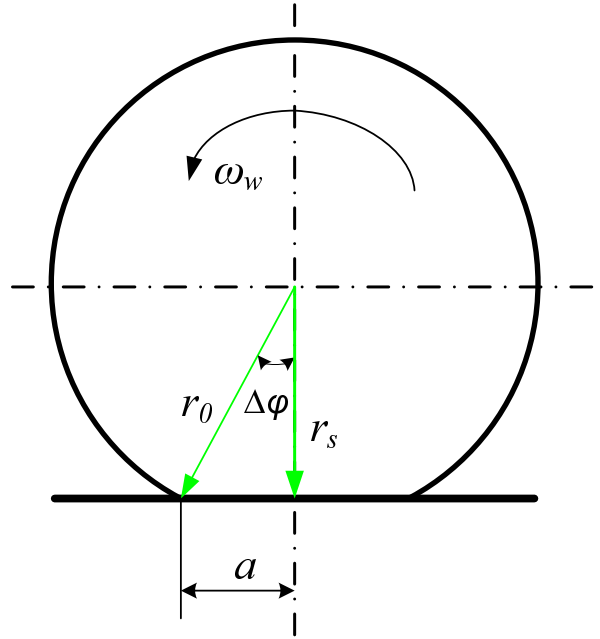


Figure 2.6: Calculation of tyre effective radius

can get [Kiencke 2005],

$$V_w = r_{eff}\omega_w = \frac{a}{t} \quad (2.16)$$

The rotation speed of the wheel is

$$\omega_w = \frac{\Delta\phi}{t} \quad (2.17)$$

Thus

$$r_{eff} = \frac{a}{\Delta\phi} \quad (2.18)$$

Replacing  $a$  from (2.14),

$$r_{eff} = \frac{r_0 \sin(\Delta\phi)}{\Delta\phi} \quad (2.19)$$

For  $\Delta\phi$  is small, the sine-function and cosine-function be approximated by the first terms of its Taylor-Expansion

$$\sin(\Delta\phi) \approx \Delta\phi - \frac{\Delta\phi^3}{6} \quad (2.20)$$

$$\frac{r_s}{r_0} = \cos(\Delta\phi) \approx 1 - \frac{1}{2}\Delta\phi^2 \Rightarrow \Delta\phi^2 \approx 2\left(1 - \frac{r_s}{r_0}\right) \quad (2.21)$$

Then (2.19) can be rewritten as

$$\begin{aligned}
 r_{eff} &= r_0 \frac{\Delta\varphi - \frac{1}{6}\Delta\varphi^3}{\Delta\varphi} \\
 &= r_0 \left(1 - \frac{1}{6}\Delta\varphi^2\right) \\
 &= r_0 \left(1 - \frac{1}{3}\left(1 - \frac{r_s}{r_0}\right)\right) \\
 &= \frac{2}{3}r_0 + \frac{1}{3}r_s
 \end{aligned} \tag{2.22}$$

The static tyre radius is influenced by the vertical load of the tyre,

$$r_s = r_0 - \frac{F_z}{k_z} \tag{2.23}$$

where  $k_z$  is the vertical tyre stiffness.

## 2.3.2 Powertrain dynamics

In the previous discussions, the vehicle longitudinal dynamics are described in equation (2.1), rewrite this equation

$$m\ddot{x} = F_{xf} + F_{xr} - F_{aero} - R_{xf} - R_{xr} - mg \sin(\alpha)$$

where  $F_{xf}$  and  $F_{xr}$  are the longitudinal tyre forces at front and rear tyres respectively, and they are the primary forces that drive the vehicle moving forward. These two forces depend on the *slip ratio* of the driving tyre, which is determined by the difference between the actual longitudinal velocity at the axle of the wheel  $V_x$  and the rotational wheel velocity  $r_e\omega_w$ , as discussed in section 2.3.1.2. The rotational velocity  $\omega_w$  is produced by the powertrain system of the vehicle. A typical powertrain system of a vehicle is shown in Fig. 2.7, which includes the subsystems of engine, torque convert, transmission, drive shafts, final drive, and differentials. In the rest of this subsection, the modeling of these subsystems will be discussed.

### 2.3.2.1 Engine model

The internal combustion engines are commonly equipped on road vehicles. Normally, we consider the engine output is the engine torque, which is a nonlinear function of the air/fuel ratio, the exhaust gas recirculation (ERG), the cylinder total mass charge, the

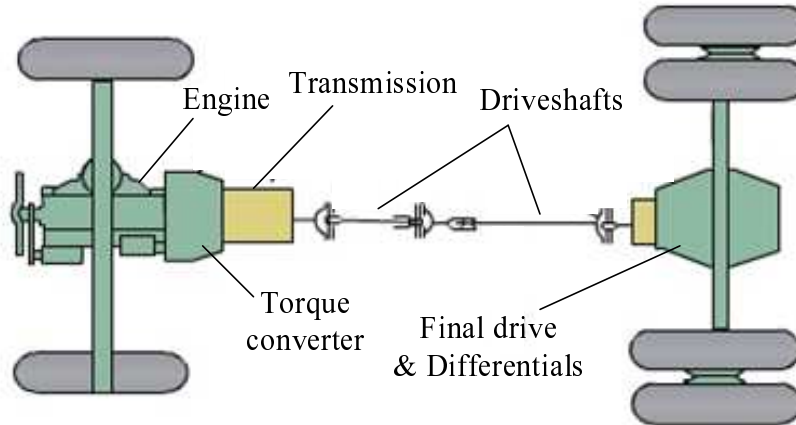


Figure 2.7: Vehicle powertrain system

spark advance, the engine speed and the drivetrain load as well as the throttle angle. Various engine models have been proposed in the early researches [Powell 1987, Cho 1989, Sun 2000]. But these models are so complex, which always contain many parameters need to be defined, that make them inconvenient to be used in the engine controller design.

An often used alternative to the parametric engine model is one in which engine maps from experimental data are used to replace several parametric functions. For example, the torque  $T_e$  of a combustion engine can be characterized as a function of its angular velocity  $\omega_e$  and the gas pedal input  $P_{th}$  ( $P_{th} \in [0, 1]$ ):

$$T_e = Eng(\omega_e, P_{th}) \quad (2.24)$$

In *Matlab Simulink*, the Look-up Table block can be used to describe the nonlinear relationships between  $T_e$ ,  $\omega_e$ ,  $P_{th}$ , an example of engine map is shown in Fig. 2.8.

### 2.3.2.2 Torque converter

The torque converter is a type of fluid coupling that connects the engine to the transmission. It includes three major components: pump, turbine and the stator. Torque converter modeling has been studied by different researches [Kotwicki 1982, Assanis 2000, Cho 1989]. Usually, the torque converter model can be described as a quasi-steady model based on

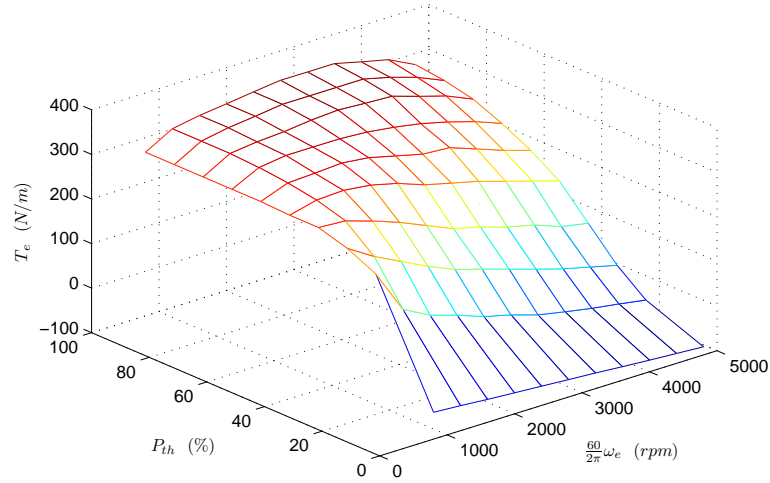


Figure 2.8: Example of engine map

experimental data, it can be written as

$$i_{con} = \frac{n_t}{n_i} \quad (2.25)$$

$$\Psi(i_{con}) = \frac{T_t}{T_i} \quad (2.26)$$

$$T_i = \frac{n_i^2}{K^2} \quad (2.27)$$

where,

- $n_t$  rotation speed of turbine
- $n_i$  rotation speed of pump
- $i_{con}$  speed ratio
- $\Psi$  torque ratio
- $T_t$  turbine torque
- $T_i$  pump torque
- $K$  capacity factor

A torque converter model is shown as a block diagram in Fig. 2.9. Two lookup table blocks are used to convert the speed ration  $i_{con}$  to torque ratio  $\Psi$  and capacity factor  $K$ . The data that we use in the lookup tables can be obtained from the experiments, which are usually provided by the suppliers.

### 2.3.2.3 Gearbox

#### 1. Gear transmission basic

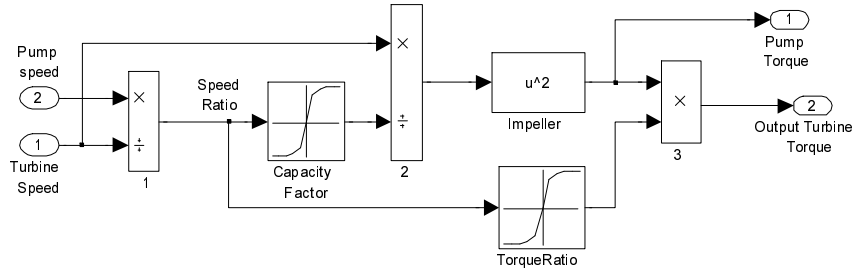


Figure 2.9: Block diagram of torque converter subsystem

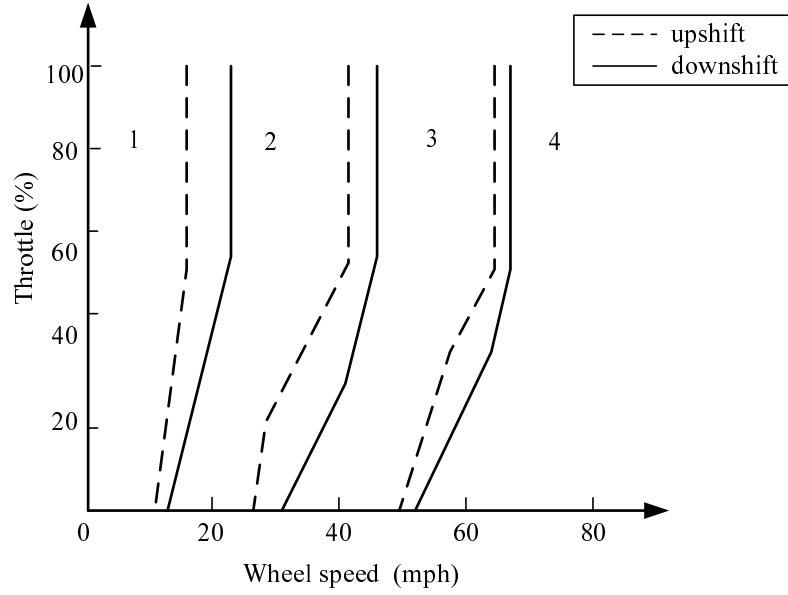


Figure 2.10: Gear shift schedule

The gearbox allows the gear ratio to be adjusted. By shifting the gears manually or automatically, the engine works at its most efficient region while allowing the vehicle to drive at a large range of speed. In our work, a 4-speed automatic gearbox is considered. Let  $R_g$  be the gear ratio of the gearbox, the value of  $R_g$  depends on the operating gear. Usually the gear ratio is defined as

$$R_g = \frac{\omega_t}{\omega_s} = \frac{T_s}{T_t} \quad (2.28)$$

where,  $\omega_t$  and  $\omega_s$  denote the angular speed of the turbine and the drive shaft.  $T_t$  and  $T_s$  denote the turbine torque and the drive torque acting on the drive shaft respectively.

## 2. Gear shift schedule

The operating gear is decided by a gear shift schedule that depends on both the

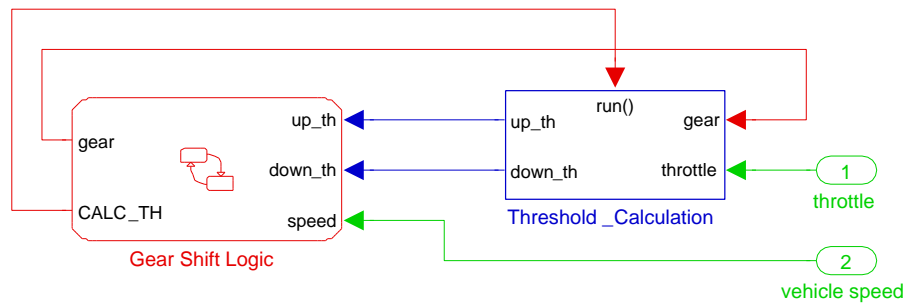


Figure 2.11: Model of automatic gear shift control

vehicle speed and the throttle opening (ranged form 0 to 100%). Fig. 2.10 shows a shift schedule for a 4-speed automatic transmission, which determines the current gear number and whether or not to perform an upshift or a downshift operation. The solid and dashed lines denote upshift and downshift thresholds respectively.

### 3. Modeling of automatic transmission

The automatic gearbox model is built up on the platform of *Matlab/Stateflow*. Fig. 2.11 shows the automatic gear shift model. This model includes two sub-systems: the *Threshold calculation* and the *Gear shift logic*. The *Threshold calculation* subsystem receives the input signals of throttle angle and the current gear number, and then it calculates the upshift threshold speed and downshift threshold speed for the vehicle at current gear. These two threshold speeds combined with the current vehicle speed are then transferred to the *Gear shift logic* subsystem, where the vehicle current speed is compared with the upshift and downshift threshold speed, and then it determines whether or not to perform an upshift or a downshift operation.

Modeling of the gear shift logic is the kernel in the automatic gearbox modeling. Traditionally, the gearbox has several fixed gears, 4 or 5 for instance. Under certain conditions, it changes the current gear to an other gear. Thus, the automatic gearbox system is a typical event-driven system with several prescribed states. The FSM (Finite State Machine) theory is then used in the modeling of automatic transmission system. *Matlab/Stateflow*<sup>®</sup> which provides a powerful environment for the analysising&modeling of the finite state machine is then employed in our research.

The stateflow diagram shown in Fig. 2.12 illustrates the functionality of the *Gear shift logic* model. This model has two *Parallel(AND)* states, named *gear\_state* and *selection\_state*. The *gear\_state* keeps track the current gear state, and the

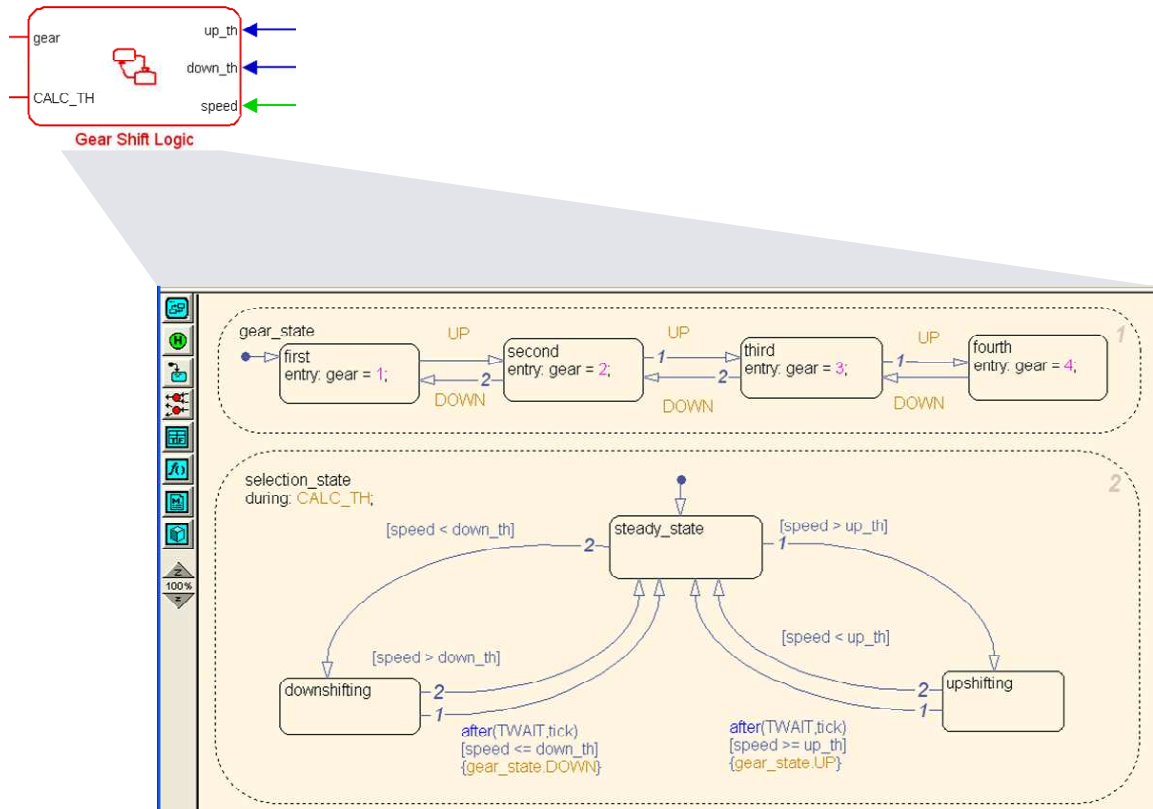


Figure 2.12: Stateflow diagram of the gear shift logic

*selection\_state* in charge of the gear selection process.

Let us begin with the *selection\_state* to illustrate the functionality of the ***Gear shift logic*** model. The state action “*during : CALC\_TH*”, which is always active, call the function *CALC\_TH* to calculate the upshift and downshift speed thresholds as a function of the instantaneous values of gear and throttle. While in *steady\_state*, the model compare the vehicle current speed to the upshift and downshift speed thresholds to judge if a shift operation is required. If one of the transit condition (as shown in Fig. 2.12) is satisfied, it enters one of the confirm state: *upshifting* or *downshifting*.

In the confirm state, if the vehicle speed no longer satisfies the shift condition, the model give up the shift and get back to the *steady\_state*. This will prevent the undesired shift due to noise disturbance. If the shift condition remains valid for a duration of *TWAIT* ticks(determined by the function: *after(TWAIT,tick)*), the model performs the transition, changes its state to *steady\_state* and at the same time effectuates one of the shift events *UP* or *DOWN*. As a result, this shift event

will lead to a shift operation in the *gear\_state*. The value of the gear will change consequently, and this value will be sent to the *Threshold\_Calculation* block for calculating the new speed threshold for the next circle.

### 2.3.2.4 Drive shaft, Final drive & Differential

#### 1. Drive shaft

A drive shaft is a mechanical component for transmitting torque and rotation. In an automobile, the drive shafts are usually used to connect other components of a drive train that cannot be connected directly because of distance or the need for relative movement between them, as shown in Fig.2.7 . In our work, we neglect the flexibility of the drive shafts and regard them as a rigid connection, the speed ratio and the torque ratio of the drive shaft is always 1.

#### 2. Final drive & Differential

The basic function of a final drive in the powertrain of an automobile is to provide an additional and constant gear reduction in the transmission system. In the longitudinally mounted engines, two basic types of final drive reduction gear have been used : bevel gear and worm. For the cars with transversely mounted engines, the final drive reduction gears are usually the helical pinions.

In addition, a differential is included in the final drive unit, which is capable of transmitting torque and rotation through three shafts: one input shaft which is connected to the drive shaft or the gearbox layshaft, and two output shafts which drive the driving wheels. The differential allows the two driving wheels to rotate at different speeds, while supplying equal torque to each of them for most vehicles. As in our work, the vehicle is assumed to drive in the good road condition, the two driving wheels in the both sides always have the same adhesion conditions. Thus the influences of the differential to the vehicle dynamics are neglected. The final drive dynamics are written as:

$$R_f = \frac{\omega_s}{\omega_w} = \frac{T_w}{T_s} \quad (2.29)$$

where,

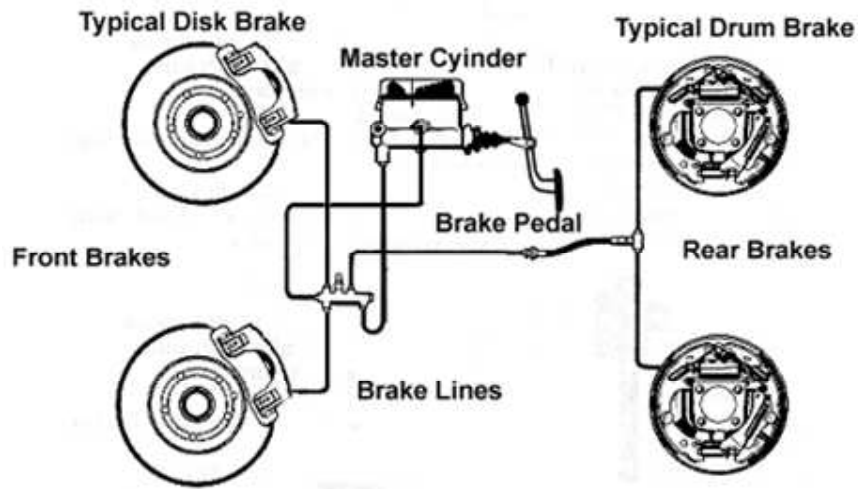


Figure 2.13: Typical braking system

- $R_f$  speed ratio of final drive
- $\omega_s$  rotation speed of drive shaft
- $\omega_w$  rotation speed of wheel
- $T_w$  driving wheel torque
- $T_s$  drive shaft torque

### 2.3.2.5 Braking system modeling

The typical automotive brake system is shown in Fig. 2.13. The front and rear wheel brakes (disk brake or drum brake) are connected by a system of tubes and hoses that link each brake to the master cylinder. When we step on the brake pedal, we are actually pushing against the piston in the master cylinder which forces hydraulic oil through a series of tubes and hoses to the braking unit at each wheel.

The braking torque is approximated to be proportional to the pressure in the brake chamber and brake fade is ignored [Kienhöfer 2006, Hedrick 1996]:

$$T_b = 2A_c P_c \mu_{br} r_{br} \quad (2.30)$$

where,

$T_b$  braking torque

$A_c$  effective area of the brake chamber diaphragm

$P_c$  brake chamber pressure

$\mu_{br}$  coefficient of friction between the brake disk and brake pads

$r_{br}$  effective radius through which the disk and brake pad friction acts

Let  $K_b = 2A_c\mu_{br}r_{br}$ , which is a constant that is determined by the vehicle brake system construction. Then equation (2.30) is reduced to

$$T_b = K_b P_c \quad (2.31)$$

Considering the deformation of the tubes and hoses as well as the volume nuance of the hydraulic oil during the braking period, the transfer function of the brake demand pressure to the pressure in the brake chamber is approximated as a first order system [Kienhöfer 2006]:

$$P_c = P_d \frac{1}{1 + \tau s} e^{-sT_d} \quad (2.32)$$

where,

$P_d$  brake demand pressure

$\tau$  time constant of the transient response of the brake system,  $\tau = 0.01s$

$T_d$  time delay in the brake system

### 2.3.3 Longitudinal model for simulation

The objective of this subsection is to present the longitudinal model for the simulations in the later chapters. The longitudinal model should consider the most significant phenomena in the vehicle longitudinal control. As consequence, we build a longitudinal vehicle model which starts from the engine and then the transmission till to the tyre/road, as described in the powertrain system in Fig. 2.7.

#### 2.3.3.1 Assumptions

In order to build a longitudinal model for the controller design in this work, we propose the following hypotheses:

- The vehicle is considered as driving in a straight road, and the vehicle lateral movement has no effect on longitudinal movement, which implies:

$$\delta = 0$$

where,  $\delta$  means the steering angle

- Negligible roll, pitch and vertical motions
- Negligible wind speed

### 2.3.3.2 Longitudinal model

According to longitudinal dynamics described in equation 2.1, considering the assumptions in the previous subsection, we get the new equation of longitudinal dynamics,

$$m\ddot{x} = F_{xf} + F_{xr} - F_{aero} - R_{xf} - R_{xr} - mg \sin(\alpha) \quad (2.33)$$

Let  $F_t = F_{xf} + F_{xr} - R_{xf} - R_{xr}$ , which means the traction force. Substituting  $F_{aero}$  from equation (2.6), vehicle longitudinal motion is then written as:

$$m\ddot{x} = F_t - \frac{1}{2}\rho C_d A_F V_x^2 - mg \sin(\alpha) \quad (2.34)$$

However, this equation is in terms of longitudinal tract force instead of engine and brake torques which are considered to be controlled. Therefore, the powertrain dynamics which we discussed in the section 2.3.2 should be added in the expression of longitudinal dynamics. The diagram of the different forces acting on the body and wheels of a rear drive vehicle during a acceleration driving is shown in Fig 2.14.

Each wheel can provide a torque equation as:

$$-F_{tf}r_{eff} - T_{bf} - T_{yf} = J_{wf}\dot{\omega}_{wf} \quad (2.35)$$

$$T_d - F_{tr}r_{eff} - T_{br} - T_{yr} = \bar{J}_{wr}\dot{\omega}_{wr} \quad (2.36)$$

where,

$F_{tf}/F_{tr}$	Tractive forces at the front and rear wheel
$T_d$	Drive torque referred to the axel
$T_{bf}/T_{br}$	Brake torque at the front and rear wheel
$T_{yf}/T_{yr}$	Rolling resistance torque at front and rear wheel
$J_{wf}/\bar{J}_{wr}$	Front axle inertia and the effective inertia of the rear axle, transmission and engine, which are related to the rear axle
$\omega_{wf}/\omega_{wr}$	Angular speed of the front and rear wheel
$r_{eff}$	Effective radius of the wheels

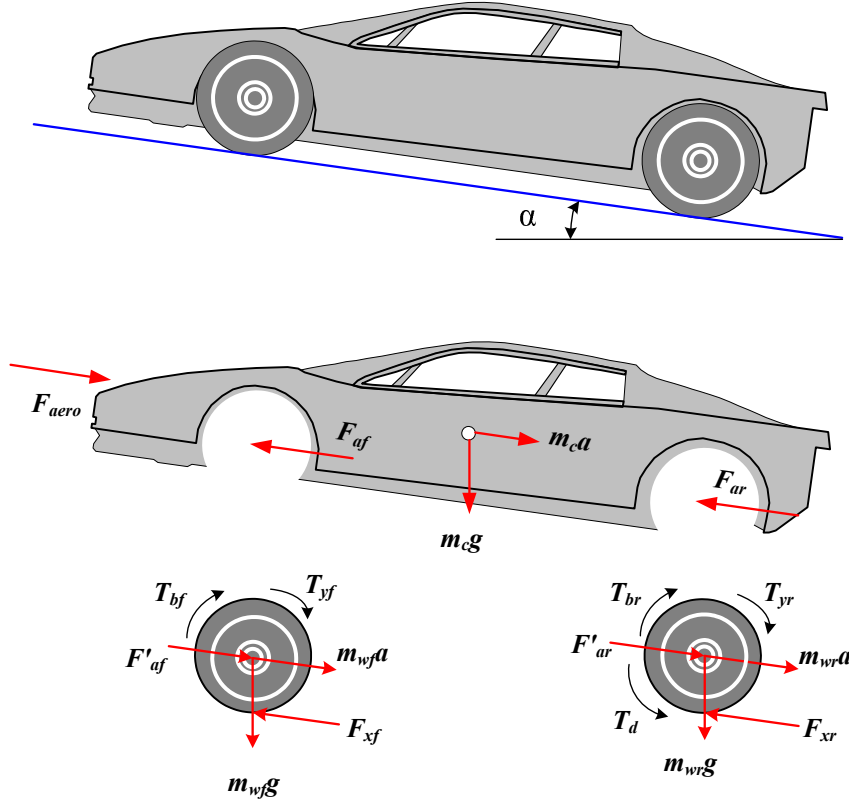


Figure 2.14: The different forces acting on the body and wheels

Solving  $F_{tf}$ ,  $F_{tr}$  from equations (2.35) and (2.36)

$$F_{tf} = \frac{1}{r_{eff}}(-J_{wf}\dot{\omega}_{wf} - T_{bf} - T_{yf}) \quad (2.37)$$

$$F_{tr} = \frac{1}{r_{eff}}(T_d - \bar{J}_{wr}\dot{\omega}_{wr} - T_{br} - T_{yr}) \quad (2.38)$$

Note that the total traction force  $F_t = F_{tf} + F_{tr}$ , then substituting (2.37) and (2.38) into (2.34), yields:

$$m\ddot{x} = \frac{1}{r_{eff}}(T_d - T_{bf} - T_{br} - T_{yf} - T_{yr} - J_{wf}\dot{\omega}_{wf} - \bar{J}_{wr}\dot{\omega}_{wr}) - \frac{1}{2}\rho C_d A_F V_x^2 - mg \sin(\alpha) \quad (2.39)$$

In order to simplify the analysis procedure, we make a father assumption that no slip occurs at the wheels. Strictly speaking, this assumption is not true, since in the discussions in the section 2.3.1.2, the longitudinal traction force depends on the slip ratio of the tyre. However, at the low acceleration conditions in this work for general operation in highway maneuvers, the slip is quite small and thus the tyre slip may safely be neglected. The no slip assumption has been employed in several previous researches [McMahon 1992,

Hedrick 1993, Hedrick 1997]. Using this assumption, we get:

$$\dot{\omega}_{wf} = \dot{\omega}_{wr} = \frac{\ddot{x}}{r_{eff}} \quad (2.40)$$

The next step relates to the drive torque  $T_d$ . Considering a mechanical transmission system,  $T_d$  is given by:

$$T_d = T_e R_g R_f \quad (2.41)$$

where,  $T_e$  denotes the engine torque,  $R_g$ ,  $R_f$  refer to the gear ratios of the gearbox and final drive respectively. However, in our work, an automatic transmission system with a hydraulic torque converter is considered, thus by using the expressions of (2.25, 2.26, 2.27), the axel drive torque can be written as:

$$T_d = T_e \Psi R_g R_f \quad (2.42)$$

In case that the torque converter is locked, as appeared in some models for reducing the power loss, the hydraulic transmission is thus regarded as a mechanical transmission system as described in equation (2.41).

Finally, we assume that the distribution of rolling resistance or braking torque on the front and rear axle is always appropriate. And we do not consider the influences caused by the different distributions of the rolling resistance and braking torque on the axels. We define  $T_y = T_{yf} + T_{yr}$  and  $T_b = T_{bf} + T_{br}$ , equation (2.39) is then reduced to:

$$\ddot{x} \left( m + \frac{J_{wf} + \bar{J}_{wr}}{r_{eff}^2} \right) = \frac{1}{r_{eff}} (T_e \Psi R_g R_f - T_b - T_y) - \frac{1}{2} \rho C_d A_F V_x^2 - mg \sin(\alpha) \quad (2.43)$$

This final equation represents the longitudinal vehicle dynamics. It considers both the engine and brake torques, and will be used in the controller design in the later chapters.

### 2.3.4 Simulations

In order to validate the vehicle longitudinal dynamics described in equation 2.43, we build a vehicle longitudinal system diagram as shown Fig. 2.15. The basic elements in longitudinal powertrain system are modeled as *Engine*, *Torque converter*, *Gear box* (Stateflow model) and *Final drive*, respectively. The *Vehicle longitudinal dynamics subsystem* is built upon the equation 2.43. The system inputs are throttle and brake, and the output is vehicle longitudinal speed. In our work, the throttle is expressed by the value of open

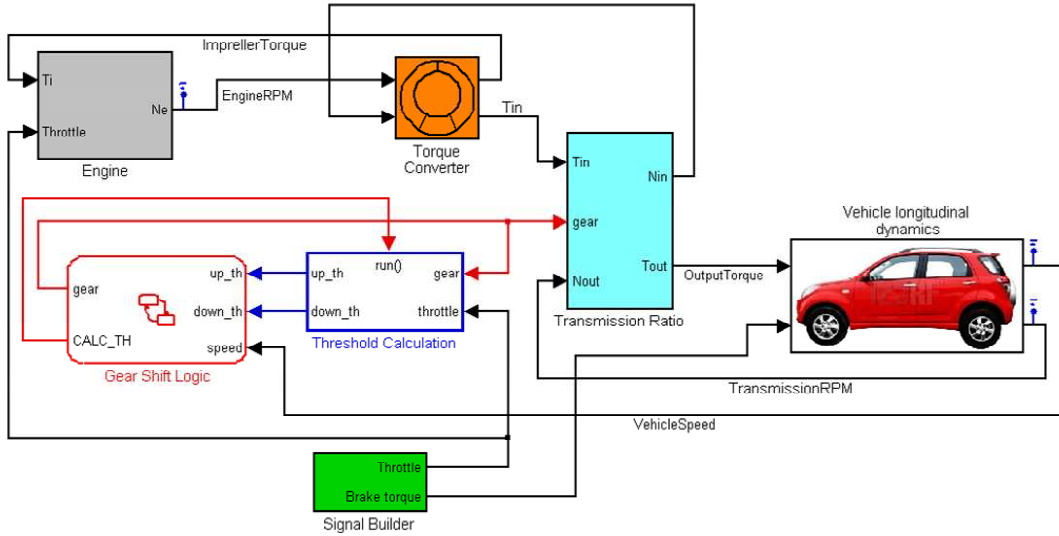


Figure 2.15: Vehicle longitudinal system diagram

percentage, ranged from 0 to 100%, where 0 means closed and 100% means full open. Since, the relationship between the brake torque and the brake oil pressure is approximated to be proportional as described in equation 2.31, therefore, we use brake torque as the input parameter and it is easy to transform, if necessary, the brake torque to the brake oil pressure.

We perform the following operations of throttle and brake pedal to drive the experimental vehicle: at first, we press down slowly the throttle pedal from 0 to 70%, next, we release slowly from 70% to 20%, and then we release the pedal completely. After that, we begin to press down the brake pedal to provide the brake torque from 0 to 400 ( $n * m$ ), afterwards, we keep the brake operation for 15s, and finally, we release the brake pedal gradually. The operation details of this acceleration and then deceleration scenario are described in Fig. 2.16.

The simulation results are shown in Fig. 2.17. Figure 2.17(a) shows the gear shift history, where we can find the operation trace of the automatic gearbox in this acceleration and then deceleration scenario. In the acceleration period, with the increases both in throttle open and vehicle speed, the gearbox changes up under the following sequence:  $1^{st} \rightarrow 2^{nd} \rightarrow 3^{rd} \rightarrow 4^{th}$ . While, in the deceleration period, it changes down reversely as:  $4^{th} \rightarrow 3^{rd} \rightarrow 2^{nd} \rightarrow 1^{st}$ . Figure 2.17(b) shows the *Up threshold* (red solid line) and *Down threshold* speed (green dashed line) for the shift up or shift down operations respectively. The values for the up and down thresholds are determined by the current gear number and throttle percentage. Note that the *Up threshold* curve is broken between 15s and 63s, this is because the gearbox is already engaged in the  $4^{th}$  gear, the highest gear, in

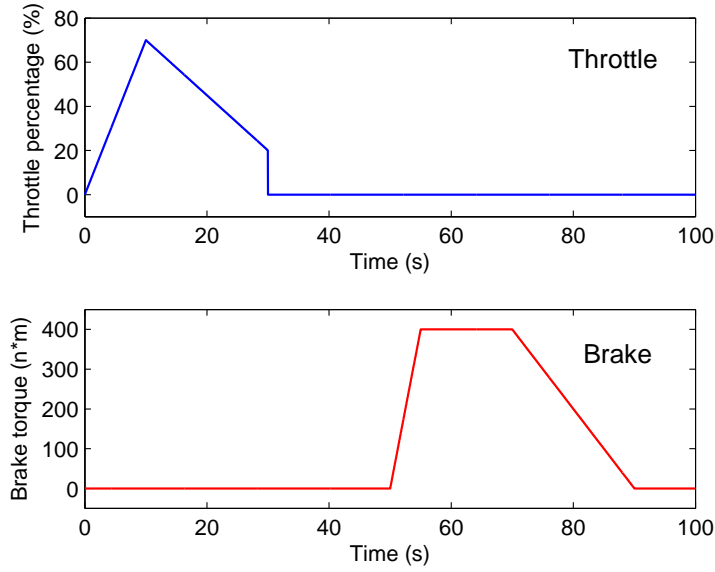


Figure 2.16: Throttle and brake input for simulation

this period. So the up threshold speed becomes to infinity.

The engine speed is shown in Fig. 2.17(c). Several peaks in engine speed curve are caused by the gear shift operations. Figure 2.17(d) and 2.17(e) show the evolution of speed and acceleration respectively. Note that in the acceleration curve, there are two sudden oscillations at 10.5s and 13.8s. These oscillations are caused by the gear change shocks between  $2^{nd} \rightarrow 3^{rd}$  and  $3^{rd} \rightarrow 4^{th}$ .

The above results are reasonable. They can reflect the interior movements of the different subsystems during the vehicle driving process. Therefore, this model will be employed in the longitudinal controller design in the later chapters.

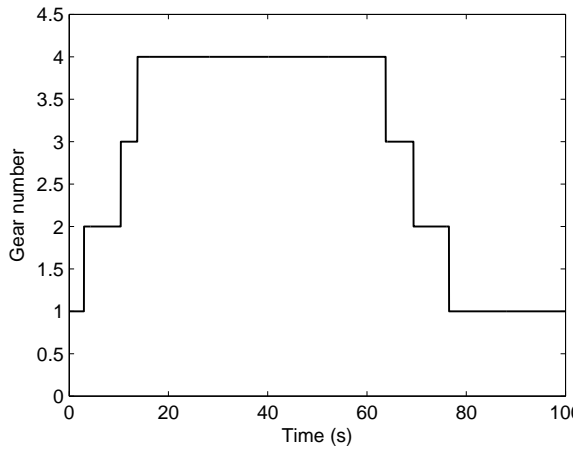
## 2.4 Modeling of Lateral vehicle dynamics

### 2.4.1 Lateral kinematic model

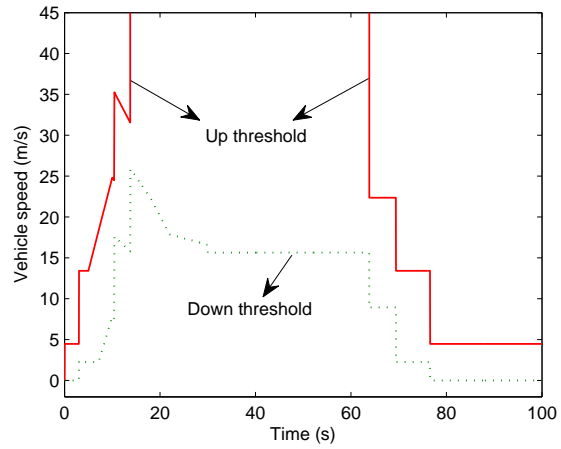
The kinematic model of the vehicle motion provides a mathematic description of the vehicle motion without considering the forces that affect the motion. We consider only the geometric parameters in the equations of kinematic model. This model can be used in the low speed application, such as car-like robot.

The vehicle lateral motion can be simplified as a bicycle model, as shown in Fig. 2.18, under the assumptions follows:

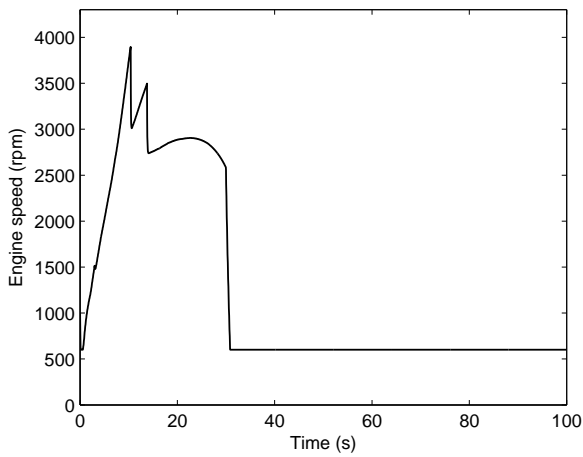
- The velocity vectors at front and rear wheels are in the direction of the orientation of



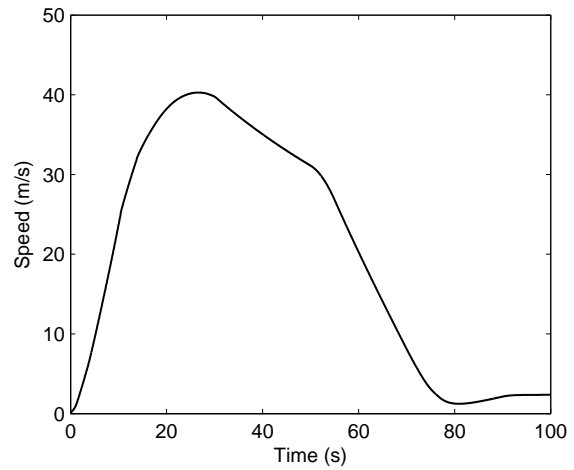
(a) Gear shift history



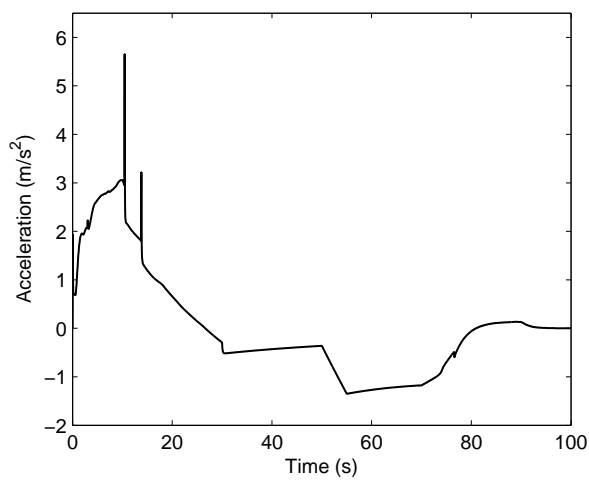
(b) Gear shift thresholds



(c) Engine speed



(d) Vehicle speed



(e) Vehicle acceleration

Figure 2.17: Simulation of longitudinal model

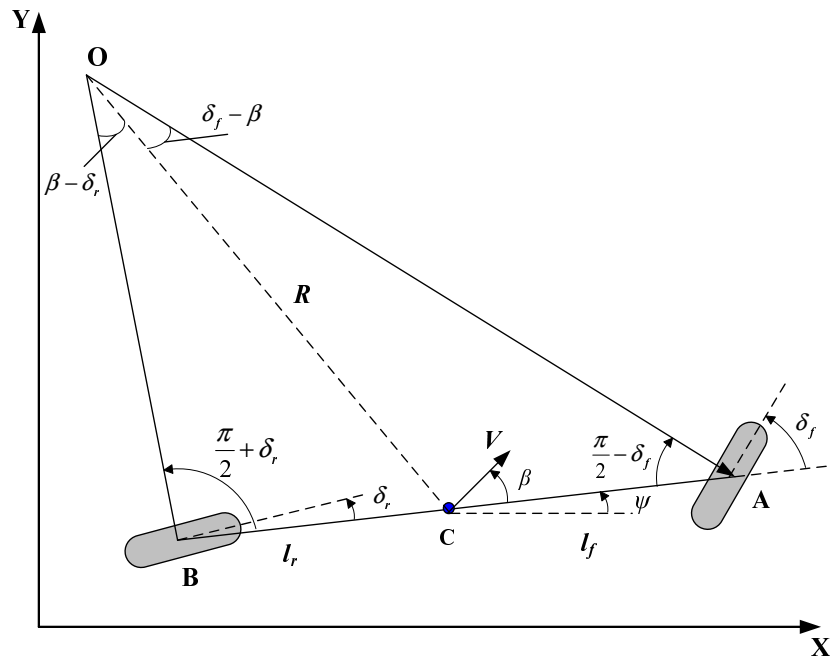


Figure 2.18: Kinematic bicycle model

the front and rear wheels respectively, which means the "slip angle" at both wheels are zero.

- The two wheels in both side of a axle have a same steering angle. Thus, we can combine the two wheels of one axle into a single wheel. The four wheels vehicle is modeled as a two wheels bicycle.

In Fig. 2.18, points  $A$ ,  $B$  and  $C$  represent the center of the front, the rear axle and the center of gravity (c.g.) of the vehicle respectively. The point  $O$  is the instantaneous rolling center for the vehicle.  $\delta_f$  and  $\delta_r$  represent the steering angle of the front and rear wheel respectively. In the case of front wheel steering, the parameter  $\delta_r$  can be set to zero. The velocity at the c.g. of the vehicle is  $V$ , which has an angle  $\beta$  with the longitudinal axis of the vehicle. The angle  $\beta$  is called the slip angle of the vehicle.  $R$  is the radius of the vehicle's path.

We use three coordinates to describe the motion of vehicle:  $X, Y$  and  $\psi$ .  $(X, Y)$  are inertial coordinates of the location of the c.g. of the vehicle while  $\psi$  is the yaw angle of the vehicle. Therefore, the kinematic model of vehicle lateral motion is given by:

$$\begin{cases} \dot{X} = V \cos(\psi + \beta) \\ \dot{Y} = V \sin(\psi + \beta) \\ \dot{\psi} = \frac{V \cos(\beta)}{l_f + l_r} (\tan(\delta_f) - \tan(\delta_r)) \end{cases} \quad (2.44)$$

where, the vehicle slip angle  $\beta$  is written as:

$$\beta = \tan^{-1} \left( \frac{l_f \tan \delta_r + l_r \tan \delta_f}{l_f + l_r} \right) \quad (2.45)$$

### 2.4.2 Lateral dynamic model

At higher vehicle speed, the assumption of zero “slip angle” at each wheel can no longer be made. In this case, the kinematic model cannot be used, and a dynamic model for lateral vehicle motion must be developed.

A “bicycle” model for vehicle lateral dynamics, which has two degrees of freedom, is shown in Fig. 2.19. The two degrees of freedom are denoted by the vehicle lateral position  $y$  and the vehicle yaw angle  $\psi$ . Two coordinate systems are used in this analysis: the global coordinate system is fixed to the ground, denoted by  $X, Y$  axes. The body fixed coordinate system is fixed to the vehicle body, denoted by  $x, y$  axes, the origin of this system,  $C$ , is the c.g. of the vehicle. Point  $O$  is the rotating center. The longitudinal velocity of the vehicle at the c.g. is denoted by  $V_x$ .

According to the Newton’s second law for motion along the  $y$  axis,

$$ma_y = F_{sf} \cos(\delta) + F_{sr} \quad (2.46)$$

where  $a_y$  is the inertial acceleration of the vehicle at the c.g. in the direction along the  $y$  axis,  $a_y = \frac{d^2y}{dt^2}$ .  $F_{sf}$  and  $F_{sr}$  are the lateral tyre forces of the front and rear wheels respectively.

Consider  $a_y$ , it is composed by two elements:  $\ddot{y}$  is due to the motion along the  $y$  axis and  $V_x \dot{\psi}$  is the centripetal acceleration. Thus

$$a_y = \ddot{y} + v_x \dot{\psi} \quad (2.47)$$

Substituting from (2.47) into (2.46), the equation of lateral translational motion is given by

$$m(\ddot{y} + v_x \dot{\psi}) = F_{sf} \cos(\delta) + F_{sr} \quad (2.48)$$

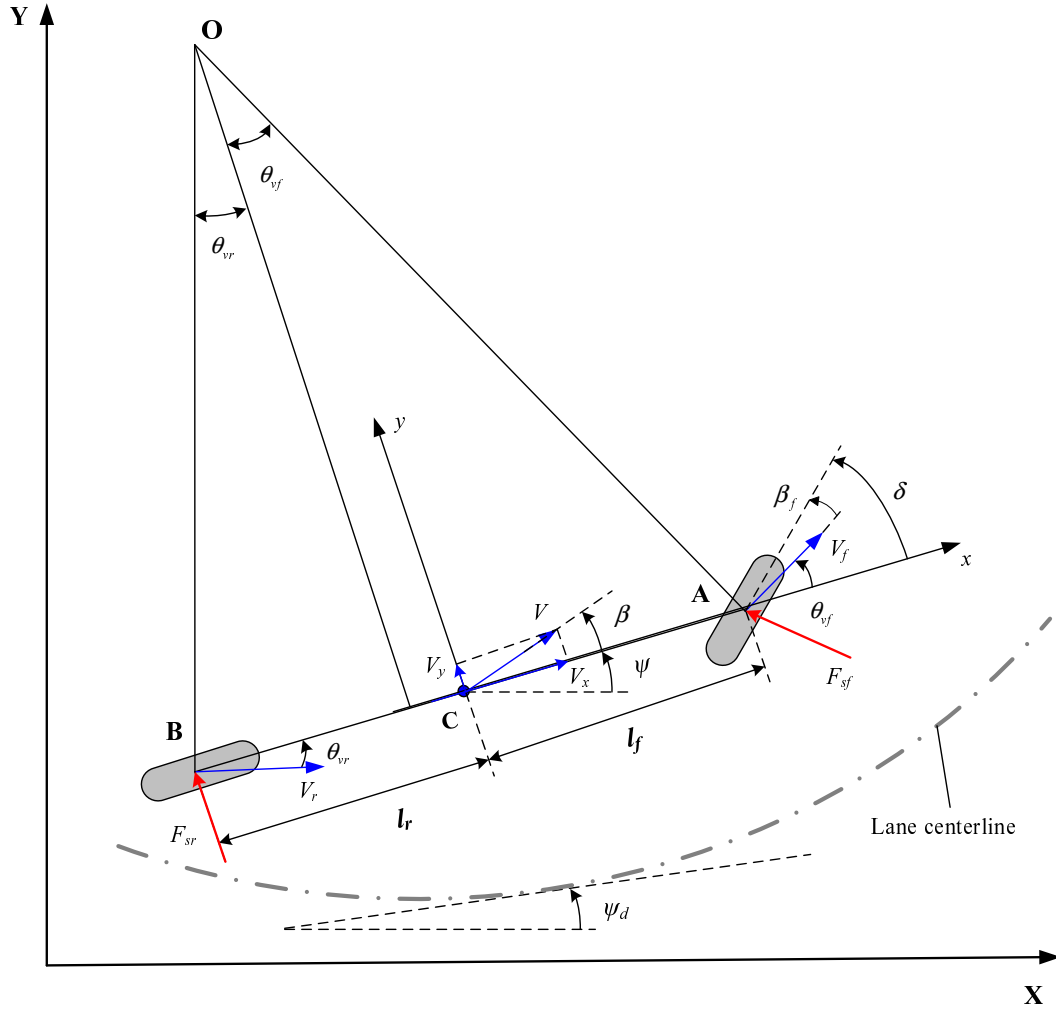


Figure 2.19: Bicycle model for vehicle lateral dynamics

Moment balance about the  $z$  axis can be obtained as:

$$I_z \ddot{\psi} = l_f F_{sf} \cos(\delta) - l_r F_{sr} \quad (2.49)$$

where,  $l_f$  and  $l_r$  are the distances of the front wheel and rear wheel respectively from the c.g. of the vehicle.

We assume that the vehicle steering angle is small thus,  $\cos(\delta) \approx 1$ <sup>3</sup>, the equations of (2.48) and (2.49) can be rewritten as:

$$\begin{cases} m(\ddot{y} + V_x \dot{\psi}) = F_{sf} + F_{sr} \\ I_z \ddot{\psi} = l_f F_{sf} - l_r F_{sr} \end{cases} \quad (2.50)$$

<sup>3</sup>The assumption of small steering angle is reasonable for the vehicles in highway driving conditions. In this work, a small steering angle means  $\delta \in [-15^\circ, 15^\circ]$ .

On account of the lateral tyre force is proportional to the “slip angle” for small slip angle. The slip angle of a tyre is the angle between the orientation of the tyre and the orientation of the velocity vector of the wheel, as shown in Fig.(2.19). In this figure, the slip angle of the front and rear wheel can be obtained as

$$\beta_f = \delta - \theta_{vf} \quad (2.51)$$

and

$$\beta_r = -\theta_{vr} \quad (2.52)$$

where  $\delta$  is the steering angle.  $\theta_{vf}$  is the angle between the velocity vector of the front wheel and the longitudinal axis of the vehicle, while  $\theta_{vr}$  is the angle between the velocity vector of the rear wheel and the longitudinal axis of the vehicle.

The slip angle results in a force perpendicular to the wheel’s direction of travel- lateral tyre force (cornering force). This lateral force increases approximately linearly for the small slip angle, we can get

$$\begin{cases} F_{sf} = 2C_{af}(\delta - \theta_{vf}) \\ F_{sr} = -2C_{ar}\theta_{vr} \end{cases} \quad (2.53)$$

where  $C_{af}$  and  $C_{ar}$  are the cornering stiffness of each front and rear tyre respectively. The factor 2, in both the two equations, is due to the fact that there are two wheels in each axle of vehicle.

Using the following relations, we can calculate  $\theta_{vf}$  and  $\theta_{vr}$

$$\tan(\theta_{vf}) = \frac{V_y + l_f\dot{\psi}}{V_x} \quad (2.54)$$

$$\tan(\theta_{vr}) = \frac{V_y - l_r\dot{\psi}}{V_x} \quad (2.55)$$

Using small angle approximations and let  $V_y = \dot{y}$ , we can get

$$\theta_{vf} = \frac{\dot{y} + l_f\dot{\psi}}{V_x} \quad (2.56)$$

$$\theta_{vr} = \frac{\dot{y} - l_r\dot{\psi}}{V_x} \quad (2.57)$$

Substituting from equations 2.51, 2.52, 2.56 and 2.57 into equation 2.50, the state space model of vehicle lateral dynamics can be written as

$$\dot{X} = AX + B\delta \quad (2.58)$$

where,  $X$  is the state variable,  $X = [y, \dot{y}, \psi, \dot{\psi}]^T$ , and

$$A = \begin{bmatrix} 0 & 1 & 0 & 0 \\ 0 & -\frac{2C_{af} + 2C_{ar}}{mV_x} & 0 & -V_x - \frac{2C_{af}l_f - 2C_{ar}l_r}{mV_x} \\ 0 & 0 & 0 & 1 \\ 0 & -\frac{2l_f C_{af} - 2l_r C_{ar}}{I_z V_x} & 0 & -\frac{2l_f^2 C_{af} + 2l_r^2 C_{ar}}{I_z V_x} \end{bmatrix}$$

$$B = \begin{bmatrix} 0 \\ \frac{2C_{af}}{m} \\ 0 \\ \frac{2l_f C_{af}}{I_z} \end{bmatrix}$$

Equation (2.58) describes the vehicle dynamics using the state variables lateral position and yaw angle. But when our objective is to design a steering control system, it is more practical to utilize a dynamic model in which the state variables are the position and orientation error with respect to the road. Hence, the lateral model described in (2.58) should be re-defined with the new state variables.

We define the following variable as state variables:

- $e_1$ , the distance of the c.g. of the vehicle from the center line of the lane, as shown in Fig. 2.20.
- $e_2$ , the orientation error of the vehicle with respect to the road.

From the above definition, we obtain

$$e_2 = \psi - \psi_d \quad (2.59)$$

where,  $\psi_d$  denote the desired yaw angle of vehicle (i.e. the orientation angle of the road).

Consider a vehicle traveling with a constant longitudinal velocity  $V_x$  on a curve of constant radius  $R$ . Assume that the curve radius  $R$  is large enough so that small steering angle assumption can be made. Then, the desired yaw rate of the vehicle is given by:

$$\dot{\psi}_d = \frac{V_x}{R} \quad (2.60)$$

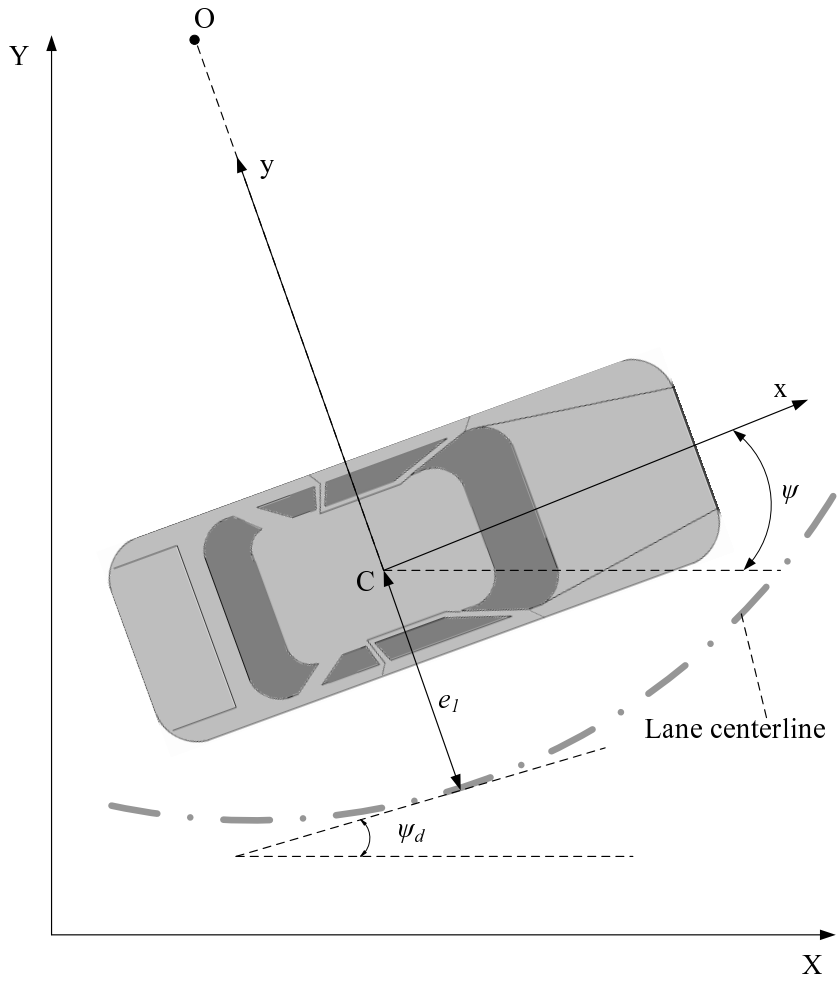


Figure 2.20: The vehicle lateral system

The desired acceleration along the  $y$  axis of the vehicle is then written as:

$$a_{yd} = \frac{V_x^2}{R} = V_x \dot{\psi}_d \quad (2.61)$$

From the definition of  $e_1$ , we can get [Rajamani 2006]

$$\ddot{e}_1 = a_y - a_{yd} = (\ddot{y} + V_x \dot{\psi}) - \frac{V_x^2}{R} = \ddot{y} + V_x(\dot{\psi} - \dot{\psi}_d) \quad (2.62)$$

Then we can get

$$\dot{e}_1 = \dot{y} + V_x(\psi - \psi_d) \quad (2.63)$$

Substituting from Equations (2.59) and (2.63) into (2.49), we get

$$\begin{aligned}
 m\dot{e}_1 &= \dot{e}_1 \left( \frac{-2C_{af} - 2C_{ar}}{V_x} \right) + e_2 (2C_{af} + 2C_{ar}) \\
 &+ \dot{e}_2 \left( \frac{-2C_{af}l_f + 2C_{ar}l_r}{V_x} \right) + 2C_{af}\delta \\
 &+ \dot{\psi}_d \left( \frac{-2C_{af}l_f + 2C_{ar}l_r}{V_x} - mV_x \right)
 \end{aligned} \tag{2.64}$$

and

$$\begin{aligned}
 I_z\ddot{e}_2 &= \dot{e}_1 \left( \frac{-2C_{af}l_f + 2C_{ar}l_r}{V_x} \right) + e_2 (2C_{af}l_f - 2C_{ar}l_r) \\
 &\dot{e}_2 \left( \frac{-2C_{af}l_f^2 - 2C_{ar}l_r^2}{V_x} \right) + 2C_{af}l_f\delta - I_z\ddot{\psi}_d \\
 &+ \dot{\psi}_d \left( \frac{-2C_{af}l_f^2 - 2C_{ar}l_r^2}{V_x} \right)
 \end{aligned} \tag{2.65}$$

From (2.64) and (2.65), the state space model can therefore be written as

$$\dot{X} = AX + B_1\delta + B_2\rho \tag{2.66}$$

where,  $X$  is the state variable,  $X = [e_1, \dot{e}_1, e_2, \dot{e}_2]^T$ , and

$$\begin{aligned}
 A &= \begin{bmatrix} 0 & 1 & 0 & 0 \\ 0 & -\frac{2C_{af}+2C_{ar}}{mV_x} & \frac{2C_{af}+2C_{ar}}{m} & \frac{-2C_{af}l_f+2C_{ar}l_r}{mV_x} \\ 0 & 0 & 0 & 1 \\ 0 & -\frac{2C_{af}l_f-2C_{ar}l_r}{I_zV_x} & \frac{2C_{af}l_f-2C_{ar}l_r}{I_z} & -\frac{2C_{af}l_f^2+2C_{ar}l_r^2}{I_zV_x} \end{bmatrix}, \\
 B_1 &= \begin{bmatrix} 0 & \frac{2C_{af}}{m} & 0 & \frac{2C_{af}l_f}{I_z} \end{bmatrix}^T, \\
 B_2 &= \begin{bmatrix} 0 & -\frac{2C_{af}l_f-2C_{ar}l_r}{m} - V_x^2 & 0 & -\frac{2C_{af}l_f^2+2C_{ar}l_r^2}{I_z} \end{bmatrix}^T.
 \end{aligned}$$

Consider the simplified vehicle lateral dynamic model shown in (2.66), it is a 4<sup>th</sup> order linear model and a LTI model as well, when all the parameters in the matrices  $A$ ,  $B_1$  and  $B_2$  are constant. If the parameters' values vary, for example the vehicle velocity  $V_x$  or tyre cornering stiffness  $C_a$  varies, the LTI model is then replaced by a LTV (Linear Time Variant) model.

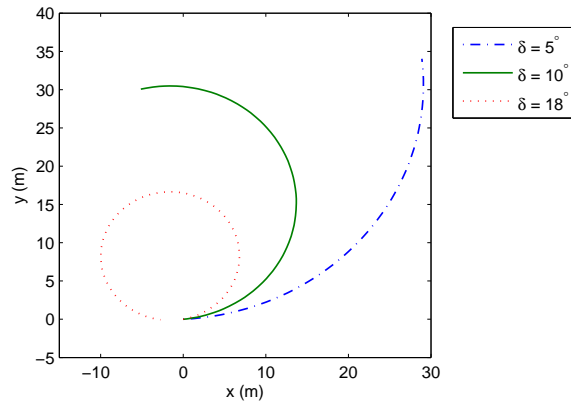


Figure 2.21: Kinematic model results with different steering angles  $\delta$

### 2.4.3 Simulations

In this part, the vehicle lateral kinematic model and dynamic model will be tested using *Matlab/Simulink*<sup>®</sup>. The kinematic model is given by equation (2.44), while the dynamic model is written by equation (2.66).

#### 2.4.3.1 Kinematic model simulations

Since the kinematic model considers only the geometric parameters of the vehicle and ignores the forces that will affect its motion. This model is appropriated only in the low speed applications, such as during the parking operation or for the low speed car-like robots. Therefore, we will simulate the model only in the low speed region. In this case, the big steering angle is allowed.

The vehicle longitudinal speed is set to a constant  $5 \text{ m/s}$ , a typical low speed for a real scale vehicle. The front wheel steering angle is set to  $5^\circ$ ,  $10^\circ$  and  $18^\circ$  respectively. The simulation time is set to 10 seconds. The results of vehicle positions are shown in Fig. 2.21. We can find that the two vehicle tracks are two parts of two circles with different radius. These results are reasonable because the kinematic model do not consider the lateral forces that caused by the lateral motion. Thus the vehicle will track a circle in the proposed simulation conditions.

#### 2.4.3.2 Dynamic model simulations

At first, consider the dynamic model which is given in equation (2.66), the small steering angle assumption is proposed to linearize the lateral model. Thus, in our simulation, the experimental steering angle is set to be small (less than  $10^\circ$ ) as the first simulation

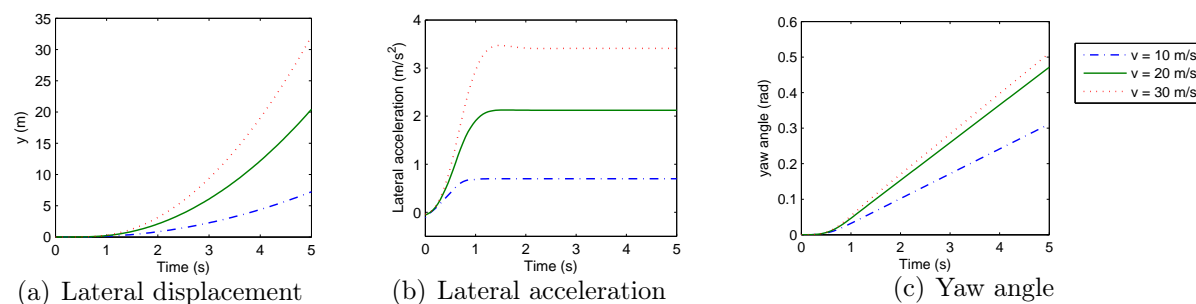


Figure 2.22: Dynamic model results with different speeds

requirement. This requirement is reasonable for the vehicles in highway driving situations. Second, it is known that the vehicle speed varies in a wide range during the highway operations. Therefore, we need to consider a wide range of speed variations in our simulations.

We test the dynamic model with the following conditions. The vehicle longitudinal speed is set to 10  $m/s$ , 20  $m/s$  and 30  $m/s$  respectively. The steering angle is set to be increased from  $0^\circ$  to  $1.2^\circ$  during the first 0.9 second, and then it keeps the steering angle of  $1.2^\circ$ .

The vehicle lateral displacement, lateral acceleration and yaw angle results are shown in Fig 2.22. We can find that the vehicle responses are varied notably with the variation of vehicle speed, which means the vehicle speed has a great influence on vehicle lateral dynamics. In Fig. 2.22(b), when the vehicle speed is high,  $v = 30 m/s$ , the maximum lateral acceleration is about  $3.5 m/s^2$ , a rather high value, even when the steering angle is small  $\delta = 1.2^\circ$ . Generally, for the reason of security, the vehicle lateral acceleration should not exceed  $4 m/s^2$ , otherwise, there is a risk of rollover. The phenomena that vehicle lateral dynamics is notably affected by the vehicle speed will be an important element to be considered in the lateral controller design.

The two different vehicle lateral model, kinematic and dynamic models, were developed and tested in this section. However, the assumptions for the two models are different. Thus, when we use these models, the utilization requirements and road conditions are the essential factors to be considered.

## 2.5 Conclusion

In this chapter, we have presented the vehicle longitudinal and lateral models, which will be employed in the controller design in the following chapters.

For the vehicle longitudinal model, at first, we established the non-linear **longitudinal dynamic model** based on the Newton's second law, with the hypothesis of no-slip at the tyre-road interface. In this model, all the forces that influence the vehicle longitudinal dynamics are expressed in only one equation. Moreover, the engine and brake torques, which are considered to be controlled in the longitudinal controller, are included in this equation. This makes it convenient for the controller design. Second, the **powertrain dynamic model** of a passenger car with an automatic gearbox was built, which includes the sub-models of different parts in the powertrain system, the engine, torque converter, automatic gearbox, drive shafts, final drive and differential, as well as the braking system. By using this powertrain model, we can simulate the vehicle behavior thus to test the controllers' results in the following sections.

For the lateral model, the **kinematic** and **dynamic** models were studied respectively. The kinematic model provides a mathematic description of the vehicle motion without considering the forces that affect the motion, and it considers only the geometric parameters. This model can be used in the low speed applications. A "bicycle" model was proposed to express the vehicle lateral dynamics. Under the assumptions of small steering angle and small slip angle, the bicycle model can be described by a 4<sup>th</sup> order linear model.

Although the bicycle model is simple, it has been proven to be a good approximation for vehicle dynamics when lateral acceleration is limited to 0.4g on normal dry asphalt roads.

# Chapter 3

## Longitudinal Control for Vehicle Platoons

### Contents

---

<b>3.1</b>	<b>Introduction</b>	<b>64</b>
<b>3.2</b>	<b>Architecture of longitudinal control system</b>	<b>65</b>
<b>3.3</b>	<b>Upper level control</b>	<b>66</b>
3.3.1	Introduction	66
3.3.2	String stability	68
3.3.3	Traffic flow stability	71
3.3.4	Evaluation of the Constant Time Gap spacing policy	74
3.3.5	Proposed Safety Spacing Policy	78
3.3.6	Simulation tests	86
<b>3.4</b>	<b>Lower level control</b>	<b>89</b>
3.4.1	Introduction	89
3.4.2	Coordinated Throttle and Brake Fuzzy Controller	90
3.4.3	Simulation tests	96
<b>3.5</b>	<b>Conclusion</b>	<b>101</b>

---

## 3.1 Introduction

With the increasing problems of traffic congestion and safety, the idea of using automated vehicles driving in automated highway is growing steadily more attractive. Longitudinal control and lateral control are the two basic functions of the vehicle automation. Longitudinal control system controls the longitudinal motion of the vehicle, such as longitudinal velocity, acceleration or the its longitudinal distance from the proceeding vehicle in the same lane, by using throttle and brake controllers [Rajamani 2006], while the vehicle lateral control system senses the road centerline using a road based reference system and other on-board sensors and generates steering command to keep the vehicle running along the desired path, thus to realize the lane-keeping or lane-changing tasks for the automatic vehicles.

The longitudinal vehicle motion control has been pursued for several decades and at many different levels by researchers and automotive manufactures. From 1970s to 1980s, there appeared some researches in the control system design for vehicle engines and brake systems, as shown in [Fisher 1970, Guntur 1972, Guntur 1980, Moskwa 1987, Powell 1987]. Since then, some first generation of engine control systems appeared in [Cho 1989, Grizzle 1994], and some results in the brake system control have obtained great success, such as the ABS (Anti-lock Brake System), which have been widely accepted in the automobile industry. Based on these results, and since 1990s, the researches in the longitudinal control combined with throttle and brake control has become steadily more attractive, and a variety of solutions have been proposed in [Tan 1990, McMahan 1990] and [Hedrick 1991, McMahan 1992]. In addition, in 1986, the California PATH (U.S.A.), one of the most fruitful organization in transportation researches, was established. Almost in the same time, the program of AHSS (Advanced Highway Safety System) in Japan, and the program of PROMETEUS (PROgram for an European Traffic with Highest Efficiency and Unprecedented Safety) in Europe were carried out. These programs have contributed a considerable efforts and encouraging results in such a control system.

Nowadays, the standard Cruise Control (CC) system, which can automatically control the throttle to maintain the pre-set speed, is widely available on passenger cars. Furthermore, the Adaptive Cruise Control (ACC) and the Cooperative Adaptive Cruise Control (CACC) system were developed, which are extensions of the CC system, have the capacity of detecting the preceding vehicle and then maintain a proper distance from it [Marsden 2001, Wang 2004a, van Arem 2006]. In the case of absence of preceding vehicles, the ACC/CACC vehicle travels as a CC vehicle. Another cruise control system is

the “collision avoidance” (CA) system. A CA system operates like a cruise control system to maintain a constant desired speed in the absence of preceding vehicles. If a preceding vehicle appears, the CA system will judge the operation speed is safe or not, if not, the CA will reduce the throttle and/or apply brake so as to slow the vehicle down, at the same time a warning is provided to the driver.

A completely different concept proposed by the California PATH Program, is the vehicle “platoon”, where the vehicles travel together with a close separation [Rajamani 2000]. It was estimated that the traffic capacity is about three times the capacity of a typical highway if all the vehicles travel in the closely packed platoons [Varaiya 1993].

Inspired by the concept of “platoon”, our principal objective is to design a vehicle longitudinal control system which can enhance vehicle safety while at the same time improving traffic capacity. Thus, we need to envisage not only the control problems of a single vehicle but also the behaviors of a string of vehicles and its impacts to traffic flow.

This chapter concentrates on the design problems of vehicle longitudinal control system design. At first the longitudinal control system architecture was designed to be hierarchical, with an upper level controller and a lower level controller. And then the design of upper and lower level controllers will be carried out respectively. To validate the proposed controllers, simulation tests will be carried out. And some conclusion will be given in the end of this chapter.

## 3.2 Architecture of longitudinal control system

As we have introduced in chapter 1, the control architecture of an Automated Highway System (AHS) is hierarchical and has 4 layers shown in Fig.4.18(c). In the (regulation layer), the longitudinal control system is in charge of the steady and transient longitudinal maneuvers. The longitudinal control system is designed to be hierarchical [Rajamani 2006], with an upper level controller and a lower level controller as shown in Fig. 3.1. The upper level controller determines the desired acceleration or speed for the controlled vehicle, while the lower level controller decides the throttle and brake commands required to track the desired acceleration or speed.

Based on this hierarchical control architecture, the overall longitudinal control system design is thus divided into two steps: (i) upper level controller design, which includes the design of the specific spacing policy and the associated control laws. The spacing policy means the desired spacing that an automated vehicle attempts to maintain with respect to the preceding vehicle. The desired spacing, which is the value of  $(x_{i-1} - x_i - w_{i-1})$

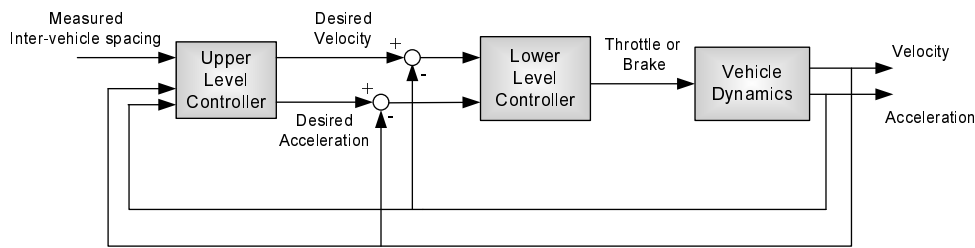


Figure 3.1: Two-level structure for longitudinal control

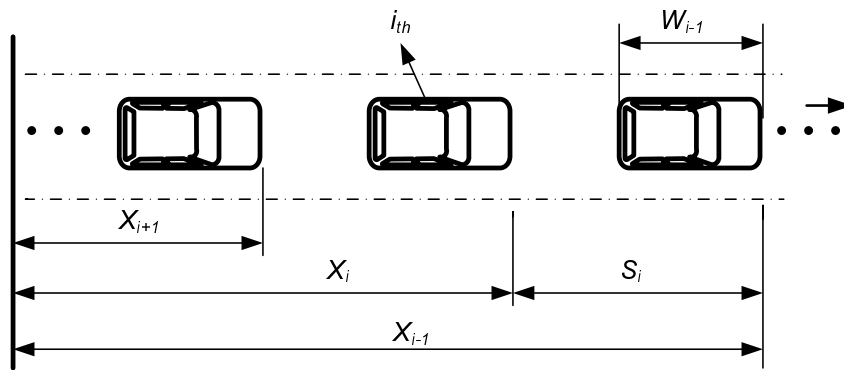


Figure 3.2: Vehicle platoon

as shown in Fig 3.2, is typically a function of the vehicle speed, however it could also be a constant or a function of other variables such as the relative velocity. (ii) lower level controller design, which involves the throttles and brakes controllers design. The rest of this chapter will be expanded following the above two steps.

### 3.3 Upper level control

#### 3.3.1 Introduction

As we have introduced in the previous section, the first-generation of longitudinal control systems like CC or ACC systems are primarily being developed from the point of view of increased driving comfort with some potential in increasing vehicle safety. However, the impacts of these longitudinal control systems on highway traffic have been inadequately studied [Swaroop 1999, Santhanakrishnan 2003]. From the transportation planners' point of view, the automated vehicles equipped with the longitudinal control systems should heavily impact the traffic characteristics, including highway safety, efficiency and capacity because of their more uniform behavior compared with human drivers [Zwaneveld 1998]. Before the longitudinal control systems are widely equipped on automated vehicles, their

impacts on string behavior and flow characteristics need to be carefully investigated. Otherwise traffic congestion may become worse instead of being better.

Two of the most important macroscopic behaviors of ACC vehicles are string stability and traffic flow stability. Such a distinction between the two stability has been first recognized by D. Swaroop [Swaroop 1999]. The string stability of a string of vehicles refers to a property in which spacing errors are guaranteed not to amplify as they propagate towards the tail of the string [Swaroop 1994b, Santhanakrishnan 2003]. This property ensures that any spacing error present at the head of the string does not amplify into a large error at the tail of the string. A general method to evaluate string stability is to examine the transfer function from the spacing error of the proceeding vehicle to that of the following vehicle. If the infinite norm of this transfer function is less than 1, string stability is ensured [Swaroop 1996, Wang 2004a].

Traffic flow stability refers to a macroscopic property associated with speed and density of traffic in a section of a highway. It guarantees that density disturbances attenuate as they propagate upstream. For example, density disturbances may occur as a result of a sudden influx of vehicles from a ramp. An unstable traffic flow characteristic would imply that such density or velocity disturbances are felt at every point upstream from the source without attenuation. A traffic flow is said to be stable when the slope  $\partial Q/\partial \rho$  is a positive value, where,  $Q$  is the traffic flow and  $\rho$  denotes the traffic density.

Besides, the early ACC systems are designed mainly for applications where the vehicle speed is higher than 30 km/h and, consequently are not useful in traffic jams or urban driving. This is mainly because the conventional ACC systems only manage the throttle pedal. In an extended version, the brake pedal also needs to be controlled. Stop&Go cruise control system, which includes both throttle and brake control systems, were introduced to overcome this drawback.

Based on the above discussions, the upper level controller, which includes the specific spacing policy and the associated control laws, should be designed to achieve the following objectives:

1. It should guarantee string stability in a string of vehicles.
2. The spacing policy should lead to increased traffic capacity and a stable traffic flow up to a higher characteristic traffic density.
3. The control effort required by the control law should be within the vehicle's traction/braking capability.

4. It should be used for a wide range of speed for vehicle operations in highway, which includes low and high speed scenarios.

The rest of this section is organized as follows: at first the theories of platoon string stability and traffic flow stability, which are required in the design upper level controller, are introduced; next, the traditional spacing policy (CTG: Constant Time Gap policy) will be evaluated; then, the proposed spacing policy will be introduced. It will be evaluated by the objectives that we proposed in this section and will be compared also with the CTG policy. Finally, some simulation results will be given.

### 3.3.2 String stability

For an interconnected system, such as a platoon of automated vehicles, stability of each component system itself is not sufficient to guarantee a certain level of performance, such as the boundedness of the spacing errors for all the vehicles. This is reasonable because our research object is a string of vehicles instead of only one vehicle. Therefore, besides the individual stability of each vehicle, another stability criterion known as the string stability is also required [Horowitz 2004, Rajamani 2006].

#### 3.3.2.1 Definition of string stability

String stability is generally defined as the spacing errors are guaranteed not to amplify as they propagate towards the tail of the string. In fact, the conditions for string stability were already provided in the works of Sheikholeslam and Desoer [Sheikholeslam 1990], which indicated that the norm magnitude  $|G(j\omega)| < 1$  and the impulse response  $g(t) > 0$  of the linear operator  $G(s)$ , where  $G(s)$  maps the deviation in the assigned distances between vehicle  $i$  and  $i - 1$ .

The more formalized and generalized definition of string stability was given by Swaroop [Swaroop 1996]. The mathematical definitions for *string stability*, *asymptotically stability*, and  *$l_p$  string stability* were made. We use the definitions proposed by Swaroop [Swaroop 1994a, Swaroop 1996]. At first, we use the following notations:  $\|f_i(\cdot)\|_\infty$ , denotes  $\sup_{t \geq 0} |f_i(t)|$ , and  $\|f_i(0)\|_\infty$  denotes  $\sup_i |f_i(0)|$ . For all  $p < \infty$ ,  $\|f_i(\cdot)\|_p$  denotes  $(\int_0^\infty |f_i(t)|^p dt)^{\frac{1}{p}}$  and  $\|f_i(0)\|_p$  denotes  $(\sum_1^\infty |f_i(0)|^p)^{\frac{1}{p}}$ .

Consider an interconnected system:

$$\dot{x}_i = f(x_i, x_{i-1}, \dots, x_{i-r+1}) \quad (3.1)$$

where  $i \in \mathbb{N}$ ,  $x_{i-j} \equiv 0 \forall i \leq j$ ,  $x \in \mathbb{R}^n$ ,  $f : \underbrace{\mathbb{R}^n \times \dots \times \mathbb{R}^n}_{r \text{ times}} \rightarrow \mathbb{R}^n$  and  $f(0, \dots, 0) = 0$ .

**Definition 3.1 (String stability).** The origin  $x_i = 0$ ,  $i \in \mathbb{N}$  of (3.1) is string stable, if given any  $\epsilon > 0$ , there exist a  $\delta > 0$  such that :

$$\|x_i(0)\|_\infty < \delta \Rightarrow \sup_i \|x_i(\cdot)\|_\infty < \epsilon$$

**Definition 3.2 (Asymptotically (exponential) stability).** The origin  $x_i = 0$ ,  $i \in \mathbb{N}$  of (3.1) is asymptotically (exponentially) string stable if it is string stable and  $x_i(t) \rightarrow 0$  asymptotically (exponentially) for all  $i \in \mathbb{N}$ .

A more general definition of string stability is given in follow:

**Definition 3.3 ( $l_p$  String stability).** The origin  $x_i = 0$ ,  $i \in \mathbb{N}$  of (3.1) is  $l_p$  string stable if for any  $\epsilon > 0$ , there exist a  $\delta > 0$  such that :

$$\|x_i(0)\|_p < \delta \Rightarrow \sup_i \left( \sum_1^\infty |x_i(t)|^p \right)^{\frac{1}{p}} < \epsilon$$

It is clear that Definition 3.1 can be obtained as  $l_\infty$  string stability of Definition 3.3. The generalized string stability implies uniform boundedness of the system states if the initial conditions are uniformly bounded.

### 3.3.2.2 String stability in vehicle following system

In the case of vehicle following system, such as a vehicle platoon as shown in Fig. 3.2, for the  $i$ th vehicle,  $x_i$  is the location measured from an inertial reference, as shown in the same figure. We define the spacing error for the  $i$ th vehicle as:

$$\delta_i = x_i - x_{i-1} + S_i \tag{3.2}$$

where  $S_i$  is the desired spacing measured from vehicle  $i - 1$  to  $i$ , and it includes the preceding vehicle's length  $W_{i-1}$ . A sufficient condition for string stability is that [Swaroop 1994a, Swaroop 1996]:

$$\|\delta_i\|_\infty \leq \|\delta_{i-1}\|_\infty \tag{3.3}$$

If we define the transfer function from  $\delta_{i-1}$  to  $\delta_i$  to be

$$\hat{H}(s) = \frac{\delta_i(s)}{\delta_{i-1}(s)} \tag{3.4}$$

where  $\delta_i(s)$  is the Laplace transform of  $\delta_i(t)$ . Let  $h(t)$  be the impulse response of  $\hat{H}(s)$ , thus the condition (3.3) for string stability becomes

$$\|h(t)\|_1 \leq 1 \quad (3.5)$$

due to the result in system theory that

$$\|h(t)\|_1 = \sup_{x \in L_\infty} \frac{\|\delta_{i-1}\|_\infty}{\|\delta_i\|_\infty} \quad (3.6)$$

Then the condition of (3.5) can be replaced by

$$\|\hat{H}(s)\|_\infty \leq 1 \text{ and } h(t) > 0 \quad (3.7)$$

This transformation from (3.5) to (3.7) is realized by the following Lemma:

**Lemma 3.4** (*[Swaroop 1994a]*)

*If  $h(t) > 0$ , then all the Input/Output induced norms are equal.*

**Proof:**

*Let  $\gamma_p$  be the  $p$ th induced norm, i.e.*

$$\gamma_p = \sup_{x \in L_p} \frac{\|y\|_p}{\|x\|_p} \quad (3.8)$$

*Then, from linear systems theory*

$$|H(0)| \leq \|\hat{H}(j\omega)\|_\infty \leq \gamma_p \leq \|h\|_1 \quad (3.9)$$

*If  $h(t) > 0$  then  $|\hat{H}| = \|h\|_1 \Rightarrow \gamma_p = \|h\|_1$ , as shown below,*

$$|\hat{H}(0)| = \left| \int_0^\infty h(t) dt \right| \leq \int_0^\infty |h(t)| dt = \|h\|_1$$

■

**Remark 3.5** *As mentioned above, if  $h(t) > 0$ , and  $\|\hat{H}(s)\|_\infty \leq 1$ , results in string stability. However, if  $h(t)$  is not positive, then the condition  $\|\hat{H}(s)\|_\infty \leq 1 \Rightarrow \|\delta_{i-1}\|_2 \leq \|\delta_i\|_2$ , which means  $L_2$  string stability.  $L_2$  string stability ensures the energy in the signal  $\delta_{i-1}(t)$  is less than the energy in the signal  $\delta_i(t)$ , but it is not sufficient for the strong condition of  $\|\delta_{i-1}\|_\infty \leq \|\delta_i\|_\infty$  for string stability. Therefore,  $L_2$  string stability is less suitable for this type of applications.*

We use the condition of (3.7) instead of (3.5), because it is much easier to design the control system to ensure (3.7) is satisfied rather than to design the system to ensure (3.5) is satisfied. In the later Sections, the condition of (3.7) will be used to evaluate the proposed spacing policy for the vehicle longitudinal control system.

### 3.3.3 Traffic flow stability

As we have mentioned before, the traffic flow stability is a macroscopic characteristic of traffic flow dynamics. It is different from the conception of string stability. Normally, in the study of string stability, no vehicle enters or leaves the string is considered. However, in a macroscopic scale, traffic flow is the aggregation of strings and single vehicles in many sections of highway. Traffic flow stability deals with the evolution of aggregate velocity and density in response to addition and/or removal of vehicles from the flow.

For decades, in the fields of traffic dynamics, the functional relations between the traffic volume (vehicle current) and the traffic density (vehicle density) have highly attracted attention of traffic researchers. A well known relation between traffic volume (vehicle current) and traffic density (vehicle density), which is also called fundamental diagram, is shown in Fig. 3.3. At low densities, it shows the linear dependence of the traffic flow on the density, which denotes a free traffic (FT) state, i.e. the vehicles move freely at low density. In contrast, at high densities, the traffic flow decreases with increasing density, which denotes a congested traffic state [Nagatani 2002].

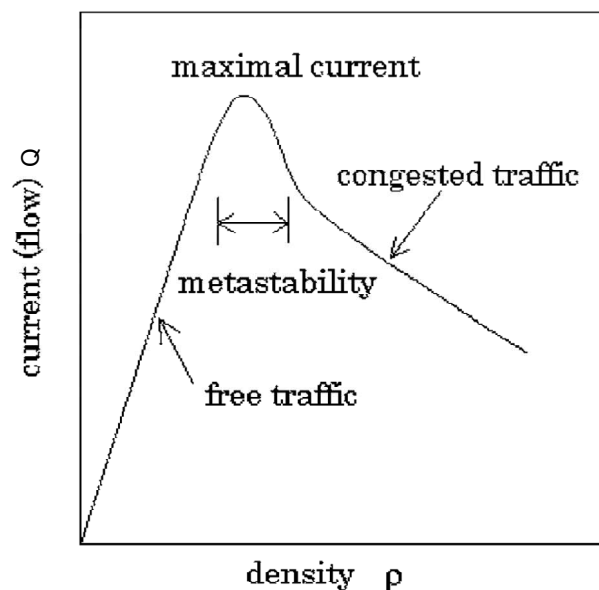


Figure 3.3: Fundamental diagram

In the late of 1980s, with the development of vehicular technology, the first generation of cruise control systems were developed from the point of view of driving comfort and safety. After that, Adaptive Cruise Control (ACC) system appeared, which is an extension of the standard cruise control system. As the ACC vehicles have the more similar longitudinal behaviors than the manual derived vehicles, the traffic dynamic characteristic of the automated traffic flow is thus deeply influenced by the ACC systems. Therefore, in the design of ACC control systems, its influence on the traffic dynamics is an important aspect to be considered.

### 3.3.3.1 Definition of traffic flow stability

The conception of traffic flow stability was proposed to evaluate the traffic flow dynamics [Swaroop 1999]. Traffic flow stability refers to the evolution of density and velocity disturbances. In this work, for the sake of simplicity, a one-lane highway will be considered with every vehicle on the highway is equipped with an ACC system. The traffic flow is modeled as a continuum.

Let  $x$  denotes the position of a vehicle at time  $t$ , i.e.,  $x = x(X, t)$ , where  $X$  is the state of the vehicle at some initial time,  $t_0$ . The velocity of the vehicle is given by  $v(x, t)$ .  $\rho(x, t)$  denotes the traffic density. Then the traffic flow stability is defined as [Swaroop 1999]:

**Definition 3.6 (Traffic flow stability).** Let  $v_0(x, t)$ ,  $\rho_0(x, t)$  denote the nominal state of traffic. Let  $v_p(x, t)$ ,  $\rho_p(x, t)$  be the velocity and density perturbations to the traffic, consistent with the boundary conditions and are such that  $v_p(x, 0) \equiv 0$ ,  $\rho_p(x, 0) \equiv 0 \quad \forall x \geq x_u$ . The traffic flow is stable, if

1. given  $\varepsilon > 0$ , there exists a  $\delta > 0$  such that

$$\sup_{x \leq x_u} \{|v_p(x, 0)|, |\rho_p(x, 0)|\} < \delta \Rightarrow \sup_{t \geq 0} \sup_{x \leq x_u} \{|v_p(x, t)|, |\rho_p(x, t)|\} < \varepsilon$$

and

2.  $\lim_{t \rightarrow \infty} \sup_{x \leq x_u} \{|v_p(x, t)|, |\rho_p(x, t)|\} = 0$

The concept of traffic flow stability can be illustrated by Fig. 3.4. A traffic density perturbation of the main lane happens in the entrance of the inlet ramp due to the inlet traffic joins into the main lane. An unstable traffic flow implies that such a density perturbation are felt by every point upstream from the source without attenuation. While, in a stable traffic flow, this perturbation attenuates when it propagates upstream.

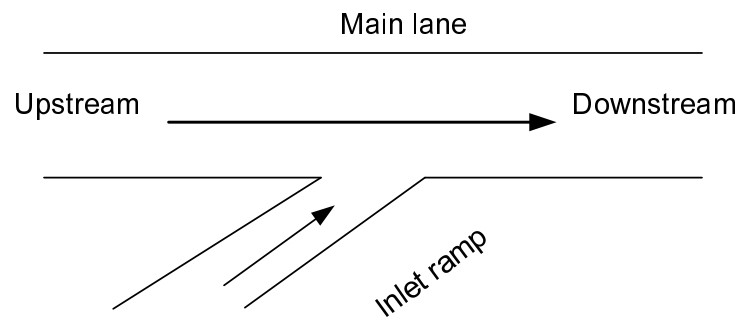


Figure 3.4: Main lane and inlet ramp

In the following sections, the above definition will be used to judge traffic flow stability of the automated highway traffics.

### 3.3.3.2 Effect of spacing policy on traffic flow stability

As mentioned in previous sections, the spacing policy denotes the desired spacing that an automated vehicle attempts to maintain with respect to the preceding vehicle. Clearly, spacing policy has an important effect on the traffic flow dynamics by regulating the spacing of the ACC vehicles. In order to analyze its effect on the traffic flow dynamics, consider the spacing policy is a function of the vehicle velocity,

$$S = g(v) \quad (3.10)$$

where,  $S$  is the desired spacing for the controlled vehicle. Then, this relation can be translated as the following equation:

$$\frac{1}{\rho} = g(v) \Rightarrow v = h(\rho) := g^{-1}\left(\frac{1}{\rho}\right) \quad (3.11)$$

Similarly to the fluid dynamics, traffic volume at any point is given by

$$Q = \rho v = \rho h(\rho) \quad (3.12)$$

According to the conservation of mass equation, the evolution of traffic density is represented as

$$\frac{\partial \rho}{\partial t} + \frac{\partial Q}{\partial x} = 0 \Rightarrow \frac{\partial \rho}{\partial t} + \frac{\partial Q}{\partial \rho} \frac{\partial \rho}{\partial x} = 0 \quad (3.13)$$

Substituting for  $Q$  from equation (3.12)

$$\frac{\partial \rho}{\partial t} + \frac{\partial(\rho h(\rho))}{\partial \rho} \frac{\partial \rho}{\partial x} = 0 \quad (3.14)$$

Considering the above partial equation, let  $\rho_0$  be a base solution for the density. In order to study the stability of the base solution, consider some density perturbations  $\varepsilon \rho_p$  to the base solution. Neglecting second-order terms in  $\varepsilon$  and defining  $c$  as

$$c := h(\rho_0) + \rho_0 \frac{\partial h}{\partial \rho}(\rho_0) \quad (3.15)$$

(Note that  $c = \frac{\partial Q}{\partial \rho}$ ). We get

$$\frac{\partial \rho_p}{\partial t} + c \frac{\partial \rho_p}{\partial x} = 0 \quad (3.16)$$

Equation (3.16) describes the evolution of a density disturbance of the traffic flow. Thus, the behavior of the solution to the linear partial differential equation (3.16) depends on the sign of  $c$ . It is clear that the sign of  $c$  is dependent on the density of base flow,  $\rho_0$ .

The solution of equation (3.16) is a traveling wave, i.e.,  $\rho_p = F(x - ct)$ . If  $c > 0$ , the solution is a forward traveling wave. If  $c < 0$ , the solution is a backward traveling wave. Thus, in the traffic flow dynamics, when  $c < 0$ , arbitrarily small density disturbances are propagated upstream without any attenuation. According to the Definition 3.6, the traffic flow is thus unstable when  $c < 0$ . In contrast, the traffic flow stability can be ensured when  $c > 0$ .

According to the above discussions, we can draw the conclusion that if the condition  $c > 0$  or  $\partial Q / \partial \rho > 0$  is satisfied, then the traffic flow is a stable traffic flow, otherwise, an unstable traffic flow. This conclusion will be used in the subsequent sections in the design and evaluation of different spacing policies.

### 3.3.4 Evaluation of the Constant Time Gap spacing policy

At present, the most common spacing policy used by researchers and vehicle manufactures is the constant time-gap (CTG) spacing policy [Wang 2004a]. Much research works have been done in the study of ACC system with CTG spacing policy [Marsden 2001, Nouveliere 2003, Ioannou 1994]. And some manufactures have more recently launched their ACC systems based on CTG algorithm [McDonald 1999]. However, there still exists some problems in the use of CTG algorithm:

- Using the CTG policy, the current cruise control system isn't suitable for use in high-density traffic conditions, and the operating speed should be higher than 40

km/h [Marsden 2001, Zhao 2007].

- Using the standard CTG policy, traffic flow stability cannot be ensured [Swaroop 1999].

### 3.3.4.1 The Traditional Constant Time-gap (CTG) Spacing Policy

The constant time-gap spacing policy is given by:

$$S_i = L + h\dot{x}_i \quad (3.17)$$

where  $S_i$  denotes to the desired inter-vehicle spacing for the  $i$ th vehicle,  $L$  is a constant that includes the vehicle length  $W_{i-1}$  of the preceding vehicle as shown in Fig.3.5.  $h$  is the headway time.

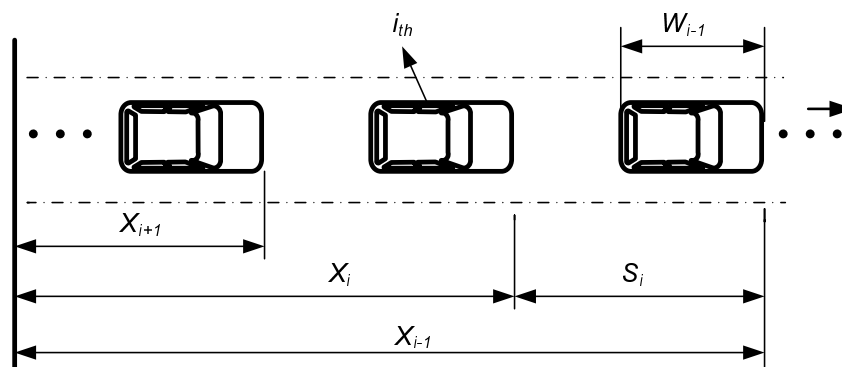


Figure 3.5: Vehicle platoon

The spacing error under the CTG policy is given by:

$$\delta_i = \varepsilon_i + L + h\dot{x}_i \quad (3.18)$$

where  $\varepsilon_i = x_i - x_{i-1}$ .

The corresponding longitudinal controller ensuring that the spacing error converges to zero is described by

$$\ddot{x}_{i\_des} = -\frac{1}{h}(\dot{\varepsilon}_i + \lambda\delta_i) \quad (3.19)$$

### 3.3.4.2 String stability of CTG

In Section 3.2, we have shown that the ACC control architecture is designed to be hierarchical, with an upper and a lower level controller, as shown in Fig. 3.1. The upper level

controller determines the desired acceleration or speed for the controlled vehicle, while the lower level controller decides the throttle and brake commands required to track the desired acceleration or speed. The behavior of this two level control system can be approximated by a first-order system:

$$\tau \dot{a}_i + a_i = a_{i\_des} \quad (3.20)$$

where  $a_i$  is the vehicle's actual acceleration,  $a_{i\_des}$  is the desired acceleration, and  $\tau$  is a constant time lag.

Substituting  $a_{i\_des}$  from equation (3.19), we get

$$\tau \ddot{x}_i + \dot{x}_i = -\frac{1}{h}(\dot{\varepsilon}_i + \lambda \delta_i) \quad (3.21)$$

Differentiating  $\delta_i$  twice from equation (3.18), we get

$$\ddot{\delta}_i = \ddot{\varepsilon}_i + h \ddot{x}_i \quad (3.22)$$

Substituting for  $\ddot{x}_i$  from equation (3.21),

$$\ddot{\varepsilon}_i = \ddot{\delta}_i + \frac{1}{\tau}(\dot{\delta}_i + \lambda \delta_i) \quad (3.23)$$

Consider equation (3.18), the difference between errors of successive vehicles can be give by

$$\delta_i - \delta_{i-1} = \varepsilon_i - \varepsilon_{i-1} + h \dot{\varepsilon}_i \quad (3.24)$$

Differentiating equation (3.24) twice,

$$\ddot{\delta}_i - \ddot{\delta}_{i-1} = \ddot{\varepsilon}_i - \ddot{\varepsilon}_{i-1} + h \ddot{\varepsilon}_i \quad (3.25)$$

Using equation (3.23) to rewrite equation (3.25), we obtain

$$h\tau \ddot{\delta}_i + h\ddot{\delta}_i + (1 + \lambda h)\dot{\delta}_i + \lambda \delta_i = \dot{\delta}_{i-1} + \lambda \delta_{i-1} \quad (3.26)$$

Taking the laplace transform of equation (3.26), we get

$$\frac{\delta_i}{\delta_{i-1}}(s) = \frac{s + \lambda}{h\tau s^3 + hs^2 + (1 + \lambda h)s + \lambda} \quad (3.27)$$

By using the above transfer function, the string stability of CTG system can be analyzed. Substituting  $s = j\omega$  and evaluating the magnitude of the above transfer function,

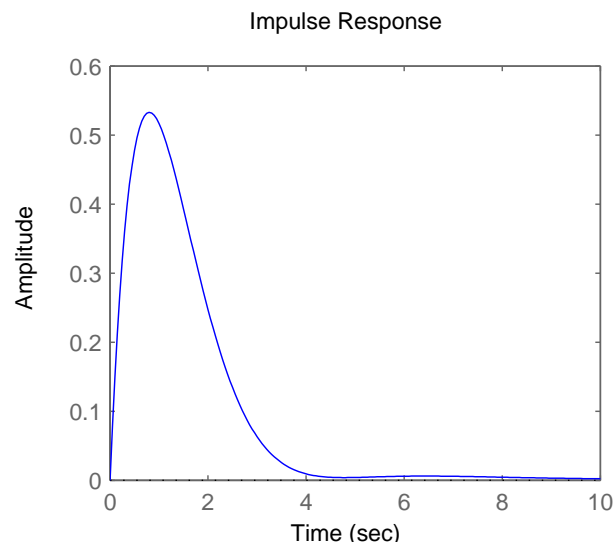


Figure 3.6: Impulse response of the CTG system

it can be shown that the condition ( $\|\hat{H}(s)\|_\infty \leq 1$ ) is ensured only if

$$h \geq 2\tau \quad (3.28)$$

According to the string stability condition shown in equation (3.7), the condition that impulse response  $h(t) > 0$  should also be satisfied. Figure 3.6 shows the impulse response of the transfer function in equation (3.27) with the values of  $\lambda = 0.4$ ,  $\tau = 0.4$  and  $h = 1.5$  s. The impulse response is positive for these values of the transfer function parameters. Therefore, the string stability condition  $\|\hat{H}(s)\|_\infty \leq 1$  and  $h(t) > 0$  can be ensured by this choice of controller parameters.

In fact, the requirement  $\|\hat{H}(s)\|_\infty \leq 1$  can be satisfied by choosing a sufficient big value of  $h$  based on equation (3.28). However, for the specification that impulse response  $h(t) > 0$ , there are no results available that provide a direct design method for ensuring this specification, and it needs to be studied further. The results in [Darbha 2003] show an indirect method for this issues, two necessary conditions are proposed for the non-negative impulse response,

1. The dominant poles of the system should not be a complex conjugate pair.
2. There should not be any zeros of the system that are completely to the right of all poles of the closed-loop system.

### 3.3.4.3 Traffic flow stability of CTG

For the CTG policy, the steady-state spacing is given by  $S = L + hv$ , where  $v$  is aggregate highway velocity, and  $h$  is the headway time, this lead to a steady density of

$$\rho = 1/(L + hv) \quad (3.29)$$

Solving  $v$  in terms of  $\rho$  from (3.29), one can get  $v = (1 - \rho L)/(\rho h)$ , and the traffic flow is

$$Q = \rho v = (1 - \rho L)/h \quad (3.30)$$

As we have shown in section 3.3.3.2 that the condition  $\partial Q/\partial \rho > 0$  should be satisfied for a stable traffic flow. In equation (3.30) the variable  $\partial Q/\partial \rho = -L/h$  is a negative value, which means the CTG policy is always traffic flow unstable.

**Remark 3.7** *The results of Shrivastava and Li [Shrivastava 2000, Li 2002] have shown that the CTG policy could ensure traffic flow stability, which appeared to be contrary to the above conclusion that we have just made. In fact, according to [Shrivastava 2000, Li 2002], traffic flow stability of the CTG system is proofed to be stable in a circular highway without inlets and exits. The premise of road condition can be viewed as a boundary condition for the stability of CTG system. However the specification  $\partial Q/\partial \rho > 0$ , which we used in this work, can be viewed as a condition for stable traffic flow without any boundary conditions. Thus the traffic stable with this condition is called unconditional traffic flow stability.*

### 3.3.5 Proposed Safety Spacing Policy

According to the above evaluation results of the traditional CTG policy, and comparing them to the design objectives for the upper level controller proposed in section 3.3.1, it is shown that the CTG policy is not appropriate for the Adaptive Cruise Control systems.

In order to overcome the shortcomings of the CTG policy, we propose a new spacing policy named ‘‘Safety Spacing Policy’’, which considers both the information of the controlled vehicle’s state (speed, inter-vehicle spacing) and capacity (braking capacity, reaction time) to maintain a safety headway from the vehicle ahead. In addition, the specifications of string stability and traffic flow stability will also be considered in the design of this new policy. It is expected that this new spacing policy would satisfy the design objectives that we proposed in section 3.3.1.

To begin with, a vehicle platoon is shown in Fig. 3.5. We assume that the following information is available for the controlled vehicle:

- A1: The relative velocity and relative distance between the  $i - 1$ th and  $i$ th vehicle, i.e.  $v_{i-1} - v_i, x_{i-1} - x_i - W_{i-1}$ .
- A2: The velocity of the controlled vehicle  $i$ , i.e.  $v_i$ .
- A3: The braking capacity  $j_i$  of controlled vehicle.

**Remark:** Currently available on board radar and sensors can provide measurements given in A1, A2. And the value of A3 can be obtained from the vehicle manufactures or by experiments.

By using the measurements given in A1-A3, we propose the following safety spacing policy (SSP).

$$S_i = L + t_d \dot{x}_i + \gamma d_i \quad (3.31)$$

where :

- $S_i$ : Desired inter-vehicle spacing for the  $i$ th vehicle.
- $L$ : A constant distance that includes the vehicle length  $W_{i-1}$  of the preceding vehicle.
- $t_d$ : The time delay of the longitudinal control system. It consists of two components: One is the time used for recognizing a hard brake in the controller. In current system, the duration of this time delay is about 60ms; The other is the time delay in the brake hardware, which ranges from 10 to 100 ms. Thus the total time delay ranges from 70 to 160ms [Hedrick 1996].
- $d_i$ : The  $i$ th vehicle's braking distance on horizontal and dry pavement. Let  $j_i$  be the average deceleration value of the  $i$ th vehicle during the maximum brake action, which is always a negative value. Then  $d_i = -\dot{x}_i^2 / (2j_i)$ .
- $\gamma$ : Safety coefficient, a parameter that could be selected by the driver, which is relevant to road condition and vehicle position in a platoon. For instance, we can select a bigger value of  $\gamma$  if the road surface is wet. In addition, considering the leading vehicle has the greatest impact on safety of a platoon, we give a bigger value of  $\gamma$  for the leading vehicle to improve platoon safety, while we select a smaller  $\gamma$  for the following vehicles thus to improve traffic capacity. In Fig. 3.7, the inter-vehicle spacing is shown as a function of velocity under different Safety coefficient  $\gamma$ . The using parameters are shown in Table 3.1.

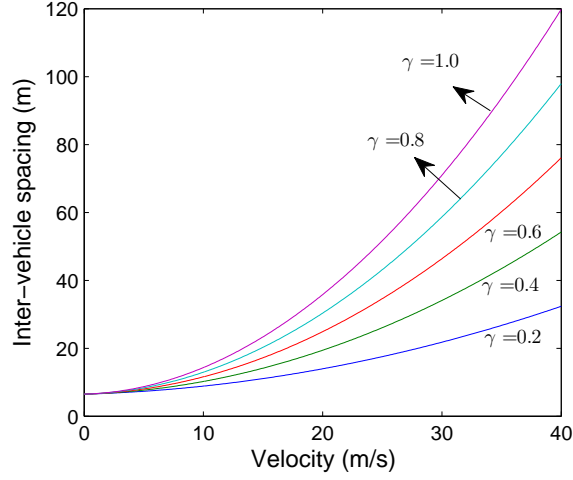


Figure 3.7: Inter-vehicle spacing with different safety coefficients  $\gamma$

Then, the spacing error of SSP is given by

$$\delta_i = \varepsilon_i + L + t_d \dot{x}_i + \gamma d_i \quad (3.32)$$

where  $\varepsilon_i = x_i - x_{i-1}$ . In order to ensure the error  $\delta_i$  converges to zero, the dynamic of  $\delta_i$  is set as  $\dot{\delta}_i = -\lambda \delta_i$ , where  $\lambda$  is a positive control gain. Differentiating (3.32), the desired acceleration with the SSP can be obtained as

$$\ddot{x}_{i\_des} = -(\lambda \delta_i + \dot{\varepsilon}_i) / (t_d - \frac{\gamma}{j_i} \dot{x}_i) \quad (3.33)$$

Table 3.1: Parameters for longitudinal controller

Parameters	L	$w_i$	$t_d$	$\lambda$	j
Value	6.5 m	4.5 m	0.1 sec	0.4	-7.32 m/s <sup>2</sup>

### 3.3.5.1 String stability of SSP

At first, in Section 3.2, we have shown that the ACC control architecture is designed to be hierarchical, with an upper and a lower level controller, as shown in Fig. 3.1. The upper level controller determines the desired acceleration or speed for the controlled vehicle, while the lower level controller decides the throttle and brake commands required to track the desired acceleration or speed. The behavior of this two level control system can be approximated by a first-order system:

$$\tau \dot{a}_i + a_i = a_{i\_des} \quad (3.34)$$

where  $a_i$  is the vehicle's actual acceleration,  $a_{i\_des}$  is the desired acceleration, and  $\tau$  is a constant time lag. Then, this first order system will be used in the analysis of the string stability of the SSP system.

Recall equation (3.7), the condition for the string stability of vehicle following system is :

$$\|\hat{H}(s)\|_\infty \leq 1 \quad \text{and} \quad h(t) > 0 \quad (3.35)$$

where  $\hat{H}(s)$  is the transfer function relating the spacing errors of consecutive vehicles,  $\hat{H}(s) = \delta_i(s)/\delta_{i-1}(s)$ ,  $h(t)$  is the impulse response of  $\hat{H}(s)$ .

In order to investigate the string stability property of the proposed spacing policy, the SSP system is linearized around a nominal velocity  $v_0$ , i.e.  $v_{0,i} = v_{0,i+1} = v_0$ . And the inter-vehicle spacing is equal to the desired spacing  $R_{0,i} = L + t_d v_0 - \frac{\gamma}{2j_i} v_0^2$ . At a certain moment, the velocity of the leading vehicle is perturbed, thus introduce disturbance to the tail of the platoon. Let  $v_i = v_0 + \Delta v_i$ ,  $\dot{v}_i = \Delta \dot{v}_i$ , and  $R_i = R_0 + \Delta R_i$ ,  $\dot{R}_i = \Delta \dot{R}_i$ , then for linearized systems the transfer function of the spacing error is the same as that of the velocity variation [Zhou 2005]:

$$\hat{H}(s) = \frac{\delta_i}{\delta_{i-1}}(s) = \frac{\Delta v_i}{\Delta v_i}(s) \quad (3.36)$$

Combine (3.34) and (3.33), we can get

$$\tau \dot{a}_i + a_i = -\frac{\lambda \delta_i + \dot{\epsilon}_i}{t_d - \frac{\gamma}{j_i} \dot{x}_i} \quad (3.37)$$

Let  $T_v = t_d - \frac{\gamma}{j_i} \dot{x}_i$ . Rewrite (3.37):

$$\tau \dot{a}_i + a_i = -\frac{\lambda \delta_i + \dot{\epsilon}_i}{T_v} \quad (3.38)$$

Under the assumption that deviations from the nominal velocity is small, and the SSP system is linearized around the nominal speed, differentiating (3.38) to obtain

$$\tau \ddot{a}_i + \dot{a}_i = -\frac{\lambda \dot{\delta}_i + \ddot{\epsilon}_i}{T_v} \quad (3.39)$$

Then we get

$$T_v\tau\ddot{v}_i + T_v\ddot{v}_i + (\lambda T_v + 1)\dot{v}_i + \lambda v_i = \dot{v}_{i-1} + \lambda v_{i-1} \quad (3.40)$$

Using the relation  $\dot{v}_i = \Delta\dot{v}_i$  that we mentioned above, equation 3.40 can be rewritten as:

$$T_v\tau\Delta\ddot{v}_i + T_v\Delta\ddot{v}_i + (\lambda T_v + 1)\Delta\dot{v}_i + \lambda\Delta v_i = \Delta\dot{v}_{i-1} + \lambda\Delta v_{i-1} \quad (3.41)$$

Taking Laplace transforms of (3.41),

$$\frac{\Delta v_i}{\Delta v_{i-1}}(s) = \frac{s + \lambda}{T_v\tau s^3 + T_v s^2 + (\lambda T_v + 1)s + \lambda} \quad (3.42)$$

Substituting  $s = j\omega$  in equation (3.42),

$$\frac{\Delta v_i}{\Delta v_{i-1}}(j\omega) = \frac{\lambda + j\omega}{-T_v\tau j\omega^3 - T_v\omega^2 + (\lambda T_v + 1)j\omega + \lambda} \quad (3.43)$$

In order to ensure the string stability, the magnitude of the transfer function should no bigger than 1, i.e.  $\|\frac{\Delta v_i}{\Delta v_{i-1}}(s)\| \leq 1$ . Then we obtain,

$$\frac{\omega^2 + \lambda^2}{(\lambda - T_v\omega^2)^2 + \omega^2(\lambda T_v + 1 - T_v\tau\omega^2)^2} \leq 1 \quad (3.44)$$

Following algebraic reduction, it can be shown that this inequality constraint is always satisfied if

$$T_v \geq 2\tau \quad (3.45)$$

i.e.  $t_d - \frac{\gamma}{j_i}\dot{x}_i \geq 2\tau$ . Thus, by using the linearization method, one condition for the string stability of the nonlinear spacing policy was obtained. For example, for the set of values as  $t_d = 0.1s$ ,  $\tau = 0.1s$ ,  $\gamma = 0.4$ , and  $j_i = -7.32m/s^2$ , the condition (3.45) is satisfied if  $v \geq 1.83m/s$ .

Another condition for string stability is  $h(t) > 0$ , as shown in equation (3.45). Consider the transfer function shown in equation (3.42), we use the following values:  $t_d = 0.1s$ ,  $\tau = 0.1s$ ,  $\gamma = 0.4$ ,  $j_i = -7.32 m/s^2$ ,  $\lambda = 0.4$ . Then the impulse responses of the transfer function (equation (3.42)) at different velocities can be obtained and shown in Fig. 3.8.

One can find, the condition  $h(t) > 0$  is not satisfied when the velocity  $v = 2 m/s$ , however, with the increasing of vehicle velocity, when velocity is higher than  $5 m/s$ , the

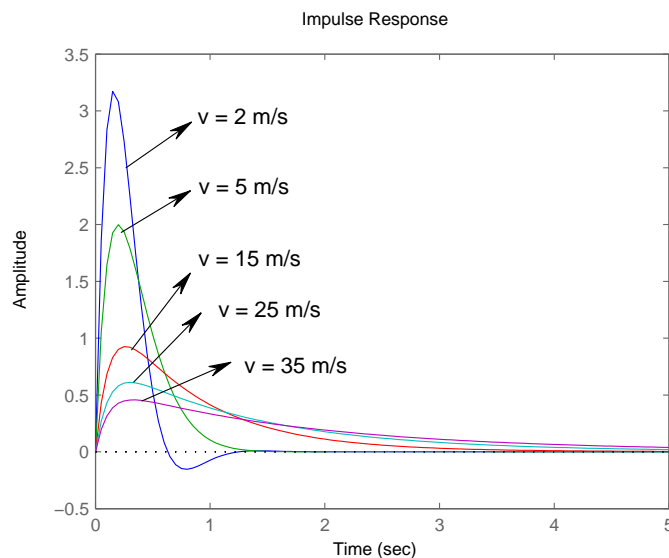


Figure 3.8: Impulse responses at different velocities of the SSP system

condition  $h(t) > 0$  is then always satisfied. Combine with the requirement of  $v > 1.83 \text{ m/s}$  for the condition  $\|\hat{H}(s)\|_\infty \leq 1$ , thus, in our SSP system, the final string stability condition is  $v > 5 \text{ m/s}$ .

### 3.3.5.2 Traffic flow stability of SSP

In the traffic analysis, it is assumed that all the automated vehicles possess the same braking capacity  $j$ . Recall the expression of the SSP policy given in equation (3.31),

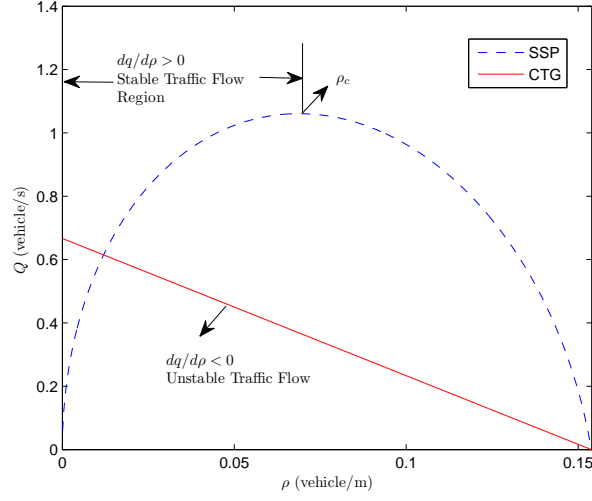
$$S_i = L + t_d v_i - \frac{\gamma v_i^2}{2j}$$

Then the traffic density at steady state is given by

$$\rho = \frac{1}{L + t_d v - \gamma v^2 / (2j)} \quad (3.46)$$

Solve equation (3.46) for  $v$  in terms of  $\rho$ . Two solutions can be obtained. Since a negative value of velocity is not acceptable for highway operation, we eliminate the negative solution. The positive solution is given by

$$v = j \frac{t_d - \sqrt{t_d^2 + 2\gamma(L - 1/\rho)/j}}{\gamma} \quad (3.47)$$


 Figure 3.9:  $Q - \rho$  curves of the CTG and SSP

Then we obtain the traffic flow

$$Q = \rho j \frac{t_d - \sqrt{t_d^2 + 2\gamma(L - 1/\rho)/j}}{\gamma} \quad (3.48)$$

So that

$$\frac{\partial Q}{\partial \rho} = \frac{t_d j}{\gamma} - \frac{j\rho[t_d^2 - 2\frac{\gamma}{j}(\frac{1}{\rho} - L)] + \gamma}{\gamma\rho\sqrt{t_d^2 - 2\frac{\gamma}{j}(\frac{1}{\rho} - L)}} \quad (3.49)$$

In order to show the advantages of SSP than CTG in the aspect of traffic flow stability, the  $Q - \rho$  (Traffic flow - Density) curves of the two policies are shown in Fig. 3.9. The parameters' values for the SSP are shown in Table 3.1, and the safety coefficient  $\gamma = 0.4$  is set for the SSP system. For the CTG system, the relationship between  $Q$  and  $\rho$  is shown in equation (3.30), and the time headway  $h = 1.5$  s is used for the plot in Fig. 3.9.

One can find that the SSP system holds a stable traffic flow ( $\partial Q/\partial \rho > 0$ ) when the density  $\rho$  is below a critical density  $\rho_c (\approx 0.069$  vehicle/m). However, the CTG system is always traffic unstable for  $\partial Q/\partial \rho < 0$ .

### 3.3.5.3 Traffic flow capacity comparison between SSP & CTG

In this subsection, we consider a highway pipe, a single lane highway without entrances and exits and estimate the maximum possible steady state flow in vehicles per lane per hour through such a pipe. We call this the AHS pipeline capacity [Godbole 2000]. Then, the two spacing policies will be compared using lane capacity in vehicles/lane/hour as a

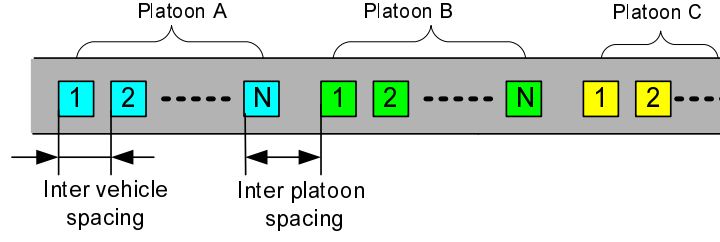


Figure 3.10: Single lane highway

measure. We assume that all the vehicles are driven in platoons which have the same size (number of vehicles). Each platoon contains  $N$  vehicles, and the inter-platoon spacing is determined by the leading vehicle's inter-vehicle spacing, as shown in Fig. 3.10.

In the case of CTG system, the headway time between 1 and 2 seconds has been widely accepted in the former research [Marsden 2001]. Thus, we choose the headway time  $h_l = 2$  s for the leading vehicle of a platoon and headway time  $h_f = 1.5$  s for all the following vehicles in a platoon. Here, we select a bigger headway time for the leading vehicle in consideration of improving platoon safety, and a smaller headway time for the following vehicles in consideration of improving traffic capacity. Then the line capacity is given by

$$Q_c = \frac{3600v}{(L + h_f v) + \frac{1}{N}(L + h_l v)} \quad (3.50)$$

In the case of SSP system, we assume that all the vehicles have the same braking capacity. Corresponding to the discussion in Section 3.3.5, we let the leading vehicle's safety coefficient  $\gamma_l = 1$ , and for the following vehicles,  $\gamma_f = 0.4$ . Then the lane capacity is:

$$Q_s = \frac{3600v}{(L + t_d v - \gamma_f \frac{v^2}{2j}) + \frac{1}{N}(L + t_d v - \gamma_l \frac{v^2}{2j})} \quad (3.51)$$

The lane capacities given by the two equations above are shown in Fig. 3.11 where  $N$  in the plot refers to the corresponding platoon sizes. One can find that the SSP system can provide more traffic capacity than the CTG system. When the aggregate traffic velocity is 100 Km/h (27.8 m/s), the SSP system has about 50% more traffic capacity than that of the CTG system.

Furthermore, as we know in the peak-hour traffic, the aggregate traffic velocity drops down due to the increase of traffic density. In Fig. 3.11, it can be found that with the velocity decreases, the capacity of the SSP system increase notably while that of the CTG system decreases gradually. That means the SSP system can relieve congestion in the peak hour while the situation becomes worse by using the CTG system. At the cruise speed

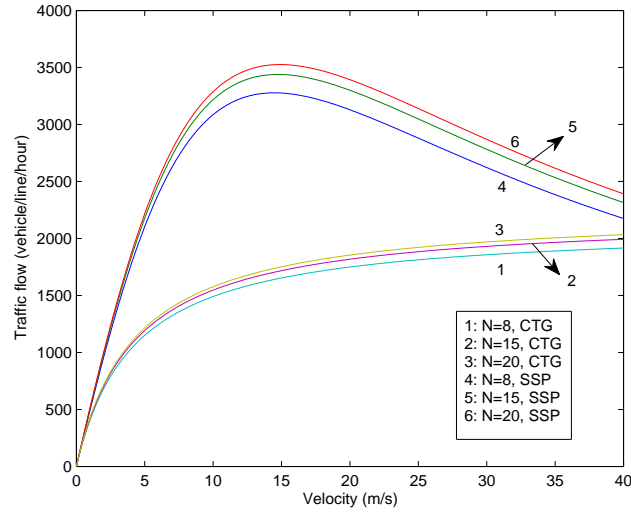


Figure 3.11:  $Q - v$  curves of CTG and SSP

of 50Km/h, the SSP control system can provide a traffic flow of 3518 vehicles/line/hour, about the double traffic flow than that of the CTG control system.

In conclusion, the SSP has the following advantages than the tradition CTG policy:

- The SSP can provide stable traffic flow while the CTG policy failed to do so.
- In the high speed operation, the SSP can provide higher traffic capacity than the CTG. At a common cruise speed of  $100km/h$ , the SSP system can provide about 50% more traffic capacity than the CTG system.
- A significant advantage of SSP is that with the traffic speed drops, the traffic capacity increases notably. This characteristic shows that the SSP can be used to relieve traffic congestion in the peak hour. However, the CTG can provide less traffic capacity in low speed than in high speed, which means the traffic situation becomes worse in peak hour.

### 3.3.6 Simulation tests

In this section, we test SSP vehicle platoon's behavior when the leading vehicle performs a hard brake and then acceleration scenario. The vehicle lateral movement isn't considered in this scenario. Three platoons of 8 vehicles with different braking capacities were considered as shown in Table 3.2, these values as well as the sequence of each vehicle are set randomly. The vehicle's maximum acceleration limit is assumed to be  $0.35g$ . In

simulation, all the following vehicles employ the same SSP controller that described in (3.33), and the safety coefficient  $\gamma = 0.4$  is used.

Table 3.2: Platoon vehicles' braking capacities ( $m/s^2$ )

	Vehicle No. in platoon							
	1	2	3	4	5	6	7	8
Platoon 1	-7.62	-7.32	-6.72	-7.08	-7.8	-6.9	-7.26	-6.54
Platoon 2	-7.93	-6.85	-7.42	-6.53	-7.84	-7.64	-7.18	-7.24
Platoon 3	-6.76	-7.88	-7.69	-7.42	-6.93	-7.61	-6.69	-7.17

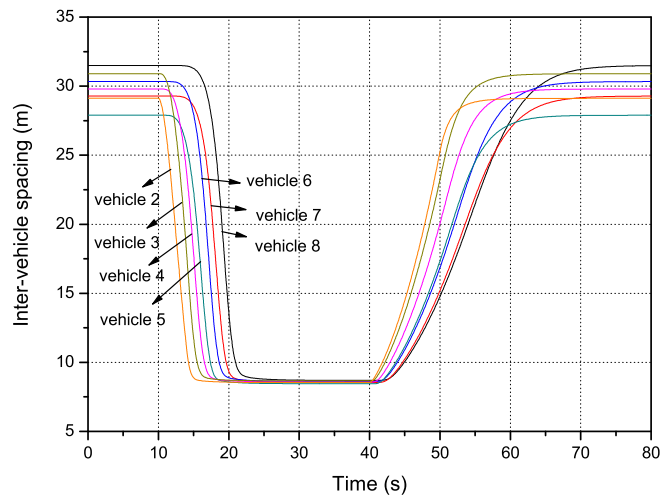
The platoon performs the following manoeuvres, starting from 27m/s with correct inter-vehicle spacing, after 10 seconds, the leading vehicle of the platoon decelerates with an acceleration of  $-5m/s^2$  for 4 seconds, and comes to a significant low speed of 7 m/s. At  $t = 40s$ , the leading vehicle accelerates back up to the initial speed with an acceleration of  $2m/s^2$ . Then we will test the following vehicles' behavior by using the SSP policy.

In order to avoid to get the results which do not exist in the real world, the following assumptions are made in this simulation test:

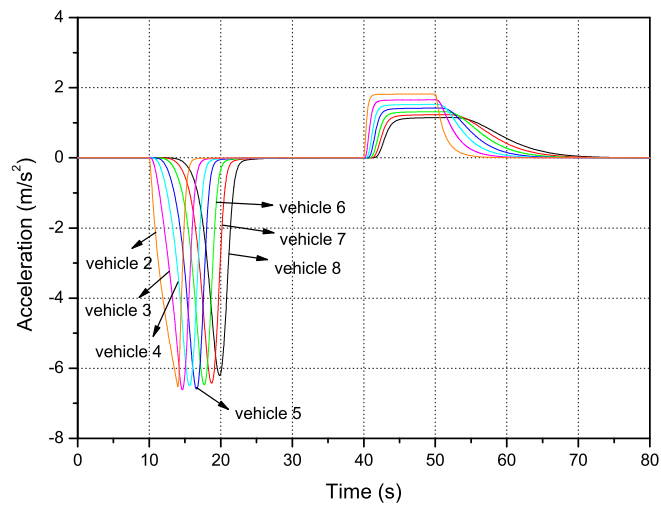
- In simulations, if the desired following vehicle's acceleration or deceleration calculated from the control law exceeds the vehicle's acceleration/deceleration limits, then the desired value is made to saturate at the appropriate limit.
- To prevent the vehicles from going backwards on highway, assume that the acceleration of each ACC vehicle becomes to zero as soon as the vehicle stops.
- To prevent the inter-vehicle spacing from being negative, the inter-vehicle spacing of two vehicles keeps zero after the two vehicles happen to collide.

Fig. 3.12(a), 3.12(b) show the time histories of the inter-vehicle spacing and the "ideal" control efforts of all the following vehicles in this hard brake and acceleration scenario with the experiment vehicle **platoon 1**. Fig. 3.12(a) shows that no matter in the deceleration or acceleration manoeuvres each vehicle can keep a safe headway according to its state and capacity, no collision occurs in this scenario. And it can also be found that all the controlled vehicle can be operated within their corresponding decelerate and accelerate capacity in Fig. 3.12(b).

From the above results, along with the analyses of string stability, traffic flow stability and traffic capacity in the previous three subsections, we can find that the proposed SSP



(a) Inter-vehicle spacing of the following vehicles



(b) Acceleration of the following vehicles

Figure 3.12: Results of longitudinal control

can satisfy the four design objectives that we proposed in section 3.3.1. Thus, we can draw the conclusion that the proposed SSP policy can provide good performances both in safety and in traffic capacity for the ACC system. And it has shown better performances than the traditional CTG policy. It is a promising policy to be implemented on ACC vehicle on today's highway.

**Remark 3.8** *In the case of using **Platoon 2** and **3**, the similar results as with **Platoon 1** could be obtained. So we don't show them respectively.*

## 3.4 Lower level control

### 3.4.1 Introduction

The vehicle longitudinal control system architecture is typically designed to be hierarchical, with an upper level and a lower level controllers as shown in Fig. 3.1 in section 3.2. In section 3.3, the issue of upper level controller was studied. In this section, the control problems of the lower level controller will be investigated. And then combine with the two level controllers, we will have a complete longitudinal control system for the automated vehicles.

The design objective of the lower level controller is to decide the required throttle and brake commands to track the desired acceleration/speed which is given by the upper level controller. Obviously, the basic elements of the lower level controller are the throttle controller and brake controller. Two main challenges to be envisaged in the lower level controller design are:

- The nonlinearities and uncertainties in vehicle longitudinal dynamics
- Coordination between the throttle and brake controllers (since a good human driver never uses the throttle and brake pedals simultaneously)

To handel with the model nonlinearities and uncertainties, a combined engine and brake control system based on multiple-surface sliding control method is presented in [Gerdes 1997]. The proposed system consists three basic elements: an upper sliding controller that incorporates vehicle acceleration as a synthetic input, a logic switch that chooses between throttle or brake control, and lower sliding controllers for the engine and brake operations. In [Ioannou 1993], fixed gain and gain scheduling PID controllers as well as the adaptive control method are proposed. The controllers are simulated using a

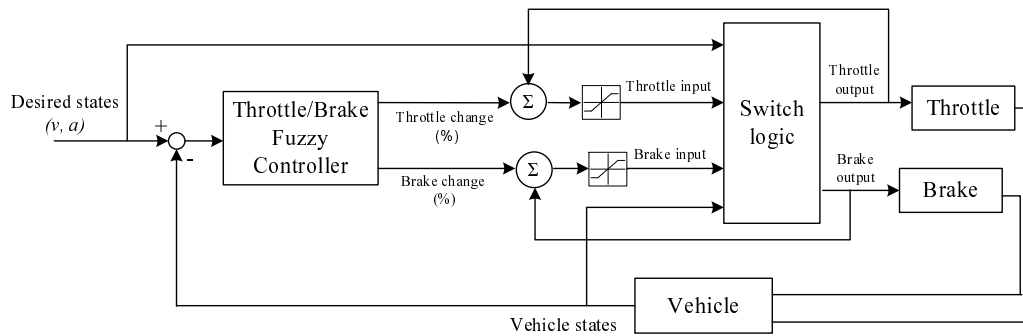


Figure 3.13: Coordinated throttle and brake control system diagram

validated full order nonlinear longitudinal model and tested also on a real vehicle, and the results are satisfied. However, in order to use these PID based controllers, an exact throttle angle to vehicle speed and position model is required as a premise. To get this model, it needs a lot of experiments to determine the required parameters and in some cases it is confidential.

The fuzzy logic is also proposed for this subject. In [Naranjo 2006], a throttle and brake fuzzy control system is proposed to perform the ACC+Stop&Go maneuvers. Two separate fuzzy controllers are designed to control the throttle and brake pedals. In order to avoid simultaneous actions of both the pedals, the values of the membership functions of the two controllers are well defined. The constant time gap spacing policy is used to give the desired spacing for the controlled vehicle. This system has been equipped in a two-vehicle platoon. The results show that the automated vehicle behave very similarly to human-driven car and is adaptive to the speed variations.

Since the using of the fuzzy control approach has the main advantages of no requirement of an exact mathematic model of the controlled system, such as vehicles, where the exact engine and brake dynamics are not always available; and it uses the linguistic expressions to represent the human drivers experiences instead of the mathematical expressions [Naranjo 2006, Zhao 2009a]. Inspired by this, we propose a fuzzy logic control system to perform the throttle/brake control, and a logic switch is used to coordinate the two controllers.

## 3.4.2 Coordinated Throttle and Brake Fuzzy Controller

### 3.4.2.1 Coordinated Throttle and Brake Fuzzy Control System Architecture

To cope the design problems of the lower level controller, we propose a coordinated throttle and brake control system as shown in Fig. 3.13.

At first, a fuzzy logic controller is designed for the task of throttle control. The fuzzy input variables are the *speed error*  $E_v$  and the *acceleration error*  $E_{acc}$ , and the output variable is the *throttle change*  $\Delta Th$ . In order to facilitate the expression in this work, we use the percentage value for the throttle control signals, where 0% means the throttle valve is fully closed, while 100% means fully opened. Then, the current throttle percentage  $Th(n)$  is the summation of the *throttle change*  $\Delta Th(n)$  and the throttle percentage at the previous time step  $Th(n - 1)$ , where  $n$  denotes the time step number of discrete process:

$$Th(n) = \Delta Th(n) + Th(n - 1) \quad (3.52)$$

Second, from the similar consideration, a fuzzy controller is also proposed for the brake control. Since, for a human driver, the fundamental operation logic for the brake pedal is just the opposite to the throttle pedal, we use the same fuzzy controller that is used in the throttle control. The only difference between the two controllers is the output variable of the brake controller *brake torque change*  $\Delta Br(n)$  is always negative to the output of the throttle controller  $\Delta Th(n)$ , i.e.

$$\Delta Br(n) = -\Delta Th(n) \quad (3.53)$$

Similarly, the current brake torque percentage is given by:

$$Br(n) = \Delta Br(n) + Br(n - 1) \quad (3.54)$$

where,  $Br(n)$  and  $Br(n - 1)$  are the values of brake percentage at  $n$ th and  $(n - 1)$ th time step respectively, and 0% means no brake action, while 100% means the maximum brake action.

Next, after each fuzzy controller, there exists a saturation block as shown in Fig.3.13. The lower and upper limits of these saturation blocks are set to 0 and 1 respectively, which ensure the throttle and brake percentage do not exceed the range of [0,1].

Finally, a Switch Logic Block is designed to avoid the simultaneously operation of throttle and brake, and to ensure the smooth coordination between the two controllers.

### 3.4.2.2 Throttle and Brake Fuzzy Controllers

We begin with the throttle controller. The base knowledge of the fuzzy throttle controller, formed by the inputs, outputs, rules and inference method, is detailed as follows.

**Input and output variables:** The two fuzzy inputs variables, *acceleration error*

$E_{acc}$  and speed error  $E_v$ , are given by:

$$E_{acc} = a_{des} - a \quad (3.55)$$

$$E_v = v_{des} - v \quad (3.56)$$

where,  $a_{des}$  and  $v_{des}$  denote the desired acceleration and speed which are given by the upper level controller.  $a$  and  $v$  mean the real acceleration and speed of the controlled vehicle, which can be obtained from the on board sensors. The output variable of the throttle controller is the *throttle change (%)*:  $\Delta Th$ .

We define five fuzzy sets for both the two inputs, as  $Nb$ ,  $Ns$ ,  $Null$ ,  $Ps$  and  $Pb$ . And also five fuzzy sets for the output, as  $D\_inten$ ,  $D\_sof$ ,  $Null$ ,  $A\_sof$  and  $A\_inten$ , described as follows:

$$\{E_{acc}, E_v\} = \{Nb, Ns, Null, Ps, Pb\} \quad (3.57)$$

$$\{\Delta Th\} = \{D\_inten, D\_sof, Null, A\_sof, A\_inten\} \quad (3.58)$$

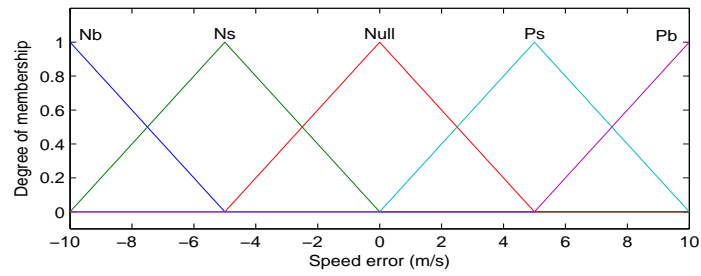
Figure 3.14(a), 3.14(b) and 3.14(c) show the input and output variables' membership functions. The values that we give to each fuzzy set are derived from expert experiences and simulation experiments.

**Fuzzy rule base:** The expert's knowledge and experience are represented by a fuzzy rule base, with the fuzzy control rules in the form of "IF (premise) THEN (consequent)". The proposed fuzzy control rule base is shown in Table 4.5.

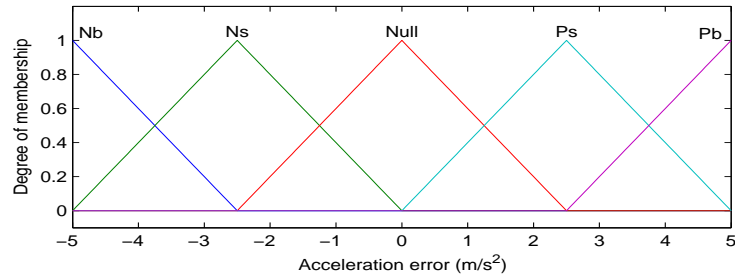
**Fuzzy Reasoning Process:** The fuzzy reasoning process can be divided into three steps: fuzzification, inference engine and defuzzification. In this work, we use triangle and trapezoids shaped membership function for the fuzzification process as shown in Fig. 3.14. The Mamdani's inference method is employed to solve the fuzzy implication. And we use the centroid method for defuzzification process.

Table 3.3: Fuzzy Rule Base

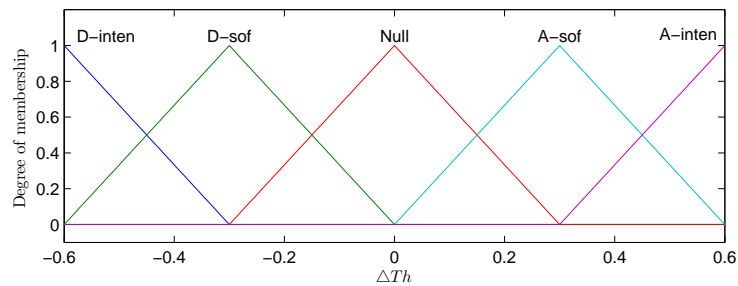
		Input 2: Acceleration Error				
		Nb	Ns	Null	Ps	Pb
Input 1:	Nb	D-inten	D-inten	D-sof	D-sof	Null
Speed	Ns	D-inten	D-sof	D-sof	null	A-sof
Error	Null	D-sof	D-sof	Null	A-sof	A-sof
	Ps	D-sof	Null	A-sof	A-sof	A-inten
	Pb	Null	A-sof	A-sof	A-inten	A-inten



(a) Input 1: Speed error



(b) Input 2: Acceleration error



(c) Output: Throttle change

Figure 3.14: Variables of fuzzy throttle controller

Concerning the brake controller, we use the same fuzzy logic controller that is used for the throttle control. The only difference is the output variable, as we have mentioned in Section 3.4.2.1. Now we can find the advantage of choosing the percentage measurement for the output variables of both the throttle and brake controllers: in fact, the throttle angle and the brake torque are two variables that have different physic meanings and different scales. By using the measurement of “percentage”, we can unify the two output values into the same value range  $[0,1]$ , thus, to allow us to simplify the throttle and brake controllers into one controller. The relationship between the two output variables is just given by (3.53).

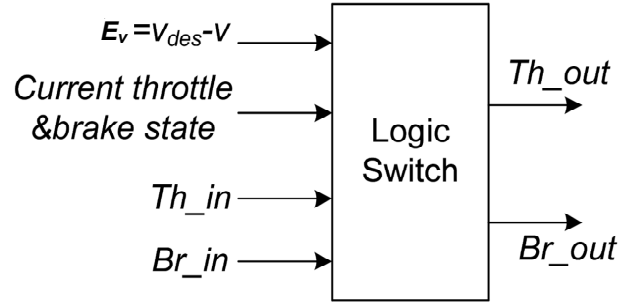


Figure 3.15: Block diagram of logic switch

### 3.4.2.3 Switch Logic Between Throttle and Brake

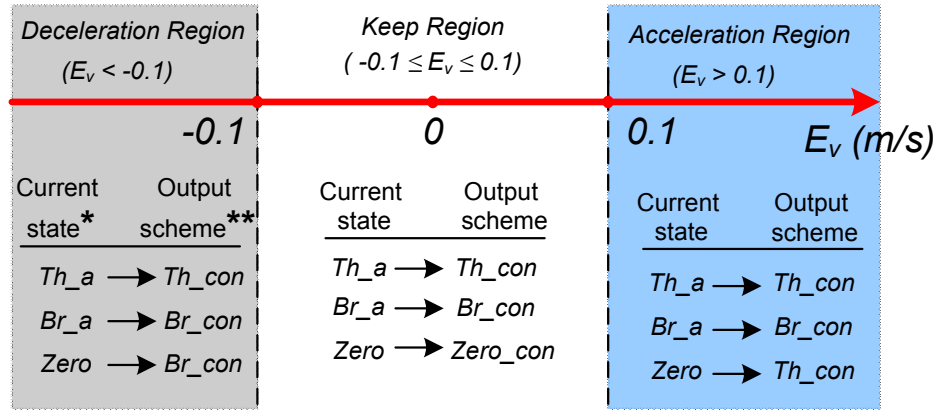
In the previous subsections, we designed the throttle and brake controllers, which can be considered as two separate systems working simultaneously. Now, the logic switch is designed to coordinate the operations of the throttle and brake. The basic functions of the logic switch are:

- avoid simultaneous operation at both throttle and brake pedals
- before step down the throttle, it needs to step off the brake, vice versa
- avoid frequent switchings from one pedal to the other

To achieve these functions, our approach is to synthesize the information of speed error  $E_v$  ( $E_v = v_{des} - v$ ) and the current throttle&brake state as well as the throttle input  $Th\_in$  ( $Th\_in = Th(n)$ ) and brake input  $Br\_in$  ( $Br\_in = Br(n)$ ). Then, a switch logic is employed to decide the throttle and brake output  $Th\_out$  and  $Br\_out$ . The logic switch diagram is shown in Fig. 3.15.

Our switch logic is inspired by the human driver's operation logic. The details of our switch logic are shown in Fig. 3.16. At first, using the variable  $E_v$  (m/s), we divide the total operation region into three sub-regions as, *Deceleration region*, where  $E_v < -0.1$ , *Acceleration region*, where  $E_v > 0.1$ , and *Keep region*, where  $-0.1 \leq E_v \leq 0.1$ .

For each region, there is a corresponding switch logic. The switch logic is expressed by a series of judgment rules in the form of "If (premise) Then (consequence)". Take the *Deceleration region* as an example, there are totally three rules. (1) if the current throttle/brake state is  $Th\_a$ , which means the throttle pedal is being operated, then we choose the Output scheme  $Th\_con$ , which denotes  $Th\_out = Th\_in$  and  $Br\_out = 0$ . It means to decrease throttle input to decelerate the vehicle (the descriptions of *Current throttle/brake state* and *Output scheme* is detailed in the footnotes of Fig. 3.16); (2) if the



\* three throttle/brake states are :  $Th_a$  (throttle control active),  $Br_a$  (brake control active), Zero (neither throttle nor brake is active); these states are determined by the current value of  $Th_{out}$ , and  $Br_{out}$ , if  $Th_{out} > 0.01$ , it denotes the state  $Th_a$ , if  $Br_{out} > 0.01$ , it denotes the state  $Br_a$ , otherwise is the state Zero

\*\* three output schemes are:  $Th_con$ ,  $Br_con$ ,  $Zero_con$ ; where  $Th_con$  means using throttle control, thus  $Th_{out} = Th_{in}$  and  $Br_{out} = 0$ ;  $Br_con$  means using brake control, thus  $Th_{out} = 0$  and  $Br_{out} = Br_{in}$ ;  $Zero_con$  means zero action in both throttle and brake

Figure 3.16: Switching regions and conditions

current throttle/brake state changes to  $Br_a$  or  $Zero$ , then it uses the Output scheme  $Br_con$ , which denotes  $Th_{out} = 0$  and  $Br_{out} = Br_{in}$ . It means to press down the brake pedal to decelerate.

A “Keep region” is designed to avoid frequent switchings between the throttle and brake actuators. In this region, the Output scheme always keeps in accordance with its current state, as shown in Fig. 3.16. We can find that the procedures from  $Zero$  state to  $Th_con$  or to  $Br_con$  are forbidden when the speed error falls into  $[-0.1, 0.1]$ , hence to avoid frequent switchings between the two controllers.

In the *Acceleration region*, the switch logic works in a similar way as in the *Deceleration region*. Due to the page limit, we do not give the details.

Finally, the above described switch logic can be represented by the flowchart shown in Fig. 3.17. It should be noted that in the process of judging the current state of throttle (brake) pedal, a threshold value of 0.01 is used. It means if the current value of throttle (or brake) value is bigger than 0.01, i.e.  $Th_s > 0.01$ , then the current state is throttle (or brake) active:  $Th_a$  (or  $Br_a$ ). If neither of them is bigger than 0.01, than we consider the current sate as *ZERO*.

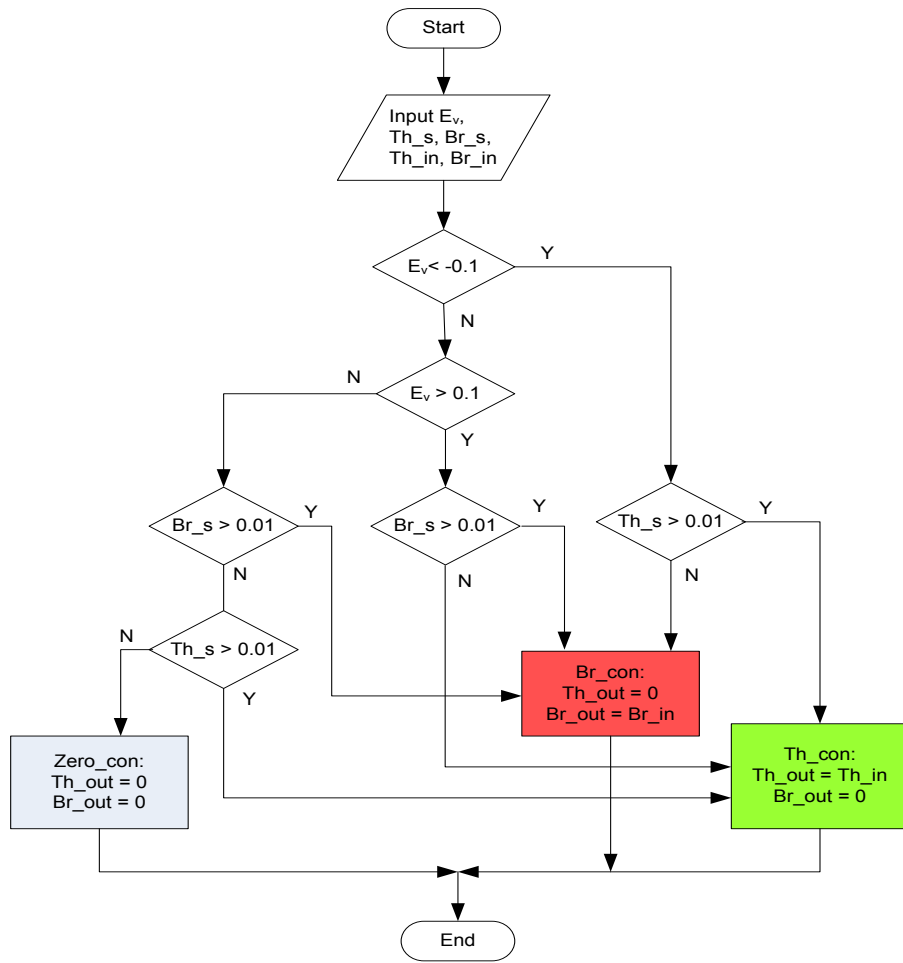


Figure 3.17: Flowchart of switch logic

### 3.4.3 Simulation tests

A two-vehicle platoon is considered. The lead vehicle is a manually-driven vehicle, and the following vehicle is an automatic vehicle equipped with the proposed longitudinal control system, which includes the upper level controller that we proposed in equation (3.33) and the lower level controller that we proposed in 3.4.2.2.

The leading vehicle performs a series of operations to change its longitudinal speed, then we test the performances of the longitudinal control system by evaluating the following vehicle's speed, acceleration and inter-vehicle spacing (headway distance), as well as the associated errors, etc. The simulation scenarios are designed to be rather "complex", which include high and low speed cruise, acceleration and deceleration. Furthermore, since the road grade can be regarded as the external disturbances, extended simulations with inclined road conditions are also carried out to test the robustness of the proposed control system.

### 3.4.3.1 Longitudinal vehicle model for simulation

A vehicle longitudinal car model is shown in Fig. 3.18 [Ioannou 1993]. There are two control inputs as throttle command and brake command, and the outputs are the vehicle speed and acceleration. The vehicle lateral movement is not considered in this model.

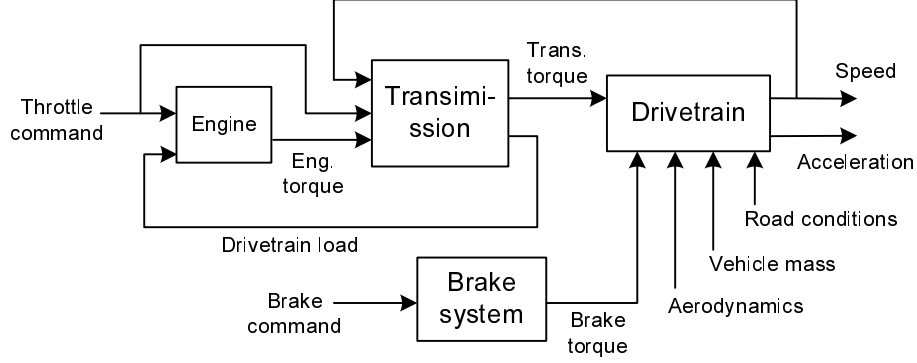


Figure 3.18: Longitudinal car model

In this model, the basic parts of vehicle are considered as subsystems with various inputs and outputs. These subsystems include Engine, Torque converter, Gearbox, Drive shaft and final drive.

Recall the vehicle longitudinal dynamic equation (2.43),

$$\ddot{x}\left(m + \frac{J_{wf} + \bar{J}_{wr}}{r_{eff}^2}\right) = \frac{1}{r_{eff}}(T_e \Psi R_g R_f - T_b - T_y) - \frac{1}{2} \rho C_d A_F V_x^2 - mg \sin(\alpha)$$

Then, the vehicle model shown in Fig. 3.18 can be described by the vehicle longitudinal simulation model shown in Fig. 2.15, which has been developed and validated in section 2.3.3.

### 3.4.3.2 Horizontal road condition

The horizontal road condition is first considered. The simulation scenario is described as follows: at beginning, the two vehicle run at a constant speed of 10m/s and the following vehicle has 5.6m headway spacing from the leader. From  $t = 5s$  to  $t = 17s$ , the leading vehicle's speed is gradually increased to a high speed of 26 m/s, and then keeps this speed till to  $t = 30s$ . After that, it begins to decelerate, at  $t = 42s$ , the speed is decreased to 5m/s. Successionally, from  $t = 42s$  to  $t = 53.3s$ , the leading vehicle accelerates back to a high speed of 20 m/s, and then keeps this speed. The profile of the leading vehicle's

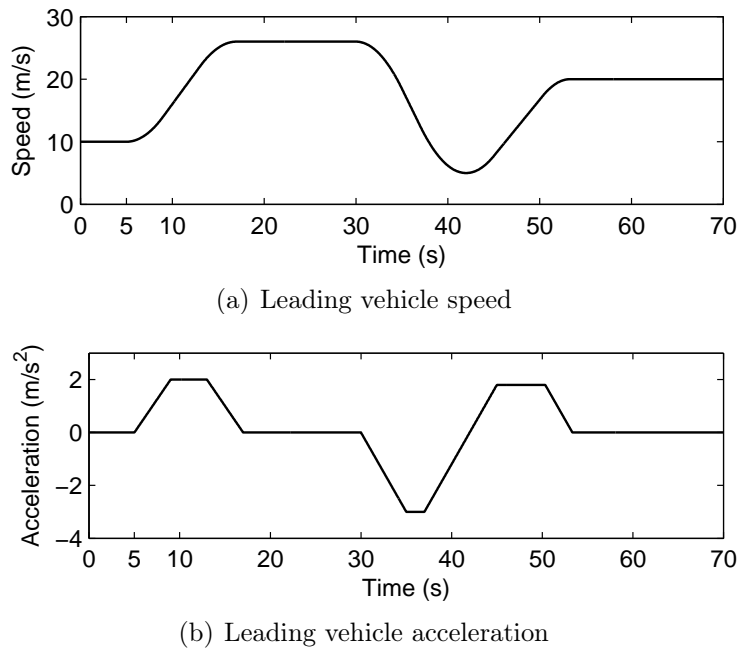


Figure 3.19: Leading vehicle's speed and acceleration

speed and acceleration are detailed in Fig. 3.19(a), 3.19(b).

The following vehicle's speed and speed error ( $\Delta v = v_{des} - v$ ) are shown in Fig. 3.20(a), 3.20(b). It is clear from these figures that, in the whole test period, good velocity tracking is achieved by the throttle/brake fuzzy controller. The speed error is less than  $0.15 \text{ m/s}$ .

Figures 3.21(a), 5.4(b) show the time history of the inter-vehicle spacing and the spacing error between the two vehicles respectively. The following vehicle can always keep a safe spacing from the proceeding one, which is decided by the Safety Spacing Policy (SSP) described in (3.33). The maximum spacing error is always less than  $0.25 \text{ m}$ , which means the vehicle safety is ensured during this test.

Figures 3.22(a), 3.22(b) and 3.22(c) show the final control results of the throttle, the brake and the gear shift operations respectively. We can find that the throttle and the brake work coordinately. There is neither simultaneous operations nor frequent switching between the two actuators during the entire period. In addition, the operations of the throttle and brake are rather smooth except several little oscillations in the throttle results. In fact, the main reason for these little oscillations is the gear shift-up operations in the hydraulic automatic transmission as shown in Fig. 3.22(c).

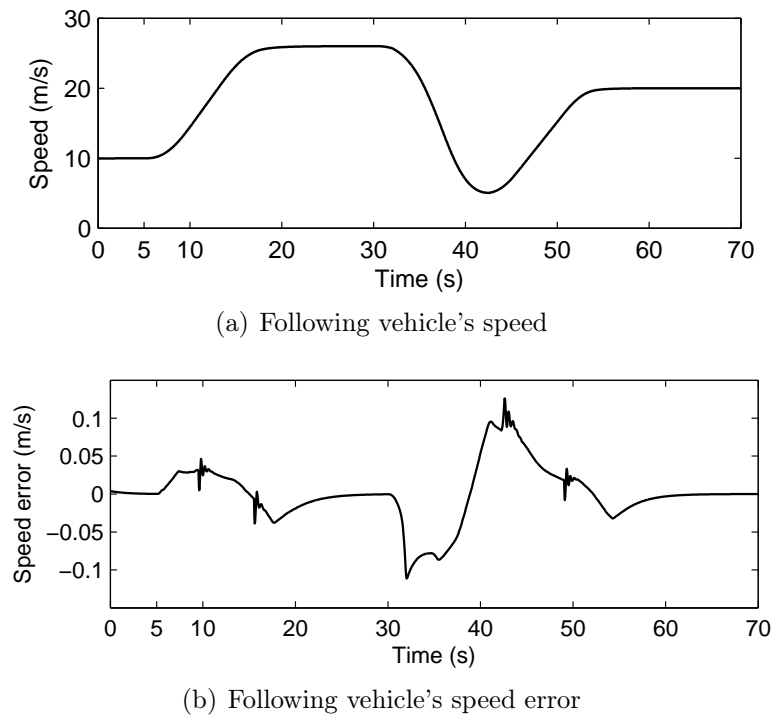


Figure 3.20: Following vehicle's speed and speed error

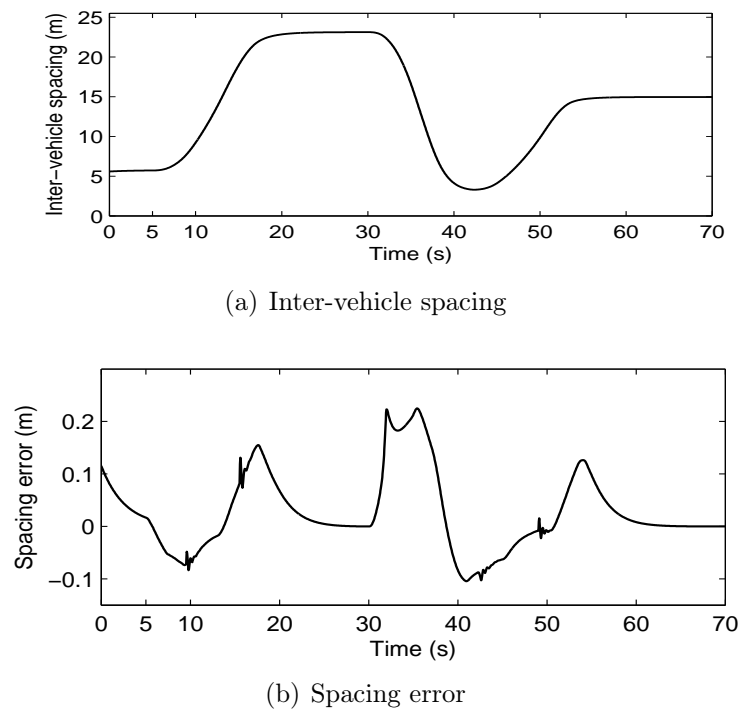


Figure 3.21: Inter-vehicle spacing and spacing error

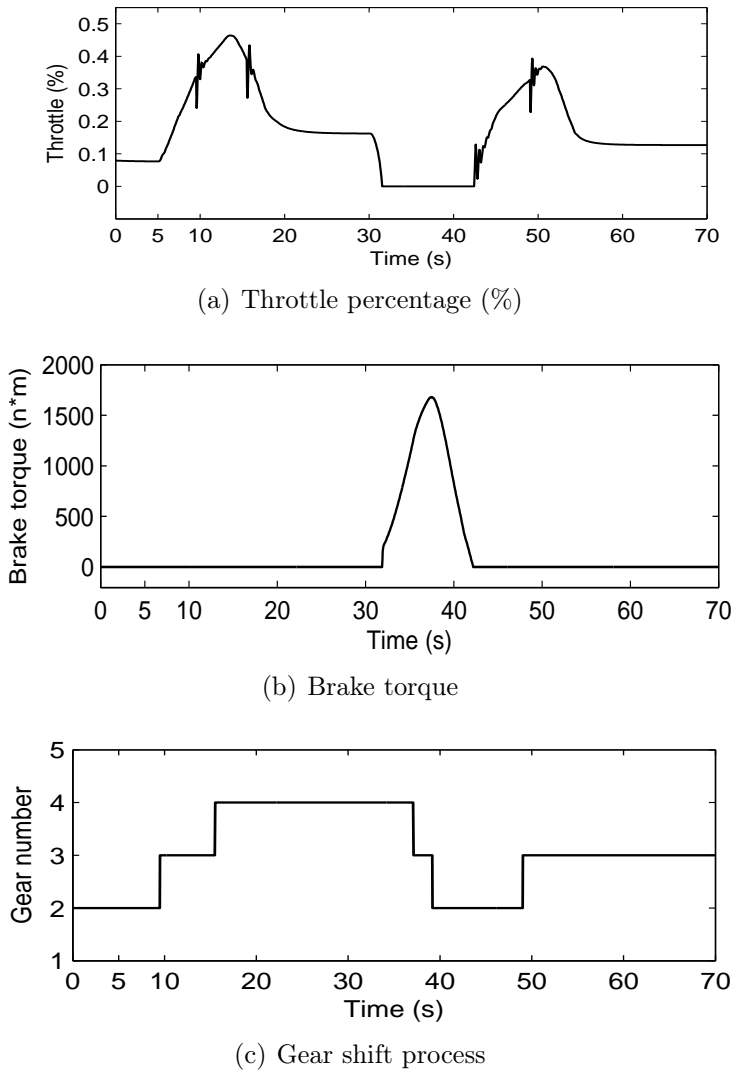


Figure 3.22: Control results of throttle and brake (horizontal road)

### 3.4.3.3 Inclined road condition

In this simulation, the road grade is considered. We use the same two-vehicle platoon and the same leading vehicle scenario that we used in the former simulation. The road grade is described as follows: for the following vehicle, from  $t = 0s$  to  $t = 5s$ , the road is horizontal, from  $t = 5s$  to  $t = 25s$ , it is a downhill with a grade of  $-2\%$ , from  $t = 25s$  to  $t = 55s$ , the road becomes to a uphill with a grade of  $3\%$ , after that, the road becomes to horizontal again. The road grade profile is given in Fig. 3.23(a).

The results of the following vehicle's speed error and spacing error are given in Fig. 3.23(b), 3.23(c). It is shown that good speed tracking and space keeping are achieved by the throttle/brake fuzzy controller even with the road disturbances. The maximum

speed error is less than  $0.2m/s$  and that of the spacing error is less than  $0.25m$ .

The control efforts of throttle and brake are shown in Fig. 3.24(a), 3.24(b) respectively. It is shown that the proposed control system is adaptive to the variations of road grade. The throttle and brake controller work coordinately.

## 3.5 Conclusion

In this chapter, we concentrated on the vehicle longitudinal control system design. The longitudinal control system architecture was designed to be hierarchical, with an upper level controller and a lower level controller.

In the upper level controller design, the spacing policy and its associated control law were designed with the constraints of string stability, traffic flow stability and traffic flow capacity. A safety spacing policy (SSP) was proposed, which uses both the information of vehicle state and vehicle braking capacity to determine the desired spacing from the preceding vehicle. It was shown that the proposed SSP could ensure both the string stability and traffic flow stability. In addition, through the comparisons between the SSP and the traditional Constant Time Gap (CTG) policy, we could find the obvious advantages of the SSP system in improving traffic capacity especially in the high-density traffic conditions.

In the lower level controller design, a coordinated throttle and brake fuzzy controller was proposed. This controller can deal with the nonlinearity in the engine and brake dynamic systems. And a logic switch was designed to avoid frequent switching between the two actuators and simultaneous operations of them.

The above proposed longitudinal control system was validated to be effective through a series of simulations.

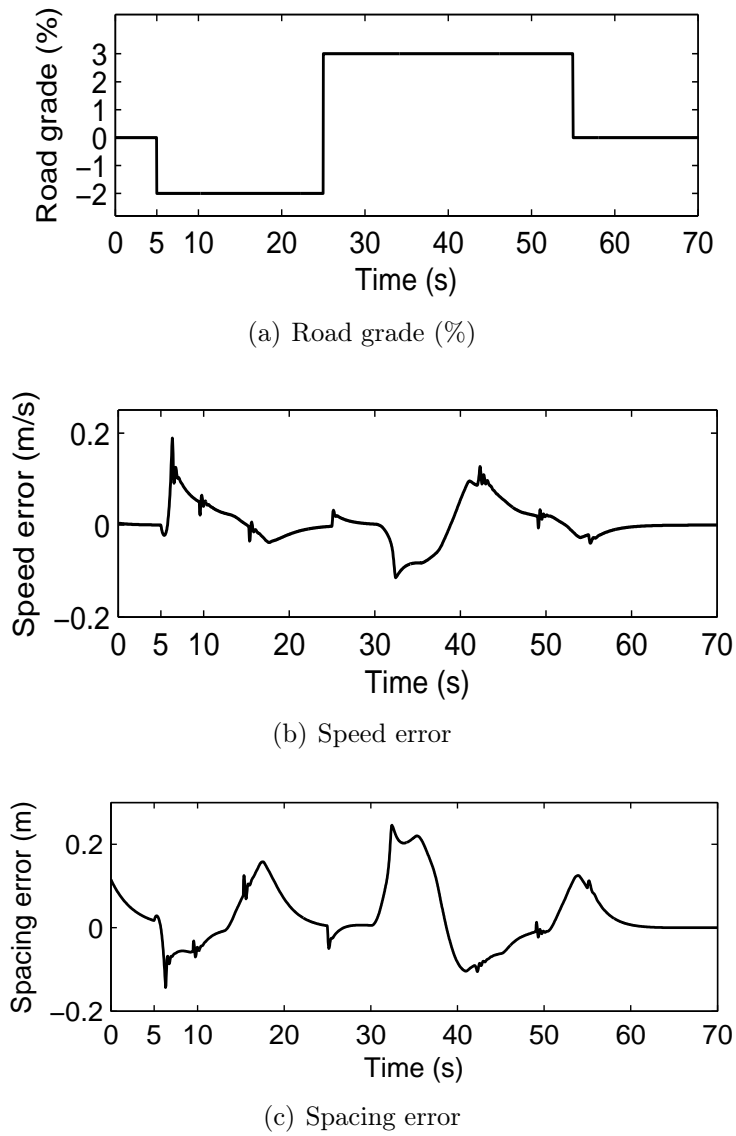
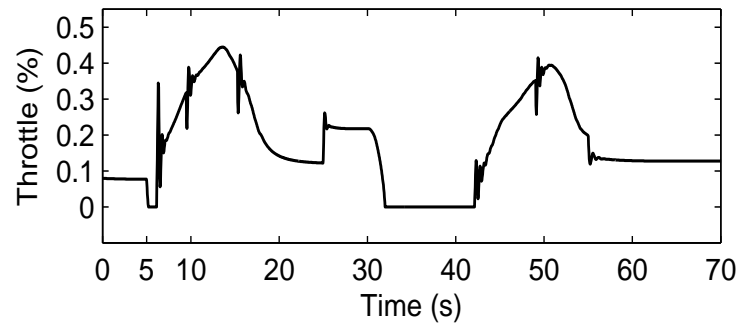
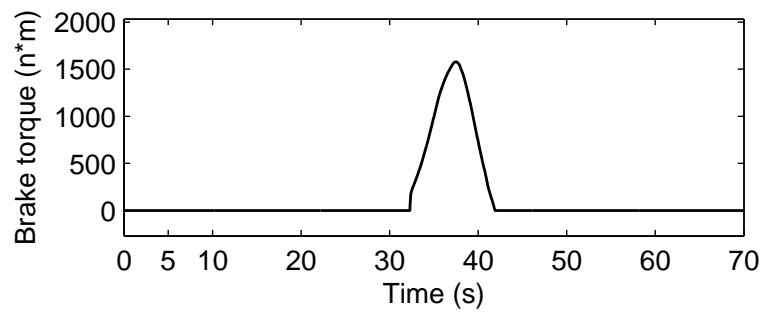


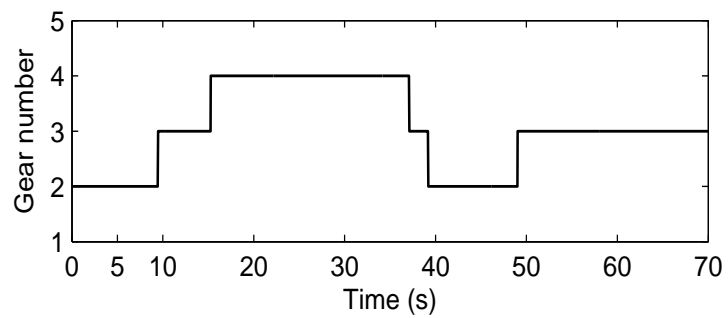
Figure 3.23: Road grade, speed error and spacing error (inclined road)



(a) Throttle percentage (%)



(b) Brake torque



(c) Gear shift process

Figure 3.24: Control results of throttle and brake (inclined road)



# Chapter 4

## Vehicle Lateral Control

### Contents

---

<b>4.1</b>	<b>Introduction</b>	<b>106</b>
<b>4.2</b>	<b>Methodology-Multiple model approaches</b>	<b>109</b>
4.2.1	Introduction	109
4.2.2	The operating regime approach& multiple model/controller approach	110
<b>4.3</b>	<b>Architecture of lateral control system</b>	<b>115</b>
<b>4.4</b>	<b>Analysis of vehicle lateral dynamics</b>	<b>117</b>
4.4.1	Bicycle Model	117
4.4.2	Open-Loop Response to the Parameter Variations	117
<b>4.5</b>	<b>Lateral controller design</b>	<b>119</b>
4.5.1	PID with anti-windup	120
4.5.2	Fuzzy control for vehicle steering	124
4.5.3	Multi-model fuzzy control	128
4.5.4	Virtual desired trajectory for lane change maneuver	133
<b>4.6</b>	<b>Simulation tests</b>	<b>134</b>
4.6.1	Test 1: Lane keeping control at different speeds (1)	135
4.6.2	Test 2: Lane keeping control at different speeds (2)	135
4.6.3	Test 3: Lane keeping control under different loads and Cornering Stiffness	137
4.6.4	Test 4: Lane changing scenarios at different speeds	137

4.6.5 Test 5: Lane changing scenarios under different loads and Cornering Stiffness . . . . .	140
<b>4.7 Conclusion . . . . .</b>	<b>141</b>

---

## 4.1 Introduction

According to the statistics of road fatalities provided by A.A.S.H.T.O.<sup>1</sup>, lane departures are the number one cause of fatal accidents, and account for over 25,000 deaths annually, almost 60% of the total deaths in the highway crashes in the United States, as shown in Fig. 4.1. It was also reported that the average crash rate in the curves is about 3 times that for straight segments. And studies have shown that the driver-related human error is involved in over 90% of highway traffic accidents [A.A.S.H.T.O 2008].

In the past two decades, the Automated Highway System (AHS)- with the main goal of eliminating traffic congestion and enhancing traffic safety - has seen significant progresses. Vehicle lateral control is one of the crucial subsystems for the AHS vehicles. It senses the road centerline using a road based reference system and other on-board sensors and generates steering command to keep the vehicle running along the desired path or steer the vehicle into an adjacent lane. The design requirement of vehicle lateral control is to ensure small lateral errors and small relative yaw angles while maintaining ride comfort under different conditions. Lane-keeping and lane-changing are the two basic functions of vehicle lateral control system [Huang 2005, Shladover 1991b].

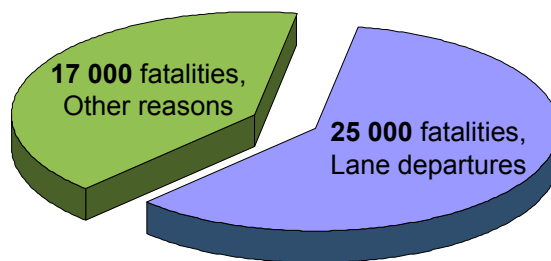


Figure 4.1: Road fatalities in U.S.A.

A lane keeping system automatically controls the steering to keep the vehicle in its lane and also follow the lane as it curves around. In [Fenton 1988], Fenton R.E. and Selim

---

<sup>1</sup>A.A.S.H.T.O.: American Association of State Highway and Transportation Officials

I designed a velocity-adaptive lateral controller using an optimization approach. The resulting controller, which is nonlinear with velocity, requires full-state feedback and thus an observer is included. In [Choi 2001], the vehicle is steered to follow the reference yaw rates which are generated by the deviations of lateral distance and the yaw angle between the vehicle and the reference lane. A PI controller was designed to minimize the error between the reference yaw rate and the measured one. In [Taylor 1999], three vision-based lateral control strategies: lead-lag control, full state feedback and input-output linearization were introduced and compared through a series of experiments. Although these unique model based approaches can lead to acceptable control results, their performance may be too sensitive to model mismatch and unmodeled dynamics. Besides, some controllers such as sliding mode solutions in [Zhang 2000], H-infinity controller in [Chaib 2004], and the self-turning regulator in [Netto 2004], appear rather complex for realtime embedded control of autonomous vehicles.

The lane changing system automatically steers the vehicle from the current lane to an adjacent lane. In fact, lane changing and lane keeping maneuvers become virtually identical when the lateral sensor can measure its location in both lanes. One major solution is Look-ahead lateral reference/sensing system (e.g. machine vision system). It can provide a long and wide range measurement of vehicle lateral displacement. By using this measurement, the lateral controller mimics human driver's behavior to perform the lane changing maneuver, see [Taylor 1999, Lee 2002]. However, the reliability of machine vision system is susceptible to variations in light or inclement weather conditions. The fact that Look-down lateral reference/sensing system (e.g. magnetic markers installed in the center of highway) improves the reliability of the sensing system can be another solution. But it suffers from the small sensor range. In this case, the lane changing control problem becomes complicated as the lateral sensing system cannot sense both lanes and the vehicle must travel a certain distance without seeing the road reference system.

The virtual desired trajectory (VDT) for a lane change operation is then designed considering passenger's ride comfort and transition time. Four candidate trajectories as (1) circular trajectory (2) cosine trajectory (3) 5th order polynomial trajectory, and (4) trapezoidal acceleration trajectory were evaluated using the transition time as a performance index, the lateral acceleration and jerk as constraints, and vehicle speed as a design parameter. The trapezoidal acceleration trajectory is selected to be the optimal trajectory [Chee 1994, Hedrick 1994]. By using VDT, the lane change maneuver is then investigated as a lane tracking problem. In this way, we consider using an uniform control algorithm to perform the lane tracking tasks for both the lane keeping and the lane

changing, so as to make the lateral control system simpler and more compact.

Considering the vehicle lateral dynamic system is a typical system where driving models, sensorial information, objectives, constraints, and control actions are under uncertainty, see [Naranjo 2008], in this work, a multi-model fuzzy controller is proposed. We choose this method for two main reasons. On one hand, there are two main advantages in fuzzy logic control: (1) The possibility of effective usage of drivers' knowledge and skills using linguistic control rules. (2) The lack of requirements for a quantified model of the control vehicles, see [Lee 1999]. In [El Kamel 2002], the authors have proposed a knowledge-based fuzzy controller for lateral guidance of buses during final approach, which involve a nonlinear model and uniquely 40 rules. On the other hand, the multi-model control appears as a powerful technique to deal with complex, non-linear and/or ill-defined systems, and is a potential solution for systems with large parameter variations. In [EL KAMEL 2000a, EL KAMEL 2000b], the multi-model approach was studied, and a multi-model controller for the vehicle longitudinal control has been suggested [El Kamel 2005]. Therefore, we propose a multi-mode fuzzy controller, and expect to combine the strong points of these two methods.

Based on the above discussions, the following design objectives are proposed for the vehicle lateral control system:

1. It can provide a framework in which the divers lateral operation scenarios can be performed (such as lane keeping, lane changing, overtaking...)
2. It can ensure small lateral errors and small relative yaw angles while maintaining ride comfort under different operations.
3. It is robust to variations of vehicle parameters (such as velocity, load mass, tyre cornering stiffness, road conditions ... )

The following of this chapter is organized as follows: section 4.2 introduces the basic theory of multiple model approach. In section 4.3, the lateral control system architecture is presented. The vehicle lateral dynamics is analyzed in section 4.4. Section 4.5 illustrates the design of 3 lateral controllers: PID with anti-windup, fuzzy controller, and multi-model fuzzy controller. Simulation tests are given in section 4.6.

## 4.2 Methodology-Multiple model approaches

### 4.2.1 Introduction

With the increasing complexity of process plant, vehicles and other engineered systems, the task of controller design for these complex systems is obviously a difficult problem. For such a situation, Zadeh has described the principle of incompatibility: “*As the complexity of a system increases, our ability to make precise and yet significant statements about its behaviour diminishes until a threshold is reached beyond which precision and significance (or relevance) become almost mutually exclusive characteristics [Zadeh 1973].*” One obvious result that we can derive from this principle is that models and analysis of complex systems will be less precise than for simple systems. Inspired by this, it appears an idea that we could look for other model representations and tools that can make use of less precise system knowledge than the traditional approaches which worked well for low and medium complexity modelling and control problems in the past. This idea just represents the trend in the field of intelligent control where fuzzy logic, neural networks, expert systems, etc, are being developed [Murray-Smith 1997, Åström 1992, Antsaklis 1991].

A common experience in daily life, as well as in engineering fields, to solve complex problem is the *divide-and-conquer* strategy, which means a complex problem can be divided into a number of simpler subproblems that can be solved independently, and these individual solutions yield the solution of the original complex problem. This strategy can be then applied in the modeling or control problems for complex systems. A complex system (nonlinear or time-varying) can be divided into a number of simpler subsystems, then the solutions for each “local” subsystems compose the solution for the global system. This is the principle of the multiple model approaches. One of the key to successful applying this approach is to find the appropriate axes along which the problem can be partitioned. One important approach to realize the partition is the operating regime approach.

The basic of the operating regime approach is to partition the operating range of the system thus to solve modeling and control problems. The operating regime approach leads to multiple model or multiple controller approaches, see Fig. 4.2 [Murray-Smith 1997]. We can see different local models or controllers work under different operating conditions, and a supervisor or scheduler will coordinate these local models or controllers. Then, the operating regime approach and multiple model/controller approach will be introduced in the subsequent sections.

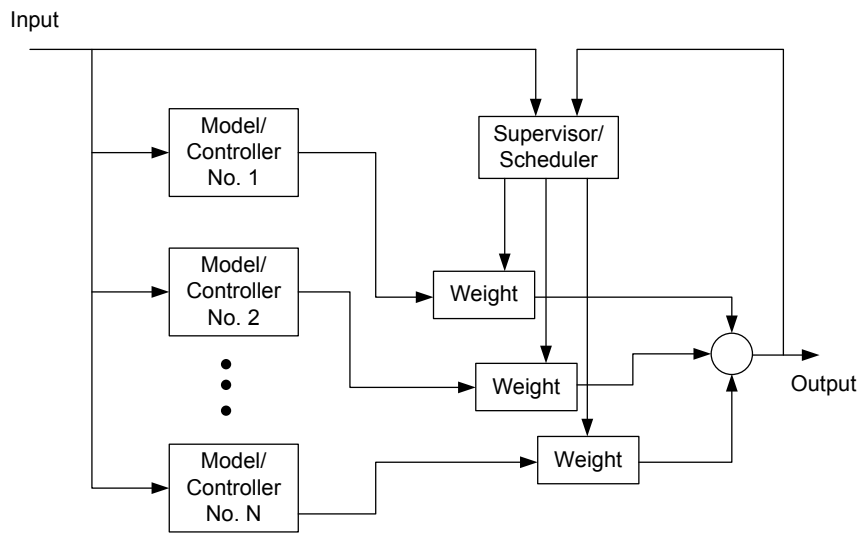


Figure 4.2: Multiple model/controller approach

## 4.2.2 The operating regime approach & multiple model/controller approach

### 4.2.2.1 Framework of operating regime approach

The decomposition of a system's full range of operation into a number of sub-regimes is illustrated in Fig. 4.3. In each operating regime, a local model or controller is applied. Of course, the final goal is a global model or controller, and it can be realized by combining the local models or controllers in some ways. Thus, the operating regime approach includes typically the following tasks [Murray-Smith 1997]:

- Decompose the system's full range of operation into several operating regimes.
- Select simple local model or controller structures within each operating regime. The local model or controller structures are usually parameterized by certain variables that must be determined.
- A method for combining the local models or controllers into a global one.

In the case of a complex system in which there has a large number of variables affecting the behaviour of system, the decomposition of the operating regimes will be a high dimensional problem. To deal with the complexity and high-dimensionality, a common method is hierarchy, which could be found in almost every area of science [Mesarovic 1970]. The first step of this idea is to decompose roughly the full operating range into several operating regimes according to the most important characteristic variables. Now each of these

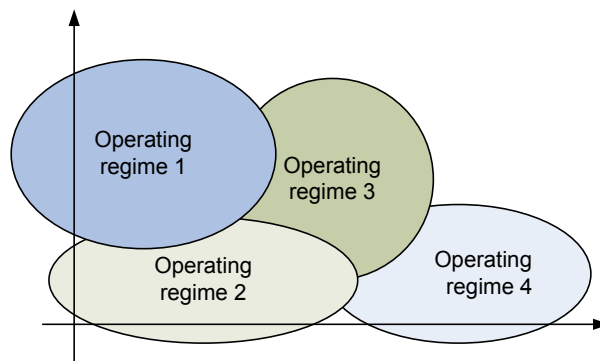


Figure 4.3: Decomposition of a complex system

operating regime can be further decomposed based on other characteristic variables, and so on, as shown in Fig. 4.4.

Despite the decomposition according to the operating regimes, the decomposition can also be implemented based on the following considerations: the physical components, phenomena, mathematical series expansion, (control) goals... (for the detail, one is referred to [Murray-Smith 1997])

#### 4.2.2.2 Dilemma between local and global

Obviously, in the operating regime approach, a trade-off between the number of operating regimes and the complexities of the local models should be made. Figure 4.5 illustrates the dilemma relationship between these two aspects. The dashed curve is the function to be approximated, while the solid lines are the local model approximations. Figure 4.5(a) shows that one can have a very fine partitioning of operating regime, then the local model can be represented by constant values. However, if we use linear local models, then 3 operating regimes are required, see Fig. 4.5(b). Furthermore, if quadratic models are employed, then we need only 2 operating regimes, see Fig. 4.5(c).

For a smooth objective function, it was shown that approximations based on operating regimes and local models can be made arbitrarily accurate either by making the operating regimes sufficiently fine, or by making the local model sufficiently complex [Johansen 1993a].

#### 4.2.2.3 Combination of local models and controllers

In the previous subsections, we have discussed briefly the issues of operating range decomposition and local controller selection, then the next step is to combine the local models

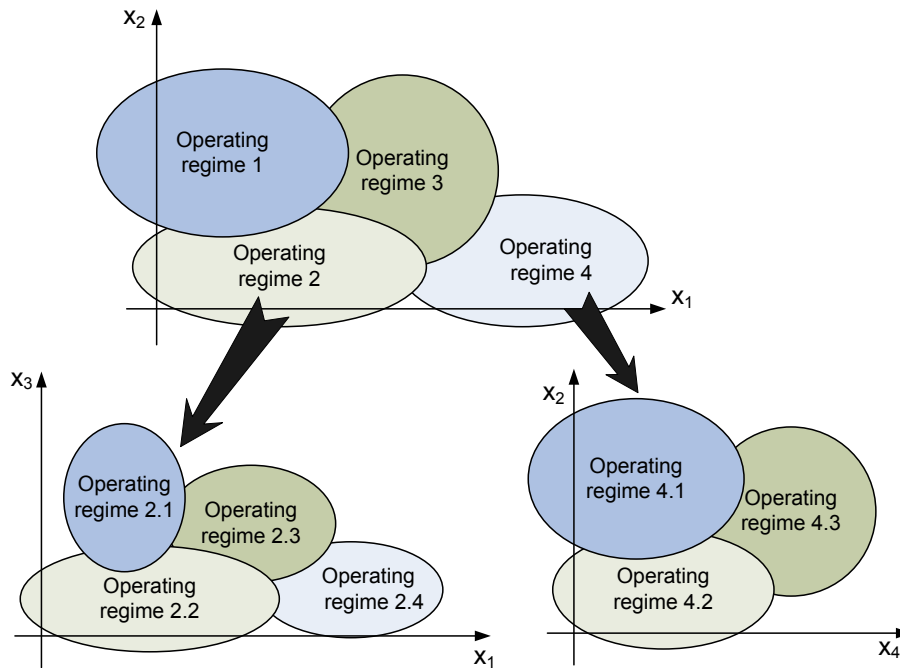


Figure 4.4: Hierarchical decomposition of a complex system

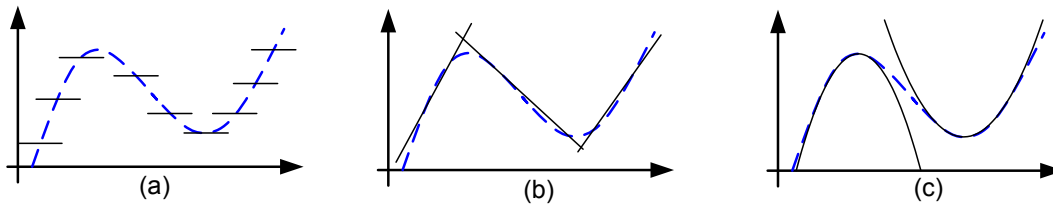


Figure 4.5: Approximation methods for local models

or controllers. In fact, the combination process is to decide when and how to “switch” between the local models or controllers. In this process, the problems of the overlap between the operating regimes, and whether a sudden switch of a smooth transition should be addressed. In previous literatures, the methods of mode switching, finite state automata, interpolation methods, fuzzy logic, and probabilistic approaches were proposed as the possible solutions for the combination of the local models [Hilhorst 1991, Zhang 1994, Johansen 1993b, Zadeh 1973, Jacobs 1991]. In the following of this subsection, we will take the mode switching and interpolation method for instance to illustrate how the combination process works.

### Hard partitions and model switching

The basic idea of hard partitions is that at each operating point, there exist exactly one local model or controller as a deterministic function of the operating point. In this

condition, the mode switching method is always employed. For example, a complex system can be decomposed into 4 operating regimes numbered from 1 to 4, see Figure 4.6. For each operating regime  $i$ ,  $i \in 1, 2, 3, 4$ , there is a corresponding local model, named as  $f_i$ . Then the total control system could be realized by using a number of logical statements of the form

$$\begin{aligned} & \text{If } x_1 \text{ is HIGH, AND } x_2 \text{ is LOW,} \\ & \text{THEN the system is operating in the Regime 4} \end{aligned} \quad (4.1)$$

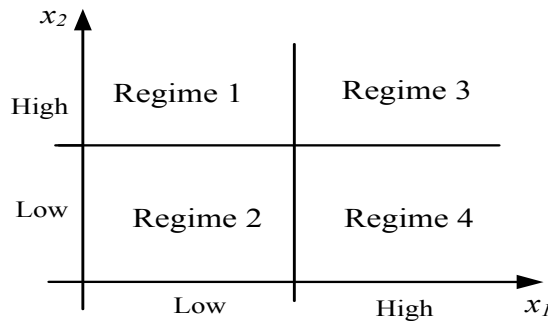


Figure 4.6: Hard partitions example

In practice, the type of hard partitions operating regime based models or controllers can be implemented using the methods from the simple discrete logic to sophisticated expert systems. A supervisory system based on discrete logic that supervises the traditional control systems to handle various situations, such as start, shut down, product change, has become the standard approach to dealing with wide operating range plants in manufacturing industry.

To give a general description of this method, we assume a modeling problem is a static function approximation problem, where the local models  $f_1, f_2, \dots, f_n$  are known for each operating regime. The operating regimes must cover the full operating range, and have not overlap between them. Then the global approximation is

$$f(u) = \sum_{i=1}^n f_i(u)r_i(u) \quad (4.2)$$

where  $r_i(u)$  is the characteristic function for the set of points that defines the operating regime with index  $i$ .

### Soft partitions and interpolation method

In the case of hard partitions of operating regime, there exist a sudden change between two adjacent operating regimes. However, in some cases, the sudden change between the operating regimes is not natural. For instance, the system behavior changes gradually as the operating point moves between different operating regimes. In such cases, the operating regimes can be described as overlapping sets and perform a smooth deterministic transition between them.

Consider again the decomposition shown in Fig. 4.6. If the boundary between the operating regimes characterized by *LOW* and *HIGH* is soft, which means there is a overlapping region between the classifications *LOW* and *HIGH*. Then a mixture of the local models or controllers should be applied.

Methods that can be applied to describe such soft boundaries between operating regimes includes fuzzy logic and interpolation methods, see [Zadeh 1973, Takagi 1985] and [Johansen 1993b]. In fuzzy logic, the logic statement described in (4.1) acts as a fuzzy rule, which is interpreted in terms of fuzzy sets defined as *LOW* and *HIGH*, as shown in Fig. 4.7. The inference system of fuzzy logic can then be built based on a series fuzzy rules. The resulting inference mechanism can be viewed as an interpolation algorithm that gives a certain weight on the local models or controllers in the different operating regimes, depending on the operating point.

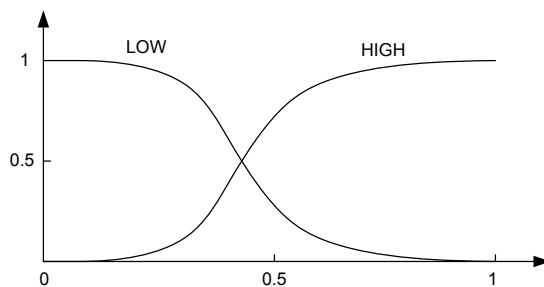


Figure 4.7: Fuzzy membership functions of *LOW* and *HIGH*

Consider again the approximation problem mentioned above. Using the interpolation method to get the global approximation,

$$f(u) = \sum_{i=1}^n f_i(u) \rho_i(u) \quad (4.3)$$

where the smooth weighting functions  $\rho_1, \rho_2, \dots, \rho_n$  provide soft transitions between the

operating regimes, and the weighting functions satisfy

$$\sum_{i=1}^n \rho_i(u) = 1 \quad (4.4)$$

for all  $u$ . In the case fuzzy logic inference, then

$$\rho_i(u) = \frac{r_i(u)}{\sum_{j=1}^n r_j(u)} \quad (4.5)$$

The function  $r_i$  is the membership function for the fuzzy set that represents the operating regimes with index  $i$ .

#### 4.2.2.4 Conclusion of multiple model approach

In order to deal with the increasing complexity of process plant, the multiple model approach provides an effective method. Inspired by the “*divide-and-conquer*” strategy, a complex system (nonlinear or time-varying) can be divided into a number of simpler subsystems, then the solutions for each “local” subsystems compose the solution for the global system. This is the principal strategy of the multiple model approach. Two key steps to successful applying this approach are: find the appropriate axes along which the problem can be partitioned; decide when and how to “switch” between the local models or controllers.

### 4.3 Architecture of lateral control system

The architecture we adopted for vehicle lateral control system is base on a two-level control model [Naranjo 2008]. This architecture is also inspired by Halle’s architecture [Halle 2005]. The resulting architecture represents the basic human driver’s behavior in vehicle lateral operations, as shown in Fig. 4.8.

The intelligent sensing module gets the information from sensors for speed, acceleration, yaw rate, lateral displacement etc. The planning module is a decision-making module. It receives and checks all the sensing data, then selects the right operation mode (lane keeping or lane changing) to continue the automatic driving. Usually, the planning module decides the vehicle keeping in its lane by using the road reference/sensing system. When a lane changing operation starts, it changes the road reference to the VDT, and then the lane changing controller starts to control the vehicle to trace the VDT. As

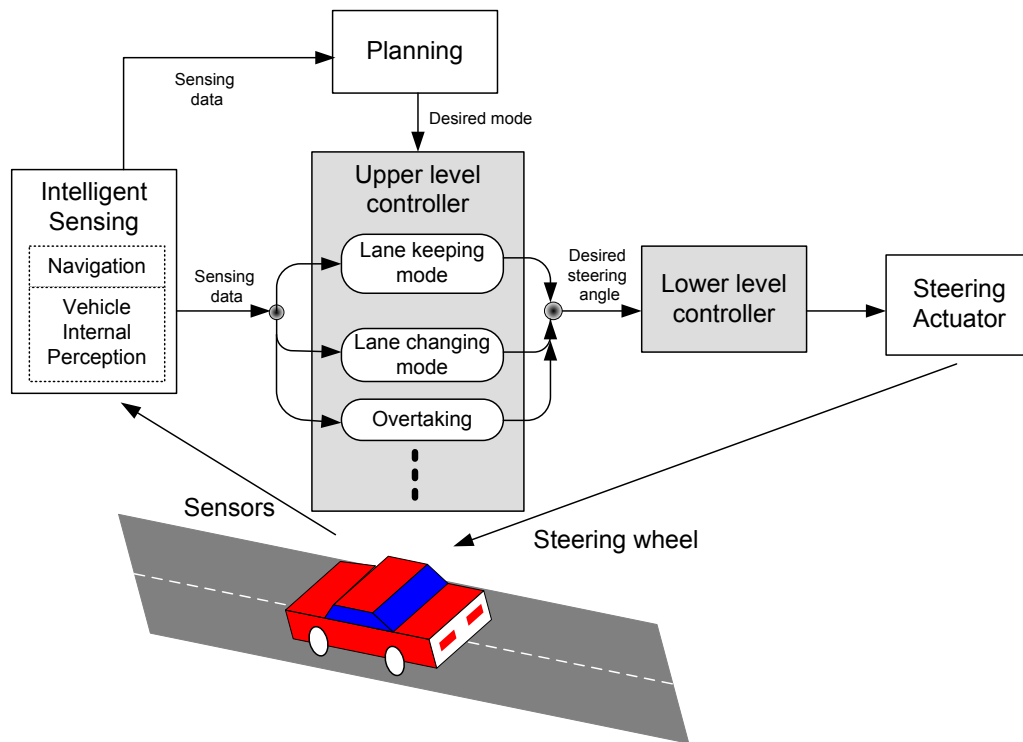


Figure 4.8: Hierarchical architecture for vehicle lateral control

the VDT is designed with consideration of ride comfort and transit time, the changeover between the two control modes is then assured to be smooth and efficient.

The module of upper level controller receives the decision from the planning module and uses the sensor data to give out the desired steering angle for the automated vehicle. A multi-model fuzzy control algorithm is designed for the lane tracking tasks in both the lane keeping and lane changing controllers. In our work, there are two major differences between the lane keeping and lane changing controllers. The first is that the two controllers use the different desired trajectories, as we mentioned earlier. The second is the method of obtaining the lateral position of the vehicle. For the lane keeping, the lateral position can be measured directly by the lateral reference/sensing system. While, the lateral position for the lane changing controller is obtained indirectly by integrating twice the data of the lateral accelerometer.

The lower level controller receives the target steering angle from the upper level controller and generates the appropriate control signals for the Steering Actuator (e.g. DC motor), hence, to control the vehicle moving in the desired direction. On account of the lower level controller is a typical DC motor control system, a PID controller will be competent.

## 4.4 Analysis of vehicle lateral dynamics

### 4.4.1 Bicycle Model

For the propose of designing an effective vehicle lateral controller, at first, we need to know the characteristics of the vehicle lateral dynamics. Since in section 2.4, we have already built the vehicle lateral kinematic model and dynamic model based on different assumptions and for different application conditions. In this chapter, our objective is to design a lateral controller for highway vehicle operations, thus the lateral dynamic model should be considered, and the kinematic model is not the case.

Recall the bicycle model described in equation (2.66), which is a 4<sup>th</sup> order system in the standard state space form,

$$\dot{X} = AX + B_1\delta + B_2\rho \quad (4.6)$$

where,  $X$  is the state variable,  $X = [e_1, \dot{e}_1, e_2, \dot{e}_2]^T$ , and

$$A = \begin{bmatrix} 0 & 1 & 0 & 0 \\ 0 & -\frac{2C_{af}+2C_{ar}}{mV_x} & \frac{2C_{af}+2C_{ar}}{m} & -\frac{2C_{af}l_f+2C_{ar}l_r}{mV_x} \\ 0 & 0 & 0 & 1 \\ 0 & -\frac{2C_{af}l_f-2C_{ar}l_r}{I_zV_x} & \frac{2C_{af}l_f-2C_{ar}l_r}{I_z} & -\frac{2C_{af}l_f^2+2C_{ar}l_r^2}{I_zV_x} \end{bmatrix},$$

$$B_1 = \begin{bmatrix} 0 & \frac{2C_{af}}{m} & 0 & \frac{2C_{af}l_f}{I_z} \end{bmatrix}^T,$$

$$B_2 = \begin{bmatrix} 0 & -\frac{2C_{af}l_f-2C_{ar}l_r}{m} - V_x^2 & 0 & -\frac{2C_{af}l_f^2+2C_{ar}l_r^2}{I_z} \end{bmatrix}^T.$$

The meaning of the symbols in (4.6) are listed in Table 4.1.

Although the bicycle model is simple, it has been proven to be a good approximation for vehicle dynamics when lateral acceleration is limited to 0.4g on normal dry asphalt roads.

### 4.4.2 Open-Loop Response to the Parameter Variations

If we fix the values of the parameters used in the system matrices in (4.6), the bicycle model represents a linear time-invariant (LTI) model. However, the longitudinal velocity of vehicle will not always be a constant in highway driving, the LTI model is then replaced by a LTV (Linear Time Variant) model. In addition, other parameters, such as the vehicle load and cornering stiffness of wheels are not always constant. The variations of these parameters will lead to the different vehicle lateral behaviors. Therefore, we use bode

Table 4.1: Nomenclature of Bicycle Model

$e_1$	distance of the Center of Gravity (C.G.) of the vehicle from the center line of the lane (m)
$e_2$	orientation error of the vehicle with respect to the lane (rad)
$\delta$	steering angle (rad)
$\rho$	road curvature (1/m)
$m$	mass (1485kg)
$V_x/V_y$	longitudinal/lateral velocity (m/s)
$I_z$	yaw moment of inertia (2872kgm <sup>2</sup> )
$l_f/l_r$	distance between the C.G. and the front/rear wheels (1.1/1.58m)
$C_{af}/C_{ar}$	cornering stiffness of the front/rear wheels ( $C_{af} = C_{ar} = 42000N/rad$ )

diagram to investigate the changes caused by the variations of vehicle parameters. The results of this investigation are important to have an insight of vehicle lateral behavior and to design the vehicle controller.

Figure 4.9(a) shows the bode diagrams of the frequency response under vehicle speeds of 30, 60, 90 km/h respectively. In the phase-angle plot, with the changing of speed, the shapes of the curves change a lot, especially in the frequency region of [1,20] rad/s, which is a common frequency region for vehicle operation. Figure 4.9(b) shows the bode plots under the loads of 0.8m, m, 1.3m respectively, with the vehicle speed of 60 km/h (m denotes the vehicle mass, and its value is shown in table 4.1). It is clear that the load variation has a very little influence on the log-magnitude curves, and the influence on phase angle curves is also very limit compared with the influence caused by speed.

From the above discussion, the very important conclusion is that the vehicle longitudinal velocity has a great influence on vehicle lateral dynamics which should be considered in lateral controller design.

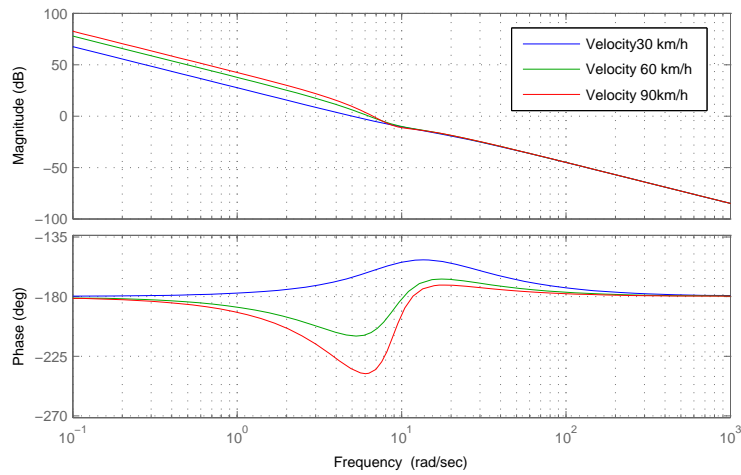
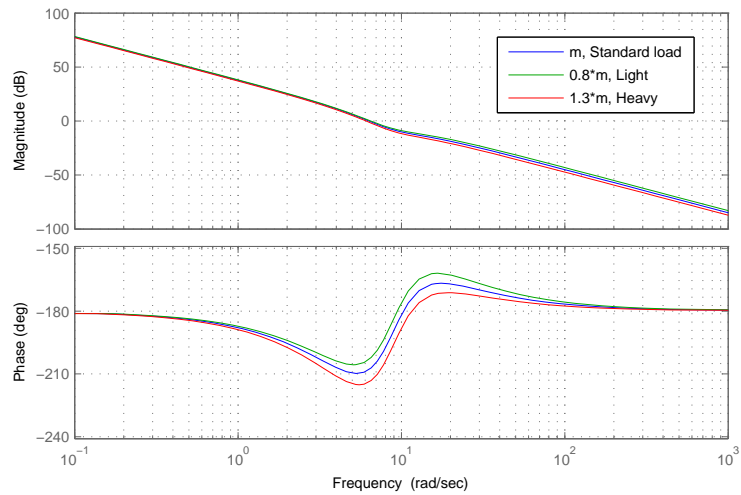
(a) Bode graph at different vehicle speeds (System Input:  $\delta$ ; Output:  $e1$  )(b) Bode graph under different loads (System Input:  $\delta$ ; Output:  $e1$  )

Figure 4.9: Open-loop responses to parameter variations

## 4.5 Lateral controller design

In the previous sections, the lateral control system architecture and vehicle lateral dynamics have been discussed. In this section, our task is to design a lateral controller, which works in the hierarchical lateral control architecture and is competent to deal with the parameter variations in vehicle lateral dynamics. The design processes of PID controller with anti-windup, fuzzy controller, and multi-model fuzzy controller will be presented, and results of these control algorithms will be compared, so as to find out the appropriate lateral control system.

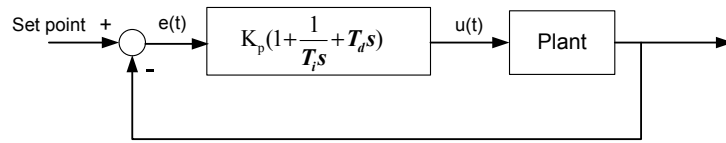


Figure 4.10: Block diagram of PID controller

## 4.5.1 PID with anti-windup

### 4.5.1.1 Traditional PID controller

The PID controller is the most common form of feedback control, which is widely used in industrial control systems. The PID controller involves three separate parameters: proportional, integral and derivative, denoted P, I, D.

Figure 4.10 shows a block diagram of PID controller. The PID algorithm is described by :

$$u(t) = K_p \left( e(t) + \frac{1}{T_i} \int_0^t e(\tau) d\tau + T_d \frac{de(t)}{dt} \right) \quad (4.7)$$

where,  $K_p$  is the proportional gain,  $T_i$  is the integral time, and  $T_d$  is the derivative time.  $u(t)$  is the control effort, and  $e(t)$  is the error. The three elements of the PID controller produce outputs with the following nature:

- P element: proportional to the error at the instant  $t$ , which is the “present” error.
- I element: proportional to the integral of the error up to the instant  $t$ , which can be interpreted as the accumulation of the “past” error.
- D element: proportional to the derivative of the error at the instant  $t$ , which can be interpreted as the prediction of the “future” error.

By tuning the three constants in the PID controller, the controller can provide control action designed for specific process requirements. There are several prescriptive rules used in PID tuning. Two of the most effective methods were proposed by Ziegler and Nichols [Ziegler 1942], and they have been widely utilized either in the original form of in modified forms.

In our case, in order to find the values of parameters of PID, equation (2.66) is used to represent the vehicle lateral dynamic model, we choose the steering angle as the system input and the lateral displacement is the system output. And the vehicle velocity is chosen as 50 *km/h*. By using Matlab/Simulink, we can find the step response of the

vehicle lateral system is not a S-shaped curve, thus the first method of Ziegler-Nichols is not available for our case. Then we use the Second Ziegler-Nichols method to determine the values of the parameters.

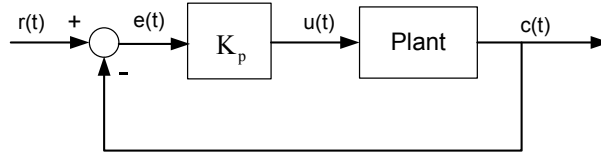


Figure 4.11: P control system

At first, let  $T_i = \infty$  and  $T_d = 0$ . Using the proportional control action only (see figure 4.11), increase  $K_p$  from 0 to a critical value  $K_{cr}$  at which the output first exhibits sustained oscillations. Thus we can get the critical gain  $K_{cr} = 2.6$  and the corresponding period  $P_{cr} = 0.693$  s. using the formulas suggested by Ziegler and Nichols shown in table 4.5.1.1, we can calculate the coefficients  $K_p$ ,  $T_i$ , and  $T_d$ :

$$K_P = 1.56, \quad T_i = 0.347, \quad T_d = 0.087 \quad (4.8)$$

Table 4.2: Ziegler-Nichols tuning rule based on critical gain  $K_{cr}$  and critical period  $P_{cr}$  (Second Method)

Type of controller	$K_p$	$T_i$	$T_d$
P	$0.5K_{cr}$	$\infty$	0
PI	$0.45K_{cr}$	$\frac{1}{1.2}P_{cr}$	0
PID	$0.6K_{cr}$	$0.5P_{cr}$	$0.125P_{cr}$

Then, with the above values, we can get the step response of the PID control system, as shown in figure 4.12. It is clear that the result is not satisfied, the transit response is oscillatory, the setting time is about 20 s, which means the amplitude decays slowly. In addition, the overshoot is rather big, and the maximum overshoot is 69%. Thus, additional fine-tuning should be done in order to get a good performance. Since, the most urgent requirement is to decrease the setting time as shown in Fig. 4.12, then we increase the value of  $T_d$  with a step of 0.05 by using a simple Matlab program, and we check the result in Matlab/Sumulink. Once the setting time gets into 3 s (allowable tolerance is 0.5%), we exit the program and it return the final value of  $T_d$ . By using this method, we

get the modified value:  $T_d = 0.385$ . Thus the new parameters values are:

$$K_P = 1.56, \quad T_i = 0.347, \quad T_d = 0.385$$

The step response of the PID controller with the new set of parameters is shown in Fig. 4.13. It should be noted that another benefit of increasing  $T_d$  is the decrease of overshoot. The control performance becomes much more better than the former one. The setting time is less than 3 s, and the maximum overshoot decreases to less than 25%.

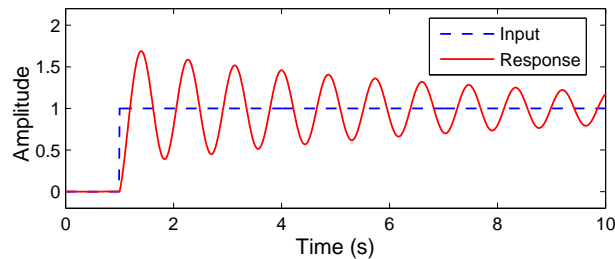


Figure 4.12: Step response of PID controller after the first tuning

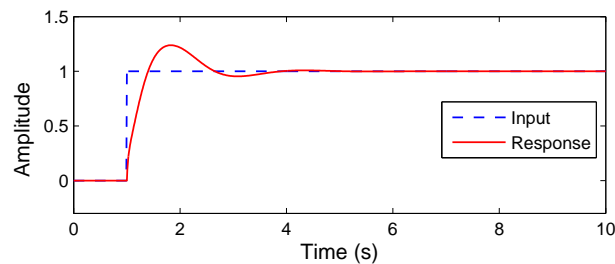


Figure 4.13: Step response of PID controller after the fine-tuning

#### 4.5.1.2 PID with Anti-Windup

Although the above designed PID controller has a good performance in this step response test, however, it should be noted that the PID output at the step time is a very big value which is far more than  $45^\circ$ , the mechanical limit of the steering system of road vehicles. In addition, for a road vehicle, the ride comfort is another constraint need to be considered, thus a limit of  $0.175 \text{ rad}$  (or  $10^\circ$ ) should be introduced to our lateral control system. A saturation block is then added in the PID control system, as shown in Fig. 4.14. The saturation algorithm is written as,

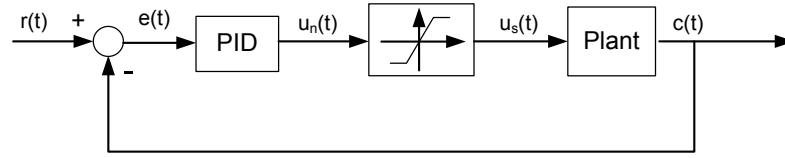


Figure 4.14: PID controller with saturation constraint

$$u_s(t) = \begin{cases} -0.175 & \text{if } u_n(t) \leq -0.175 \\ u_n(t) & \text{if } -0.175 \leq u_n(t) \leq 0.175 \\ 0.175 & \text{if } u_n(t) \geq 0.175 \end{cases} \quad (4.9)$$

The saturation block is a nonlinear element, and it will induce the integrator windup phenomenon in the PID control system, which will make worse the performance of the PID controller and even the stability of the control system. Different anti-windup algorithms have been proposed in former researches, such as the Set Point Limitation, Incremental Algorithms, Back-calculation, etc. [Åström, K.J. 2002]. In this work we use the traditional back-calculation method to deal with the anti-windup phenomenon.

The back-calculation method works as follows: When there is a output saturate, the integral term in the controller is recomputed so that its new value gives an output at the saturation limit.

Figure 4.15 shows a block diagram of a PID controller with anti-windup based on back-calculation. The system has an extra feedback path that is generated by measuring the error signal  $e_s(t)$  produced by the saturation block ( $e_s(t) = u_s(t) - u_n(t)$ ). Signal  $e_s(t)$  is fed to the input of the integrator through gain  $1/T_t$ . A rule of thumb that has been suggested is to choose  $T_t = \sqrt{T_i T_d} = 0.366$  [Åström, K.J. 2002]. Therefore, the values of the PID with anti-windup control system parameters are:

$$K_P = 1.56, \quad T_i = 0.347, \quad T_d = 0.385, \quad T_t = 0.366$$

Then we will test the proposed controller with a simple step input. As we have already shown the fact that the vehicle velocity has great influences on vehicle lateral dynamics in Section 4.4, then it is interesting to test whether the above mentioned controller is robust to the variation of vehicle speed. Therefore, the test will be performed at 80, 40, 20, 10 *km/h* respectively.

Figure 4.16 shows the step responses of the PID with anti-windup. It can be found that the results at 80 and 40 *km/h* are quite similar, which are better than the results in

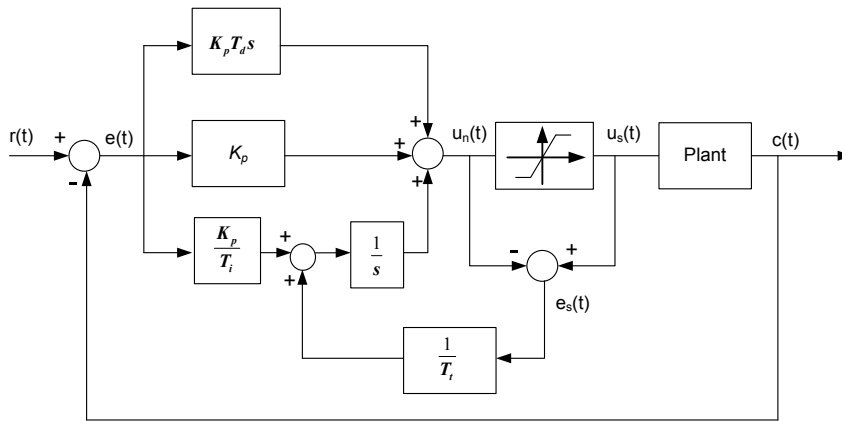


Figure 4.15: PID controller with Anti-Windup

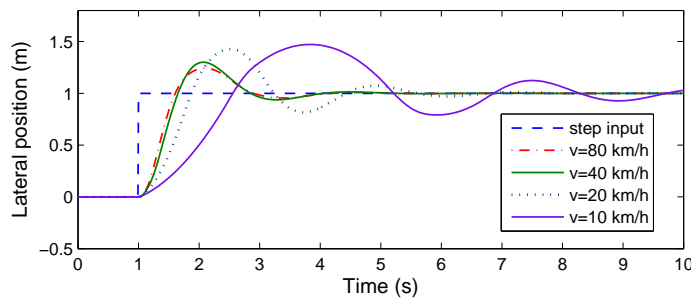


Figure 4.16: PID with anti-windup control system: step responses at different speed

low speed region. With the decreasing of speed, the control performances are degraded significantly. The proposed PID control system can work only in a certain speed region, and it is not robust to the velocity variations.

### 4.5.2 Fuzzy control for vehicle steering

It is known that fuzzy logic is a very useful nonlinear control method, that can be used to control very complex models or plants, which are difficult to model. As the vehicle lateral dynamic system is a typical system where driving models, sensorial information, objectives, constraints, and control actions are under uncertainty, thus different fuzzy logic controllers were proposed for the vehicle lateral control [Chunyan 2003].

In [Chunyan 2003] an adaptive fuzzy logic controller was designed, which has two inputs, one output, and an adaptive fuzzy search table deduced by lingual information from experienced drivers. Simulations and experiments have been done in straight lane with the speed of 80 *km/h* and in curve lanes with the speeds of 40 *km/h*. The given results showed the effectiveness of the proposed fuzzy approach. However the tracking

results in low speed have not been shown in this work.

Works carried out by Wijesoma and Kodagoda [Wijesoma 1999, Kodagoda 2002] have shown a fuzzy lateral controller for a golf car-like AGV (Autonomously Guided Vehicle). In their works, the coupling effects of vehicle speed on steering angle (and hence angular velocity), and vice versa, was not explicitly accounted for. Thus, two independent controllers of longitudinal controller and lateral controller were designed. Simulation experiments were carried out with the variation of vehicle loads and vehicle velocities. However, the variations of vehicle speed is only from  $3\text{m/s}$  to  $7\text{m/s}$  ( $[10.8\text{ km/h}, 25.2\text{ km/h}]$ ), which is reasonable for their Golf Car but not sufficient for the highway vehicle operations, because this speed region covers only the low speed region for the vehicles driving in highway.

As we know the fact that vehicle velocity has great influences on vehicle lateral dynamics, then it is interesting to investigate how the above mentioned fuzzy controllers deal with this problem using the uncoupled model of the longitudinal and the lateral controllers. In the following of this subsection, we will take the fuzzy controller in [Chunyan 2003] as an example to find out how lateral controller works with out considering the influences of vehicle speed.

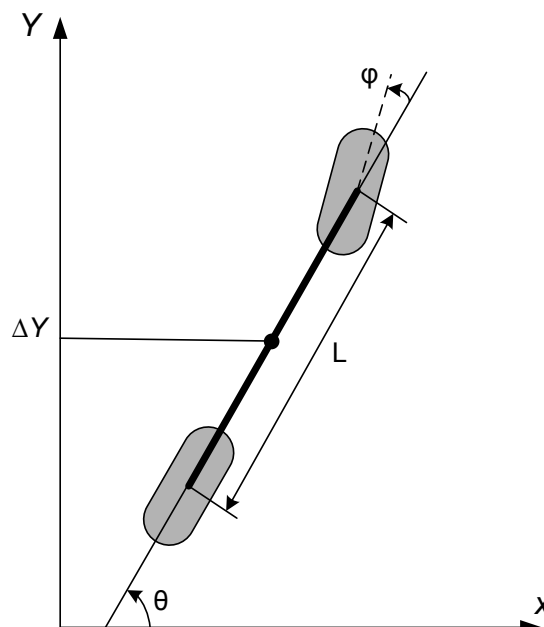


Figure 4.17: Simple bike model

#### 4.5.2.1 Vehicle lateral model

The vehicle model used in [Chunyan 2003] is a kinematic model as shown in Fig. 4.17. And it has the following formulas:

$$\begin{cases} \dot{\theta}(t) = \tan \varphi(t) \frac{v(t)}{L} \\ \dot{y}(t) = \sin \theta(t) v(t) \\ \dot{x}(t) = \cos \theta(t) v(t) \\ \varphi(t) = f(\theta, t) \end{cases} \quad (4.10)$$

where  $L$  is the wheelbase,  $\theta$  is the yaw angle, and  $\varphi$  is the steering angle.

#### 4.5.2.2 Input and output variables

The fuzzy controller has two input variables: lateral displacement  $\Delta Y$  and its change ratio  $\Delta \dot{Y}$ ; and it has one output: steering angle  $\varphi$ . For each variable, there are 7 fuzzy sets, described as follows:

$$\{\Delta Y, \Delta \dot{Y}, \varphi\} = \{s1, s2, s3, ce, b1, b2, b3\} \quad (4.11)$$

The normal distribution function as formula (4.12) is used for the membership distribution description.

$$\mu(x) = \exp \left[ -\left( \frac{x-a}{b} \right)^2 \right], (b > 0) \quad (4.12)$$

Then the membership function of the input and output variables are shown in Fig. 4.18.

#### 4.5.2.3 Fuzzy control rules

The fuzzy control rules are in the form of “IF (Premise) THEN (Consequent)”. There are totally 49 fuzzy control rules deduced from experienced drivers, as shown in Table 4.3.

#### 4.5.2.4 Simulation tests

In order to check whether the tracking performance of this fuzzy controller is robust to the variation of vehicle speed, a simple step input is used, and we will perform this step input at different vehicle speeds.

Figure 4.19 shows the step responses of the fuzzy controller. We can find the results at  $80km/h$  and  $40km/h$  are quite good, however the results become bad with the speed

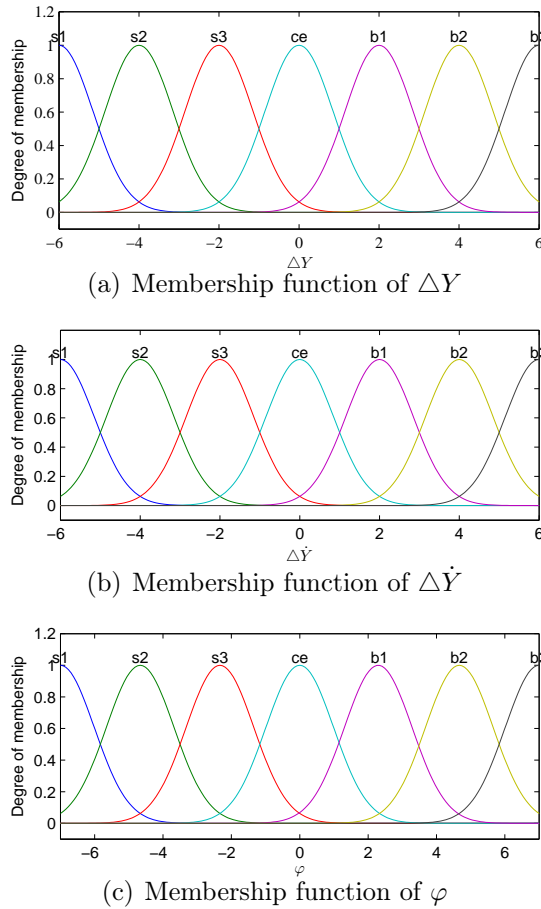


Figure 4.18: Membership functions

decreases. This results combined with the results in [Chunyan 2003] show that this fuzzy controller can provide adaptive lateral performances in middle and high speed region, however the control performances in low speed region are not acceptable. Therefore, if we want to design a adaptive lateral controller which is qualified in all vehicle speed, then the factor of speed variation must be taken into account.

An issue need to be mentioned is that the vehicle model used in the work of [Chunyan 2003] is a kinematic model which is just a simplified version of the equation (2.44) given in section 2.4. As we have discussed already that the kinematic model neglects the dynamic factors which is acceptable in the low speed operations. However, it is not the case for highway vehicles.

Since we have obtained step responses with both the fuzzy controller and PID controller which are shown in Figures 4.19 and 4.16 respectively. Then it is interesting to compare the two control results. Although the two vehicle models are not the same, but nevertheless we can find some rough conclusions by comparing the two results:

Table 4.3: Fuzzy Rule Base

		Input 2: $\Delta Y$						
		s1	s2	s3	ce	b1	b2	b3
Input 1: $\Delta Y$	s1	b3	b3	b2	b2	b1	ce	ce
	s2	b3	b3	b2	b2	b1	ce	ce
	s3	b3	b3	b2	b1	ce	s2	s2
	ce	b3	b3	b2	ce	s2	s1	s1
	b1	b2	b2	ce	s3	s2	s1	s1
	b2	ce	ce	s3	s2	s2	s1	s1
	b3	ce	ce	s3	s2	s2	s1	s1

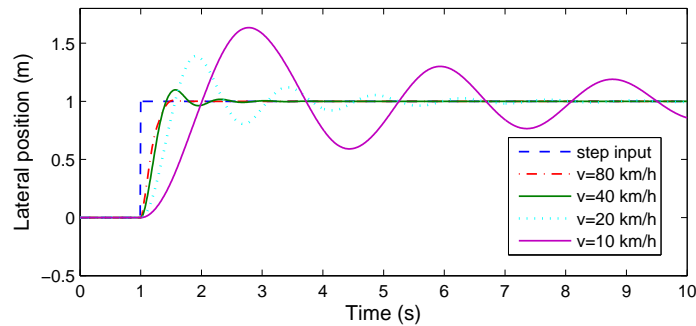


Figure 4.19: Traditional fuzzy controller: step responses at different speeds

- Both the two controller can work better in middle and high speed region than in the low speed region.
- It seems that the fuzzy controller works better than the PID, because at the speed of 80, 40, and 20  $km/h$ , the fuzzy controller has always less overshoot and less set time than that of the PID controller.

### 4.5.3 Multi-model fuzzy control

In the previous two subsections, the PID with Anti-Windup and fuzzy control algorithms have been studied. Although the fuzzy control method has shown some advantages than the PID, the results are still not satisfied if the vehicle velocity varies. This is because the above mentioned methods did not consider the influences of the variations of vehicle speed. However, for a highway vehicle, the operation speed varies in a wide range from low speed to high speed. Therefore, in the rest of this section, we will dedicate to the

task of designing a lateral control method which is robust to the velocity variations.

In section 4.2, the multiple model approach has been introduced as an effective method to deal with the complex systems where nonlinearity and wide range of parameter variations exist. Thus we will use this method to deal with the problem of velocity variations in vehicle lateral controller design.

#### 4.5.3.1 Decomposition of the operating regime

The first step of the application of multiple model approach is to find the appropriate axes along which the control system can be partitioned. Obviously, the vehicle velocity is the “appropriate axe” in our case. In highway operations, the vehicle speed varies in a wide range from low to high speed, normally in the range of  $[0, 120]$   $km/h$ . Then, how to decompose the vehicle speed into the operation regimes is the problem need to envisaged. Two questions should be answered in this procedure:

1. How many operating regimes should be decomposed? (It is associated with the question that how much is the speed interval that one operating regime should cover.)
2. Whether an overlap is required for two adjacent regimes? (It concerns the question of which kind of partition should be selected: hard partition or soft partition.)

#### How many operating regimes should be decomposed?

Consider the first question, since the velocity is the sole “axe” used to decompose the operating regime in our case, the decomposition procedure is then less complex than the systems with several decomposition “axes”. Then, we need to decide how many operating regimes that the full velocity range should be divided. In this procedure, a trade-off between the number of operating regimes and the complexities of the local models should be made (see the discussions in section 4.2.2).

One feasible idea is that we divide the full speed range into fine partitions, and a simple local model is proposed for each partition. For example, we can divide the speed range into 12 equal operating regimes as:  $[0, 10]$ ,  $[10, 20]$ ,  $\dots$ ,  $[110, 120]$   $km/h$ . Since the partitions of speed are rather fine, then in each operating regime, we consider the vehicle lateral dynamic behaviors are similar when the speed varies in each regime. For each regime, a simple local controller can be designed, such as a PID controller, which can be designed using the method that we have shown in section 4.5.1. Thus, a candidate method with 12 operating regimes and 12 local PID controllers could be generated.

On the contrary, another idea is that we divide the full velocity range into several rough partitions, and a more complex local controller is proposed for each partition. For example, we can divide the speed range into four operating regimes, and each regime covers an interval of 30 *km/h* as: [0, 30], [30, 60], [60, 90], [90, 120] *km/h*. As the speed range becomes wider in each regime, then more adaptive local controllers are required. In section 4.5.2, it has already shown the advantages of fuzzy logic controller than PID controller in vehicle lateral control. Thus, a second candidate method with only 4 operating regimes and 4 local fuzzy controllers is proposed.

Compare the two methods suggested above, the latter one is considered to be better. Two main reasons contribute to this choice. One main reason is that, from the system constructor point of view, the latter method has only 4 local controllers which is more simple and clear than the former one, which has 12 local controllers. A further reason is that the fuzzy controller is more accurate and more adaptive than the PID controller, as shown in section 4.5.2.

### **Whether an overlap is required for two adjacent regimes?**

Then we need to consider the second question that whether an overlap is required for two adjacent regimes. As we have discussed in section 4.2.2, the hard partitions with model switch method will induce discontinuities in the global control control law. Besides, undesirable peaks which may appear very detrimental to the vehicle in terms of quality of service and passenger comfort. Therefore, an overlap should be introduced to the operating regimes which can perform a smooth deterministic transition between them. Thus, the soft partition method is used in this work.

Consider the four operating regimes that we have just proposed: [0,30], [30,60], [60,90], [90,120] *km/h*, we make an overlap of 10 *km/h* for every two adjacent regimes. Then the modified four regimes are: [0,35], [25,65], [55,95], [85,120] *km/h*. For the sake of expression, we give each regime a name, as : *Low*, *Medium-Low*, *Medium-High*, and *High*. Then the decomposition of the operating regimes is shown in Fig. 4.20.

In the following sections, we will design the multi-model controller based on the above operating regimes.

#### **4.5.3.2 Multi-model fuzzy controller design**

In this subsection, we propose a multi-model fuzzy controller to perform the lane tracking tasks for the lane keeping maneuver. At first, according to the four operating regimes that we have just proposed, four fuzzy logic-based local controllers are designed respec-

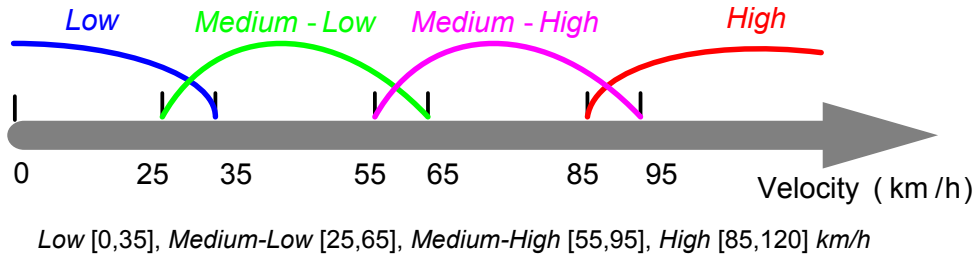


Figure 4.20: Decomposition of operating regimes

tively, named Low, Medium-Low, Medium-high and High. Then, in order to get a global controller, a fusion block is designed to combine the four independent local controllers into a global one. This fusion block determines the weighting functions for each local controller. It is designed based on a fuzzy type strategy to ensure a smooth and accurate transition between the working points. The control system structure is shown in Fig. 4.21.

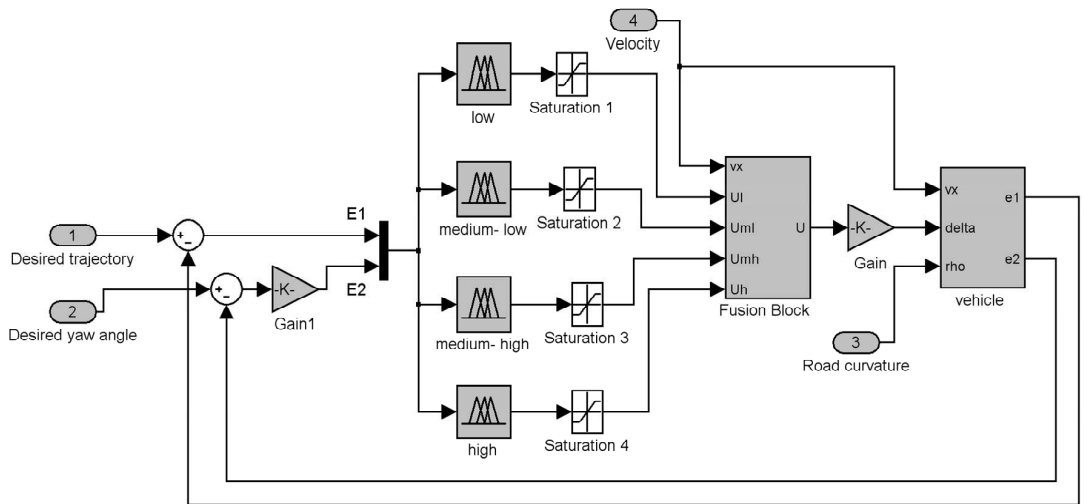


Figure 4.21: Lateral controller: Multi-model fuzzy controller block diagram

### A. Local Controller Design

For all the four local controllers, we use the same basic structure of fuzzy controller, the same fuzzy rule base and the same defuzzification method. However, the values of the membership function of the input and output variables are altered.

**Input and output variables:** We choose two inputs for the fuzzy controller, the lateral deviation  $E1$ , and the orientation error  $E2$ . The output is the steering angle of the front wheel  $\delta$ . We define three fuzzy sets for both two inputs, they are *Left*, *Center*, *Right*. Five fuzzy sets are defined for the output, named as *LeftB*, *LeftS*, *Center*, *RightS*, *RightB*.

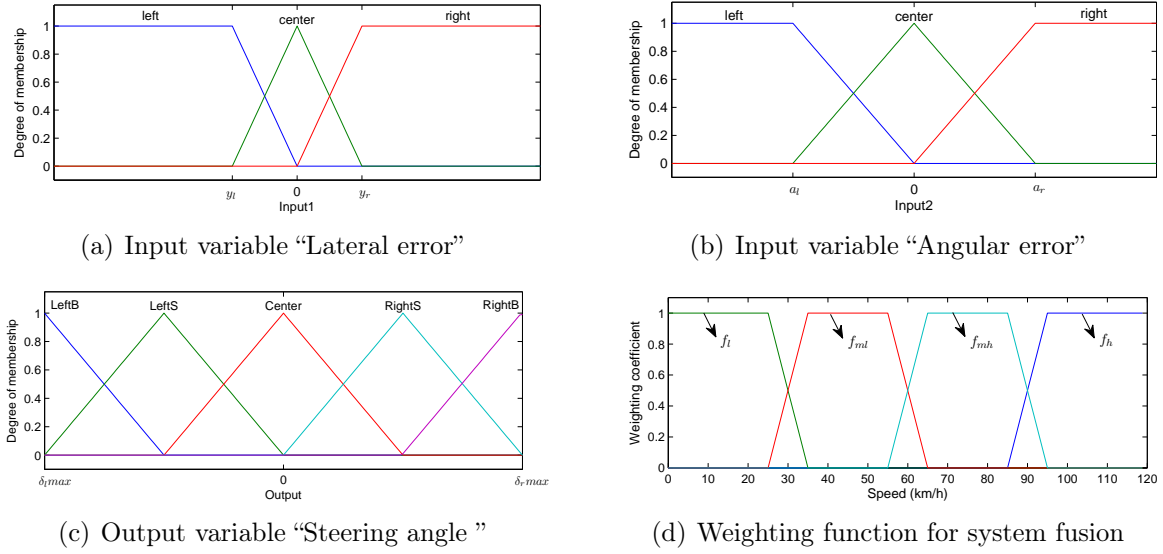


Figure 4.22: Variables in multi-model fuzzy controller

*RightB*. They can be expressed as follows:

$$\{E1, E2\} = \{Left, Center, Right\} \quad (4.13)$$

$$\{\delta\} = \{LeftB, LeftS, Center, RightS, RightB\} \quad (4.14)$$

Figures 4.22(a),4.22(b),4.22(c) show the input and output variables' membership functions. The values of the variables presented in the figures are given in Table 4.4. These values are given on the basis of expert experiences and extensive simulation experiments.

**Fuzzy Rule Base:** The expert's knowledge and experience are represented by a fuzzy rule base, with the fuzzy control rules in the form of "IF (premise) THEN (consequent)". The proposed fuzzy control rule base is shown in Table 4.5. This rule base is used for all the four local controllers.

**Fuzzy Reasoning Process:** The fuzzy reasoning process can be divided into three steps - fuzzification, inference engine and defuzzification. In this work, we use triangle and trapezoids shaped membership function for the fuzzification process as shown in Fig. 4.22. The Mamdani's inference method is employed to solve the fuzzy implication. And we use Centroid method for defuzzification process.

Table 4.4: Membership Function Variables

	Local controllers			
	Low	Medium-Low	Medium-High	High
$y_l/y_r$ (m)	-0.2/0.2	-0.3/0.3	-0.4/0.4	-0.5/0.5
$a_l/a_r$ (deg)	-10/10	-6/6	-4/4	-3/3
$\delta_{lmax}/\delta_{rmax}$ (deg)	-20/20	-12/12	-8/8	-6/6

Table 4.5: Fuzzy Rule Base

		Input 2: Angular Error		
		Left	Center	Right
Input 1: Lateral Error	Left	RightB	RightS	Center
	Center	RightS	Center	LeftS
	Right	Center	LeftS	LeftB

#### 4.5.4 Virtual desired trajectory for lane change maneuver

In the design of VDT, passenger's ride comfort, transit time are the main factors to be considered. The trapezoidal acceleration trajectory has been selected to be the optimal trajectory for a lane changing maneuver, see [Chee 1994, Hedrick 1994, Ji 2007]. The acceleration profile is specified in Fig. 4.23, where  $a_{max}$  and  $J_{max}$  represent the lateral acceleration limit and the lateral jerk limit of the trapezoidal acceleration trajectory respectively.

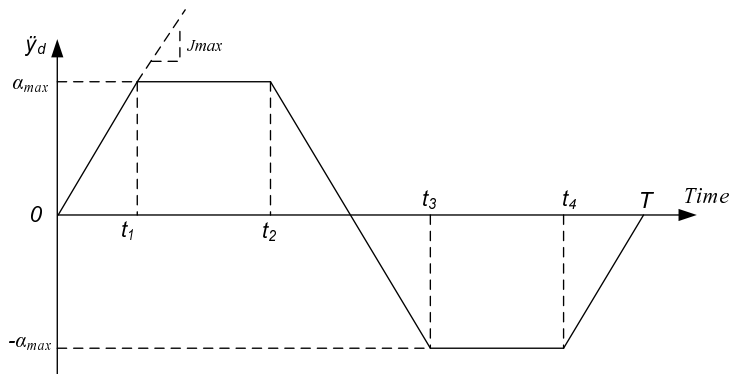


Figure 4.23: Trapezoidal acceleration profile

From Fig. 4.23, the desired lateral acceleration  $\ddot{y}_d$  can be described as

$$\begin{aligned} \ddot{y}_d = & J_{max}t \cdot u(t) - J_{max}(t - t_1) \cdot u(t - t_1) \\ & - J_{max}(t - t_2) \cdot u(t - t_2) + J_{max}(t - t_3) \cdot u(t - t_3) \\ & + J_{max}(t - t_4) \cdot u(t - t_4) - J_{max}(t - T) \cdot u(t - T) \end{aligned} \quad (4.15)$$

where,  $u(t)$  is a unit step function. Integrating (4.15) twice with respect to time and with zero initial conditions, then the lateral position can be written as:

$$y_d = \frac{J_{max}}{6} \left[ \begin{aligned} & t^3 \cdot u(t) - (t - t_1)^3 \cdot u(t - t_1) - \\ & (t - t_2)^3 \cdot u(t - t_2) + (t - t_3)^3 \cdot u(t - t_3) \\ & + (t - t_4)^3 \cdot u(t - t_4) - (t - T)^3 \cdot u(t - T) \end{aligned} \right] \quad (4.16)$$

Set  $y_d(T) = d$ , where  $d$  means the lateral distance between the target lane and the origin lane, i.e. lane width. The temporal parameters for this trajectory,  $t_1, t_2, t_3$  and  $t_4$  can be obtained as

$$\begin{aligned} t_1 = \frac{a_{max}}{J_{max}}, t_2 = \frac{-t_1^2 + \sqrt{t_1^4 + 4t_1 \frac{d}{J_{max}}}}{2t_1} \\ t_3 = 2t_1 + t_2, t_4 = t_1 + 2t_2 \end{aligned} \quad (4.17)$$

The transit time  $T$  for the lane change maneuver can be written as:

$$T = 2(t_1 + t_2) = \frac{a_{max}}{J_{max}} + \sqrt{\left(\frac{a_{max}}{J_{max}}\right)^2 + 4 \frac{d}{a_{max}}} \quad (4.18)$$

By selecting the values of design parameters  $d$ ,  $a_{max}$  and  $J_{max}$ , one can obtain the desired trajectory and the transit time from (4.16) and (4.18) respectively. The trapezoidal acceleration trajectory is easy to be parameterized. And it provides a direct method to design a desired trajectory only with several main performance constrains, which facilitates finding the optimal trade-off between the transit time and ride comfort constrains.

## 4.6 Simulation tests

In this section, we will test the performance of the proposed vehicle lateral control system throughout a series of simulations. The lane keeping and lane changing will be assessed

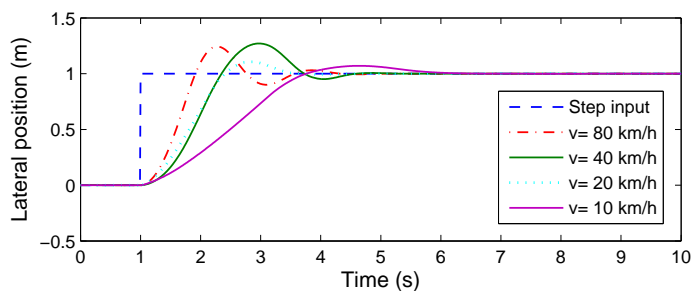


Figure 4.24: Multi-model fuzzy controller: step responses at different speeds

separately. Moreover, in order to show the robust performance of the multi-model fuzzy controller, variations in vehicle velocity, mass, movement inertia and wheel cornering stiffness are considered in our tests. The parameters of the experimental vehicle are shown in Table 4.1.

#### 4.6.1 Test 1: Lane keeping control at different speeds (1)

In this simulation, the lane keeping performance will be tested. A 600-meter trajectory includes a segment of 5-meter lateral deviation is designed, see Fig. 4.25. The test vehicle will pass through the designed trajectory at the speeds of 30, 60, 90  $km/h$  respectively, and the simulation results of steering angle, lateral position error and lateral acceleration are shown in Figs. 4.26(a), 4.26(b), 4.26(c) respectively. We can find that the experimental vehicle can steer accurately to trace the desired trajectory at all the three test speeds. In the three output results, all the maximum values occur at the speed of 90  $km/h$ , and the results at 30 and 60  $km/h$  are more accurate and more smooth. However, even at the speed of 90  $km/h$ , the maximum lateral position error is less than 0.08  $m$ , and the maximum lateral acceleration is less than 1.1  $m/s^2$ . In general, the lateral acceleration should not exceed 4  $m/s^2$  for the rollover and 2  $m/s^2$  for passenger comfort [Ackermann 1995]. Since the lateral acceleration is always below 2  $m/s^2$ , the passenger comfort is then ensured in this scenario.

#### 4.6.2 Test 2: Lane keeping control at different speeds (2)

In this simulation, the experimental vehicle will perform two times of 3-meter lateral deviation during the periods of 4 to 10  $s$  and 15 to 22  $s$ , see Fig. 4.27. This input trajectory is different from the trajectory shown in Fig. 4.25. In the latter one, we give out the time history of the desired lateral displacement. If the test vehicle performs this

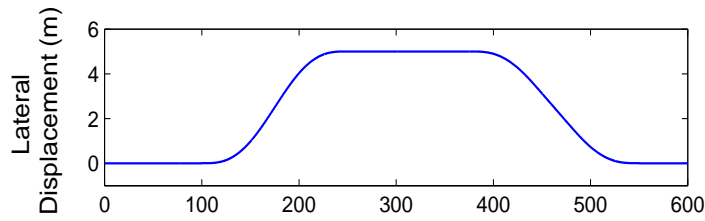
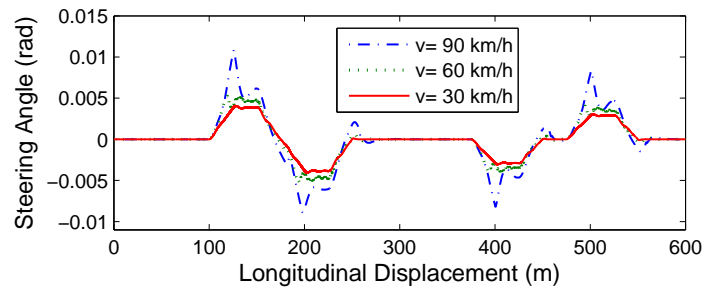
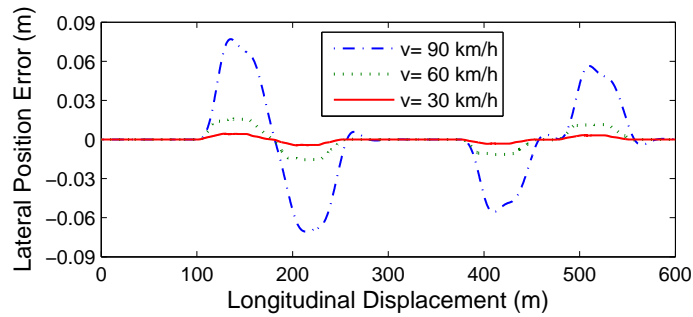


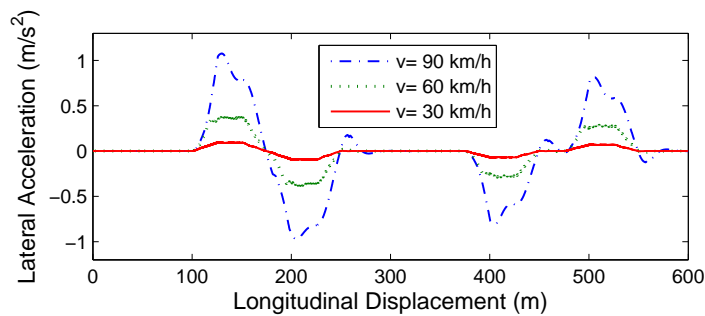
Figure 4.25: Desired trajectory (1)



(a) Steering angle



(b) Lateral position errors



(c) Lateral acceleration responses

Figure 4.26: Lane keeping control results at different speeds (1)

time history with different speed, then this time history will result in different trajectories. The objective of this scenario is to test the performance of the lateral control system when it performs a same lateral deviation during the same time, however at different speeds.

The vehicle speed is set to 30, 60, 90 km/h respectively. Figure 4.28(a) shows the steering results corresponding to the three test speeds. The steering operations are rather smooth in this scenario, and the steering angle at 30 *km/h* is bigger than the results at the higher speed. This is reasonable, because when the speed is slow, we need bigger steering angle to reach the same lateral position.

Figure 4.28(b) shows the time history of lateral position errors. We can find the proposed multi-mode fuzzy controller can assure good tracking performances in different speed scenarios. The maximum lateral position error occurs at 90 *km/h*, and the maximum value is less than 0.05 *m*. Figure 4.28(c) shows the lateral acceleration curves. The maximum value of lateral acceleration is about 0.6 *m/s<sup>2</sup>*, which means the ride comfortable is ensured. Furthermore, the acceleration results are very similar even there are big difference between the operation speeds. This shows the proposed multi-model controller can provide stable performances in a wide range of operation speed.

### 4.6.3 Test 3: Lane keeping control under different loads and Cornering Stiffness

In this simulation, the issue we address is the influences caused by the variations of vehicle mass and wheel cornering stiffness. With the variation of vehicle mass, as a result, the moment of inertia will change correspondingly. We use the same input trajectory that we used in the former simulation as shown in Fig. 4.27, and the vehicle speed is set to 60 km/h. The variations of the parameters are listed in Table 4.6. The vehicle mass changes from 1300 *kg* to 2300 *kg*, the movement inertia of vehicle body changes from 3000 *kgm<sup>2</sup>* to 4400 *kgm<sup>2</sup>*, and the wheel cornering stiffness changes from 36500 *N/rad* to 55000 *N/rad*. Fig. 4.29(a) and Fig. 4.29(b) show the time history of the lateral position error and lateral acceleration respectively. In both the two figures, the differences between the two cases are very small. The proposed controller shows a strong adaptability to the variations of vehicle load, moment inertia and wheel cornering stiffness.

### 4.6.4 Test 4: Lane changing scenarios at different speeds

The VDT for the lane changing is described in equation (4.15). In our case, the lateral acceleration limit  $a_{max}$  for the VDT is set to 0.05 *g*, and the jerk limit is set to 0.1 *g/s*,

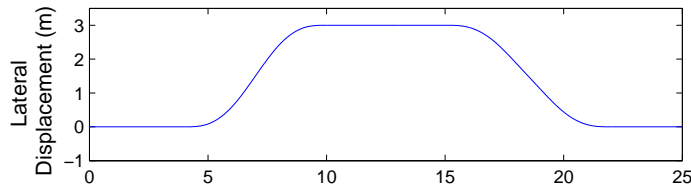
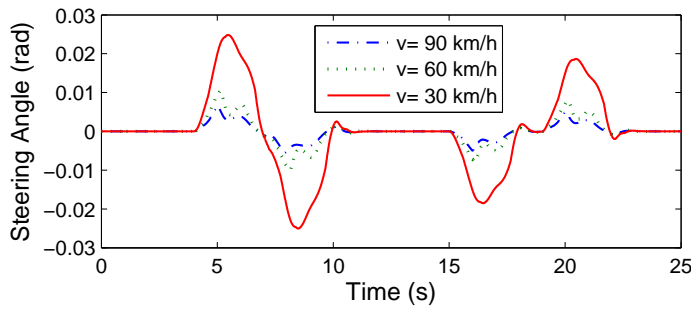
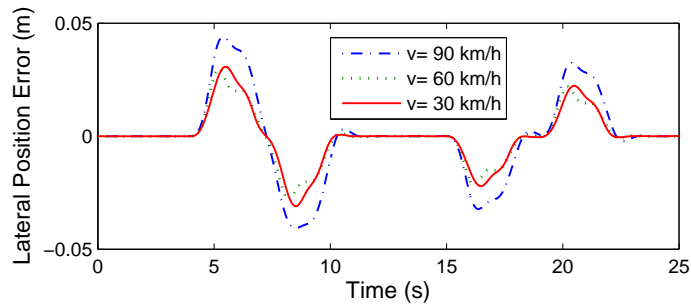


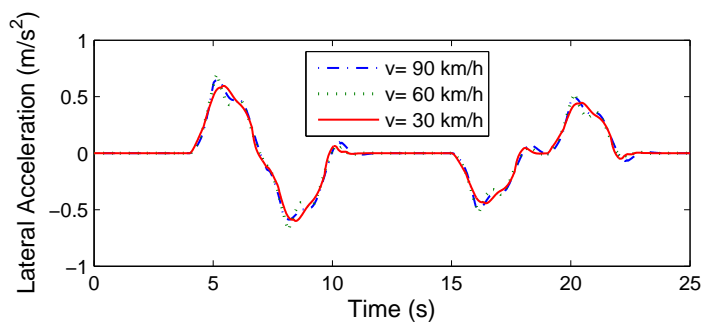
Figure 4.27: Desired trajectory (2)



(a) Steering angle



(b) Lateral position errors

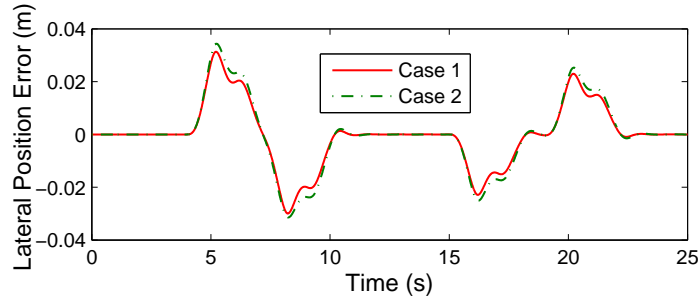


(c) Lateral acceleration responses

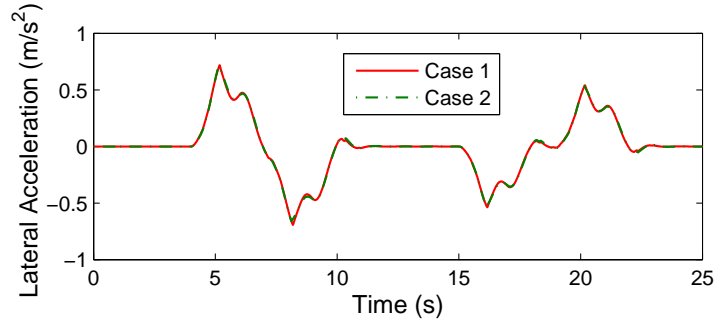
Figure 4.28: Lane keeping control results at different speeds (2)

Table 4.6: Parameter Variations

	Mass (kg)	Movement Inertia ( $kgm^2$ )	Cornering Stiffness (N/rad)
Case 1	1300	3000	36500
Case 2	2300	4400	55000



(a) Lateral position errors



(b) Lateral acceleration responses

Figure 4.29: Lane keeping control results under different loads

where  $g$  is the gravitational acceleration. The highway lane width is chosen as 3.75 m. With these values, the transit time  $T = 6.05s$ . The VDT is shown in Fig. 4.30.

We perform the lane changing scenarios at the speeds of 30, 60 and 90 km/h respectively. Fig. 4.31(a) shows the tracking errors for the three cases. The peak tracking error is about 0.06 m, which appears at the speed of 90 km/h scenario. With the speed drops down, the peak tracking errors at 60 km/h and 30 km/h decrease to about 0.04 m. Figure 4.31(b) shows the lateral acceleration results. One can find that the lateral acceleration responses are always less than  $1 m/s^2$ . Furthermore, the three curves are very similar, which means the proposed lateral controller working together with the VDT can provide stable performances under different operation speeds.

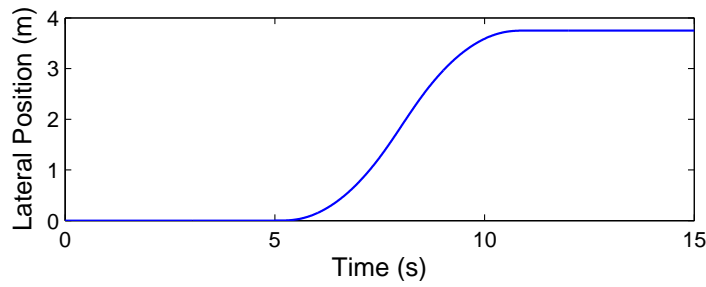
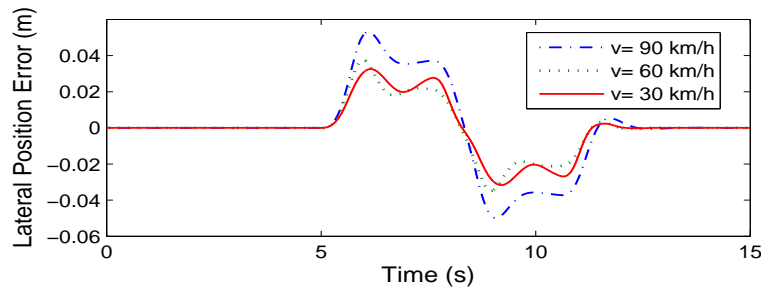
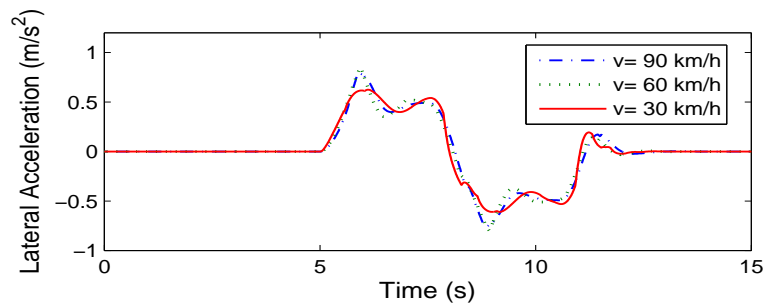


Figure 4.30: Virtual Desired Trajectory



(a) Lateral position errors



(b) Lateral acceleration responses

Figure 4.31: Lane changing control results at different speeds

#### 4.6.5 Test 5: Lane changing scenarios under different loads and Cornering Stiffness

In this test, we will test the robustness of the lane changing controller under the variations of the vehicle load and wheel cornering stiffness. We use the VDT as shown in Fig. 4.30. Two sets of vehicle parameters are shown in Table 4.6. Two simulations are carried out separately with the two sets of parameters, while the vehicle speed for these tests is set to 60 km/h. Figs. 4.32(a), 4.32(b) show the tracking error results and lateral acceleration results respectively. Although the values of the vehicle parameters change a lot in the two cases, the results are very similar. This shows the proposed controller is robust under the variations of these parameters.

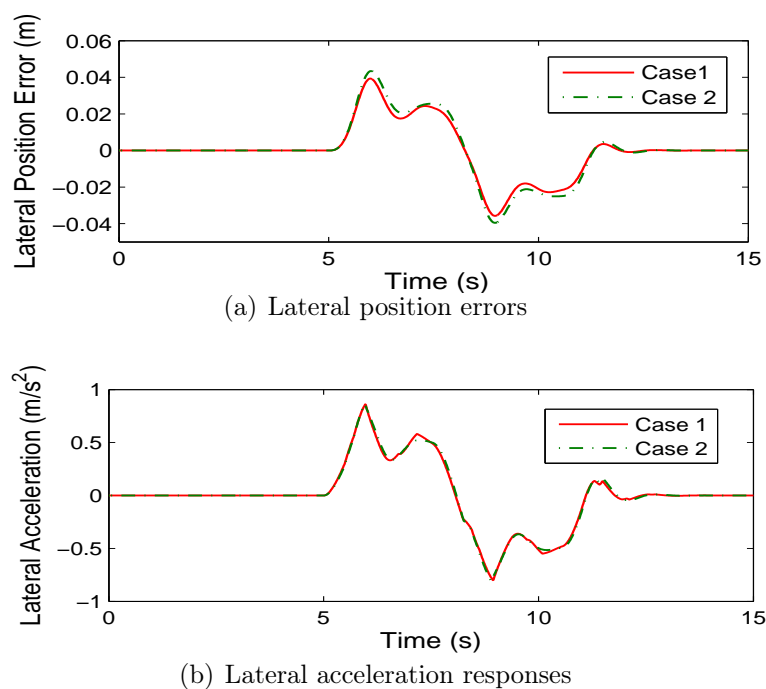


Figure 4.32: Lane changing control results under different loads

## 4.7 Conclusion

In this chapter, we presented a lateral control system, which was capable of performing lateral operations for the autonomous vehicles. This system was built on a hierarchical control architecture, with this architecture we could perform the basic lateral operations of lane keeping and lane changing. By combining the two basic operations, we could reach the more complex operations, such as overtaking, etc. One major difficulty in lane changing control is that the vehicle need to travel a certain distance without seeing any road references when the on-board sensors' range cannot cover both the two adjacent lanes. By using the concept of "Virtual Desired Trajectory"(VDT), the lane changing problem is then transferred to a lane tracking task.

Since the vehicle lateral dynamic is deeply influenced by the vehicle longitudinal speed, a multi-model fuzzy controller, which includes four local controllers and a fusion block, was then proposed for the lane tracking tasks in both the lane keeping and lane changing controllers. Simulations showed that it could provide good tracking performances while at the same time ensuring ride comfort in the whole range of operation speed, and it could also repel the system uncertainties such as changes in vehicle load, movement inertia and wheel cornering stiffness. Furthermore, as in each local controller, there are only 3 linguistic values for the input variables and 5 linguistic values for the output variable,

and there are totaly 9 fuzzy rules. Thus the calculation procedure is not complex, and is rather rapid. It appears a promising control algorithm for realtime applications and to be embedded in our reduced scale vehicle platoon platform.

## Chapter 5

# Global Control System Design-Integration of Longitudinal and Lateral Controllers

### Contents

---

<b>5.1</b>	<b>Introduction . . . . .</b>	<b>143</b>
<b>5.2</b>	<b>System integration . . . . .</b>	<b>144</b>
5.2.1	Uncoupled longitudinal and lateral control system . . . . .	144
5.2.2	Integrated longitudinal and lateral control system . . . . .	144
<b>5.3</b>	<b>Simulation experiments . . . . .</b>	<b>146</b>
<b>5.4</b>	<b>Conclusion . . . . .</b>	<b>147</b>

---

## 5.1 Introduction

In chapter 3, we have proposed a longitudinal control system, which includes an upper controller and a lower level controller, to perform the vehicle longitudinal speed control by using brake and throttle control. In chapter 4, a multi-model fuzzy control system has been proposed to perform the lateral control tasks for the autonomous vehicles. However, the objective of our work is to design a global control system which can perform the automatic driving in highway. Therefore, the above proposed longitudinal and lateral control systems should be integrated into a global control system which can perform the two control tasks simultaneously.

In this chapter, at first, we will establish a global control architecture which includes the longitudinal and lateral control systems, and then we will test the performance of the global control system throughout a series of experiments based on Matlab/Simulink. Finally, some conclusions will be given.

## 5.2 System integration

### 5.2.1 Uncoupled longitudinal and lateral control system

In the former researches, Wijesoma and Kodagoda have shown a global control architecture for a golf car-like AGV (Autonomously Guided Vehicle) [Kodagoda 2002, Wijesoma 1999]. In their works, the coupling effects of vehicle speed on steering angle (and hence angular velocity), and vice versa, was not explicitly accounted for. Thus a global control system contenting the independent longitudinal controller and lateral controller was proposed in Fig. 5.1.

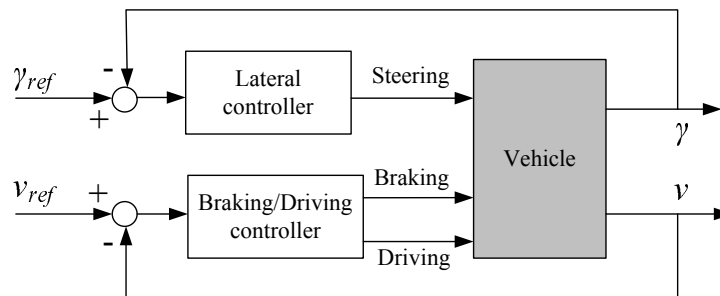


Figure 5.1: Uncoupled longitudinal and lateral control system

In this control system, the longitudinal and lateral control are achieved through separate uncoupled controllers. The single longitudinal control performance and lateral control performances were tested to be effective in their works. In addition, the simultaneous operations of the longitudinal and lateral control were also considered. But, the variation of speed is only from  $3\text{ m/s}$  to  $7\text{ m/s}$ , which is reasonable for the Golf Car but not sufficient for the highway vehicle operations, because this speed region covers only the low speed region for the vehicle driving in highway.

### 5.2.2 Integrated longitudinal and lateral control system

Although in our previous works, the longitudinal and lateral controllers have been designed separately in chapters 3, 4, but we have shown that the vehicle longitudinal speed has

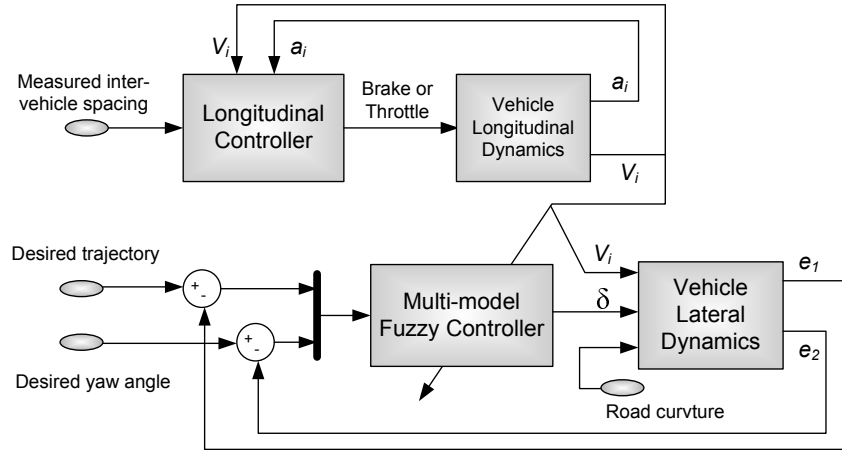


Figure 5.2: Integrated control system

a significant impact on vehicle lateral dynamics. Then, the uncoupled global control system shown in Fig. 5.1 is not appropriate in our application. Therefore, we propose an integrated control system in which the longitudinal and the lateral controllers are connected by the vehicle longitudinal speed as shown in Fig. 5.2.

In this control system, the longitudinal controller block represents the longitudinal control system which includes the upper and the lower level controllers, as we have shown in Fig. 3.1. The upper level controller in the longitudinal control system is the SSP spacing policy that we have proposed in equation (3.33), written as:

$$\ddot{x}_{i\_des} = -(\lambda\delta_i + \varepsilon_i)/(t_d - \frac{\gamma}{j_i}x_i)$$

The details of the upper level controller are described in section 3.3.5. The lower level controller included in the longitudinal control system is the coordinated throttle and brake fuzzy controller that we have proposed in section 3.4.

For the task of lateral control, we use the multi-model controller that we have proposed in section 4.5.3, see Fig. 4.21.

With this integrated control system, we can manage either the longitudinal movements or the lateral movements of autonomous highway vehicles. Furthermore, some more complex maneuvers, which require simultaneously operations both in longitudinal and lateral directions, could also be achieved in this integrated control system.

### 5.3 Simulation experiments

Since in sections 3.3.6 and 4.6, the independent longitudinal controller and lateral controller have been already examined and validated through a series of simulation tests. In this section, we will test the experiment vehicle's behavior in a more practical case where the longitudinal and lateral controllers operate simultaneously, as this will give us some results under the coupling effects between the steering and driving systems.

The values of the parameters used for the simulation are shown in Table 5.1.

Table 5.1: Parameters for longitudinal controller

Parameters	L	$w$	$t_d$	$\lambda$	j
Value	6.5 m	4.5 m	0.1 sec	0.4	-7.32 m/s <sup>2</sup>
Parameters	m	$I_z$	$l_f/l_r$	$C_{af}/C_{ar}$	
Value	1485 kg	2872 kgm <sup>2</sup>	1.1/1.58 m	42000 n/rad	

We build a scenario which requires the simultaneous operations of the longitudinal and lateral controllers. In this scenario, the controlled vehicle is supposed to follow a leading vehicle which will perform accelerate and decelerate operations. And at the same time, the controlled vehicle will trace a desired trajectory in which the steering operations are required. The profile of the proceeding vehicle's speed and the desired lateral displacement are shown in Fig. 5.3. In Fig. 5.3(a), one can find that during the period of [5, 10] s, the controlled vehicle needs to accelerate from 10 m/s to 26 m/s (36 km/h to 93.6 km/h), and then during the period of [25, 37] s, the vehicle decelerates from 26 m/s to a low speed of 5 m/s (18 km/h). While, in Fig. 5.3(b), it shows that the controlled vehicle needs to perform a 3-meter deviation during the accelerate period and it needs to steer back during the decelerate period.

The results of the longitudinal control system, which include the upper and lower longitudinal controllers, are shown in Fig. 5.4. The time history of the proceeding and the following vehicles' speeds are shown in Fig. 5.4(a). We can find that the following vehicle can follow smoothly the speed variations of the proceeding vehicle. Figure 5.4(b) shows the longitudinal spacing error of the controlled vehicle during the experiment period. The maximum longitudinal spacing error is about 0.22 m when the desired inter-vehicle spacing is about 19.7 m, thus at this time, the spacing error is only around 1.1%.

Figure 5.4(c) shows the coordinated throttle and brake controller results. One can find the throttle and brake actuators can work coordinately, and smoothly. However, there are three little oscillations in the throttle curve. In fact, these oscillations are induced by

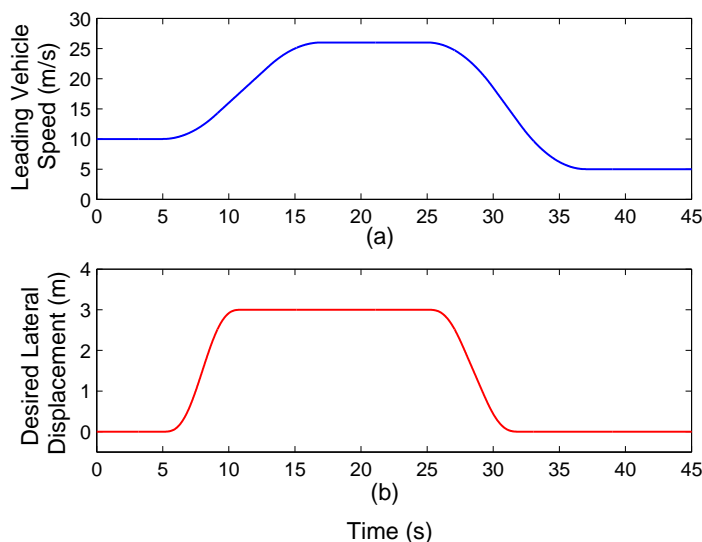


Figure 5.3: Speed and road profiles

the gear shift operations of the gearbox, see Fig. 5.4(d).

Figure 5.5 shows the results of the lateral control system. The result of the steering angle of the controlled vehicle is shown in Fig. 5.5(a). One can find the controlled vehicle can steer accurately and smoothly to trace the desired trajectory, and there is no high frequency oscillation in the steering output.

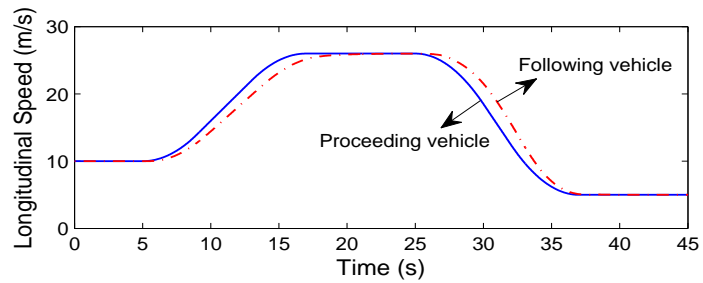
The results of the lateral position error and lateral acceleration are shown in Figs. 5.5(b) and 5.5(c) respectively. One can find that the maximum lateral position error is less than  $0.05m$ , and the maximum lateral acceleration is less than  $0.8 m/s^2$ , which mean the tracing accuracy and ride comfort are ensured during this simultaneous operations of the longitudinal and lateral controllers.

## 5.4 Conclusion

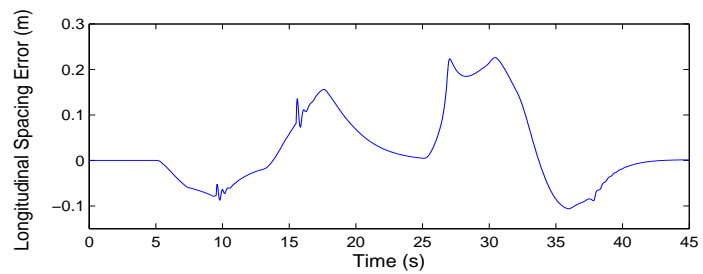
In this chapter, we concentrated on the problem of designing a global control system, which could control both the longitudinal and lateral movements of the automated vehicle by using the longitudinal controller and lateral controllers that we have proposed in chapter 3 and 4. Since, in our work, the vehicle longitudinal speed has been demonstrated as a key parameter that can influence the vehicle lateral dynamics, and we use it to build up a multi-model lateral controller. Thus, the uncoupled longitudinal and lateral control system is no longer available in our case.

Therefore, we proposed a global control system, in which the longitudinal and the

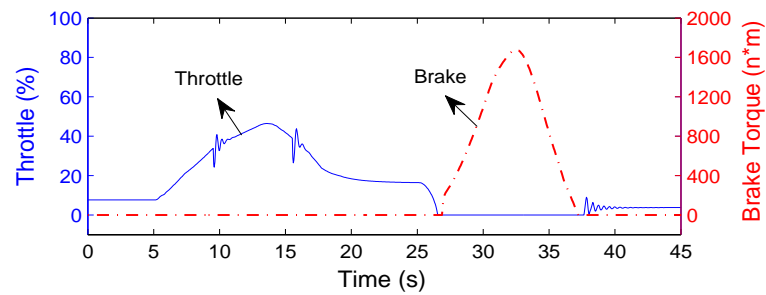
lateral controllers were connected by the vehicle longitudinal speed. In this way, the designed longitudinal control system and the multi-model fuzzy control system can work coordinately. The simulation experiments showed that the proposed global control system could provide good performances in the scenario where the steering operations and acceleration(or deceleration) operations were performed simultaneously. With this control system, we can achieve the more complex scenarios where different longitudinal and lateral operations are required.



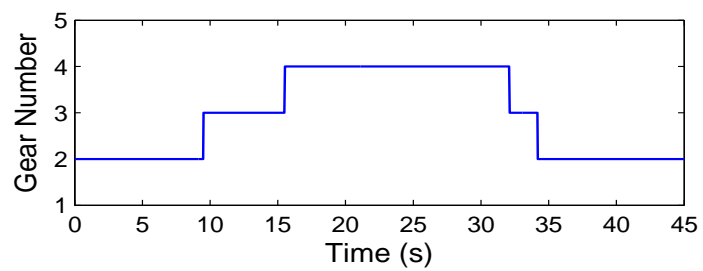
(a) Leading vehicle and following vehicle speed



(b) Longitudinal spacing error of the following vehicle

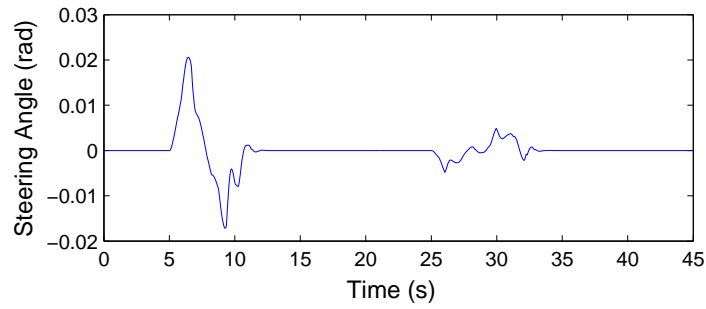


(c) Throttle and brake control results

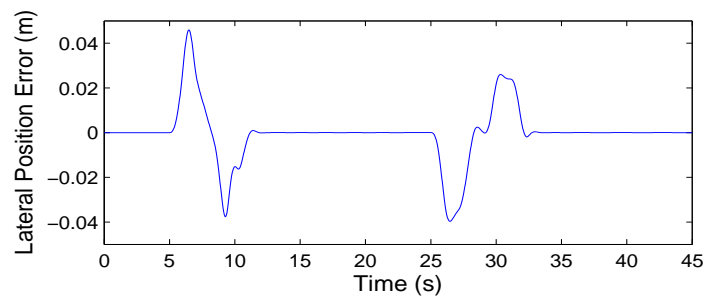


(d) Gear shift history

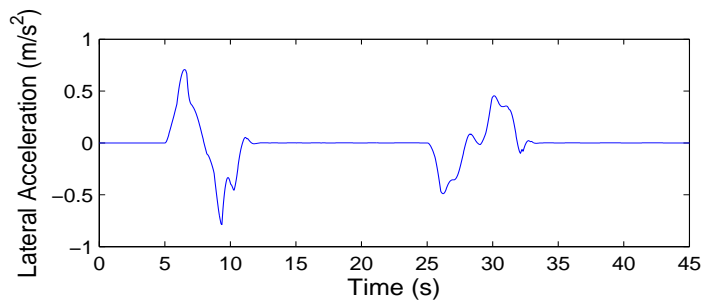
Figure 5.4: Longitudinal control results



(a) Steering angle



(b) Lateral position error



(c) Lateral acceleration

Figure 5.5: Lateral control results

# Chapter 6

## Observation of Vehicle States and Multi-Sensor Intelligent Vehicle Prototype

### Contents

---

<b>6.1</b>	<b>Introduction . . . . .</b>	<b>152</b>
<b>6.2</b>	<b>Observation of vehicle states . . . . .</b>	<b>152</b>
6.2.1	Introduction . . . . .	152
6.2.2	Kalman-Bucy Filter for LTV system . . . . .	154
6.2.3	Yaw rate and lateral velocity estimation using Kalman-Bucy filter	155
6.2.4	Estimation results . . . . .	158
<b>6.3</b>	<b>Presentation of reduced scale multi-sensor intelligent vehicle prototype . . . . .</b>	<b>159</b>
6.3.1	Technologies . . . . .	159
6.3.2	Integration . . . . .	164
6.3.3	Control strategies and first tests . . . . .	164
<b>6.4</b>	<b>Conclusion . . . . .</b>	<b>164</b>

---

## **6.1 Introduction**

In the previous chapters, the intelligent vehicle motion control systems have been studied. In the controller design process, we assume that all vehicle states are accurately measured by different type of sensors, such as longitudinal and lateral acceleration, velocity, inter-vehicle spacing, yaw angle, lateral displacement, etc. In practice, however, some states are not measurable, or some states are measurable but due to the high cost of sensors and rigorous installation requirements, we can not measure them directly. Then we need to design observers to estimate unavailable state variables. In addition, even for the states that can be directly measured, on account of the sensor noise which will degrade the control performance, and sensor fault diagnosis, the observer design is also an important issue need to be considered.

This chapter is devoted to two aspects relating to the practice: the observation of vehicle states and a multi-sensor intelligent vehicle prototype. At first, the vehicle sensor system configuration is discussed. Second, the principle of the Kalman-Bucy filter is introduced. Then a Kalman-Bucy filter is designed to estimate vehicle yaw rate and lateral velocity by using lateral acceleration measurement. Finally, a reduced scale multi-sensor intelligent vehicle prototype will be introduced.

## **6.2 Observation of vehicle states**

### **6.2.1 Introduction**

The effectiveness of a vehicle dynamic control system relies on accurate knowledge of vehicle states. Generally, the vehicle states are directly measured by the onboard sensors. However, some states are not measurable, in addition, even for the measurable states, due to the limitations in sensor accuracy, cost, reliability, we can not always get the vehicle states directly from onboard sensors. Thus the vehicle state estimation is a very important aspect in vehicle control system design. It should be noted that estimation is also one of the key technologies for onboard fault diagnosis.

Vehicle state estimation problem can be divided into four aspects: sensor configuration, physical model, estimation algorithm and parameter adaption [Yu 2009].

According to the divers application objectives, the typical estimation states are vehicle

speed, yaw rate and side-slip angle. Take ABS (Anti-lock Brake System) and ESP (Electronic Stability Program) as an example, which are the most two typical active security systems in today's market. ABS highly depends on the estimation of vehicle speed. And ESP needs the yaw rate as an important control input, although the gyroscope sensor can provide direct measurement of yaw rate, the high price of gyroscope sensor (compared to the other sensors) makes the ESP system can be only equipped in the high-end models. Using state estimation, the yaw rate can then be estimated (indirectly measured) through other already employed and low cost sensors, such as lateral acceleration sensor.

### **Selection of state to be estimated**

Since our work mainly concerns two aspects in vehicle motion control: longitudinal control (spacing control) and lateral control (steering control). In the longitudinal control system, the required information such as: longitudinal acceleration, speed, inter-vehicle spacing can be obtained by using the acceleration sensor, wheel rotation sensor and radar (or infrared sensor). While, in the lateral control system, the vehicle lateral displacement and yaw angle are two input parameters. Normally, the Magnet-Magnetometer reference system (look down system) can provide the lateral displacement measurement. Then the yaw angle is the parameter to be estimated.

### **Observation methods in former researches**

Different observation algorithms have been proposed in former literatures. For the linear system observation, the traditional Luenberger observer and Kalman filter are widely used [Luenberger 1971, Kalman 1960]. The Luenberger observer, which is based on the pole-placemen of LTI system (Linear Time Invariant), was proposed to estimate the states in vehicle lateral dynamics [Kiencke 1997]. However, the problem for this method is that the poles are shifting, caused by changes of the system parameters (for example, the vehicle speed  $v$ ). In [Venhovens 1999], the application of Kalman filter in vehicle dynamics estimation was discussed. An example of using Kalman filter to estimate lateral velocity was introduced. Gao Z.H. has proposed a "soft measurement" of vehicle yaw rate by using discrete Kalman filter [Zhenhai 2003]. The results showed that the proposed Kalman filter could provide accurate estimation of yaw rate, however, the experiment vehicle speed was assumed to be a constant (22 m/s). The results under the variations of vehicle speed have not been provided.

While, for the nonlinear system, different solutions have been proposed, such as Extend Luenberger observer, Extend Kalman filter, sliding-mode observer are the conven-

tional nonlinear observers [Stephant 2004, Shaozhong 2009]. Besides, some other nonlinear observers have been also proposed for the vehicle state estimation, such as estimation based on  $H_\infty$  algorithm, neural network estimate and fuzzy logic, and etc., see [O'Brien Jr 2006, SASAKI 2000, Shuming 2005].

In conclusion, considering the vehicle controller requirements together with sensor system configuration, we choose the yaw rate as the state to be estimated. Since in chapter 2, we have shown that the vehicle lateral dynamic equation (2.58) is a LTV (Linear Time variant) system with the consideration of vehicle parameters variations, such as the variation of vehicle speed. Therefore, the traditional Luenberger observer is not available in our case. We choose the Kalman filter to estimate the yaw rate.

### 6.2.2 Kalman-Bucy Filter for LTV system

The famous Kalman filter, based on the state-space formulation of linear dynamic systems, provides a recursive solution to the linear optimal filtering problem. The Kalman filter is a set of mathematical equations that provides an efficient computational means to estimate the state of a process, in a way that minimize the mean of the squared error. The mathematical algorithms was original provided in [Kalman 1960] for the discrete system and [Kalman 1961] for the continue system. The Kalman-Bucy filter is the continue version of the Kalman filter.

Let us consider here LTV system defined by the following state space model:

$$\begin{aligned}\dot{x}(t) &= A(t)x(t) + B(t)u(t) + G(t)w(t), \\ y(t) &= C(t)x(t) + v(t)\end{aligned}\tag{6.1}$$

where  $x(t)$  is the state vector,  $y(t)$  denotes the measured signal,  $u(t)$  is the control input,  $w(t)$  and  $v(t)$  represent the process and measurement noise respectively. The noises are assumed to be independent (of each other), white, Gaussian and with the following covariance matrices:

$$\begin{aligned}E\{w(t)w^T(t')\} &= Q(t)\delta(t-t'), \quad E\{v(t)v^T(t')\} = R(t)\delta(t-t'), \\ E\{v(t)w^T(t')\} &= 0, \quad E\{v(t)\tilde{x}^T(0)\} = 0, \\ E\{w(t)\tilde{x}^T(0)\} &= 0, \quad E\{\tilde{x}(0)\tilde{x}^T(0)\} = P_0,\end{aligned}\tag{6.2}$$

where,  $\delta(t)$  is the Dirac delta, and  $x(0)$  is a random variable with the expected value  $m_0$ ,  $\tilde{x}(0) = x(0) - m_0$ .

The filter consists of two differential equations, one for state estimate and one for the

covariance:

$$\dot{\hat{x}}(t) = A(t)\hat{x}(t) + B(t)u(t) + K(t)[y(t) - C(t)\hat{x}(t)] \quad (6.3)$$

$$\dot{P}(t) = A(t)P(t) + P(t)A^T(t) + G(t)Q(t)G^T(t) - K(t)R(t)K^T(t) \quad (6.4)$$

where the second equation is a Riccati equation, and the Kalman gain is given by:

$$K(t) = P(t)C^T(t)R(t)^{-1} \quad (6.5)$$

Equations (6.3), (6.4) and (6.5) define the continuous-time Kalman-Bucy estimator, which is also called the Kalman-Bucy filter [Kalman 1960, Kalman 1961, Borne 1990].

### 6.2.3 Yaw rate and lateral velocity estimation using Kalman-Bucy filter

The issue of vehicle lateral dynamics has been discussed in Chapter 2. The well known two degree-of-freedom “bicycle model” was introduced. Recall the bicycle model, as shown in Fig. 6.1.

Rewrite the vehicle lateral dynamic equation in the state space form:

$$\dot{X} = AX + B\delta \quad (6.6)$$

where,  $X$  is the state vector,  $X = [y, \dot{y}, \psi, \dot{\psi}]^T$ ,  $y$  and  $\psi$  denote the vehicle lateral displacement and yaw angle respectively,  $\delta$  represents steering angle, and

$$A = \begin{bmatrix} 0 & 1 & 0 & 0 \\ 0 & -\frac{2C_{af} + 2C_{ar}}{mV_x} & 0 & -V_x - \frac{2C_{af}l_f - 2C_{ar}l_r}{mV_x} \\ 0 & 0 & 0 & 1 \\ 0 & -\frac{2l_f C_{af} - 2l_r C_{ar}}{I_z V_x} & 0 & -\frac{2l_f^2 C_{af} + 2l_r^2 C_{ar}}{I_z V_x} \end{bmatrix}$$

$$B = \begin{bmatrix} 0 \\ \frac{2C_{af}}{m} \\ 0 \\ \frac{2l_f C_{af}}{I_z} \end{bmatrix}$$

the variables in the matrices  $A$  and  $B$  are shown in table 6.1.

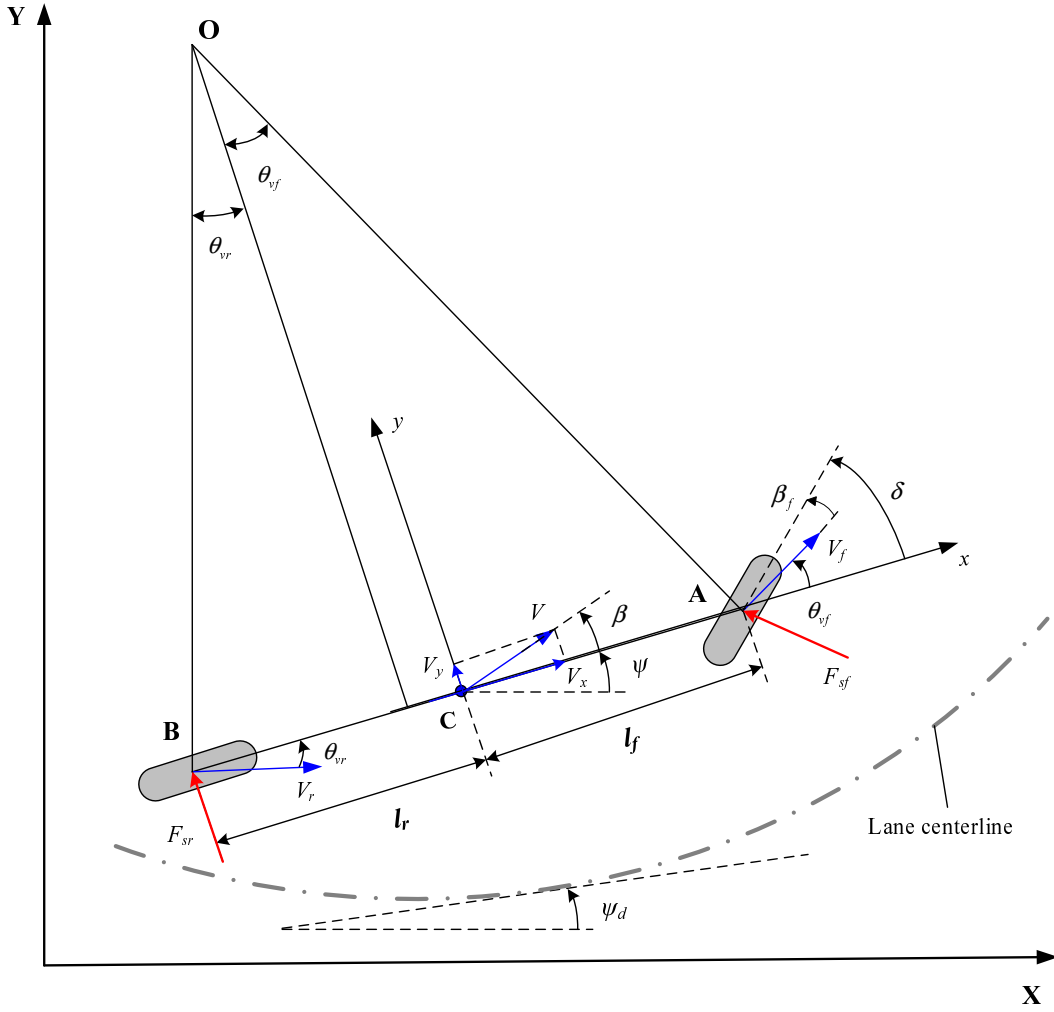


Figure 6.1: Bicycle model for vehicle lateral dynamics

Since the lateral acceleration sensor is a common sensor can be easily obtained, in our system, the lateral acceleration  $\ddot{y}$  is selected as the measured variable. Then from equation (6.6), we can get:

$$\ddot{y} = a_y = -\frac{2C_{af} + 2C_{ar}}{mV_x} \dot{y} + \left( -V_x - \frac{2C_{af}l_f - 2C_{ar}l_r}{mV_x} \right) \dot{\psi} + \frac{2C_{af}}{m} \delta \quad (6.7)$$

From equation (6.7), one can find that only the state variables  $\dot{y}$  and  $\dot{\psi}$  are related with the measured variable  $\ddot{y}$ , while the state variables  $y$  and  $\psi$  do not have an one-to-one mapping to the measurement  $\ddot{y}$ . We eliminate the states  $y$  and  $\psi$  from equation (6.6). Then, the simplified state space model for observation and measurement equation can be given by:

Table 6.1: Nomenclature of Bicycle Model

$\psi$	yaw angle (rad)
$\delta$	steering angle (rad)
$\rho$	road curvature (1/m)
$m$	mass (1485kg)
$V_x/V_y$	longitudinal/lateral velocity (m/s)
$I_z$	yaw moment of inertia (2872kgm <sup>2</sup> )
$l_f/l_r$	distance between the C.G. and the front/rear wheels (1.1/1.58m)
$C_{af}/C_{ar}$	cornering stiffness of the front/rear wheels ( $C_{af} = C_{ar} = 42000N/rad$ )

$$\begin{aligned}\dot{X} &= A_1X + B_1\delta + G_1w \\ \dot{y} &= C_1X + D_1\delta + v\end{aligned}\quad (6.8)$$

where,  $X$  is the state vector,  $X = [\dot{y} \ \psi]^T$ .  $\dot{y}$  is the measurement.  $\delta$ , steering angle, is the system input,  $w$  is the process noise,  $w = [w_1 \ w_2]^T$ ,  $v$  is the measurement noise, and

$$A_1 = \begin{bmatrix} -\frac{2C_{af} + 2C_{ar}}{mV_x} & -V_x - \frac{2C_{af}l_f - 2C_{ar}l_r}{mV_x} \\ -\frac{2l_fC_{af} - 2l_rC_{ar}}{I_zV_x} & -\frac{2l_f^2C_{af} + 2l_r^2C_{ar}}{I_zV_x} \end{bmatrix}, B_1 = \begin{bmatrix} \frac{2C_{af}}{m} \\ \frac{2l_fC_{af}}{I_z} \end{bmatrix},$$

$$C_1 = \left[ \left( -\frac{2C_{af} + 2C_{ar}}{mV_x} \right) \quad \left( -V_x - \frac{2C_{af}l_f - 2C_{ar}l_r}{mV_x} \right) \right],$$

$$D_1 = \begin{bmatrix} \frac{2C_{af}}{m} \end{bmatrix}, G_1 = \begin{bmatrix} 1 & 0 \\ 0 & 1 \end{bmatrix},$$

the meaning of the parameters in the above matrices are shown in table 6.1.

From equation(6.8), one can find that the system matrices  $A_1$  and  $C_1$  are functions of longitudinal velocity  $V_x$ . Since in our work, the vehicle speed variation is considered as an important factor in the lateral controller design (see chapter 4). The speed variation should also be considered in the estimation process. Therefore, the vehicle state estimation problem described by equation (6.8) is a LTV system estimation problem.

At first, we need to validate the observability of the system described in equation (6.8). The observability matrix of the system is

$$M = \begin{bmatrix} N_0 \\ N_1 \end{bmatrix} \quad (6.9)$$

where,  $N_0 = C_1$ , and  $N_1 = N_0 A_1 + \frac{dN_0}{d(V_x)} \frac{d(V_x)}{dt}$ .

Then we can get,

$$M = \begin{bmatrix} \frac{a_1}{V_x} & -V_x - \frac{a_2}{V_x} \\ -a_3 + \frac{a_1^2 - a_2 a_3 - a_1 a_{cc}}{V_x^2} & (-a_{cc} - a_1 - a_4 + \frac{a_2 a_{cc} - a_1 a_2 - a_2 a_4}{V_x^2}) \end{bmatrix}, \text{ rank of } M \text{ is } 2. \quad (6.10)$$

where  $a_{cc}$  is the vehicle acceleration, and

$$a_1 = -\frac{2C_{af} + 2C_{ar}}{m}, \quad a_2 = \frac{2C_{af}l_f - 2C_{ar}l_r}{m},$$

$$a_3 = -\frac{2l_f C_{af} - 2l_r C_{ar}}{I_z}, \quad a_4 = -\frac{2l_f^2 C_{af} + 2l_r^2 C_{ar}}{I_z}$$

Therefore, the system is observable.

Then, a Kalman-Bucy filter can be designed by following the equations (6.3), (6.4) and (6.5), which can be used to estimate the state variables lateral velocity and yaw rate by using the lateral acceleration measurement.

### 6.2.4 Estimation results

In this subsection, we will test the performance of the designed observer by using *Matlab/Simulink*. The vehicle parameters are given in table 6.1. The vehicle performs a sinusoidal steering operation, the steering angle is given by:

$$\delta = 0.1 \sin\left(\frac{t}{2.5} + 0.1N(t)\right) \quad (6.11)$$

where, the unit of  $\delta$  is *rad*,  $t$  denotes the time, and  $0.1N(t)$  represents the steering input noise caused by the steering mechanism and uncertainties of road conditions,  $N(t)$  is assumed to be a normal distribution with mean 0 and standard deviation 1,

$$N(t) \sim \mathcal{N}(0, 1) \quad (6.12)$$

The vehicle speed variation is described as follows: from 0s to 20 s, the vehicle keeps a constant speed of 5 m/s (18 km/h), and then the vehicle begins to accelerate from 5 m/s to 25 m/s (90 km/h) with an acceleration of 0.4 m/s<sup>2</sup>, and then the vehicle keeps the final speed of 25 m/s.

The time histories of vehicle steering angle and speed variation are shown in Fig. 6.2.

Figure 6.3 shows the plots of measured and estimated lateral acceleration. The “filtering” function of the Kalman filter is evident as the estimate appears considerably smoother than the noisy measurement.

The true and estimated values of lateral velocity and yaw rate are shown in fig. 6.4. Although the vehicle velocity varies in a wide range, and the lateral acceleration measurement is noisy, the estimated lateral velocity and yaw rate can closely follow the variations of the true values during the whole experiment period. The designed Kalman-Bucy filter is proved to be effective in the vehicle lateral dynamic estimation.

## 6.3 Presentation of reduced scale multi-sensor intelligent vehicle prototype

In this section, a reduced scale (1:10) multi-sensor intelligent vehicle prototype will be introduced [El Kamel 2006]. This prototype provides a platform for advanced technology integration, reliability analysis, real time control and monitoring... An overview of the platoon is shown in Fig. 6.5. The different parts of the car are to be explained in the following sections.

### 6.3.1 Technologies

#### 6.3.1.1 Multi-sensor system

At first, the multi-sensor system, which is necessary to perform the control strategies, will be introduced. A cost oriented principle was established when choosing the most advanced technologies which meet the operation requirements for the reduced scale cars. The multi-sensor system diagram and configuration are shown in Fig. 6.6.

#### Sensors for longitudinal control

We propose to determine distance between vehicles by using two kinds of sensors, both chosen because of their 2m-range which makes them efficient and reliable at our scale:

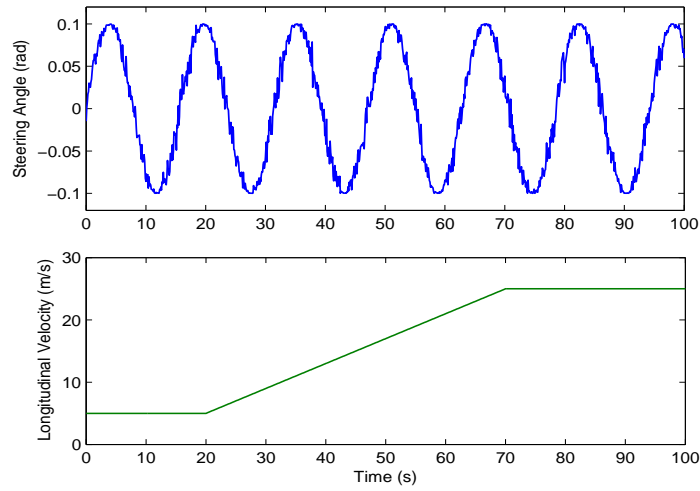


Figure 6.2: Steering angle input and vehicle longitudinal velocity

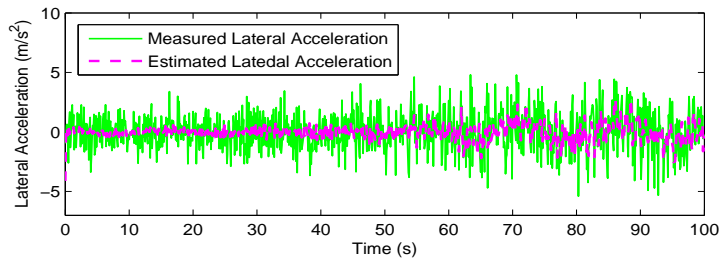


Figure 6.3: Measured and estimated lateral acceleration

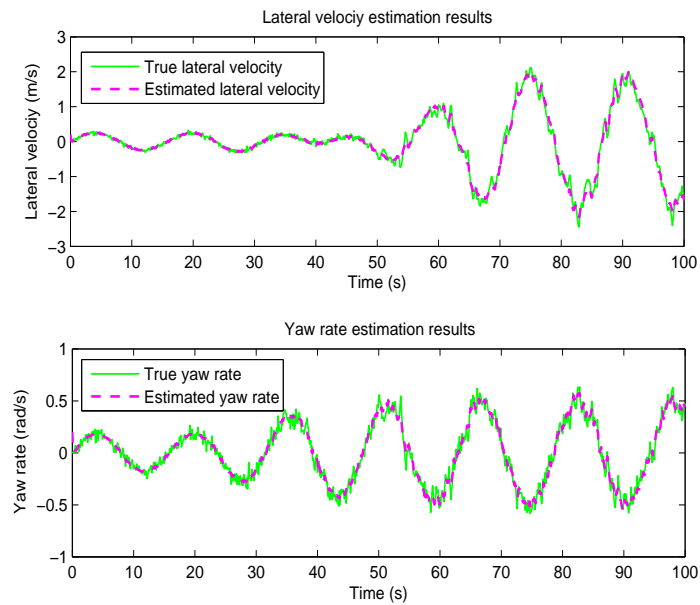


Figure 6.4: Estimation results



Figure 6.5: Two-car platoon

- Infrared telemeter: it measures the changing between the outgoing wave and the phototransistor that receives it after reflection on an obstacle.
- Ultrasonic sensors: they use the propagation time of a short ultrasonic impulsion which is proportional to the distance between vehicles.

The two distance measurements are sent to the intelligent system which compares them and deduces the reliable data based on a data fusion process.

### **Sensors for trajectory tracking**

The road (or desired trajectory) is represented by a white line drawn on the ground that the platoon has to follow. The position of the vehicle with respect to the white line is given by an integrated system camera/microprocessor. Thus, with the given color of the line, the microprocessor of the camera is able to compute the barycenter of the line and to send it digitally to the intelligent central system.

However, since the line tracking is a critical function for the vehicle and hence cannot accept any misleading without dramatic consequences, a magnet/magnetometer system is also introduced. The magnetic plots are fixed on the lane center, and two magnetometers placed on the left and right sides of the front bumper. We can compare the tensions delivered by each one and thus get the exact position with respect to the lane, see Fig. 6.7

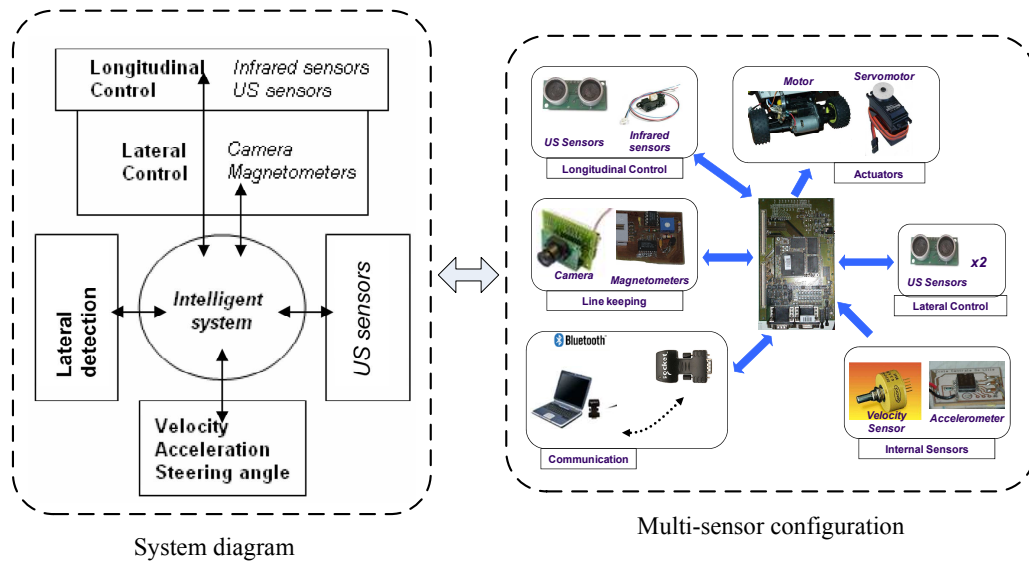


Figure 6.6: Multi-sensor system

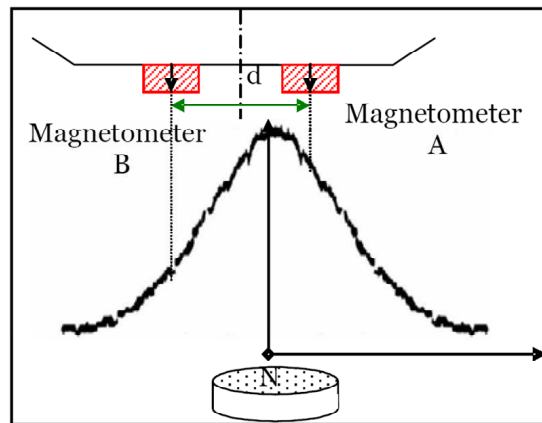


Figure 6.7: Magnetic field

### Sensors for lateral detection

In order to enable the vehicle to implement complex driving scenarios such as the insertion of a vehicle in the platoon, the lateral detection becomes essential. Indeed, to determine for instance whether a vehicle can be inserted or not, we need to be sure that there is not any other vehicle on the side. Two ultrasonic telemeters on front and end sides of the vehicle are used.

### Other sensors

We need to know at any time the specific data of each vehicle. The velocity, acceleration and steering angle are used as feedback variables for longitudinal and lateral

controls. Besides, for safety reasons, the information is sent to the supervisor using a wireless communication.

Thus, we use a sensor of angular rotation to measure the steering angle, an optical velocity sensor to determine the velocity and an accelerometer to determine the acceleration of the vehicle.

### 6.3.1.2 The microcontroller

The core of intelligent system is the microcontroller. An Infineon CS167 microcontroller has been chosen to gather all sensors' information, compute the control law, and manage the communication system. As the load of the microcontroller appears rather high and a master/slave architecture is a new solution proposed to devote a specific microcontroller to one task, communication for instance, while the second is devoted to sensor management and control strategies and an exchange protocol is developed to communicate with the main controller.

### 6.3.1.3 Wireless communication

The communication system is one of the core parts of the system. Many options are available as radio telecommunications, Wifi, Bluetooth, ZigBee. Due to the technology limitation, cost and availability in the market for the moment, a Bluetooth socket plugged on the RS-232 port of the microcontroller communicating with the PC which transmits the information to the other vehicles, see Fig. 6.8. The communication between the supervisor and a vehicle is based on a general communication protocol using a specific framework. Therefore the development of a human machine interface (HMI) is required to help the user communicate with the platoon of vehicles. The HMI is in charge of different types of data flows [El Kamel 2006].

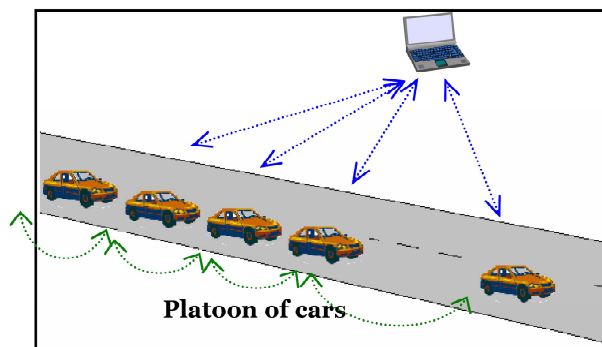


Figure 6.8: Platoon communication system

### 6.3.2 Integration

One of the main difficulties of the prototype design is to integrate all the technologies and make them work together. The integration process is explained as follows.

We have designed and built a complete architecture for the cars which takes into account interference and power issues. Figure 6.9 shows the general structure of a vehicle. It should be noted that all the devices have been organized and optimized around the microcontroller.

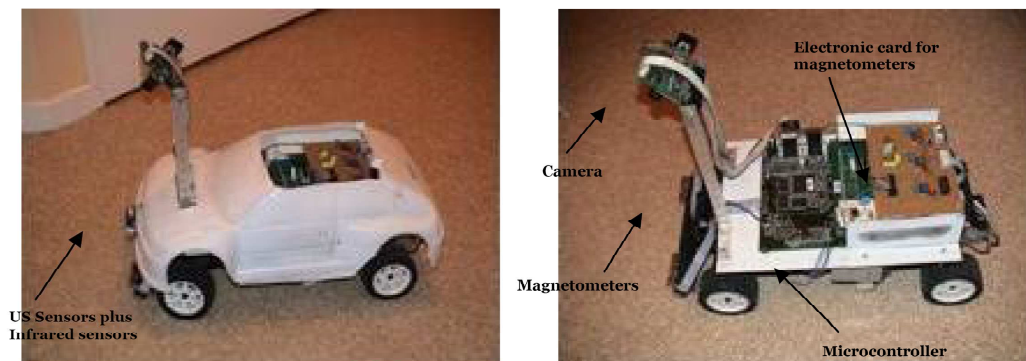


Figure 6.9: Vehicle structure

### 6.3.3 Control strategies and first tests

Two fuzzy controllers were developed for longitudinal control and lateral control separately based on the linearization of a complete two dynamical models of a car. In order to match reduced scale dynamics, the temporal and geometrical similitude was applied. Following a simulation stage, the controllers were integrated in the microcontroller based on Real Time Workshop (RTW) of *Matlab/Simulink* and embedded C-Coder toolbox destined precisely to the Infineon C 167 microcontrollers. The first tests showed that the vehicle could perform the basic following and lane tracking scenarios [El Kamel 2005, El Kamel 2007]. The more complex scenarios will be carried out in the future works.

## 6.4 Conclusion

This chapter is devoted to two aspects relating to the practice, the observation of vehicle states and the design of a multi-sensor intelligent vehicle prototype.

At first, we considered the sensor configuration problem for our intelligent vehicle control system (longitudinal and lateral control system). Due to the cost limit, the yaw

rate, which is useful in the lateral control system, is not available in our multi-sensor system. Then an observer is required to estimate the yaw rate by using the available lateral acceleration measurement.

Second, since the vehicle lateral dynamic system is a LTV system, thus the traditional observe method for LTI system (such as Luenberger observer) is not applicable in this case. A Kalman-Bucy filter was then designed to estimate the vehicle states. The designed filter can provide accurate estimation results even with the noisy lateral acceleration measurement and a wide range of speed variation.

Finally, a reduced scale multi-sensor intelligent vehicle prototype was introduced. The different aspects of the prototype from the multi-sensor system, vehicle structure, communication system, and HMI were presented. In the first-step tests, the basic functions such as vehicle following and lane tracking were realized. In the future work, the more complex operations such as platoon control with more vehicles, lane changing, join (or split from) a platoon will be carried out.



# Conclusions and Perspective

## Conclusions

This thesis is devoted to the intelligent control strategies for vehicle platoons in highway, with the main aim of resolving the traffic congestion and traffic safety problems. The whole document is structured around five themes:

1. Modeling of four wheeled vehicles
2. Longitudinal control (upper level controller, lower level controller, string stability, traffic flow stability, etc)
3. Lateral control (lane keeping control, lane changing control)
4. Integration of longitudinal and lateral control
5. Vehicle state observation and multi-sensor intelligent vehicle prototype design

The main contributions of this thesis include the following:

- At the upper level of longitudinal control system, the spacing policy and its associated control law were designed with the constraints of string stability, traffic flow stability and traffic flow capacity. A safety spacing policy (SSP) was proposed, which uses both the information of vehicle state and vehicle braking capacity to determine the desired spacing from the preceding vehicle. It was shown that the proposed SSP could provide good performances both in traffic safety and traffic capacity for highway operations. In addition, through the comparison between the SSP and the traditional Constant Time Gap (CTG) policy, we can find that the SSP system has the obvious advantage in improving traffic capacity especially in the high-density traffic conditions, i.e., it can relieve traffic congestions in peak hour. The corresponding results were published in “IEEE Intelligent Vehicle Symposium 2009”, see [Zhao 2009c].

- At the lower level of longitudinal control system, a coordinated throttle and brake fuzzy controller was proposed. One main advantage of using fuzzy approach in this case is that we can achieve the control objectives by using the linguistic expressions of driver's experiences instead of the exact mathematic model of the controlled system (such as engine or brake dynamics). The proposed controller can deal with the nonlinearity in the engine and brake dynamics. Another highlight of the lower level controller is that a logic switch is designed to coordinate the two actuators (throttle and brake pedals). It was shown that the proposed controller could successfully deal with different driving scenarios and road disturbances. The corresponding result will be published in the "IEEE Conference on Intelligent Transportation Systems 2010", see [Zhao 2010a].
- The vehicle lateral control system was designed based on a hierarchical lateral control architecture, which could effectuate flexible switch between different lateral operations. Considering the vehicle lateral dynamics is a typical LTV system which is deeply influenced by the vehicle longitudinal velocity, a multi-model fuzzy controller was then proposed. The proposed controller contains four local fuzzy controllers which correspond to four velocity intervals. In order to avoid the undesired peaks which may appear during the commutation of the different local controllers, a fusion block was designed. Simulations showed that it could provide good tracking performances while at the same time ensuring ride comfort in the whole range of operation speed, and it could also repel the system uncertainties in vehicle load, movement inertia, etc. The corresponding results can be found in [Zhao 2009b, Zhao 2010c].
- In order to reach the final goal of automated vehicle operation, the longitudinal and lateral control system should be integrated into a global controller. Since we have shown that the vehicle longitudinal velocity is a key parameter which influences the lateral controller, an integrated longitudinal and lateral control system is then proposed, in which the two controllers are connected by the vehicle longitudinal velocity. The proposed integrated system is different from the existing uncoupled control systems (such as the one in [Kodagoda 2002, Wijesoma 1999]). And it is appropriate to the real vehicle dynamics in highway than the uncoupled control system. Simulation results showed that the longitudinal controller and lateral controller could work coordinately in this global control system. The corresponding results can be found in [Zhao 2009a, Zhao 2010b].
- For the purpose of application, the estimation of vehicle states is an important issue

---

to be considered. In our case, the vehicle yaw rate is a parameter unavailable for our lateral control system. Considering the vehicle lateral dynamics is a LTV system, a Kalman-Bucy filter was designed, which could estimate the vehicle states in lateral dynamics by using the available lateral acceleration measurement. The designed filter can provide good estimation results even with the noisy lateral acceleration measurement and a wide range of speed variation. Finally, a multi-sensor intelligent vehicle prototype, which was developed in our research team, was presented.

## Perspective

Based on the results given by this thesis, several perspectives should be considered:

- In this thesis, the fuzzy logic control was used for the vehicle automation: the coordinated throttle and brake fuzzy controller and the multi-model fuzzy lateral controller. Compared with the traditional fuzzy controller, the proposed approaches provide new ways to achieve more robust and accurate control performances than the traditional approach. Based on these results, the following two suggestions should be considered for the further works:
  - 1) In this work, the stability of the proposed control algorithms was only tested by simulations in different scenarios with different disturbances. The theoretical stability analysis of the fuzzy algorithm (multi-model fuzzy system) has not been given. In fact, we choose the fuzzy control because it is a powerful approach for very complex system, non linear system and system with uncertainties... And the design of a fuzzy controller does not depend on an exact mathematic model. However, it is just the above mentioned advantages make it is often difficult or even impossible to apply nonlinear analysis techniques (such as Lyapunov method) to the fuzzy applications. In fact, to develop a mathematical theory for verification and certification of fuzzy system is still a problem for today's fuzzy controller researchers.
  - 2) The fuzzy control rules and parameters are derived from the driver experiences and time consuming simulation experiments. In order to get the "optimized" fuzzy rules and parameters, we could also introduce the Genetic algorithms or neural network to optimize the fuzzy controllers.
- The two main advantages of vehicle platoon control shown in this work are increasing traffic capacity and improving traffic safety. The related analyses were carried

out with the assumption that all the vehicles are automated controlled. However, in a mixed traffic condition, where automated vehicles operate together with manually driven vehicles, the traffic flow, traffic safety as well as fuel consumption and pollution levels are the interesting issues to be studied.

- A multi-sensors intelligent vehicle platform is introduced. In the first step experiments, some basic functions such as vehicle following and lane tracking have been realized. In the future, we need to test some more complex scenarios, such as platoon control with more vehicles, lane changing, overtaking, join (or split from) a platoon, etc. Thus, we can provide a theoretical and practical groundwork for those near term applications such as safe tunnel control, ACC system, driver assistance systems, and also for those long term applications like AHS, fully automated vehicles, etc.
- In our reduced scale vehicle platform, a communication system (Bluetooth) is introduced to communicate between the PC (supervisor) and the cars. Thus, we can supervise the system states and perform more complex scenarios. However, with the using of system communication, an important issue need to be envisaged is the time-delays which may degrade the control performance. Some constructive solutions for the time-delay problems have been proposed, such as [Moog 1996, Márquez-Martinez 2001, Márquez-Martinez 2004]. However to solve the time-delay problem in the vehicle platoon control is still an attractive topic.
- Considering the fact that a fault from any part of the vehicle control system (sensor, actuator, microcontroller, etc.) may cause serious results for vehicle safety, a fault tolerant control system is safety critical for intelligent vehicles. The subjects of fault tolerant control and reliability analysis have been studied by the researchers in BUAA (Beihang University), see [Wang 2009, Wang 2005, Wang 2004b]. In the frame of the cooperation between the two research teams from BUAA and LAGIS, the subject of fault tolerant control system for intelligent vehicles will be emphasized.

# Résumé étendu en français

Ce mémoire est consacré à la mise en oeuvre de commandes d'un train de véhicules intelligents ayant pour objectifs premiers la réduction de la congestion et l'amélioration de la sécurité routière. Au cours de ces dernières décennies, l'industrie automobile a vécu un développement considérable et par suite le secteur automobile a joué un rôle important dans l'évolution industrielle et même de notre société. Néanmoins, les problèmes de transport tels que la congestion du trafic, la sécurité routière, la pollution et la consommation de carburant sont de plus en plus graves dans le monde entier. La conception d'AHS (Automated Highway System) a été proposée pour faire face à ces problèmes et atteindre l'objectif d'une "mobilité durable", avec des véhicules pouvant rouler à terme en formation de "train de véhicules". Depuis les deux dernières décennies, des recherches sur l'AHS ont vu des progrès significatifs. Les contrôles longitudinal et latéral du véhicule représentent l'un des sujets les plus étudiés, actuellement, par les chercheurs et les constructeurs automobiles.

- **Le contrôle longitudinal**

Le système de contrôle longitudinal offre son assistance au conducteur pour contrôler le véhicule en utilisant les commandes d'accélérateur et de frein. La première génération de ces systèmes est principalement développée pour améliorer le confort de conduite avec une certaine amélioration de la sécurité. En revanche, les impacts de ces systèmes sur le trafic sont insuffisamment étudiés [Swaroop 1999]. Dans ce mémoire, nous envisageons le contrôle longitudinal pour un train de véhicules, donc nous devons tenir compte non seulement des contraintes de confort et de sécurité, mais aussi des exigences de stabilité de la chaîne, de stabilité des flux de trafic ainsi que de l'augmentation de capacité de trafic. Pour répondre à ces exigences, la structure du système de contrôle longitudinal est conçue pour être hiérarchique avec un contrôleur de niveau supérieur et un contrôleur de niveau inférieur. Le contrôleur de niveau supérieur détermine l'accélération (ou la vitesse) désirée pour le

véhicule contrôlé, tandis que le contrôleur de niveau inférieur décide des commandes d'accélération et de freinage pour suivre l'accélération (ou la vitesse) désirée.

Les tâches principales pour la conception du contrôleur de niveau supérieur sont la conception d'une régulation d'inter-distance entre les véhicules et l'algorithme de contrôle associé. La régulation d'inter-distance détermine l'espacement entre le véhicule contrôlé et le véhicule précédent, qui a des grandes influences sur les comportements du véhicule et ainsi sur le trafic. Dans ce travail de recherche, nous proposons une régulation de sécurité (SSP, Safety Spacing Policy), comme fonction non-linéaire de la vitesse du véhicule. Elle utilise à la fois les informations sur l'état du véhicule et la capacité de freinage afin d'ajuster la position et la vitesse du véhicule contrôlé. En outre, des efforts particuliers sont consacrés à l'analyse de la SSP dans les aspects de la stabilité de chaîne, et de la stabilité des flux de trafic ainsi que la capacité de trafic. Enfin, une comparaison entre la SSP et la régulation d'inter-distance traditionnelle CTG (Constant Time Gap spacing policy) est également présentée.

Les non-linéarités et les incertitudes dans la dynamique longitudinale du véhicule sont les principaux défis à relever pour la conception de contrôleurs d'accélération et de freinage (Contrôleur de niveau inférieur). Par exemple, les modèles exacts du moteur et de la dynamique du système de freinage sont toujours des modèles non-linéaires avec de nombreux paramètres. Par ailleurs, dans la plupart des cas, ces modèles sont difficiles à obtenir. En outre, afin d'avoir des opérations acceptables comme un bon conducteur humain, la commande d'accélérateur et la commande de freinage doivent être coordonnées. Pour relever ces défis, nous proposons un contrôleur de type commande floue coordonnée pour gérer l'accélérateur et le freinage. Dans un premier temps, deux commandes floues pouvant effectuer des actions additives sur les pédales d'accélération et de freinage sont proposées. Le principal avantage de cette approche est qu'elle peut réaliser le contrôle de vitesse rapidement et efficacement sans exigence de modèles exacts de moteur et de freinage. Ensuite, nous proposons une logique de commutation permettant de coordonner les actions des deux pédales (accélérateur et freinage).

- **Le contrôle latéral**

En ce qui concerne le système de contrôle latéral, il pilote l'angle de braquage du véhicule pour que le véhicule puisse suivre la trajectoire ou en changer. La loi de commande doit assurer une bonne qualité de conduite et une faible erreur

---

de poursuite. Le suivi et le changement de trajectoire sont les deux principales opérations.

Nous étudions, tout d'abord, la loi de commande pour le suivi de trajectoire. Le modèle latéral est un modèle de type "bicyclette" avec une description du pneumatique dans des conditions de faible glissement. Etant donné que les paramètres du véhicule, comme la vitesse, la masse, le moment d'inertie, la rigidité du pneu, etc., ne sont pas toujours constants, le modèle latéral est donc un système LTV (Linear Time-Variant). Nous proposons une loi de commande de type multi-modèle floue qui hérite les points forts de la commande multi-modèle et de la commande floue. Cette loi peut donner de bonnes performances pour la gamme de vitesses de conduite. Par ailleurs, elle peut maîtriser les incertitudes du système (la masse, le moment d'inertie, la rigidité du pneu, etc.).

La principale difficulté dans l'opération de changement de trajectoire est que le véhicule doit traverser une certaine distance sans les retours des capteurs si les capteurs ne peuvent pas mesurer la position du véhicule entre les deux voies, par exemple, si on utilise le capteur de type magnétomètre. Nous utilisons la trajectoire virtuelle désirée (VDT, Virtual Desired Trajectory) qui peut fournir une référence virtuelle pendant l'opération de changement de trajectoire. Afin d'effectuer des commutations flexibles entre les différentes opérations latérales, telles que le suivi de trajectoire, le changement de trajectoire, le dépassement, etc., nous proposons aussi une architecture hiérarchique pour le système de contrôle latéral.

Sur la base des résultats des commandes longitudinale et latérale, nous proposons un système de contrôle complet intégrant ces contrôles. Avec ce système complet, le contrôle pour la conduite automatisée peut être réalisé sur autoroute.

En outre, l'estimation des variables d'états du véhicule est discutée. Pour les lois de commandes que l'on a proposées, on suppose que toutes les variables utilisées sont disponibles. Néanmoins, cette hypothèse n'est pas toujours vraie dans la pratique (indisponibilité de la technologie, prix...). Par conséquent, l'observation d'état du véhicule est incontournable. Compte tenu de la configuration du système de capteurs et les états utilisés pour les contrôleurs du véhicule, nous avons choisi la vitesse de lacet du véhicule en tant que paramètre à estimer. Etant donné que la dynamique du véhicule latérale est un modèle LTV, on propose un filtre de Kalman-Bucy pour l'estimation des variables du système LTV.

Enfin, nous présentons un prototype multi-capteurs de véhicule intelligent à échelle réduite (1 :10). Les différents aspects du prototype tels que la structure du véhicule, le système de communication ainsi que l'IHM (Interface Human-Machine) sont présentés. Ce prototype offre une plate-forme pour l'intégration des technologies, l'analyse de la fiabilité, le contrôle en temps réel et la surveillance. Les performances des divers algorithmes de commande proposées dans ce mémoire ont été testées par simulations numériques, et les résultats ont été confirmés par les premières expériences en utilisant ce prototype.

## Organisation du document

**Le premier chapitre** présente l'état de l'art sur les systèmes de conduite automatisée. Dans un premier temps, le contexte et les problèmes du trafic sont mis en place. Ensuite, nous présentons les solutions les plus intéressantes : ITS, AHS et Véhicule intelligent. Enfin, les évaluations des grands projets en cours ainsi que l'évolution des contrôles longitudinal et latéral sont présentées en détail.

Dans **le deuxième chapitre**, nous réalisons, tout d'abord, les modèles de la dynamique longitudinale et latérale, afin d'élaborer des lois de commande pour la régulation de la position du véhicule suiveur dans la suite des travaux. On établit le modèle longitudinal en utilisant la formule de Newton. Puis, la description mécanique du comportement du groupe motopropulseur est présentée. Ce dernier comprend les sous-modèles des différentes parties : le moteur, le convertisseur de couple, la boîte de vitesses automatique, les arbres de transmission et le différentiel.

En ce qui concerne le modèle latéral, nous présentons à la fois le modèle cinématique ainsi que le modèle dynamique. Le modèle cinématique fournit une description mathématique du mouvement du véhicule sans tenir compte des forces influant le mouvement. Quant au modèle dynamique, le modèle retenu est un modèle de type "bicyclette" avec une description du pneumatique dans des conditions de faible glissement. Les modèles longitudinal et latéral sont utilisés par la suite pour générer les lois de commande dans les chapitres suivants.

Dans **le troisième chapitre**, nous développons la loi de commande longitudinale. Le système de contrôle longitudinal est conçu pour être hiérarchique avec un contrôleur de niveau supérieur et un contrôleur de niveau inférieur. Pour le contrôleur de niveau supérieur, une régulation d'inter-distance (SSP, Safety Spacing Policy) est proposée. Elle utilise à la fois les états du véhicule et la capacité de freinage pour déterminer la distance désirée pour le véhicule suiveur. Nous présentons aussi une comparaison entre la SSP

---

et la régulation d'inter-distance traditionnelle CTG (Constant Time Gap spacing policy). Quant au contrôleur de niveau inférieur, on propose un contrôleur de type commande floue coordonnée pour gérer l'accélérateur et le finage. Enfin, on teste le système de contrôle longitudinal par simulation numérique.

**Le quatrième chapitre** est consacré au contrôle latéral. Nous proposons une loi de commande multi-modèle floue afin d'effectuer les opérations de suivi et de changement de trajectoire. Une trajectoire virtuelle VDT (Virtual Desired Trajectory) est introduite pour fournir une trajectoire lisse et efficace pour l'opération de changement de trajectoire. Afin de réaliser des commutations flexibles entre les différentes opérations, nous proposons aussi une architecture hiérarchique pour le système de contrôle latéral.

A partir des lois de commande proposées dans les chapitres précédents, **le chapitre 5** présente un système complet intégrant le contrôle longitudinal et le contrôle latéral. Ce système complet permet de réaliser une conduite automatisée pour les véhicules sur AHS.

**Le dernier chapitre** s'attache d'écrire, d'une part, l'estimation des variables d'états du véhicule, et d'autre part l'introduction d'un prototype multi-capteurs de véhicule intelligent à échelle réduite. Nous proposons un filtre de Kalman-Bucy pour estimer des états du véhicule de la dynamique latérale. En outre, les différents aspects pour réaliser le prototype de véhicule intelligent sont présentés.

Finalement, une synthèse de ces travaux de thèse est effectuée afin d'évaluer les résultats déjà obtenus ainsi que les perspectives futures.



# Bibliography

- [A.A.S.H.T.O 2008] A.A.S.H.T.O. *Driving Down Lane-Departure Crashes-A National Priority*. Rapport technique, American Association of State Highway and Transportation Officials, Washinton, DC, April 2008.
- [Åström, K.J. 2002] Åström, K.J. *Control System Design Lecture notes*. Department of Mechanical and Environmental Engineering, University of California, Santa Barbara, 2002.
- [Abele 2005] J. Abele, C. Kerlen, S. Krueger, H Baum and et al. *Exploratory Study on the potential socio-economic impact of the introduction of Intelligent Safety Systems in Road Vehicles*. Final report, SEISS, Teltow, Germany, January 2005.
- [Ackermann 1995] J. Ackermann, J. Guldner, W. Sienel, R. Steinhauser and VI Utkin. *Linear and nonlinear controller design for robust automaticsteering*. IEEE Transactions on Control Systems Technology, vol. 3, no. 1, pages 132–143, 1995.
- [Addi 2005] K. Addi, D. Goeleven and A. Rodi. *Mathematical analysis and numerical simulation of a nonsmooth road-vehicle spatial model*. ZAMM-Journal of Applied Mathematics and Mechanics/Zeitschrift für Angewandte Mathematik und Mechanik, vol. 86, no. 3, pages 185–209, 2005.
- [Andrew H 1993] Card Andrew H. *Hearing before the subcommittee on investigations and oversight of the committee on science, space and technology*. US. House of Representatives, 103 congress, First Session, PP. 108-109, US. Printing Office, November 1993.
- [Antsaklis 1991] PJ Antsaklis, KM Passino and SJ Wang. *An introduction to autonomous control systems*. IEEE Control Systems Magazine, vol. 11, no. 4, pages 5–13, 1991.
- [Assanis 2000] D.N. Assanis, Z.S. Filipi, S. Gravante, D. Grohnke, X. Gui, L. Louca, G. Rideout, J. Stein and Y. Wang. *Validation and use of SIMULINK integrated, high fidelity, engine-in-vehicle simulation of the international class VI truck*. SAE Transactions, vol. 109, no. 3, pages 384–399, 2000.
- [Åström 1992] K.J. Åström and T.J. McAvoy. *Intelligent control*. Journal of Process Control, vol. 2, no. 3, pages 115–127, 1992.

- [Bom 2005] J. Bom, B. Thuilot, F. Marmoiton and P. Martinet. *A global control strategy for urban vehicles platooning relying on nonlinear decoupling laws*. In 2005 IEEE/RSJ International Conference on Intelligent Robots and Systems, 2005.(IROS 2005), pages 2875–2880, 2005.
- [Bonnifait 2007] Ph. Bonnifait, M. Jabbour and G. Dherbomez. *Real-Time Implementation of a GIS-Based Localization System for Intelligent Vehicles*. EURASIP Journal of Embedded Systems, vol. vol. 2007, pages 12–24, June 2007. DOI 10.1155/2007/39350.
- [Bonnifait 2008] Ph. Bonnifait, M. Jabbour and V. Cherfaoui. *Autonomous Navigation in Urban Areas using GIS-Managed Information*. International Journal of Vehicle Autonomous Systems, vol. 6, no. 1/2, pages 84–103, 2008. Special Issue on Advances in Autonomous Vehicles and Intelligent Transportation.
- [Borne 1990] P. Borne, G. Dauphin-Tanguy, J.-P. Richard, F. Rotella and I. Zamettakis. *Commande et optimisation des processus*. Éditions Technip, Paris, 1990.
- [Chaib 2004] S. Chaib, M.S. Netto and S. Mammar.  *$H_\infty$ , adaptive, PID and fuzzy control: a comparison of controllers for vehicle lane keeping*. In Intelligent Vehicles Symposium, 2004 IEEE, pages 139–144, Parma, June 2004.
- [Chaibet 2005] A. Chaibet, L. Nouveliere, S. Mammar and M. Netto. *Backstepping control synthesis for automated low speed vehicle*. In PROCEEDINGS OF THE AMERICAN CONTROL CONFERENCE, volume 1, pages 447–452, 2005.
- [Chee 1994] W. Chee and M. Tomizuka. *Vehicle Lane Change Maneuver in Automated Highway Systems*. Rapport technique, California PATH Research Report, UCB-ITS-PRR-94-22, 1994.
- [Cheon 2002] S. Cheon. *An Overview of Automated Highway Systems (AHS) and the Social and Institutional Challenges They Face*. Report 624, University of California Transportation Center, 2002.
- [Chiang 2006] H.H. Chiang, L.S. Ma, J.W. Perng, B.F. Wu and T.T. Lee. *Longitudinal and lateral fuzzy control systems design for intelligent vehicles*. In Networking, Sensing and Control, 2006. ICNSC'06. Proceedings of the 2006 IEEE International Conference on, pages 544–549, 2006.
- [Cho 1989] D. Cho and JK Hedrick. *Automotive powertrain modeling for control*. Journal of Dynamic Systems, Measurement, and Control, vol. 111, pages 568–576, 1989.
- [Choi 2001] Ju Yong Choi, Chang Sup Kim, Sinpyo Hong, Man Hyung Lee, Jong Il Bae and F. Harashima. *Vision based lateral control by yaw rate feedback*. In Industrial Electronics Society, 2001. IECON '01. The 27th Annual Conference of the IEEE, volume 3, pages 2135–2138, Denver, December 2001.

- 
- [Chunyan 2003] W. Chunyan, Q. Tongyan and W. Xiaojing. *An adaptive fuzzy controller and its application for lateral control in IHS*. 2003 IEEE Intelligent Transportation Systems, 2003. Proceedings, vol. 1, pages 244–246, 2003.
- [COMMUNITIES 2006a] COMMISSION OF THE EUROPEAN COMMUNITIES. *Keep europe moving-sustainable mobility for our continent-mid-term review of the european comission's 2001 transport white paper*. Office for Official Publications of the European Communities, 2006.
- [COMMUNITIES 2006b] COMMISSION OF THE EUROPEAN COMMUNITIES. *On the Intelligent Car Initiative: Raising Awareness of ICT for Smarter, Safer and Cleaner Vehicles*. Report COM(2006) 59 final, COMMISSION OF THE EUROPEAN COMMUNITIES, Februry 2006.
- [COMMUNITIES 2008] COMMISSION OF THE EUROPEAN COMMUNITIES. *Communication from the Commission - Action plan for the deployment of Intelligent Transport Systems in Europe*, December 2008.
- [Darbha 2003] S. Darbha. *On the synthesis of controllers for continuous time LTI systems that achieve a non-negative impulse response*. Automatica, vol. 39, no. 1, pages 159–165, 2003.
- [Day 1995] TD Day. *An overview of the HVE vehicle model*. Society of Automotive Engineers, SAE 950308, Warrendale PA, 1995.
- [EL KAMEL 2000a] A. EL KAMEL, F. BOUSLAMA and P. BORNE. *Multimodel Multi-control of Vehicles in automated Highways*. In The 4th World Automation Congress WAC'00, Hawaii, USA, June 2000.
- [EL KAMEL 2000b] A. EL KAMEL, M. KSOURI-LAHMARI and P. BORNE. *Contribution to Multimodel Analysis and Control*. Int. J. of Studies in Informatics and Control, vol. 9, pages 29–38, 2000.
- [El Kamel 2002] A. El Kamel, J.Y. Dieulot and P. Borne. *Fuzzy controller for lateral guidance of busses*. In Proceedings of the IEEE International Symposium on Intelligent Control, pages 110–115, Vancouver, October 2002.
- [El Kamel 2005] A. El Kamel and J.P. Bourey. *UML-Based Design and Fuzzy Control of Automated Vehicles*. Lecture notes in Artificial Intelligence, Springer, vol. 3613, pages 1025–1033, 2005.
- [El Kamel 2006] A. El Kamel, Q. Hembise, S. Olive and K. Mellouli. *Intelligent Transportation System Design and Monitoring*. In IEEE International Conference on Industrial Technology, 2006. ICIT 2006, pages 3020–3025, 2006.
- [El Kamel 2007] A. El Kamel. *Multi-Sensor Automated Highway Prototype Design, Instrumentation & Embedded Control*. In European Control Conference, ECC'07,, Kos, Greece, July 2007.

- [EL-KOURSI 2006] EM EL-KOURSI and L TORDAI. *Common approach for supervising the railway safety performance*. Wit Transactions on the Built Environment, vol. 88, pages 147–156, 2006.
- [EL-KOURSI 2007] EM EL-KOURSI, S MITRA and G BEARFIELD. *Harmonising Safety Management Systems in the European Railway Sector*. Safety Science Monitor, vol. 11, pages 01–14, 2007.
- [ERTICO ] ERTICO. *ERTICO homepage*, <http://www.ertico.com/>.
- [Fenton 1988] R.E. Fenton and I. Selim. *On the optimal design of an automotive lateral controller*. IEEE Transactions on Vehicular Technology, vol. 37, no. 2, pages 108–113, May 1988.
- [Fisher 1970] DK Fisher. *Brake system component dynamic performance measurement and analysis*. SAE paper, vol. 700373, pages 1157–1180, 1970.
- [Freyssenet 2009] M. Freyssenet. *La production automobile mondiale par continent et quelques pays, 1898-2008*. <http://freyssenet.com/?q=node/367>, 2009.
- [Gerdes 1997] J.C. Gerdes and JK Hedrick. *Vehicle speed and spacing control via coordinated throttle and brake actuation*. Control Engineering Practice, vol. 5, no. 11, pages 1607–1614, 1997.
- [Gillespie 1992] T.D. Gillespie. *Fundamentals of vehicle dynamics*. Society of Automotive Engineers Warrendale, PA, 1992.
- [Gim 1990] G. Gim and PE Nikravesh. *An analytical model of pneumatic tyres for vehicle dynamic simulations. Pt. 1: pure slips*. International Journal of Vehicle Design, vol. 11, no. 6, pages 589–618, 1990.
- [Gim 1991a] G. Gim and PE Nikravesh. *An analytical model of pneumatic tyres for vehicle dynamic simulations. Pt. 2: comprehensive slips*. International journal of vehicle design, vol. 12, no. 1, pages 19–39, 1991.
- [Gim 1991b] G. Gim and PE Nikravesh. *An analytical model of pneumatic tyres for vehicle dynamic simulations. Pt. 3: validation against experimental data*. International Journal of Vehicle Design, vol. 12, no. 2, pages 217–28, 1991.
- [Godbole 2000] D.N. Godbole and J. Lygeros. *Safety and throughput analysis of automated highway systems*. Rapport technique UCB-ITS-PRR-2000-1, California PATH Research Report,, 2000.
- [Grizzle 1994] JW Grizzle, JA Cook and WP Milam. *Improved cylinder air charge estimation for transient air fuel ratio control*. In American Control Conference. Citeseer, 1994.
- [Guntur 1972] R. R. Guntur and H. Ouwerkerk. *Adaptive brake control system*. Proceedings of the Institution of Mechanical Engineers, vol. 186, pages 855–880, 1972.

- 
- [Guntur 1980] RR Guntur and JY Wong. *Some Design Aspects of Anti-Lock Brake Systems for Commercial Vehicles*. *Vehicle System Dynamics*, vol. 9, no. 3, pages 149–180, 1980.
- [Halle 2005] Simon Halle and Brahim Chaib-draa. *A collaborative driving system based on multiagent modelling and simulations*. *Transportation Research Part C: Emerging Technologies*, vol. 13, no. 4, pages 320 – 345, 2005.
- [Hedrick 1991] McMahon D. Narendran V. Swaroop-D. Hedrick J.K. *Longitudinal Vehicle Controller Design for IVHS Systems*. In *American Control Conference*, pages 3107–3112, June 1991.
- [Hedrick 1993] JK Hedrick, DH McMahon and D. Swaroop. *Vehicle modeling and control for automated highway systems*. Technical Report UCB-ITS-PRR-93-24, UC Berkeley: California Partners for Advanced Transit and Highways (PATH), 1993.
- [Hedrick 1994] JK Hedrick, M. Tomizuka and P. Varaiya. *Control issues in automated highway systems*. *IEEE Control Systems Magazine*, vol. 14, no. 6, pages 21–32, 1994.
- [Hedrick 1996] J.K. Hedrick, V. Garg, J.C. Gerdes, D.B. Maciuca and D. Swaroop. *Longitudinal Control Development for IVHS Fully Automated and Semi-Automated Systems-Phase II*. Rapport technique, California Partners for Advanced Transit and Highways (PATH), PATH Report, UCB-ITS-PRR-96-1, January 1996.
- [Hedrick 1997] JK Hedrick, JC Gerdes, DB Maciuca and D. Swaroop. *Brake system modeling, control and integrated brake/throttle switching: Phase I*. California PATH Research Report UCB-ITS-PRR-97-21, California Partners for Advanced Transit and Highways (PATH), May 1997.
- [Hilhorst 1991] RA Hilhorst, J. van Amerongen, P. Lohnberg and H. TuUeken. *Intelligent adaptive control of mode-switch processes*. In *IFAC Symposium on Intelligent Tuning and Adaptive Control*, page 145, Singapore, 15-17, January 1991. Pergamon.
- [Hingwe 1997] P.S. Hingwe. *Robustness and performance issues in the lateral control of vehicles in automated highway systems*. PhD thesis, University of California, Berkeley, 1997.
- [Hoeglinger 2008] Stefan Hoeglinger, Thomas Leitner, George Yannis, Petros Evgenikos and etc. *Traffic Safety Basic Facts 2007*. Report, European Road Safety Observatory, February 2008.
- [Horowitz 2000] R. Horowitz and P. Varaiya. *Control design of an automated highway system*. *Proceedings of the IEEE*, vol. 88, no. 7, pages 913–925, 2000.
- [Horowitz 2004] R. Horowitz, C.W. Tan and X. Sun. *An efficient lane change maneuver for platoons of vehicles in an automated highway system*. Report UCB-ITS-PRR-2004-16, UC Berkeley, California PATH, May 2004.

- [Huang 2005] J. Huang and M. Tomizuka. *LTV controller design for vehicle lateral control under fault in rear sensors*. IEEE/ASME Transactions on Mechatronics, vol. 10, no. 1, pages 1–7, February 2005.
- [Ioannou 1993] P. Ioannou, Z. Xu, S. Eckert, D. Clemons and T. Sieja. *Intelligent cruise control: theory and experiment*. In Proceedings of the 32nd IEEE Conference on Decision and Control, pages 1885–1890 vol.2, Dec 1993.
- [Ioannou 1994] PA Ioannou, F. Ahmed-Zaid and D. Wuh. *A time headway autonomous intelligent cruise controller: Design and simulation*. Research Report UCB-ITS-PWP-94-07, California PATH, April 1994.
- [ITSC ] ITSC. *National ITS Center, China*. <http://www.itsc.com.cn/>.
- [Jacobs 1991] R.A. Jacobs, M.I. Jordan, S.J. Nowlan and G.E. Hinton. *Adaptive mixtures of local experts*. Neural computation, vol. 3, no. 1, pages 79–87, 1991.
- [Japanese Ministry of Land a] Infrastructure Transport Japanese Ministry of Land and Tourism. *What's ITS?* [http://www.mlit.go.jp/road/ITS/topindex/topindex\\_g02\\_1.html](http://www.mlit.go.jp/road/ITS/topindex/topindex_g02_1.html).
- [Japanese Ministry of Land b] Transport Japanese Ministry of Land Infrastructure and Tourism. *Comprehensive Plan for ITS in Japan*. <http://www.mlit.go.jp/road/ITS/>.
- [Ji 2007] J. Ji, Y. Li and L. Zheng. *Self-Adjusting Fuzzy Logic Control for Vehicle Lateral Control*. In Proceedings of the Fourth International Conference on Fuzzy Systems and Knowledge Discovery, volume 2, pages 614–618. IEEE Computer Society Washington, DC, USA, 2007.
- [Jia 2000] Yingmin Jia. *Robust control with decoupling performance for steering and traction of 4WS vehicles under velocity-varying motion*. Control Systems Technology, IEEE Transactions on, vol. 8, no. 3, pages 554–569, May 2000.
- [Johansen 1993a] T.A. Johansen and B.A. Foss. *Constructing NARMAX models using ARMAX models*. International Journal of Control, vol. 58, no. 5, pages 1125–1153, 1993.
- [Johansen 1993b] T.A. Johansen and B.A. Foss. *Constructing NARMAX models using ARMAX models*. International Journal of Control, vol. 58, no. 5, pages 1125–1153, 1993.
- [Kalman 1960] RE Kalman. *A new approach to linear filtering and prediction theory*. ASME Journal of Basic Engineering, vol. 82, pages 35–45, 1960.
- [Kalman 1961] R. Kalman and R. Bucy. *New results in linear prediction and filtering theory*. AMSE Journal of Basic Engineering, pages 95–108, 1961.

- 
- [Kiencke 1997] U. Kiencke and A. Daifl. *Observation of lateral vehicle dynamics*. Control Engineering Practice, vol. 5, no. 8, pages 1145–1150, 1997.
- [Kiencke 2005] U. Kiencke and L. Nielsen. *Automotive control systems: for engine, driveline, and vehicle*. Springer Verlag, 2005.
- [Kienhöfer 2006] FW Kienhöfer and D. Cebon. *Improving ABS on heavy vehicles using slip control*. Rapport technique, Cambridge University Engineering Department, 2006.
- [Kodagoda 2002] KRS Kodagoda, WS Wijesoma and EK Teoh. *Fuzzy speed and steering control of an AGV*. IEEE Transactions on control systems technology, vol. 10, no. 1, pages 112–120, 2002.
- [Kotwicki 1982] A.J. Kotwicki. *Dynamic models for torque converter equipped vehicles*. SAE paper, vol. 820393, 1982.
- [Lee 1999] G.D. Lee, S.W. Kim, Y.U. Yim, J.H. Jung, S.Y. Oh and B.S. Kim. *Longitudinal and lateral control system development for a platoon of vehicles*. In Proceedings. IEEE/IEEEJ/JSAI International Conference on Intelligent Transportation Systems, pages 605–610, Tokyo, October 1999.
- [Lee 2002] KB Lee, YJ Kim, OS Ahn and YB Kim. *Lateral control of autonomous vehicle using Levenberg-Marquardt neural network algorithm*. Int. J. Automotive Technology, vol. 3, no. 2, pages 71–77, 2002.
- [Li 2002] Perry Y. Li and Ankur Shrivastava. *Traffic flow stability induced by constant time headway policy for adaptive cruise control vehicles*. Transportation Research Part C: Emerging Technologies, vol. 10, no. 4, pages 275 – 301, 2002.
- [Lim 1999] E.H.M. Lim and J.K. Hedrick. *Lateral and longitudinal vehicle control coupling for automated vehicle operation*. In Proceedings of the American Control Conference, volume 5, pages 3676 –3680, San Diego, California, June 1999.
- [Lowndes 1998] E.M. Lowndes. *Development of an Intermediate DOF Vehicle Dynamics Model for Optimal Design Studies*. PhD thesis, North Carolina State University, 1998.
- [Luenberger 1971] D. Luenberger. *An introduction to observers*. IEEE Transactions on Automatic Control, vol. 16, no. 6, pages 596–602, 1971.
- [Lygeros 1998] J. Lygeros, DN Godbole and S. Sastry. *Verified hybrid controllers for automated vehicles*. IEEE Transactions on Automatic Control, vol. 43, no. 4, pages 522–539, 1998.
- [Mammar 2004] S. Mammar and M. Netto. *Integrated longitudinal and lateral control for vehicle low speed automation*. In Control Applications, 2004. Proceedings of the 2004 IEEE International Conference on, volume 1, pages 350–355, 2004.

- [Márquez-Martinez 2001] L.A. Márquez-Martinez and C.H. Moog. *Trajectory Tracking Control for Nonlinear Time-Delay Systems*. *Kybernetika*, vol. 37, no. 4, pages 370–380, 2001.
- [Márquez-Martinez 2004] LA Márquez-Martinez and CH Moog. *Input-output feedback linearization of time-delay systems*. *IEEE Transactions on Automatic Control*, vol. 49, no. 5, pages 781–785, 2004.
- [Marsden 2001] G. Marsden, M. McDonald and M. Brackstone. *Towards an understanding of adaptive cruise control*. *Transportation Research Part C*, vol. 9, no. 1, pages 33–51, 2001.
- [McDonald 1999] M. McDonald and M. Marsden. *DIATS Deployment of interurban ATC test scenarios, Final report*. Report RO-96-SC.301, DIATS Project, May 1999.
- [McMahon 1990] Hedrick J. K. Shladover-S. E. McMahon D. H. *Vehicle Modelling and Control for Automated Highway Systems*. In *American Control Conference*, pages 297–303, May 1990.
- [McMahon 1992] DH McMahon, VK Narendran, D. Swaroop, JK Hedrick, KS Chang and PE Devlin. *Longitudinal vehicle controllers for IVHS: Theory and experiment*. In *Proceedings of the 1992 American Control Conference*, pages 1753–1757, Chicago, 1992.
- [Mesarovic 1970] M.D. Mesarovic, D. Macko and Y. Takahara. *Theory of hierarchical, multilevel, systems*. Academic Press New York, 1970.
- [Moog 1996] CH Moog, R. Castro and M. Velasco. *The dynamic disturbance decoupling problem for time-delay nonlinear systems*. In *Conference on Decision and Control, 1996.*, *Proceedings of the 35th IEEE*, volume 1, pages 821–822, Kobe, Japan, December 1996.
- [Moskwa 1987] JJ Moskwa and JK Hedrick. *Automotive engine modeling for real time control application*. In *American Control Conference*, pages 341–346, 1987.
- [Murray-Smith 1997] R. Murray-Smith and T.A. Johansen. *Multiple model approaches to modelling and control*. Taylor&Francis, 1997.
- [Nagatani 2002] T. Nagatani. *The physics of traffic jams*. *Reports on Progress in Physics*, vol. 65, pages 1331–1386, 2002.
- [Naranjo 2006] J.E. Naranjo, C. Gonzalez, R. Garcia and T. De Pedro. *ACC+ Stop & Go maneuvers with throttle and brake fuzzy control*. *IEEE Transactions on intelligent transportation systems*, vol. 7, no. 2, pages 213–225, 2006.
- [Naranjo 2008] J.E. Naranjo, C. Gonzalez, R. Garcia and T. de Pedro. *Lane-Change Fuzzy Control in Autonomous Vehicles for the Overtaking Maneuver*. *IEEE Transactions on Intelligent Transportation Systems*, vol. 9, no. 3, pages 438–450, Sept. 2008.

- 
- [Netto 2004] M.S. Netto, S. Chaib and S. Mammar. *Lateral adaptive control for vehicle lane keeping*. In Proceedings of the American Control Conference, volume 3, pages 2693–2698, Boston, July 2004.
- [Nouvelière 2002] Lydie Nouvelière. *Commandes Robustes Appliquées au Control Assisté d'un Véhicule à Basse Vitesse*. PhD thesis, Université de Versailles-Saint Quentin en Yvelines, Versailles, France, Décembre 2002.
- [Nouveliere 2003] L. Nouveliere and S. Mammar. *Experimental vehicle longitudinal control using second order sliding modes*. In Proceedings of the 2003 American Control Conference, volume 6, pages 4705 – 4710, Denver, Colorado, june 2003.
- [O'Brien Jr 2006] RT O'Brien Jr and K. Kiriakidis. *A comparison of  $H_\infty$  with Kalman Filtering in vehicle state and parameter identification*. In American Control Conference, 2006, pages 3954–3959, 2006.
- [OCIA ] OCIA. *Production Statistics*, <http://www.oica.net/category/production-statistics/>.
- [Pacejka 2006] H.B. Pacejka. Tyre and vehicle dynamics. Butterworth-Heinemann Ltd, 2006.
- [PATH ] PATH. *California PATH homepage*, <http://www.path.berkeley.edu/Default.htm>.
- [Pham 1997] H. Pham, M. Tomizuka and J.K. Hedrick. *Integrated Maneuvering Control for Automated Highway Systems Based on a Magnetic Reference Sensing System*. California PATH Research Report UCB-ITS-PRR-97-28, University of California, Berkeley,, july 1997.
- [Powell 1987] BK Powell and JA Cook. *Nonlinear low frequency phenomenological engine modeling and analysis*. In Proceeding of American Control Conference, volume 1, pages 332–340, 1987.
- [PREDIT ] PREDIT. *PREDIT homepage*, <http://www.predit.prd.fr/predit3/lepredit.html>.
- [Rajamani 2000] R. Rajamani, Han-Shue Tan, Boon Kait Law and Wei-Bin Zhang. *Demonstration of integrated longitudinal and lateral control for the operation of automated vehicles in platoons*. IEEE Transactions on Control Systems Technology, vol. 8, no. 4, pages 695–708, July 2000.
- [Rajamani 2006] R. Rajamani. Vehicle dynamics and control. Springer, New York, 2006.
- [Ralph 2008] Kisiel Ralph. *Electronics overload may limit option choices; Some features may draw too much battery power*. [http://reviews.cnet.com/8301-13746\\_7-10123235-48.html](http://reviews.cnet.com/8301-13746_7-10123235-48.html), December 2008. Automotive News.
- [Santhanakrishnan 2003] K. Santhanakrishnan and R. Rajamani. *On spacing policies for highway vehicle automation*. IEEE Transactions on Intelligent Transportation Systems, vol. 4, no. 4, pages 198–204, December 2003.

- [SASAKI 2000] H. SASAKI and T. NISHIMAKI. *A side-slip angle estimation using neural network for a wheeled vehicle*. SAE transactions, vol. 109, no. 6, pages 1026–1031, 2000.
- [Shaozhong 2009] ZHU Shaozhong, GAO Xiaojie and YU Zhuoping. *Vehicle Sideslip Angle Estimation Under Extreme Driving Condition*. Journal of Tongji University (Natural Science), vol. 37, pages 1070–1074, 2009.
- [Sheikholeslam 1990] S. Sheikholeslam and C. Desoer. *Longitudinal Control of a Platoon of Vehicles*. In Proceedings of the 1990 American Control Conference, pages 291–297, San Diego, CA, May 1990.
- [Shinq-Jen Wu 2005] Jau-Woei Perng Tsu-Tian Lee Chao-Jung Chen Shinq-Jen Wu Hsin-Han Chiang. *The automated lane-keeping design for an intelligent vehicle*. pages 508 – 513, June 2005.
- [Shladover 1991a] S.E. Shladover. *Longitudinal control of automotive vehicles in close-formation platoons*. Journal of dynamic systems, measurement, and control, vol. 113, no. 2, pages 231–241, 1991.
- [Shladover 1991b] S.E. Shladover, CA Desoer, JK Hedrick, M. Tomizuka, J. Walrand, W.B. Zhang, DH McMahan, H. Peng, S. Sheikholeslam and N. McKeown. *Automated vehicle control developments in the PATH program*. IEEE Transactions on Vehicular Technology, vol. 40, no. 1, pages 114–130, Feb 1991.
- [Shrivastava 2000] A. Shrivastava and P.Y. Li. *Traffic flow stability induced by constant time headway policy for adaptive cruise control (ACC) vehicles*. In Proceedings of the 2000 American Control Conference,, volume 3, pages 1503 –1508, 2000.
- [Shuming 2005] S. Shuming, H. Lupker, P. Bremmer and J. Zuurbier. *Estimation of Vehicle Side Slip Angle Based on Fuzzy Logic* . Automotive Engineering, vol. 4, pages 426–430, 2005.
- [Stephant 2004] J. Stephant, A. Charara and D. Meizel. *Virtual sensor: application to vehicle sideslip angle and transversal forces*. IEEE Transactions on industrial electronics, vol. 51, no. 2, pages 278–289, 2004.
- [Sun 2000] P. Sun, B. Powell and D. Hrovat. *Optimal idle speed control of an automotive engine*. In Proceedings of the American Control Conference, volume 2, 2000.
- [Swaroop 1994a] D. Swaroop. *String stability of interconnected systems: An application to platooning in automated highway systems*. PhD thesis, University of California at Berkeley, 1994.
- [Swaroop 1994b] D. Swaroop, JK Hedrick, CC Chien and P. Ioannou. *A Comparison of Spacing and Headway Control Laws for Automatically Controlled Vehicles 1*. Vehicle System Dynamics, vol. 23, no. 1, pages 597–625, 1994.

- 
- [Swaroop 1996] D. Swaroop and JK Hedrick. *String stability of interconnected systems*. IEEE Transactions on Automatic Control, vol. 41, no. 3, pages 349–357, 1996.
- [Swaroop 1999] D. Swaroop and K. R. Rajagopal. *Intelligent cruise control systems and traffic flow stability*. Transportation Research Part C: Emerging Technologies, vol. 7, no. 6, pages 329 – 352, 1999.
- [Takagi 1985] T. Takagi and M. Sugeno. *Fuzzy identification of systems and its applications to modeling and control*. IEEE transactions on systems, man, and cybernetics, vol. 15, pages 116–132, 1985.
- [Tan 1990] HS Tan and M. Tomizuka. *An adaptive sliding mode vehicle traction controller design*. In Proceedings of the American Control Conference, volume 2, pages 1856–1861, San Diego, CA, 1990.
- [Taylor 1999] C.J. Taylor, J. Kosecka, R. Blasi and J. Malik. *A comparative study of vision-based lateral control strategies for autonomous highway driving*. The International Journal of Robotics Research, vol. 18, no. 5, pages 442–453, May 1999.
- [Tomizuka 1993] M. Tomizuka and JK Hedrick. *Automated vehicle control for ivhs systems*. In IFAC Conference, Sydney, Australia, pages 109–112, 1993.
- [Toulotte 2006] PF Toulotte, S. Delprat and TM Guerra. *Longitudinal and lateral control for automatic vehicle following*. In IEEE Vehicle Power and Propulsion Conference, 2006. VPPC’06, pages 1–6, 2006.
- [Tsugawa 2000] S. Tsugawa, S. Kato, T. Matsui, H. Naganawa and H. Fujii. *An architecture for cooperative driving of automated vehicles*. 2000 IEEE Intelligent Transportation Systems, 2000. Proceedings, pages 422–427, 2000.
- [Unsal 1998] Cem Unsal. *Intelligent navigation of autonomous vehicles in an automated highway system: Learning methods and interacting vehicles approach*. PhD thesis, Virginia Polytechnic Institute and State University, 1998.
- [van Arem 2006] B. van Arem, C.J.G. van Driel and R. Visser. *The Impact of Cooperative Adaptive Cruise Control on Traffic-Flow Characteristics*. IEEE Transactions on Intelligent Transportation Systems, vol. 7, no. 4, pages 429–436, Dec. 2006.
- [Varaiya 1993] P. Varaiya. *Smart cars on smart roads: problems of control*. IEEE Transactions on Automatic Control, vol. 38, no. 2, pages 195–207, 1993.
- [Venhovens 1999] P.J.T.H. Venhovens and K. Naab. *Vehicle dynamics estimation using Kalman filters*. Vehicle System Dynamics, vol. 32, no. 2, pages 171–184, 1999.
- [Wang 2004a] J. Wang and R. Rajamani. *The impact of adaptive cruise control systems on highway safety and traffic flow*. Proceedings of the Institution of Mechanical Engineers, Part D: Journal of Automobile Engineering, vol. 218, no. 2, pages 111–130, 2004.

- [Wang 2004b] Shaoping Wang, Jianfeng Tao and Zongxia Jiao. *Reliability analysis based on simulation modular to control system*. Journal of Beijing University of Aeronautics and Astronautics, vol. 30, pages 813–818, 2004.
- [Wang 2005] Shaoping Wang, Mingshan Cui, Shi Jian and Kang Ming. *Performance Degradation and Reliability Analysis for Redundant Actuation System*. Chinese Journal of Aeronautics, vol. 18, pages 359–365, November 2005.
- [Wang 2009] Shaoping Wang, Sijun Zhao and M.M. Tomovic. *Failure decision-making based on contracted support vector machine for indiscernible system*. In Advanced Intelligent Mechatronics, 2009. AIM 2009. IEEE/ASME International Conference on, pages 693–698, 14-17 2009.
- [Wijesoma 1999] W.S. Wijesoma, K.R.S. Kodagoda and E.K. Teoh. *Uncoupled fuzzy controller for longitudinal and lateral control of a golf car-like AGV*. In Proceedings of 1999 IEEE/IEEJ/JSAI International Conference on Intelligent Transportation Systems, pages 142–147, 1999.
- [Wu 2009] Jia Wu, A. Abbas-Turki and A. El Moudni. *Discrete Methods for Urban Intersection Traffic Controlling*. In Vehicular Technology Conference, 2009. VTC Spring 2009. IEEE 69th, pages 1–5, 26-29 2009.
- [Yan 2009] Fei Yan, M. Dridi and A. El Moudni. *Autonomous vehicle sequencing algorithm at isolated intersections*. In Intelligent Transportation Systems, 2009. ITSC '09. 12th International IEEE Conference on, pages 1–6, 4-7 2009.
- [Yang 2007] Jing Yang and Nanning Zheng. *An Expert Fuzzy Controller for Vehicle Lateral Control*. pages 880–885, Nov. 2007.
- [Yu 2009] Z. Yu and X. Gao. *Review of vehicle state estimation problem under driving situation*. Chinese Journal of Mechanical Engineering, vol. 45, no. 5, pages 20–33, 2009.
- [Zadeh 1973] L.A. Zadeh. *Outline of a new approach to the analysis of complex systems and decision processes*. IEEE Transactions on Systems, Man, and Cybernetics, vol. 3, no. 1, pages 28–44, 1973.
- [Zhang 1994] X.C. Zhang, A. Visala, A. Halme and P. Linko. *Functional state modelling approach for bioprocesses: local models for aerobic yeast growth processes*. Journal of Process Control, vol. 4, no. 3, pages 127–134, 1994.
- [Zhang 2000] J.R. Zhang, S.J. Xu and A. Rachid. *Robust sliding mode observer for automatic steering of vehicles*. In Intelligent Transportation Systems, 2000. Proceedings. 2000 IEEE, pages 89–94, Dearborn, 2000.
- [Zhao 2007] Jin Zhao, Masahiro Oya, Ting Wang and Qiang Wang. *Impacts of the ACC System on Highway Traffic Safety and Capacity*. Journal of China Mechanical Engineering, vol. 18, no. 12, pages 1496–1500, June 2007.

- 
- [Zhao 2009a] Jin Zhao and A. El Kamel. *Integrated Longitudinal and Lateral Control System Design for Autonomous Vehicles*. In The 2nd IFAC International Conference on Intelligent Control Systems and Signal Processing, ICONS, Istanbul, Turkey, September 2009.
- [Zhao 2009b] Jin Zhao and A. El Kamel. *Multi-Model Fuzzy Controller for Lateral Guidance of Vehicles*. In CSCS-17, the 17th International Conference on Control Systems and Computer Science, Bucharest, Romania, May 2009.
- [Zhao 2009c] Jin Zhao, M. Oya and A. El Kamel. *A safety spacing policy and its impact on highway traffic flow*. In 2009 IEEE Intelligent Vehicles Symposium, pages 960–965, Xi'an, China, June 2009.
- [Zhao 2010a] Jin Zhao and A. El Kamel. *Coordinated Throttle and Brake Fuzzy Controller Design for Vehicle Following*. In ITSC2010, the 13th International IEEE Conference on Intelligent Transportation Systems, Madeira Island, Portugal, September 2010.
- [Zhao 2010b] Jin Zhao and A. El Kamel. *Integrated Longitudinal and Lateral Control System Design for Autonomous Vehicles*. Submitted to the IEEE Transactions on Intelligent Transportation Systems, in June, 2010.
- [Zhao 2010c] Jin Zhao, Gaston Lefranc and A. El Kamel. *Lateral Control of Autonomous Vehicles Using Multi-Model and Fuzzy Approaches*. In IFAC 12th LSS Symposium, Large Scale Systems: Theory and Applications, Villeneuve D'Ascq, France, July 2010.
- [Zhenhai 2003] G. Zhenhai. *Soft sensor application in vehicle yaw rate measurement based on Kalman filter and vehicle dynamics*. Proceeding of IEEE Intelligent Transportation Systems, vol. 2, pages 1352–1354, 2003.
- [Zhou 2005] J. Zhou and H. Peng. *Range policy of adaptive cruise control vehicles for improved flow stability and string stability*. IEEE Transactions on Intelligent Transportation Systems, vol. 6, no. 2, pages 229–237, 2005.
- [Ziegler 1942] JG Ziegler and NB Nichols. *Optimum settings for automatic controllers*. Transactions of the A.S.M.E, vol. 64, pages 759–768, November 1942.
- [Zwaneveld 1998] P. Zwaneveld and B. van Arem. *Traffic effects of automated vehicle guidance systems*. In Fifth World Congress on Intelligent Transportation Systems, Seoul, Korea, October 1998.



## Résumé

Ce mémoire est consacré à la mise en oeuvre de commandes d'un train de véhicules intelligents sur autoroute ayant pour objectifs principaux de réduire la congestion et d'améliorer la sécurité routière. Après avoir présenté l'état de l'art sur des systèmes de conduite automatisée, des modèles de la dynamique longitudinale et latérale du véhicule sont présentés. Ensuite, des stratégies de contrôle longitudinal et latéral sont étudiées.

D'abord, le contrôle longitudinal est conçu pour être hiérarchique avec un contrôleur de niveau supérieur et un contrôleur de niveau inférieur. Pour celui de niveau supérieur, une régulation d'inter-distance SSP (Safety Spacing Policy) est proposée. Nous avons constaté que la SSP peut assurer la stabilité de la chaîne et la stabilité des flux de trafic et augmenter ainsi la capacité de trafic. Puis, pour celui de niveau inférieur, une loi de commande floue coordonnée est proposée pour gérer l'accélérateur et le freinage.

Ensuite, une loi de commande multi-modèle floue est conçue pour le contrôle latéral. De plus, pour réaliser des transformations lisses entre les différentes opérations latérales, une architecture de contrôle hiérarchique est proposée. Puis, l'intégration des commandes longitudinale et latérale est étudiée.

Enfin, l'estimation des variables d'états du véhicule est discutée. Un filtre de Kalman-Bucy est conçu pour estimer les états du véhicule. En outre, un prototype de véhicule intelligent à échelle réduite est également présenté. Les performances des divers algorithmes de commande proposés ont été testées par simulations, et les résultats ont été confirmés par les premières expériences en utilisant le prototype.

**Mots-clés:** Véhicule intelligent, Train de véhicule, Commande longitudinale, Commande latérale, Commande multi-modèle, Commande floue

## Abstract

This PhD thesis is dedicated to the control strategies for intelligent vehicle platoon in highway with the main aims of alleviating traffic congestion and improving traffic safety. After a review of the different existing automated driving systems, the vehicle longitudinal and lateral dynamic models are derived. Then, the longitudinal control and lateral control strategies are studied respectively.

At first, the longitudinal control system is designed to be hierarchical with an upper level controller and a lower level controller. For the upper level controller, a safety spacing policy (SSP) is proposed. It is shown that the proposed SSP can ensure string stability, traffic flow stability and improve traffic capacity. Then, a coordinated throttle and brake fuzzy controller (lower level controller) is designed, in which a logic switch is designed to coordinate the two actuators (throttle and brake pedals).

Second, for the lateral control, a multi-model fuzzy controller is designed. And a hierarchical lateral control architecture is also proposed, which can effectuate flexible switch between different lateral operations. After that, the integration of the longitudinal controller and lateral controller is also studied.

Finally, the estimation of vehicle states is discussed. A Kalman-Bucy filter is designed to estimate vehicle states in lateral dynamics. Moreover, a reduced scale multi-sensor intelligent vehicle prototype is also presented. The performances of the divers control algorithms proposed in this thesis have been tested in numerical simulations, and the first step experiments with the reduced scale vehicle prototype gave encouraging results.

**Keywords:** Intelligent vehicle, Vehicle platoon, Longitudinal control, Lateral control, Multi-model control, Fuzzy control.

